

Evaluating the Role of Bacterial Lipopolysaccharide on Etiology and Pathogenesis of
Transmissible Spongiform Encephalopathies

by

Seyed Ali Goldansaz

A thesis submitted in partial fulfillment of the requirements for the degree of

Master of Science

in

Animal Science

Department of Agricultural, Food and Nutritional Science
University of Alberta

© Seyed Ali Goldansaz, 2014

Abstract

Transmissible spongiform encephalopathies (TSEs) or otherwise known as prion diseases are a class of fatal neurodegenerative diseases related to irreversible brain damage. Presently, there is no effective treatment or preventive strategy for this disease because the etiology and biological behavior of the causative agent, prion protein, is not yet understood very well. Although the disease is related to misfolding of a normal cellular prion protein (PrP^C) into an abnormal one, known as scrapie (PrP^{Sc}), there is increasing evidence for a potential role of endogenous/exogenous cofactors in the pathogenesis of the disease. Furthermore, it has been reported that in presence of cofactors prion disease tends to aggravate. Of note, none of the cofactors identified so far have been able to independently induce prion disease in various animal models.

In this study, we hypothesized that bacterial lipopolysaccharide (LPS), derived from Gram-negative bacteria, and recombinant PrP converted *in vitro* into a beta-rich isoform resistant to proteinase K digestion (moPrP^{res}) through incubation with bacterial LPS, can cause prion-like disease in a murine model. LPS is a cell wall component of all Gram-negative bacteria commonly found in the environment, and highly abundant in the digestive tract. Lipopolysaccharide has been extensively used to mimic bacterial infection in various studies. In neurodegenerative diseases, LPS has shown to contribute to exacerbating existing neurodegenerative disease conditions. Recently our team reported that incubation of LPS with PrP^C under normal *in vitro* conditions and without presence of other cofactors can convert PrP^C to an isoform rich in beta sheets and resistant to proteinase K digestion, which we are defining as resistant mouse recombinant prion protein (moPrP^{res}).

To test this hypothesis and to investigate the degree of moPrP^{res} pathogenicity and infectivity, one experiment was conducted in which FVB/N female mice were inoculated subcutaneously with the infectious agents. To do so, 90 FVB/N female mice at the age of 6 week (wk) were randomly assigned into 6 treatment groups (n=15 per group) including: 1) saline (negative control), 2) LPS, 3) moPrP^{res}, 4) moPrP^{res}+LPS, 5) RML (Rocky mountain laboratory scrapie prions) +LPS, and 6) RML (positive control). Lipopolysaccharide and saline were administered subcutaneously for a period of 6 wk, whereas moPrP^{res} and RML were injected one time subcutaneously at the start of the experiment.

Mice inoculated with LPS or moPrP^{res} exhibited prion-like disease signs with weight loss accompanied with 50% and 60% mortality rates, respectively, over long incubation days in comparison to the positive controls. Immunohistochemical (IHC) staining of brain sections from the mice treated with LPS or moPrP^{res} showed extensive vacuolation patterns comparable to the positive control although with larger size and some degree of PrP^{Sc} accumulation in the brain. In addition presence of astrogliosis and deposition of amyloid plaques were detected in some brain regions. However, when chronic subcutaneous administration of LPS was accompanied with RML, IHC stainings revealed aggravation in vacuolation, accumulation of PrP^{Sc}, and astrogliosis in comparison to the RML-only treated mice. Furthermore, gene expression profiling of all treatment groups in comparison to the negative control indicated various alterations most importantly down-regulation in expression level of genes encoding the prion protein (*Prnp*) and shadow of prion protein (*Sprn*), with the exception of the LPS-only treated group that had no effect on *Prnp*. Down-regulation of *Prnp* and *Sprn* are considered gene expression signatures specific to prion diseases. In addition, using non-targeted metabolomics approach multiple

metabolite alterations were detected in the serum and urine of RML- and RML+LPS-infected mice, which might serve as predictive biomarkers of disease at early stages of pathogenesis.

Preface

This thesis is an original work by Seyed Ali Goldansaz as part of a team of colleagues under supervision of Dr. Burim N. Ametaj at University of Alberta. This research project was led by Dr. Burim N. Ametaj and with collaboration of Dr. David Wishart and his team from Departments of Biological Sciences and Computer sciences and Dr. David Westaway and his colleagues from Centre for Prions and Protein Folding Diseases both at University of Alberta. The research project, of which this thesis is a part, received research ethics approval from the University of Alberta Animal Care and Use Committee, Health Sciences, “Evaluating the Role of Bacterial Lipopolysaccharides in the Etiology and Pathogenesis of Transmissible Spongiform Encephalopathies”, No. HS 660, February 2011. No part of this thesis has been previously published.

Acknowledgments

During the course of my research at University of Alberta, part of which is presented in this thesis, I have had the opportunity and pleasure of working with various people in different laboratories. The success to bringing this project to an end is indebted to a successful team work in collaboration with other research groups. Therefore, it is now my responsibility to acknowledge all those who have contributed to my research work, partially presented in this thesis.

I would like to foremost and sincerely extend my gratitude to my family who have been a great supporter of me during this time. Without their presence and support I would have not been able to make this journey and accomplish my degree. Throughout my life, my father has been the first and most influential teacher of my life providing his experience and love to me. My beloved mother, whom I don't think I will ever be able to make up for all she has done for me, has sacrificed a lot for my sake and went through a lot of hardship with my absence back home. My brother, which I am very much proud of, has also done a lot to fill my space at home in my absence. All of this and many more that cannot be expressed with words have given me the environment to be able to concentrate on my research and pursue my education. I am thankful and blessed to have this family.

I would like to extend my appreciations to my supervisor, Dr. Burim N. Ametaj, who has been patient in training me through the course of my degree at University of Alberta, Canada. I was mostly inspired by his enthusiasm in research, coming up with new and challenging ideas. I have also appreciated his perspective in evaluating scientific issues and strategies to overcome

the existing problems. I would like to thank him for all the dedication he has put in supervising this research and providing detailed instructions in training me for the scientific world.

I would like to also thank my dear colleague and post doctorate fellow of our team, Dr. Dagnachew Hailemariam Worku, who has been greatly involved in this research from day one. My appreciations to all of my colleagues in our research group who spiritually supported me during the course of my studies. Most specifically, I would like to sincerely thank Dr. Suzanna M. Dunn, the lab technician of our team. Her positive spirit and thoughtfulness has been a blessing to the team.

In this research, two other research teams from the Faculty of Science and Centre for Prions and Protein Folding Diseases, University of Alberta, have been collaborating. I would like extend my appreciations to both Drs. David Wishart and David Westaway, in interacting with myself during the course of this research. I have been most inspired by the humbleness, respectful manner, patience in listening, and precision in providing feedback from Dr. Wishart. I would like to also thank all the members of these two collaborating teams who have interacted with me in conducting different parts of this investigation. I would like to also thank my committee members, Drs. Richard Uwiera and Judd Aiken, who had kindly spent time evaluating my thesis. In addition, I would like to thank Jody Forslund, Graduate Program Administrator, and all other staff of the Faculty of AFNS who have guided me through my program with different administrative tasks.

This research would have not been made possible without the financial supports of the Alberta Livestock and Meat Agency Ltd. (ALMA), Alberta Prion Research Institute (APRI), and the Natural Sciences and Engineering Research Council (NSERC) of Canada.

Table of Contents

List of Tables	xii
List of Figures	xiii
List of Abbreviations	xv
Chapter One: Literature review	1
1. Prion Protein.....	2
1.1. General characteristics	2
1.2. Structure	3
1.3. Forms and functions.....	5
1.4. Conversion of PrP ^C from α - to β -isoform.....	7
1.5. Hypotheses about prion disease initiation and development.....	8
1.6. Transmissible spongiform encephalopathy	14
1.7. TSE in humans and animals	15
1.8. Immune response of the body to TSE	16
1.9. Genetics of the prion protein.....	17
1.10. Cofactors in prion disease.....	27
2. Lipopolysaccharide	28
2.1. Structure	29
2.2. Function.....	31
2.3. General impact on the body	32
2.4. Influence on prion disease.....	35
3. Hypotheses	37
4. Objectives	38
References	39
Chapter Two: Chronic subcutaneous administration of lipopolysaccharide and LPS-converted mouse PrP ^C induced neurodegeneration in FVB/N wild type female mice.....	51
Abstract	52

1. Introduction	54
2. Materials and Methods	56
2.1. Experimental design and animals	56
2.2. Mouse recombinant prion protein	56
2.3. Euthanasia	58
2.4. Tissue preparation	58
2.5. Hematoxylin and eosin staining	59
2.6. PrP ^{Sc} staining	59
2.7. Amyloid plaque staining	60
2.8. Astrogliosis staining	60
2.9. Western blot assay	61
2.10. Scrapie cell assay	62
2.11. Statistical analysis	64
3. Results	65
3.1. Weight change	65
3.2. Survival analysis	66
3.3. Immunohistochemical stainings	67
3.4. Western blot	73
3.5. Scrapie cell assay	74
4. Discussion	74
4.1. Infectivity and pathogenicity of LPS-converted recombinant moPrP ^{res}	74
4.2. Prion-like pathogenesis induced by LPS-only inoculation	76
4.3. Aggravation of prion pathogenesis in the presence of LPS in conjugation with RML	79
5. Conclusions	81
6. Acknowledgment	82
References	83
Figure Captions	89

Chapter Three: Subcutaneous injection of lipopolysaccharide (LPS)-converted mouse PrP^{res} or LPS alone are associated with brain gene expression signatures typical of prion pathology..... 102

Abstract	103
1. Introduction	105
2. Materials and Methods	107
2.1. Animals and experimental design	108
2.2. Euthanasia at 11 wk post inoculation (pi) and terminal stage	109
2.3. Total RNA isolation	110
2.4. Custom-made PCR array.....	110
2.5. First strand cDNA synthesis and quantitative PCR (qPCR) assay.....	111
2.6. Protein expression and purification	112
2.7. Statistical analysis	113
3. Results	113
3.1. Differentially expressed genes in the brains of mice treated at 11 wk postinfection	113
3.2. Differentially expressed genes in the brains of mice treated with moPrP ^{res} and moPrP ^{res} +LPS at terminal stage	114
3.3. Differentially expressed genes in the brains of mice treated with LPS.....	115
3.4. Differentially expressed genes in the brains of mice treated with RML and RML+LPS	116
4. Discussion	116
5. Conclusions	134
6. Acknowledgement.....	135
References	136
Figure Captions	156

Chapter Four: Metabolomics approach reveals alterations in the urine and serum of FVB/N female mice infected with RML

Abstract	163
1. Introduction	164
2. Materials and Methods	165
2.1. Experimental Design	165

2.2. Euthanasia	165
2.3. Sample Collection	166
2.4. Direct flow injection mass spectrometry (DI-MS).....	166
2.5. Nuclear Magnetic Resonance (¹ H-NMR).....	168
2.6. Statistical analysis	171
3. Results	171
3.1. Direct Injection-Mass Spectrometry	171
3.2. Nuclear Magnetic Resonance (¹ H-NMR).....	175
4. Discussion	177
4.1. Common RML and RML+LPS predictive metabolites	178
4.2. RML specific metabolites	184
4.3. RML plus lipopolysaccharide specific metabolites.....	190
4.4. Creatine	193
5. Conclusions	194
6. Acknowledgments	195
References	196
Figure Captions	215
Chapter Five: Overall Discussion.....	228
References	238

List of Tables

Table 3.1. List of differentially expressed genes in the brains of mice treated with LPS, moPrP ^{res} , moPrP ^{res} +LPS, RML+LPS and RML at 11 weeks of post inoculation	178
Table 3.2. List of differentially expressed genes in the brains of FVB/N mice treated with LPS at terminal stage	179
Table 3.3. List of differentially expressed genes in the brain tissue of terminally sick mice after subcutaneous injection of LPS-converted resistant mouse recombinant prion protein (moPrP ^{res}) and moPrP ^{res} +LPS injection	180
Table 3.4. List of differentially expressed genes in brain tissue of terminally sick mice after RML and RML+LPS injection	181
Table 4.1. RML urine metabolite profile alteration over time	239
Table 4.2. RML serum metabolite profile alteration over time	241
Table 4.3. RML+LPS urine metabolite profile alteration over time	241
Table 4.4. RML+LPS serum metabolite profile alteration over time	242

List of Figures

Figure 1.1. Structural features of the cellular prion protein.....	25
Figure 1.2. Structure of lipid A and the whole LPS.....	52
Figure 2.1. Weight comparison of FVB/N female mice	113
Figure 2.2. Survival analysis of terminally sick FVB/N female mice	114
Figure 2.3. Early demonstration of minor prion-like vacuolation in the Hematoxylin and Eosine staining of the brain of FVB/N wild type female mice (10X magnification).....	115
Figure 2.4. Prion-like vacuolation profile in brain Hematoxylin and Eosine staining of terminally sick FVB/N wild type female mice (10X magnification).....	116
Figure 2.5. PrP ^{Sc} deposition in brains of FVB/N wild type female mice at 11wk post inoculation (10X magnification).....	117
Figure 2.6. PrP ^{Sc} deposition in brains of FVB/N wild type female mice at terminal sickness (10X magnification).....	118
Figure 2.7. Astrogliosis in brains of FVB/N wild type female mice	119
Figure 2.8. Staining for amyloid plaque in brains of FVB/N wild type female mice.....	120
Figure 2.9. Western blot of brain (A) and spleen (B) homogenates	121
Figure 2.10. Scrapie cell assay using L929 mouse fibroblast cell line and brain homogenates of terminally sick FVB/N female mice	122
Figure 3.1. Genes differentially expressed in the brain of mice terminally sick that were euthanized after treatment with: 1) resistant mouse recombinant prion protein (moPrP ^{res}); 2) moPrP ^{res} +LPS; 3) RML; and 4) RML+LPS.	180
Figure 4.1. Partial least squares Discriminant Analysis (PLSDA) of urine metabolite profile data for the RML treatment group at 11wk post inoculation	243
Figure 4.2. Partial least squares Discriminant Analysis (PLSDA) of urine metabolite profile data for the RML treatment group one month prior to death	243

Figure 4.3. Partial least squares Discriminant Analysis (PLSDA) of urine metabolite profile data for the RML treatment group at death	244
Figure 4.4. Partial least squares Discriminant Analysis (PLSDA) of urine metabolite profile data for the RML+LPS treatment group at 11 wk post inoculation	244
Figure 4.5. Partial least squares Discriminant Analysis (PLSDA) of urine metabolite profile data for the RML+LPS treatment group one month prior to death	245
Figure 4.6. Partial least squares Discriminant Analysis (PLSDA) of urine metabolite profile data for the RML+LPS treatment group at death	245
Figure 4.7. Partial least squares Discriminant Analysis (PLSDA) of urine metabolite profile data comparing the RML and RML+LPS treatment groups at 11 wk post inoculation	246
Figure 4.8. Partial least squares Discriminant Analysis (PLSDA) of urine metabolite profile data comparing the RML and RML+LPS treatment groups one month prior to death	246
Figure 4.9. Partial least squares Discriminant Analysis (PLSDA) of urine metabolite profile data comparing the RML and RML+LPS treatment groups at death	247
Figure 4.10. Partial least squares Discriminant Analysis (PLSDA) of urine metabolite profile data comparing the RML treatment group at 11 wk post inoculation, one month prior to death and at death	247
Figure 4.11. Partial least squares Discriminant Analysis (PLSDA) of urine metabolite profile data comparing the RML+LPS treatment group at 11 wk post inoculation, one month prior to death and at death	248

List of Abbreviations

3MH - 3-methylhistidine
Ach - acetylcholine
Ache - acetylcholinesterase
AD - Alzheimer's disease
ADMA - asymmetric dimethylarginine
ALMA - Alberta Livestock and Meat Agency Ltd.
ALS - amyotrophic lateral sclerosis
ANS - autonomic nervous system
Ap - amyloid plaque
Apaf - apoptotic protease activating factor
ApoE - gene coding for apolipoprotein E
App - acute phase protein
APP - amyloid- β precursor protein
APR - acute phase response
APRI - Alberta Prion Research Institute
Arg - L-arginine
ATP - adenosine triphosphate
Atp1b1 - gene coding for ATPase, Na⁺/K⁺ transporting, beta 1 polypeptide
A β - amyloid- β
Bax - bcl2-associated X
BBB - blood brain barrier
BC3 - RT buffer 3
BCAA - branched chain amino acids
BSE - bovine spongiform encephalopathy
BW - body weight
Cc - cerebral cortex
Ccl5 - gene coding for Chemokine (C-C motif) ligand 5
CD - circular dichroism
cDNA - complementary deoxyribonucleic acid

CJD - Creutzfeldt-Jakob disease
CNS - central nervous system
COX-2 - cyclooxygenase-2
Cr - cerebellum
CT - comparative threshold
CVO - circumventricular organs
CWD - chronic waste disease
CXCL - CXC chemokine ligand
D - at death
D-1 - one month prior to death
D-2 - two months prior to death
Da - dalton
DDAH - dimethylarginine dimethylaminohydrolase
ddH₂O - double distilled water
DI-MS - direct flow injection mass spectrometry
dpi - day post inoculation
Dpl- gene coding for Doppel
DSS - disodium-2,2-dimethyl-2-silapentane-5-sulphonate
E. coli - *Escherichia coli*
ENS - enteric nervous system
FcγRs - Fcγ receptors
FDCs - follicular dendritic cells
FFI - fatal familial insomnia
FIDs - free induction decays
FTLD - frontotemporal lobar degeneration
Fyn - Fyn proto-oncogene
g - gram
GAGs - glucosaminoglycans
GALT - gut associated lymphoid tissues
GBP - guanylate binding protein
GDC - genomic DNA contamination control

Gfap - gene coding for Glial fibrillary acidic protein
GIT - gastrointestinal tract
Glu - glutamate
GNB - gram-negative bacteria
GPI - glycosphosphatidyl inositol
GSS - Gerstmann-Straussler-Scheinker
H&E - hematoxylin and eosin
H₂O₂ - hydrogen peroxide
HCl - hydrochloride
HD - Huntington's disease
hr - hour
i.c. - intracerebral
i.p. - intraperitoneal
i.v. - intravenous
iCJD - iatrogenic Creutzfeldt-Jakob disease
ID - infectious dose
Ifitm3 - gene coding for interferon induced transmembrane protein 3
IFN - interferon
Ifitm3 - interferon-induced transmembrane
IGF - insulin growth factor
IgG - immunoglobulin G
IHC - immunohistochemistry
IL - interleukin
Ile - isoleucine
IP-10 - interferon-inducible protein 10
IRF7 - interferon regulatory factor
kD - kilodalton
KDO - 2-keto-3-deoxyoctonic acid
Leu - leucine
LPS - Lipopolysaccharide
LRP - lipoprotein receptor-related protein

LRS - lymphoreticular system
LT - lymphotoxin
lysoPC a - lysophosphatidylcholine acyl
Mb - midbrain
MBM - meat and bone meal
Mdk - gene coding for midkine
MHz - mega hertz
Min - minute
moPrP - mouse recombinant PrP
moPrP^{res} – mouse recombinant resistant PrP
mqH₂O - milli-Q water
MRM - multiple reaction monitoring
mRNA - messenger ribonucleic acid
MS - multiple Sclerosis
Myd88 - gene coding for myeloid differentiation primary response gene 88
NA - not available
Ncam - neural cell adhesion molecule
NF-κB - nuclear factor-κB
NMDA - N-methyl-D-aspartate
NMR - nuclear magnetic resonance
NO - nitric oxide
NOS - nitric oxide synthase
NS - not significant
NSERC - Natural Sciences and Engineering Research Council of Canada
ODC - ornithine decarboxylase
OR - octapeptide repeat
P2 - primer and external control mix
PAMP - pathogen-associated molecular pattern
PBS - Phosphate buffered saline
PC aa - phosphatidylcholine diacyl
PC ae - phosphatidylcholine acyl-alkyl

PCR – polymerase chain reaction
PD - Parkinson's disease
PFG - pulsed-field gradient
pi - post inoculation
PK - proteinase K
PLSDA - partial least square discriminant analysis
PMCA - protein misfolding cyclic amplification
PMSF - phenylmethylsulfonyl fluoride
PNS - peripheral nervous system
POPG - phospholipid 1-palmitoyl-2-oleoylphosphatidylglycerol
PP - Peyer's patches
Prkaca - gene coding for Protein kinase, cAMP dependent, catalytic, alpha
Prnd - gene coding for prion protein 2 (duplet)
Prnp - gene coding for prion protein
Prnp^{0/+} - heterozygous for gene coding for prion protein
Prnp^{0/0} - knockout for gene coding for prion protein
PrP - prion protein
PrP^C - Cellular prion protein
PrP^{res} - Resistant prion protein
PrP^{Sc} - scrapie prion protein
qPCR - quantitative polymerase chain reaction
RDA - RNA dilution buffer
RE3 - RT enzyme mix 3
RIPA - radioimmunoprecipitation assay buffer
RLA - RNA lysis buffer
RML - Rocky Mountain Laboratory
RNA - ribonucleic acid
ROS - reactive oxygen specie
rPrP - recombinant prion protein
RT PCR - real time polymerase chain reaction
RTC - reverse transcription control

SAS - statistical analysis software
sc - subcutaneous
SCA - scrapie cell assay
SM – sphingomyeline
SM(OH) – hydroxysphingomyeline
Sprn - gene coding for shadow of prion protein
TBS - tris-buffered saline
TGF - transforming growth factor
Th - thalamus
TLR - toll-like receptor
Tlr4 - gene coding for Toll-like receptor 4
TME - transmissible mink encephalopathy
Tnf - gene coding for tumor necrosis factor
TNF - tumor necrosis factor
TSE - Transmissible spongiform encephalopathy
UK - United Kingdom
USA - United States of America
UV - ultraviolet
Val - valine
vCJD - variant Creutzfeldt-Jakob disease
Wk - week
Wild type – wt
 α 2m - alpha-2-macroglobulin

Chapter One: Literature review

1. Prion Protein

1.1. General characteristics

Prions are a unique group of proteins capable of changing conformation while keeping the same amino acid sequence (Aguzzi and Heikenwalder, 2006). The term "prion", referring to a proteinaceous and infectious particle (Prusiner, 1982), is generally used for proteins capable of aggregating into amyloids (Norrby, 2011). Their resistance to proteinase K (PK) digestion is an important characteristic that allows to further purify them (Aguzzi and Heikenwalder, 2006; Siso et al., 2009). However, PK resistance does not necessarily reflect the depth of infectivity (Soto and Castilla, 2004). Other characteristics of prions include abundance in beta sheets, resistance to high temperature and pressure, formaldehyde treatment, detergent resistance, and UV radiations (Aguzzi and Heikenwalder, 2006). They are known to be the fundamental components of prion disease (Isaacs et al., 2006).

The normal cellular form (PrP^C) is originally synthesized by the host gene, *Prnp*, containing 254 amino acids and a molecular weight of 27-30 kD. Comparison between different sequences of prion protein (PrP) of different species show great amounts of similarities highlighting the essential function of PrP preserved throughout evolution. On the other hand, slight differences in the sequence or structure could propose an idea why transmission of the disease from some species to others is not attained (Norrby, 2011). Healthy PrPs are membrane bound but perform in a non-membrane bound manner when converted into the pathogenic isoform (Norrby, 2011). PrP^C is also detergent resistant, a characteristic shared by glycosphosphatidyl inositol (GPI)-linked proteins (Aguzzi and Heikenwalder, 2006).

1.2. Structure

PrP^C, synthesized within the endoplasmic reticulum and transited through the Golgi apparatus, is a glycoprotein with a GPI anchor, which bounds it to the outer membrane of the cell (Aguzzi and Heikenwalder, 2006; Hachiya et al., 2007). It includes two sites of glycosylation at the N-terminus of the protein (Aguzzi and Heikenwalder, 2006). It is noteworthy that all molecules exerting their normal physiological function have glycosylation sites and an internal disulphide bond (Norrby, 2011).

The structure of PrP^C is similar among different epitopes whereas, some show minor differences. Mouse, human, Syrian hamster, and cattle PrP^C share common structural characteristics; an amino acid terminal tail, three α -helices that are bound by a large flexible loop to a two-stranded anti-parallel β -sheet which connects the second β -sheet to the third α -helix (Figure 1.1.; Aguzzi and Heikenwalder, 2006). A disulfide bond also binds α -helix two and three from the carboxyl terminus (Aguzzi and Heikenwalder, 2006). Predominance of large α -helix structures is evident in the cellular isoform compared to the pathogenic isoform that is highly abundant in β -sheets (Norrby, 2011). The N-terminal of PrP^C is composed of an octameric amino acid sequence repeated five times, generally referred to as octapeptide repeat region (OR) and a hydrophobic segment predicted to function as a transmembrane region (Aguzzi and Heikenwalder, 2006). It is postulated that there are two copper binding sites in the OR segment (Aguzzi and Heikenwalder, 2006). Inbetween these two sites is a hydrophilic segment referred to as the charge cluster (Aguzzi and Heikenwalder, 2006). The N-terminal is thought to be essential for modulation of prion endocytosis and transportation from the Golgi apparatus to the cell membrane (Hachiya et al., 2007).

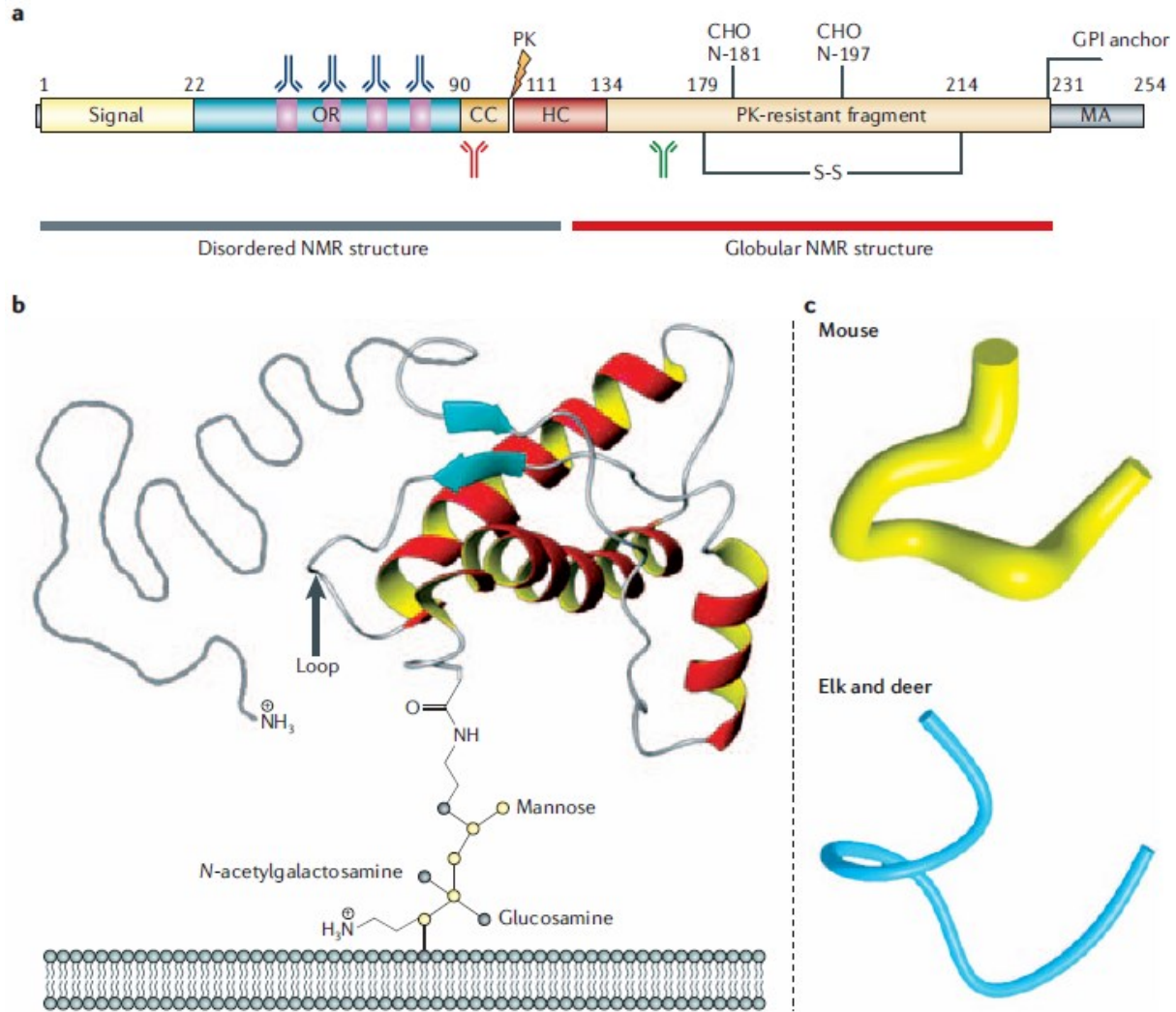


Figure 1.1. Structural features of the cellular prion protein. **a** | An outline of the primary structure of the cellular prion protein including post-translational modifications. A secretory signal peptide resides at the extreme N terminus. The numbers describe the position of the respective amino acids. CC (orange) defines the charged cluster. HC (red) defines the 'hydrophobic core'. S-S indicates the single disulfide bridge. The proteinase K (PK) resistant core of PrP^{Sc} is depicted in gold and the approximate cutting site of PK within PrP^{Sc} is indicated by the lightning symbol. MA denotes the membrane anchor region. The epitopes recognized by the POM antibodies, some of which have extremely high affinities, are also indicated. According to competition assays in solution and in surface plasmon resonance assays, POM2 (dark blue) binds to residues 58–64, 66–72, 74–80 and 82–88 (QPXXGG/SW); POM3 (red) to residues 95–100 (HNQWNK), and POM5 (green) to residues position 168–174. **b** | Tertiary structure of the cellular prion protein inserted into a lipid bilayer, as deduced from NMR spectroscopy, including the 'unstructured' N-terminal tail (grey) and the glycosyl phosphatidylinositol (GPI) anchor. The loop connecting the second β -sheet and the third α -helix is indicated by the black arrow. OR, octarepeat region. **c** | The loop region is extremely flexible in most species (for example, mouse), but it is almost entirely rigid in the prion protein of elk and deer as indicated by the average of the three dimensional space occupied during its oscillations. The figure shows amino acids 165 to 172 of the cellular prion protein of mouse, and elk and deer.

Picture from Aguzzi and Heikenwalder, 2006

Different strains of the misfolded protein obtained from different species have been reported. In vitro experiments have shown that distinct secondary structures of different strains could impose their structure onto the normal protein (Soto and Castilla, 2004; Caughey et al., 1998). Distinct incubation periods and neuropathological targeting patterns (lesion profiles) are biological properties that distinguish different epitopes (Wadsworth and Collinge, 2012; Collinge and Clarke, 2007).

1.3. Forms and functions

Some studies have focused on PrP^C expression in the central nervous system (CNS) and immune cells. PrP^C in CNS is known to be important for long-term maintenance of neuronal functions, maintaining brain cells in good condition, protecting them from overexcitement, and induction of or protection against apoptosis (Norrby, 2011; Aguzzi and Heikenwalder, 2006). It has been found that during mammalian development, PrP takes part in neurogenesis by positively regulating neural precursor proliferation (Aguzzi and Heikenwalder, 2006). Similar to neurons, PrP^C acts to maintain its role in survival, differentiation, and proliferation of astrocytes (Aguzzi and Heikenwalder, 2006; Norrby, 2011). PrP^C also interacts with glial fibrillary acidic protein in order to maintain glial cell functions. Synaptic membranes have also been found to express high levels of PrP^C (Aguzzi and Heikenwalder, 2006).

Although the role of PrP^C in the immune system is not completely understood, immune cells such as lymphocytes have been found to express this protein, taking part in immunoregulation. Reports indicate that follicular dendritic cells (FDCs) express high levels of this protein (Aguzzi and Heikenwalder, 2006). PrP^C expression also serves long-term, repopulating hematopoietic stem cells (Aguzzi and Heikenwalder, 2006).

Generally, PrP^C has been proposed to modulate signaling pathways important for cell survival, protection against oxidative stress, and binding to copper (Norrby, 2011; Aguzzi and Heikenwalder, 2006).

High titres of PrP^C have also been detected in many other tissues and organs such as the skeletal muscles, lymphoid tissues, kidney, and heart, which suggest a broad function of the protein, yet to be found (Aguzzi and Heikenwalder, 2006). Interestingly, high titres of the converted prion protein have been detected in inflamed organs such as the mammary gland at times of mastitis or the kidneys in case of nephritis.

Fatal neurodegenerative prion disease is developed by the misfolded isoform both in humans and animals (Norrby, 2011; Siso et al., 2009; Soto and Castilla, 2004). This isoform, rich in β -sheets, can aggregate within the CNS into insoluble fibrous proteins known as amyloids, consequently leading to brain degeneration (Norrby, 2011; Soto and Castilla, 2004). The infectious agent is associated with spongiform vacuolization and lesions in the brain, neural loss and apoptosis led by exaggerated activation and proliferation of microglial cells and astrocytes as well as accumulation and aggregation in the CNS (Aguzzi and Heikenwalder, 2006; Soto and Castilla, 2004).

The pathogenicity of the misfolded isoform has shown correlation with the presence and abundance of the protein in the CNS (Soto and Castilla, 2004). However, various reports have mentioned infectivity in presence of very low and undetectable amounts of PrP, whereas others reported high quantity of the hamster misfolded prion inoculated to mice showing little or no infectivity (Soto and Castilla, 2004; Hill et al., 2000). This in turn shows the possible infectiousness of the prion protein at subclinical levels in which clinical signs of the disease have

not yet manifested and the host appears to be healthy (Hill et al., 2000). Nevertheless, formation and presence of the scrapie protein is the main reason for infectivity, strain variability, species barrier, and strain adaptation (Diaz-Espinoza and Soto, 2010).

1.4. Conversion of PrP^C from α - to β -isoform

Reports indicate that prion conversion and pathogenesis is achieved by changes in the conformation of α -helices into β -sheets (Soto and Castilla, 2004). Two models have been proposed in this regard; the nucleation-polymerization model argues that in the presence of PrP^{Sc}, conversion from PrP^C to PrP^{Sc} is favored. On the other hand, the template-assistance model explains that in the absence of PrP^{Sc}, PrP^C might convert into an intermediate form and then into PrP^{Sc}. The pathogenic and also the intermediate PrPs of both models act as catalyzers in order to enhance the process of conversion, known as the snowball effect (Norrby, 2011). Conversion of the host PrP to the pathogenic isoform in both models is irreversible and results in amyloid aggregation (Norrby, 2011).

Some experiments have used physicochemical procedures in order to initiate misfolding of the recombinant prion protein in vitro (Diaz-Espinoza and Soto, 2010). However, most attempts to produce pathogenic recombinant PrP (rPrP) *de novo* have not been fully successful due to either the need of transgenic as opposed to wild type mice as the host to receive the prion inoculum or failure to create the disease with one time administration of rPrP (Diaz-Espinoza and Soto, 2010). A recent technique has been developed to convert and amplify the level of the misfolded prion isoform in a given sample known as the protein misfolding cyclic amplification (PMCA). Based on this technique small amounts of the brain homogenate of scrapie-infected animal, containing the misfolded protein and other compounds in the brain homogenate, is used

to rapidly convert large quantities of PrP^C to the pathogenic isoform (Saborio et al., 2001). The final product is then able to show similar characteristics to the pathogenic isoform, rich in β -sheets and resistant to proteinase digestion (Saborio et al., 2001).

1.5. Hypotheses about prion disease initiation and development

One of the preliminary suppositions about prion disease assumed that the key agent in disease initiation and development is a virus. This justification was made after observing long incubation periods from the time of exposure to the onset of clinical symptoms. However, further experiments showed that the pathogenic agent is resistant to heat, acetyleneimine, and UV or ionizing radiation that are all destructive for nucleic acids (Alper et al., 1967). In addition, the size of the agent was found to be smaller than a virus, a molecular weight of about 2×10^5 Da. An alternative hypothesis was introduced; the pathogenic agent was thought to be a virino, a small informational nucleic acid capsulated within a protein coat (Cho, 1976; Soto and Castilla, 2004).

The virino model explains the infectiousness of the prions in that the small genetic informational RNAs have the main role in imposing the pathogenic phenotype and initiating the disease (Dickinson and Outram, 1988). In turn, PrP^{Sc}-formed aggregates are thought to protect these noncoding nucleic acids. Purified RNAs extracted from brain-origin infectious particles are thought to be evidence in support of this model (Safar et al., 2005). Wang and colleagues in 2010 had primarily supported this idea by incubating synthetic phospholipid 1-palmitoyl-2-oleoylphosphatidylglycerol (POPG) with total RNA isolated from normal mouse liver and rPrP in the context of PMCA, generating misfolded prion proteins that could terminate in prion disease when administered to wild type mice with comparable incubation days to the naturally occurring disease. However, later on, they had modified their protocol by omitting RNA and

adding polyriboadenylic acid and running PMCA for more than 20 rounds. The resulting PrP product showed PK resistance, formed aggregates, and infected mouse neuronal CAD5 cells, similarly to the infectious particle. The common belief at this time of writing is that although there are some external factors affecting different properties of prion diseases, the infectivity is encoded within the prion protein itself (Diaz-Espinoza and Soto, 2010).

Previous studies suggested that the responsible particle for prion disease might have a non-nucleic acid origin and guesses were that it may be a protein. It was not until 1967 when a pathogenic self-replicating protein in the body was more or less argued to be the cause of prion disease (Griffith, 1967; Alper et al., 1967; Pattison and Jones, 1967). Thereafter, the proteinaceous infectious particle was named 'prion' and the 'protein-only' hypothesis came to birth (Prusiner, 1982; Soto and Castilla, 2004). Somatic cell mutations are also other pathways proposed of leading to TSE initiation (Norrby, 2011).

After administration of the infectious particle, during the incubation period, the pathogenic agent propagates and PrP^{Sc} accumulates silently in different organs. It seems that the prime target of prion accumulation and replication through most routes of inoculation involves the lymphoreticular system (LRS) including spleen, lymph nodes, Peyer's patches (PP), and tonsils prior to invading the CNS (Aguzzi and Heikenwalder, 2006; Siso et al., 2009). Translocation of the inoculated infectious particle to the secondary lymphoid organs is done by immune cells and systemic circulation. It has been shown that after oral inoculation, prions immediately replicate in the PP (Brandner et al., 1999). Intraperitoneal (i.p.) inoculation of the Rocky Mountain Laboratory (RML) prion strain has shown to infect the spleen and lymph nodes in mice within the first 4-8 weeks post inoculation (Aguzzi and Heikenwalder, 2006). Thereafter, the infectivity reaches its plateau after 6-9 weeks and is found to affect the brain approximately

4-5 months post inoculation (Büeler et al., 1993). Splenectomy before or right after prion inoculation has prolonged lifespan of the infected mice (Aguzzi and Heikenwalder, 2006). However, high titre of infectious prions in peripheral organs does not seem to be accompanied by toxicity or destructive effects (Aguzzi and Heikenwalder, 2006). From the LRS, the enteric nervous system (ENS) in the gastrointestinal tract (GIT) is the first neural tissue to be affected. Sheep inoculated orally with TSE have shown neuroinvasion of the sympathetic and parasympathetic nerves of the autonomic nervous system (ANS) (Siso et al., 2009).

In addition to the LRS, other components of the immune system are reservoirs for PrP incubation and replication. Brandner and colleagues (1999) and others (Aguzzi and Heikenwalder, 2006) have postulated that components of the immune system, including immune cells, are essential for propagation and transfer of the scrapie protein from periphery to lymphoid tissues and then to the CNS. However, it seems that the major cells hosting prion replication and accumulation in the CNS should not be able in restoring themselves, as opposed to hematopoietic cells, in order for neuroinvasion to be achieved (Kaeser et al., 2001). FDC, B and T cells, and macrophages are hematopoietic cells and the main immune cells in the periphery that host prion incubation which are involved in transport of the prion protein (Aguzzi and Heikenwalder, 2006; Brandner et al., 1999; Clarke and Kimberlin, 1984). B-cell deficient mice have been shown to prolong development of disease beyond the normal life expectancy of the animal (Brandner et al., 1999). B cells are also proposed to act as transporters of PrP from lymphoid tissues to CNS, after peripheral inoculation (Brandner et al., 1999; Aguzzi and Heikenwalder, 2006). PrP^C expression on B cells is not a requirement for its transport as they are part of the antigen presenting cells and can engulf non-self compounds (Aguzzi and Heikenwalder, 2006).

FDC on the other hand seem to meet the criteria to be the major cells in peripheral prion circulation and propagation due to their close interaction with B cells, their stromal origin in lymphoid tissues, and expression of the cellular prion protein on their cell surface (Aguzzi and Heikenwalder, 2006; Clarke and Kimberlin, 1984). Due to the contribution of B cells in FDC maturation, it is thought that interaction between these two immune cells is required in order to direct PrP^{Sc} to the autonomic nervous system. FDCs also express homeostatic chemokines such as CXCL13 to support lymphoid microarchitecture in order to maintain the structure of these tissues, contributing to prion incubation (Magliozzi et al., 2004). FDC-deficient mice have shown low prion replication within the lymph nodes (Aguzzi and Heikenwalder, 2006).

Pro-inflammatory cytokines have been recognized as essential mediators for peripheral prion contamination. One of the main cytokines contributing to FDC generation and maintenance in immunopathological conditions are lymphotoxins (LTs) (Mabbott et al., 2003). This pro-inflammatory cytokine is mainly expressed by B cells and activated T cells and is structurally related to the tumor necrosis factor (TNF) family. Therefore, B cells could be implicated for induction of chemokine and cytokine secretion, i.e. LT and TNF, leading to prion spread and replication in the stromal compartments of the lymphoid organs (Aguzzi and Heikenwalder, 2006; Mabbott et al., 2003; Fu and Chaplin, 1999). This is thought to be an indirect role of B cells, which is more important than its direct role mentioned above.

The complement system, as part of the innate immunity, is also found to have a role in prion pathogenesis although not yet clearly understood how. Experiments have shown higher resistance to peripheral prion inoculation when some complement factors such as C1q or C3 are lacking (Klein et al., 2001).

One of the conditions that favor conversion, propagation, and accumulation of the prion protein is chronic inflammation (Aguzzi and Heikenwalder, 2005). All phagocytic immune cells such as DC, FDC, macrophages, and B lymphocytes are accumulated in sites inflammaed chronically. In addition, a whole range of pro-inflammatory cytokines and chemokines are secreted with the aim of attracting more immune cells to the inflamed tissue. Up-regulation of LT and subsequent induction of FDCs expressing PrP^C would also favor prion propagation.

Organs once thought to be prion free, i.e., mammary gland, kidney, liver, and pancreas are reported to be prion infected during inflammation. Indeed, reports indicate the presence of PrP^{Sc} in mice with inflamed kidney both at subclinical and terminal scrapie. Prionuria, the state in which prions are found in urine as a consequence of kidney inflammation, has been reported in infected mice with nephritis (Seeger et al., 2005). Muscle tissue of individuals suffering from inclusion body myositis also accumulates high amounts of PrP^{Sc}. Elk and deer with chronic waste disease (CWD) are found to have their muscle tissues contaminated with the prion protein (Aguzzi and Heikenwalder, 2006). Mice suffering from hepatitis and pancreatitis have been shown to have the same pattern with regards to prion infectivity. Infected sheep with PrP^{Sc} are observed to accumulate in their mammary gland at times of mastitis (Ligios, C. et al., 2005).

Mechanism of prion contamination within the body and pathways of its translocation into the CNS has been a great issue in research. However, the mechanism of how prions are spread and transported from the periphery to the CNS and vice versa is not yet fully understood. The neuronal pathways, blood stream, and exosome formation and secretion into the extracellular environment are possible routes (Lawson et al., 2010).

The nervous system innervating the lymphoid organs is mostly the sympathetic branch of the ANS (Aguzzi and Heikenwalder, 2006). It is thought that the ENS as part of the ANS is the main route of neuroinvasion after oral inoculation of the pathogenic isoform; the dorsal motor nucleus of the vagus nerve together with the hypothalamus, are thought to be the main accumulation sites (Siso et al., 2009). Patients suffering from vCJD have shown affected sympathetic nervous system (Haik et al., 2003). Moreover, contribution between the peripheral nervous system (PNS) and immune cells has been reported in sporadic cases of prion disease (Aguzzi and Heikenwalder, 2006).

The hematogenous route is proposed as another possible way of prion transmission and circulation. The circumventricular organs (CVO), part of the brain lacking the blood brain barrier (BBB) in which brain cells are in close contact with brain parenchyma and blood circulation, are the portal of entry for the TSE agents leading to further distribution of the pathogenic isoform to the neighboring regions via the efferent connections. This proposes initial triggering of neuroinvasion from CVO prior to any other brain region through this route. In correlation to disease progression, scrapie accumulation in the CVO is increased to some extent (Siso et al., 2009).

Animals infected subcutaneously or intravenously have had similar CVO involvement compared to oral infusion or naturally occurring disease. Therefore, infection through the ENS/ANS seems not to be the only way of the TSE spread in ruminants and thought to perform parallel, if not prior to, spreading the disease. This has been shown in cows infected with BSE through oral inoculation with no signs of ENS involvement while PrP^{Sc} deposits were found in their brains. Similar observations have been made for sheep (Siso et al., 2009). Therefore, two phases are proposed for pathogen entry to the blood circulation; 1) after the uptake of the

misfolded protein from the gut lumen into the local lymphoid tissues, which seems to happen immediately, and 2) after propagation in the LRS, mainly through the secondary lymphoid tissues.

1.6. Transmissible spongiform encephalopathy

TSEs or prion diseases are fatal neurodegenerative diseases that progress independently and rapidly after the onset of clinical symptoms. They are found to happen both in humans, i.e., Kuru, CJD, Gerstmann-Straussler-Scheinker (GSS), and fatal familial insomnia (FFI), and animals, i.e., scrapie in sheep and goats, bovine spongiform encephalopathy (BSE), chronic wasting disease (CWD), transmissible mink encephalopathy (TME), and feline spongiform encephalopathy (Lawson et al., 2010).

Clinical manifestations of disease generally appear as brain injury caused by amyloid formation, neuronal loss, spongiform changes, motor dysfunction, and dementia (Lawson et al., 2010). Some clinical signs of prion invasion in mice include exaggerated weight loss, kyphosis (i.e., hunched back), head tilt, shabby and dirty hair coat, bradykinesia (slow reflex and movement), stupor (reduced responsiveness), and ataxia (i.e., poor balance). However, different strains of TSE tend to target different brain regions selectively and produce somewhat different clinical symptoms and neuropathological alterations (Soto and Castilla, 2004). This is characterized by slight difference in their conformation, protein aggregation, and incubation periods, which brings about different catalyzing ability in PrP conversion (Soto and Castilla, 2004).

1.7. TSE in humans and animals

TSE was originally found and reported in sheep in the UK more than 250 years ago (Smith and Bradley, 2003). Initial research indicates that feeding prion-contaminated animal protein supplements to cows resulted in wide spread of BSE, otherwise known as mad cow disease (Norrby, 2011; Smith and Bradley, 2003). Meat and bone meal (MBM) protein supplements were prepared by recycling offal and fallen stock of cattle, sheep, pigs, chickens, animal tissues unsuitable for human consumption, abattoir and butcher's waste (Norrby, 2011; Smith and Bradley, 2003).

By the late 1900s, massive epizootic spread of BSE in Europe lead to an astonishing estimate of more than 180,000 BSE cases with 1-3 million cases at a subclinical stage, most probably slaughtered for human consumption (Norrby, 2011; Smith and Bradley, 2003). Due to no therapeutic approach, the only way to confront disease widespread was to cull the contaminated herds (Norrby, 2011). Over the last 2 decades, more than 280,000 cases of BSE have been reported, impacting the food supply (Aguzzi and Heikenwalder, 2006). This has led to over 4 billion pounds loss in the UK alone (Smith and Bradley, 2003). Yet still, different cases of TSE are being reported even in regions once known to be prion free (Aguzzi and Heikenwalder, 2006).

Transmission of the disease to mankind through consumption of contaminated animal products raised suspicion in disease spread between different species (Norrby, 2011). More than 150 cases of variant Creutzfeldt-Jakob disease (vCJD) have been reported in recent years due to transmission from animals to humans (Aguzzi and Heikenwalder, 2006). However, previous investigations have shown that not all the infected species are able to transmit their disease to

other species; mice can only contract TSE from other mice and rodents but not from distant species (Norrby, 2011).

The first TSE reported in humans was vCJD with bovine origin in 1994 (Norrby, 2011). Kuru has been found to be the leading death cause in cannibalistic tribes of Papua New Guinea till mid twentieth century (Aguzzi and Heikenwalder, 2006; Soto and Castilla, 2004). Creutzfeldt-Jakob disease is also known to arise sporadically, due to somatic mutation or rare misfolding processes initiated in the brain (Lawson et al., 2010). In addition, as a consequence of medical procedures in humans, many cases of iatrogenic CJD (iCJD) have been reported till the late twentieth century (Aguzzi and Heikenwalder, 2006). Another form of familial TSE is also reported known as GSS syndrome (Smith and Bradley, 2003). Familial cases have been linked to genetic mutations of the corresponding gene (Soto and Castilla, 2004).

1.8. Immune response of the body to TSE

Under normal and healthy conditions the body does not generate immunological responses to its own molecules. Therefore, due to the expression of PrP by the host genes, at times of TSE development, the body does not generate any inflammatory response. It is noteworthy that the infectious PrP and the healthy isoform have identical amino acid sequences despite their differences in conformation (Norrby, 2011).

Possible therapeutic methodologies aiming the immune system have been proposed but not yet fully approved. Use of antibodies as possible prevention or curing approach, and in drug production in order to delay disease onset or reduce infectivity has been considered as one (Soto and Castilla, 2004; Peretz et al., 2001). Treatments with different antibodies such as Fab D18 and D13 in mouse neuroblastoma cell (ScN2a) media has shown to not only brake down prion

replication but also help in clearance of pre-existing PrP^{Sc} (Peretz et al., 2001). However, this process did not last long and returned to normal levels of infectivity shortly after removal of the antibodies. In vivo experiments using CD-1 Swiss mice with similar antibodies has increased incubation time, over 265 days, and the disease onset when injected i.c. (Peretz et al., 2001).

1.9. Genetics of the prion protein

Prion disease has been categorized as a post-translational disease. However, later studies not only showed that mutations in the host gene encoding for PrP can lead to cases of prion disease but also, in the process of scrapie infection many genes with diverse functions, i.e., genes related to immunity, lipid metabolism, protein synthesis, cell proliferation and etc., tend to be altered in the brain. Therefore, studying the genetic background of the prion protein and inter-related genes could bring new insights into better understanding of the protein at the genetic level.

The healthy and cellular isoform is originally synthesized by the host gene, *Prnp*, containing 254 amino acids and a molecular weight of 27-30 kD (Norrby, 2011). Purification of the prion protein led to identification of the gene encoding for this protein (Oesch et al., 1985). Studies show that the PrP mRNAs are expressed at the same level in normal and scrapie infected hamster brain and other normal organs (Oesch et al., 1985). In addition, purifications showed that there is no nucleic acid within the prion protein, which could possibly encode for the infectious agent.

However, in order for the pathogenic prion to propagate and impose its structure, the presence of host *Prnp* gene is essential to express the cellular isoform (Norrby, 2011; Lawson et al., 2010; Aguzzi and Heikenwalder, 2006; Bueler et al., 1993). The presence of PrP^C is essential

because it seems that this protein itself has the core involvement in transporting the infectivity; however, it is insufficient when only by itself (Aguzzi and Heikenwalder, 2006; Bueler et al., 1993). Knockout animals for this gene (*Prnp*^{0/0}) have been found to develop normally even after being exposed to the infectious particle (Norrby, 2011). Not only *Prnp*^{0/0} but also heterozygous *Prnp*^{0/+} mice are reported to be resistant to the pathogenic agent (Bueler et al., 1993). Genetic manipulation has also led to overcome the species barrier in transmitting the disease; introducing the Syrian hamster prion gene into a mouse line has successfully made mice sick (Bueler et al., 1993).

Many studies have recently been conducted to understand the interplay between genetic networks and their alteration during the course of a prion infection. Interestingly, different gene networks have shown to be affected due to the diseased state of the host. These include related genes to immune activation and inflammatory response, apoptosis, synaptic transmission, lipid metabolism and etc. (Sorensen et al., 2008). Interestingly, genes like apolipoprotein E are reported to be altered in prion disease, similar to other neurodegenerative diseases (Keene et al., 2011; Sorensen et al., 2008). Some of the gene categories related to neurodegenerative diseases are briefly explained below.

1.9.1. Amyloid- β generation, oligomerization, clearance, and degeneration

Amyloid- β (A β), made from A β precursor protein (APP), was first described by Glenner and Wong (1984) in Alzheimer's disease (AD) as a "purified protein derived from the twisted β -pleated sheet fibrils". Recent reports show that A β is toxic to neurons when in oligomeric form leading to fibril formation and aggregation in the brain with eventual plaque deposition (Honjo et al., 2012). Abundant presence of this protein in the brain is thought to play a major role in brain lesions associated with AD (Tanzi and Bertram, 2005). Other functions of A β in brain include

disruption of synaptic plasticity, synaptic loss, and neuronal death (Honjo et al., 2012; Tanzi and Bertram, 2005).

Currently, several genes have been reported associated with A β generation, oligomerization, clearance, and degeneration. Some induce α -secretase activity (i.e., Adam9), which leads to transduction of APP into A β formation (Sastre et al., 2008). ADAM proteinase family is a major mediator of proteolytic release of extracellular domains such as A β from their membrane bound precursors, in this case APP (Sastre et al., 2008). They are activated during the time course of inflammation leading to pro-inflammatory and neurotoxic properties via the microglia (Sastre et al., 2008).

Some genes like the apolipoprotein E (ApoE), alpha-2-macroglobulin (α 2m), and acetylcholinesterase (Ache) have also been proposed in the A β metabolism. ApoE, specifically the ϵ 4 allele, has been associated with increased A β aggregation and deposition, decreased clearance, and accumulation in the brain, which is highly correlated with AD (Keene et al., 2011). In addition to ApoE, α 2m has also been recognized as the second late onset AD gene (Kovacs, 2000). Other than promoting clearance of A β , α 2m has been associated with A β catabolism by building α 2m-proteinase complexes which binds A β to its specific binding sites in order for the proteinases to take action (Lauer et al., 2001; Kovacs, 2000). Similarly, Ache gene has been investigated to be responsible for aggregating activity of A β and promoting amyloid fibril formation (Anand et al., 2012).

1.9.2. Synaptic functions

Ache gene is also known to promote hydrolysis and reduction of acetylcholine at the synaptic level and termination of synaptic transmission as part of cholinergic signaling (Anand et

al., 2012; Zimmerman and Sorreq, 2006). Adding to its catalytic function, Ache-homologous domains have been found to take part in facilitating synaptic formation and maturation with declining expression levels of Ache as synaptogenesis occurs (Dong et al., 2004). In addition, ApoE is involved in maintaining synaptic connections, synaptogenesis, membrane repair and synaptic plasticity by releasing lipids and cholesterol from ApoE-containing lipoproteins in the CNS, specifically at times of neuronal injury and repair (Kim et al., 2009). Neural cell adhesion molecule 1 (Ncam1) is another gene belonging to the NCAM family, which has a role in synaptogenesis and synaptic plasticity by mediating cell-cell and cell-extracellular Ca^{2+} -dependent matrix interactions (Senkova et al., 2012).

1.9.3. CD molecules

Genes expressing various Toll-like receptors (TLRs) are one of the categories of the CD molecule family. TLRs are one of the many pattern recognition receptors of the innate immunity with specific recognition to a range of pathogen-associated molecular patterns (PAMPs). Nine different functional varieties of TLRs in humans localized on the cellular surface or within cellular compartments have been reported which are able to detect bacterial and viral antigens (Iwasaki and Medzhitov, 2004). Following a contact and recognition of PAMPs, TLRs signal the presence of infection to the host (Bradford and Mabbott, 2012). TLR signaling triggers the host immune response by mobilizing immune cells to inspect, attack and clear the invading pathogens, and activating the adaptive immunity (Iwasaki and Medzhitov, 2004). TLR activation and signaling, specifically TLR4, has shown to interfere with prion infection capable of activating innate immune responses to suppress scrapie infection (Spinner et al., 2008).

1.9.4. Endogenous and chemokine ligands

A range of genes regulating the expression of pro-inflammatory chemokines are a subset of these two categories. Chemokines are a resultant product of inflammatory conditions expressed by immune cells of the host such as microglia and astrocytes in the brain. Presence of microglia and their chronic activation during the course of a neurodegenerative disease is found to be detrimental and a requirement for neuronal cell death. In this context, pro-inflammatory chemokines play a vital role by triggering the migration and activation of immune cells, such as glial cells, astrocytes, and T-cells, towards the damaged region, induction of neuronal cytotoxicity, and enhancement of gliosis (Burwinkel et al., 2004). Chemokine expressing genes have been reported to be strongly up-regulated in the brains of scrapie-infected animals (Burwinkel et al., 2004).

1.9.5. Complement system

The complement system is part of the innate immunity recognizing and confronting the pathogens. Prion diseases seem to take advantage of this family by altered activation to facilitate infection in the lymphoid organs and the brain (Mabbott, 2004). Activated gene products of this category opsonize pathogens, lyse infected cells and induce pro-inflammatory responses by immune cells including brain glial cells. Chronic uncontrolled activation of this innate immune defense mechanism, as a response to sustained brain inflammation, managed by brain astrocytes, microglia, and neurons have been associated with various neurodegenerative diseases (Bonifati and Kishore, 2007). Prion infected animals have been reported with active complement components in their brain tissues (Mabbott, 2004). For instance C3 complement protein, converged in both classical and alternative pathways of complement activation, seems to play an

important role in localization of PrP to FDCs, whereas lack of this component has prolonged the survival times of the experimental animals (Mabbott, 2004). Also, scrapie infected rodents have been reported with increased level of mRNA specific for C1q complement component (Riemer et al., 2000).

1.9.6. Immunoglobulin-like domain containing

It has long been believed that there is no specific humoral response from the host to the presence of PrP^{Sc} in the body. Since the first PrP^{Sc}-specific antibody production by Korth and colleagues (1997) much has been learned about prion-specific antibody production and functions; however, there is no effective definitive antemortem diagnostic tool developed presently. Expressing genes responsible for the production of immunoglobulin G (IgG) are highly of interest due to their high affinity for the prion protein and smaller molecular size as compared to IgM (Alrey and Cashman, 2013; Tayebi et al., 2009). Anti-PrP IgM antibody response; however, has been reported to be induced in wild type mice when injected with a native PrP^{Sc}-containing vaccine (Tayebi et al., 2009).

Genes expressing NCAM are also categorized in this group with contribution to many neural functions and development such as synaptic plasticity and binding to various molecules such as to PrP^C in lipid rafts (Gnanapavan and Giovannoni, 2013). Altered NCAM levels in the brain has been reported to lead to pathology to the extent that NCAM null mice are reported to develop prion disease when injected with RML prions (Gnanapavan and Giovannoni, 2013; Schmitt-Ulms et al., 2001). Prion misfolding is thought to destabilize NCAM-PrP^C complexes which perturbs one of many NCAM functions and neuritogenesis (Gnanapavan and Giovannoni, 2013).

1.9.7. Tumor necrosis factor (ligand) superfamily

Tumor necrosis factor (TNF) is one of the many cytokines produced in the body with quite a role in neurodegeneration. Up-regulation of TNF has been correlated with incidence of various neurodegenerative disorders such as Parkinson's and Alzheimer's disease (PD and AD; Fontaine et al, 2002; Mabbott et al., 2000). At times of scrapie infection however, TNF levels are increasingly expressed from glia cell in the brain (Sakudo et al., 2003). TNF null mice have lower susceptibility to peripheral scrapie challenge as compared to the controls with failure in accumulating infectious PrP in their spleen (Mabbott et al., 2000). TNF also tends to show biphasic behavior inducing both apoptosis in cells and exerting neuroprotective behaviors (Sakudo et al., 2003). Being a cytokine, TNF is excreted as a signaling molecule as means of communication between immune agents specifically FDCs (Mabbott et al., 2000).

1.9.8. Interleukins and interleukin receptors

Interleukins (ILs) are a large class of cytokines highly active in the body at times of immune alterations. Pro-inflammatory ILs share a lot in common with the TNF family, described above, in evoking further inflammatory responses in the host to deal with the infection (Kawanokuchi et al., 2008). Activation of these pro-inflammatory genes, specifically in the nervous system, has been closely correlated with generation of neurodegenerative diseases, i.e., increased production of IL-1 β , IL-6, and IL-8, and has been associated with PD (Träger and Tabrizi, 2013). Intraperitoneal challenge with LPS using a mice model of prion disease has similarly shown increased levels of cytokine activity, including IL-1 α and IL-1 β , leading to exaggerated impairment of neural functions (Cunningham et al., 2009). Peripheral alterations in

blood cytokines such as the ILs family have provided potential biomarker candidates in new therapeutic approaches (Träger and Tabrizi, 2013).

1.9.9. Methods and mechanisms of transmission

One of the main and original routes of prion entrance is through oral inoculation being transmitted via the digestive tract (Siso et al., 2009; Smith and Bradley, 2003). This route has been challenged experimentally in many species and found to be successful in transmitting PrP^{Sc} (Smith and Bradley, 2003). The oral route is thought to lead to prion infection after translocation from the GIT to the local lymphoid tissues including the PP. Thus, involvement of the ENS and blood contamination would subsequently take place (Siso et al., 2009).

The intestine is known to perform an important role in prion transmission. Prion infectivity has been observed in the distal ileum early after oral inoculation (Aguzzi and Heikenwalder, 2006). The PP has shown to subsequently accumulate high titers of PrP^{Sc} (Aguzzi and Heikenwalder, 2006). M cells located in the intestinal wall, as part of the local lymphoid aggregates, are possible portal of entrance for this protein (Aguzzi and Heikenwalder, 2006). In association with M cells, neighboring immune cells present for antigen sampling such as DC could serve as means to translocate the prion from the lumen into the lymphoid tissues (Aguzzi and Heikenwalder, 2006). Oral ingestion of PrP^{Sc} is thought to lead to neuroinvasion through gut associated lymphoid tissues (GALT) and the autonomic nervous system (ANS), especially the enteric nervous system (ENS) (Lawson et al., 2010; Aguzzi and Heikenwalder, 2006). On the other hand, contaminated GIT possesses high risk of disease transmission and environmental TSE contamination through feces (Lawson et al., 2010).

Intraperitoneal inoculation is another route for prion transmission. This route is proposed to be closely related to prion expansion through the LRS (Klein et al., 1997). B lymphocytes have been reported to be most effective in prion i.p. expansion to an extent that mutations disrupting B cell differentiation and response prolonged the onset or prevented clinical development of scrapie in immune-deficient mice (Klein et al., 1997). This may be due to lymphocytes themselves transporting the prions to the nervous system or their corresponding antibodies. Their close contact with FDC, which is needed for the process of FDC maturation and formation of germinal centers could also be another reason (Klein et al., 1997). As mentioned previously, FDC are major sites of PrP^C expression. They can accumulate high quantities of PrP^{Sc} and have been found to transfer them to tonsils in cases with vCJD (Klein et al., 1997).

The hematogenous route has been introduced as a way of prion propagation. Infectivity is found in the blood of infected sheep and humans leading to human-to-human transmission of prion disease due to contaminated blood transfusion (Aguzzi and Heikenwalder, 2006). Protein aggregate deposits of PrP^{Sc} have been found in hypothalamus capillaries in sheep. Blood analyses have revealed presence of scrapie after oral inoculation (Siso et al., 2009). Blood transmission from preclinically infected animals that had shown no or very little PrP^{Sc} deposits in their brain to healthy animals has shown to be infectious (Siso et al., 2009). As a result of infectivity circulation, not only the lymphoid tissues but also other organs such as kidney, placenta, salivary and mammary glands have been found to be infected from scrapie. Intravenous (i.v.) injection of the scrapie has also shown the highest prion deposition in the CVO compared to other routes (Siso et al., 2009).

Intracerebral (i.c.) infection is also a means of experimentally infecting the animals with TSE. When injected i.c., the prion would start its replication from the site of administration. It could then be spread to the cerebrospinal fluid in which through the dural venous sinuses or regional lymphoid tissues through the cribriform plate could lead its way into the blood and circulate back into the brain (Siso et al., 2009). Delivering prions directly to the CNS through i.c. injections seems to infect the brain without detectable influence on the immune status of the host (Klein et al., 1997).

Astrocytes and enteric glial cells are thought to be the primary target cells for prion invasion after i.c. injection. Subsequently, neural injury occurs due to the loss of glial cell support. In this transmission method other peripheral organs such as the spleen and muscles have been found to be contaminated with PrP^{Sc}. Interestingly, i.c. injection of the infectious prion agent has proven to be associated with protein contamination in the intestine. It has been remarked that after translocation of the pathogenic protein through neurons from the brain to the gut, the PP serve as a reservoir for PrP^{Sc} accumulation and propagation (Lawson et al., 2010; Aguzzi and Heikenwalder, 2006).

Subcutaneous (sc) inoculation of the prion protein has been reported to lead to neurodegeneration through dorsal motor nucleus of the vagus nerve, similar to orally infected animals. In sheep, accumulation of the agent in the ENS has also been reported (Siso et al., 2009). In addition, sc injection of the infectious agent seems to invade the local lymphatics and/or blood vessels thereby, getting into the blood circulation. However, the sc and i.v. routes seem to be less effective compared to the oral or naturally infected routes in sheep to generate PrP^{Sc} aggregates (Siso et al., 2009).

1.10. Cofactors in prion disease

As studies continue and new findings emerge, more evidence is being found showing that the process of prion misfolding and pathogenesis is mediated by other factors found with an endogenous or exogenous source. This context proposes the propagation of disease-associated isoforms in the absence of pre-existing prions (Deleault et al., 2007). Some have mentioned that presence of PrP^C is essential for prion replication, but not sufficient (Aguzzi and Heikenwalder, 2006). Different cofactors have been reported to facilitate conversion of the healthy to the pathogenic isoform of PrP in vitro or de novo (Caughey and Baron, 2006; Wang et al., 2011; Hachiya et al., 2007).

Hachiya and colleagues (2007) proposed a possible role for a ‘protein X’ in changing the conformation of PrP^C when accompanied by this protein. As a result, an intermediate form of the protein, referred to as PrP^{*}, is made which finally converts to PrP^{Sc} with a subsequent release of protein X.

Polyanionic compounds are other proposed cofactors in prion conversion (Wang et al., 2010; Deleault et al., 2007). Small noncoding RNAs had once been reported as a potential catalyzers promoting de novo prion formation (Wang et al., 2010; Deleault et al., 2007). It was originally proposed that small RNAs dictate the pathogenic phenotype of the protein on the host PrP, not as a coding factor for the pathogenic protein but rather a facilitator in the process of conversion, and in return, formed PrP^{Sc} aggregates will serve as a protective shield for the genetic informational nucleic acid. Wang and colleagues (2010 and 2011) extracted RNA from mice liver and incubated it with PrP^C using PMCA resulting in prion conversion. However, later reports show that genetic informational RNA is not a necessity for conversion of endogenous PrP

to the misfolded pathogenic form (Wang et al., 2011). Further purification showed that these infectious agents lack a nucleic acid and have a proteinaceous structure (Norrby, 2011).

Due to the GPI-anchored property of PrP^C which attaches it to the lipid membrane of host cells, it is thought that the interfacial lipid bilayer region of the cells may have possible facilitating effects on misfolding PrP (Wang et al., 2010; White et al., 2001). To test this hypothesis, a synthetic anionic phospholipid, POPG, was incubated with PrP^C using PMCA. The final product showed similar characteristics to PrP^{Sc}, C-terminal PK-resistant core able to form aggregates. This had been accompanied with and without small RNAs, which showed similar results in both cases. The final PMCA products were tested in murine neuronal cells susceptible to prion infections, SN56 cells, and injected i.c. in wild type mice which terminated in prion disease. Terminal phenotypic behavior and pathology induced by the recombinant (r)PrP were different of those from the RML infected mice (Wang et al., 2010).

Other mutant PrP-like molecules that show many biochemical properties of the pathogenic isoform have been produced but none of them were able to infect the host when inoculated to a healthy animal (Diaz-Espinoza and Soto, 2010).

2. Lipopolysaccharide

Many bacterial populations co-exist within different parts of the body. Those bacteria are referred to as commensal bacteria which, under normal conditions, do not harm the body. Their presence is very essential, specifically for the digestive tract, for proper function of biological and biochemical processes, i.e., food digestion in the digestive tract (Van Amersfoort et al., 2003).

However, if pathogenic or commensal bacteria or their constituents breach through the barriers of the body, the immune system will be alerted and activated in order to combat the infection and eradicate the microbes (Van Amersfoort et al., 2003). Normally, this immune feedback is not so fierce to lead to any self-damage.

Discovery of LPS lays back in the late 1800s when a heat-stable toxin was synthesized by *Vibrio Cholera* (Van Amersfoort et al., 2003).

2.1. Structure

LPS is the main component of the outer layer of all Gram-negative bacterial cell-wall membranes (Van Amersfoort et al., 2003). They are the only lipid constituent in the outer leaflet of bacterial membrane comprising for almost all the outer layer surface of the membrane (Van Amersfoort et al., 2003). Other bacterial cell-wall constituents such as glycerolphospholipids and proteins are associated with the LPS molecules (Van Amersfoort et al., 2003).

There are four parts to the LPS molecule; lipid A, inner core, outer core, and O antigen. The most essential and critical part of this molecule is the linked lipid component known as lipid A (Van Amersfoort et al., 2003). It contains two phosphorylated glucosamine sugars with six or more fatty acid residues linked to it (Van Amersfoort et al., 2003). Of these fatty acids, four are hydroxylated on their third carbon and two of them do not have hydroxyl groups (Van Amersfoort et al., 2003). Variation in the lipid A brings uniqueness to LPS which lies in: 1) acylation patterns which are mostly asymmetric and some with symmetric configurations, 2) length of fatty acids which is an average of 14 carbon atoms however, can vary between 10 to 16 carbon atoms in three or four of its different fatty acids, 3) presence of 4-amino-deoxy-L-arabinose and/or phosphoethanolamine which is bound to the phosphor groups of glucosamine

sugars, and 4) the amount of fatty acids present which is commonly observed to be six (Van Amersfoort et al., 2003). Lipid A is found to be the toxic moiety of LPS, alerting the host immunity (Van Amersfoort et al., 2003).

The inner core of LPS consists of two or more 2-keto-3-deoxyoctonic acid (KDO) sugars (Van Amersfoort et al., 2003). From one side, it is bound to the glucosamine of lipid A and from the other it is linked to two or three heptose (L-glycerol-D-manno-heptose) sugars (Van Amersfoort et al., 2003).

The outer core is more variable compared to the inner core (Van Amersfoort et al., 2003). It is consisted of three sugars that could have side chains of one or more other sugars (Van Amersfoort et al., 2003).

The fourth part of LPS molecule is called O antigen. It is considered as the immunogenic component of the LPS molecule, which is attached to the terminal sugar of the outer core from one side and free from the other, extending from the bacterial surface (Van Amersfoort et al., 2003). It consists of repeated units of sugars (Van Amersfoort et al., 2003). These units can vary from 0 to 40 whereas more commonly, 20 to 40 repeating units make the O antigen segment (Van Amersfoort et al., 2003). Numerous interspecies and interstrain variations have been reported from this part with regards to its length and composition (Van Amersfoort et al., 2003).

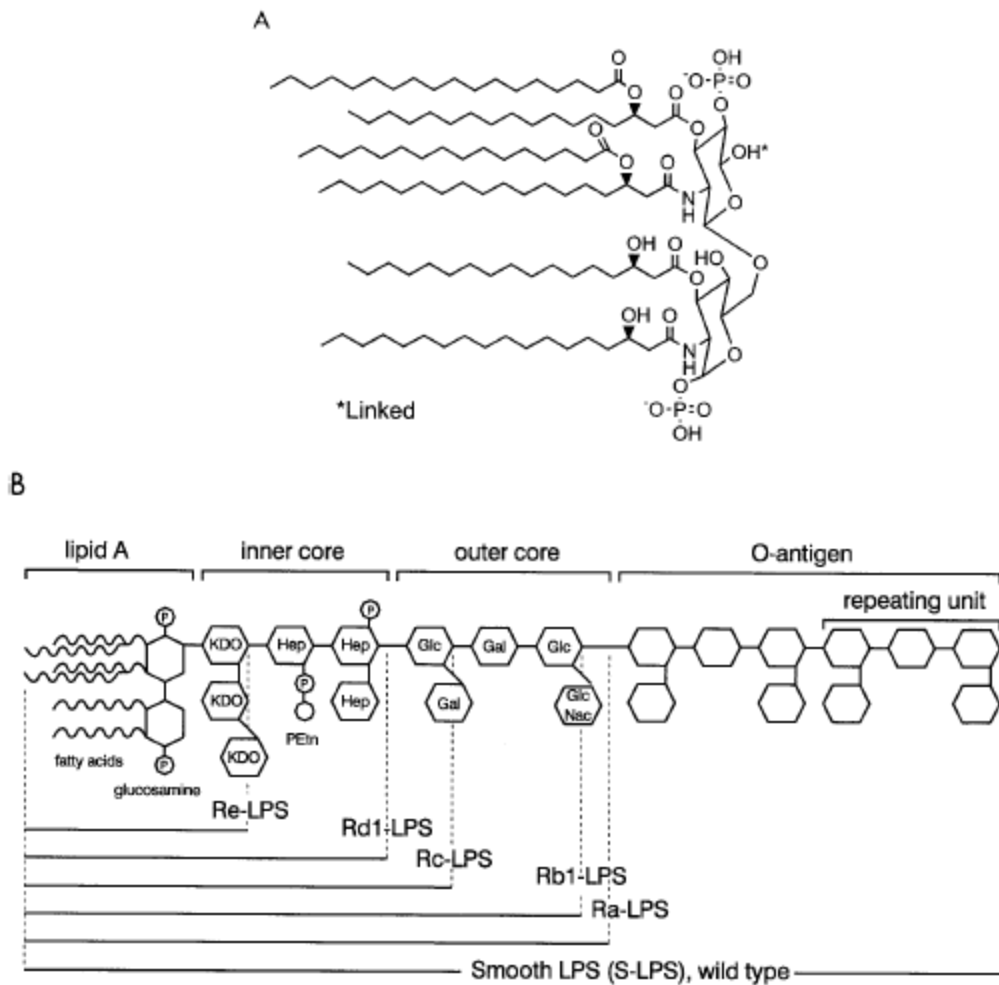


Figure 1.2. Structure of lipid A (443) (A) and whole LPS (B). The composition and length of several LPS serotypes are indicated.

Picture from Van Amersfoort et al., 2003

2.2. Function

LPS has been proven to be crucial for the normal functionality, stability, growth, and viability of Gram-negative bacteria (GNB) (Van Amersfoort et al., 2003). Interestingly enough, LPS as part of bacterial membrane is found not to be toxic; however, when released from the cell-wall membrane, it acts as a toxic agent evoking the host immune system and subsequent inflammatory responses (Van Amersfoort et al., 2003). The toxicity of LPS however, derives

from its lipid A component (Van Amersfoort et al., 2003). LPS is mainly released at times of bacterial death, lysis, or bacterial multiplication (Van Amersfoort et al., 2003).

LPS has the ability to form aggregates when in solution because of its hydrophobic and hydrophilic segments (Van Amersfoort et al., 2003). Due to many acyl residues in the lipid A, they can form micellar structures (Van Amersfoort et al., 2003). Based on temperature and ionic strength of each LPS serotype their shape can vary from lamellar to cubic and/or hexagonal micellar structures (Van Amersfoort et al., 2003). Interestingly, the endotoxic activity of each LPS serotype is related to its micellar structure and fluidity (Van Amersfoort et al., 2003).

2.3. General impact on the body

In the body, generally as a result of any injury to the host or harmful stimuli such as LPS, a non-specific immune response accompanied by a change in the surrounding vascular tissues is delivered; this is known as the state of inflammation (Ferrero-Miliani et al., 2007). The host inflammatory response, as part of the innate immune mechanism, is a protective attempt to fight back the leading reason of inflammation and furthermore, initiate the healing process (Wyss-Coray and Mucke, 2002). Interestingly, inflammation induced in the periphery affects the CNS and leads to what is known as neuroinflammation (Lee et al., 2008). Neuroinflammation on the other hand is the inflammatory response occurring within the CNS mediated mostly by resident immune cells. When the source of neuro/inflammation, in this case LPS, is constantly introduced, chronic inflammation takes place. Chronic and also cases of acute neuro/inflammation have been reported to lead to deleterious consequences such as neurodegenerative or peripheral disorders (Block et al., 2005).

Breaching of commensal or pathogenic bacteria or their constituents, such as LPS, through the barriers of the body would be detected as non-self particles which give rise to a series of immune responses in the host (Van Amersfoort et al., 2003). This includes an array of inflammatory responses such as release of cytokines and chemokines, prostaglandins and lipid mediators, and other inflammatory mediators (Van Amersfoort et al., 2003). It is believed that immune cells resident in the submucosal layers of the gastrointestinal tract are being continuously exposed to LPS, after its translocation through the mucosal layer (Van Amersfoort et al., 2003). Indeed, continuous challenge of the immune system with small quantities of bacterial constituents has been found to keep the immune system activated in responding to infections over time, in healthy individuals (Van Amersfoort et al., 2003).

LPS entering the body initiates both the humoral and cell-mediated immune response in the periphery (Van Amersfoort et al., 2003). As part of the humoral defense mechanism, the complement system is activated through both the classical and alternative pathways (Van Amersfoort et al., 2003; Amor et al., 2010). The complement component factors opsonize LPS to promote phagocytosis conducted by macrophages, form membrane attack complexes, and are chemoattractive and vasoactive (Amor et al., 2010). Acute phase response (APR) is another part of the humoral response activating production of acute phase proteins (Aps) from liver parenchymal cells with the aim of regaining the lost homeostasis (Cunningham et al., 2005; De Pablos et al., 2011). Aps production is stimulated by pro-inflammatory cytokines, i.e., TNF- α , IL-1 & 6, to encounter pathogens, neutralize proteases, opsonize and clear debris, and as part of the APR, assist the inflammatory response to re-maintain host homeostasis (Cunningham et al., 2005).

The cellular response to the presence of LPS in the body comprises of majorly the polymorphonuclear leukocytes and phagocytic cells (Amor et al., 2010). These cells commonly detect LPS by their specific pathogen recognition receptor, TLR 4 (Van Amersfoort et al., 2003; Okun et al., 2009; Amor et al., 2010). As a result of LPS recognition, a wide range of pro-inflammatory molecules including but not limited to cytokines and microbicidal agents are produced (Combs et al., 2001). The inflammatory mediators produced and secreted through various routes are potentially seeking to alert the host for effective action to be taken. In addition, resident macrophages of the liver, Kupffer cells, play a major role in LPS detoxification and clearance from the blood (Van Amersfoort et al., 2003; Amor et al., 2010).

LPS activated immune cells produce, store and secrete a wide range of inflammatory mediators such as cytokines, microbicides and free radicals (Amor et al., 2010). These inflammatory mediators potentially seek in altering and further regulating the host's immune system to take effective actions against the unwanted particle. Exacerbation or long term production of these mediators, i.e., during chronic inflammation, tends to be destructive rather than constructive. The ongoing battle between the host and the injurious process provides fertile ground for tissue destruction and resultant chronic inflammation (Wyss-Coray and Mucke, 2002). Chronic inflammation is determined by the intensity and depth of tissue based monocytic phagocyte activity, i.e., microglia in the brain, referred to as autotoxicity (McGeer and McGeer, 2004). As a result of over production of these mediators, the brain, once thought to be immune privileged, is affected and responds by inducing neuroinflammation (Frank-Cannon et al., 2009; Nguyen et al., 2002).

As a consequence of neuroinflammation, a whole range of inflammatory cytokines, such as IL-1 β , IL-6, TNF- α , and also transforming growth factor (TGF)- β are produced and secreted

(Lee et al., 2008). These factors are known to increase expression of amyloid precursor protein and up-regulate transcription of β -secretase mRNA, protein, and enzymatic activity (Lee et al., 2008). Therefore, production of cerebral amyloid proteins is thought to be majorly up-regulated at times of neuroinflammation (Lee et al., 2008). Formation of amyloid aggregates has been observed in many neurodegenerative diseases such as AD and TSEs (Lee et al., 2008). In addition, various neurotoxic factors secreted at times of neuroinflammation have been observed to lead to neurological disorders specifically at times of chronic inflammation (Nguyen et al., 2002; Wyss-Coray and Mucke, 2002).

2.4. Influence on prion disease

Presence of systemic inflammation at the times of neurodegenerative diseases increases circulatory pro-inflammatory cytokines in the host therefore, negatively influencing the CNS and worsening disease efficacy (Lee et al., 2008). Peripheral inflammation has shown direct and indirect correlation in activating a proportional immune response, mainly by activating microglial cells, in the CNS. It has been proposed that LPS can affect neurons in both a direct and/or indirect way; affecting the neurons directly through their receptors such as toll like receptors and/or stimulating microglia cells and astrocytes (Lee et al., 2008). Microglia cells and astrocytes are responsible to regulate the surrounding environment of neurons (Lee et al., 2008). By causing inflammation and production of subsequent inflammatory products, LPS promotes amyloidogenesis both in vitro and in vivo (Lee et al., 2008). LPS has also been found to promote neural apoptosis in the brain. LPS treated animals were found to have significant increase in apoptotic cells in hippocampus (Lee et al., 2008). This could be one of the impacts of amyloidogenesis after incidence of neuroinflammation (Lee et al., 2008). In addition, activated

astrocytes and induced cytotoxic cytokines in the surrounding neural environment can also be one of the reasons leading to neural death (Lee et al., 2008).

Microglia are resident macrophages in the brain belonging to the innate immune system which actively monitor their microenvironment. Any excess change in their surrounding homeostasis can activate them resulting in production of cytotoxic factors, i.e., superoxide, nitric oxide, and further production of pro-inflammatory cytokines such as TNF- α (Combs et al., 2001). In case of additional inflammatory stimuli, microglia tend to become persistently activated with exaggerated and prolonged pro-inflammatory response that could lead to neurotoxicity and neuronal damage even after the stimulus is removed (Qin et al., 2007). Consequently, neuronal damage creates a positive feedback loop that will lead to further microglial pro-inflammatory response, resultant progressive inflammation and cumulative neuronal loss over time (Block and Hong, 2005). The number of activated microglia tends to increase 10-20 fold in neurodegenerative disorders such as prion disease (Perry et al., 2007). As a consequence, many regions of the brain including the dopaminergic neurons are damaged over time (Gao et al., 2002).

Microglia seem to have a central role in inducing an inflammatory state in the brain during the course of chronic neuroinflammation and neurodegeneration. Interestingly, microglia are primed in most neurodegenerative diseases, including prion diseases, in robustly responding to peripheral or central inflammatory challenges (Murray et al., 2011). Peripheral administration of LPS has shown to activate microglia in several regions of the brain including the substantia nigra, hippocampus, and the cortex increasing the chance of neural degeneration (Qin et al., 2007). Activation of microglia and their synthesis of pro-inflammatory cytokines, most importantly TNF- α , could result in reactive microgliosis causing additional release of pro-

inflammatory factors and beginning of a self-propelling vicious cycle leading to further neuronal damage (Qin et al., 2007). Microglia exhibiting anti-inflammatory behaviors in the context of prion diseased animal models have shown to switch to producing increased levels of pro-inflammatory cytokine mRNA such as IL-1 β , TNF- α , and IL-6, leading to apoptosis and exaggerated sickness behaviors after peripheral LPS stimulation (Combrinck et al., 2002; Perry et al., 2007). Intracerebral challenge with LPS in prion infected animals has also shown to produce detectable levels of microglial neurotoxic factor, inducible nitric-oxide synthase (Cunningham et al., 2005a).

Overall although much is known about the etiopathogenesis of prion disease our understanding of the causes of prion misfolding and the factors involved are far from clear. Multiple labs have confirmed the protein only hypothesis by causing prion disease administering de novo generated prions in vitro. However, all the infectious PrP^{res} strains have been generated using a mixture of lipids, RNA, and multiple cycles of treatments with sonication PMCA protocols. None of these co-factors injected alone i.c. have not been reported to cause prion disease. Therefore, the search for the ‘golden’ co-factor that would be able to induce prion disease if administered to the host by itself continues. Recently we reported that incubation of LPS with mouse recombinant PrP (moPrP) induces conversion of moPrP into a proteinase K resistant isomer (moPrP^{res}) (Ametaj et al., 2010). In this research investigation we are testing whether this newly de novo generated moPrP^{res} is able to cause prion disease in experimental murine animals with the following hypotheses and objectives.

3. Hypotheses

This project was conducted with the aim of addressing the following hypotheses: 1) LPS-converted moPrP^{res} can exhibit infectivity and pathogenicity when inoculated subcutaneously

(sc) to a murine model; 2) Chronic subcutaneous administration of bacterial LPS (*Escherichia coli* 0111:B4) can by itself induce prion infectivity and pathogenicity using a murine model; 3) Chronic subcutaneous administration of bacterial LPS (*E. coli* 0111:B4) accompanied with one time sc injection of RML or moPrP^{res} aggravates prion pathogenicity and infectivity using a murine model; 4) moPrP^{res} and chronic subcutaneous administration of bacterial LPS (*E. coli* 0111:B4) would alter gene expression profiling when inoculated to murine models; 5) Urine metabolic profile of the murine models infected with subcutaneous RML and/or LPS (in a chronic manner)+RML is altered in a longitudinal manner over different time points.

4. Objectives

The objectives of this study were to: 1) evaluate the infectivity and pathogenicity of LPS-converted mouse (mo)PrP^{res} inoculated sc to FVB/N female mice; 2) test the potential role of LPS from *E. coli* 0111:B4 in brain neurodegeneration by chronically administering bacterial LPS sc in a murine model; 3) assess whether LPS would aggravate of prion pathogenicity and infectivity by chronically administering bacterial LPS (*E. coli* 0111:B4) sc and accompanied with one time sc injection of RML or moPrP^{res} using a murine model; 4) determine alterations in gene expression profiling of LPS and LPS-converted mouse moPrP^{res} treatment groups together with groups receiving chronic sc administration of bacterial LPS (*E. coli* 0111:B4) using a murine model; 5) analyze alterations in the urine and serum metabolic profile of murine models infected with sc administration of RML and/or chronic sc RML+LPS in a longitudinal manner over different time points by metabolomics technologies.

References

1. Aguzzi, A., and M., Heikenwalder, 2005, Prions, cytokines, and chemokines: a meeting in lymphoid organs, *Immunity*, Volume 22, p. 145–154.
2. Aguzzi A., and M., Heikenwalder, 2006, Pathogenesis of prion diseases: current status and future outlook, *Nature Reviews, Microbiology*, Volume 4, p. 765-775.
3. Airey, T. D., and N. R., Cashman, 2013, The Tyr-Tyr-Arg Prion-Specific Epitope: Update and Context, *Prions and Diseases: Volume 2, Animals, Humans and the Environment*, Chapter 15.
4. Alper, T., W. A., Cramp, D. A., Haig, and M. C., Clarke, 1967, Does the agent of scrapie replicate without nucleic acid?, *Nature*, Volume 214, p. 764–766.
5. Ametaj, B. N., F., Saleem, V., Semenchenko, C., Sobsey, and D. S., Wishart, 2010, Lipopolysaccharide interacts with prion protein and catalytically converts it into a protein resistant β -sheet-rich isoform, *Prion Congress, Salzburg, Austria*.
6. Amor, S., F., Puentes, D., Baker, and P., van der Valk, 2010, Inflammation in neurodegenerative diseases, *Immunology*, volume 129, p. 154-169.
7. Anand, P., B., Singh, and N., Singh, 2012, A review on coumarins as acetylcholinesterase inhibitors for Alzheimer's disease, *Bioorganic & Medicinal Chemistry*, Volume 20, p. 1175–1180.
8. Block, M. L., and J. S., Hong, 2005, Microglia and inflammation-mediated neurodegeneration: Multiple triggers with a common mechanism, *Progress in Neurobiology*, Volume 76, p. 77–98.
9. Bonifati, D. M., and U., Kishore, 2007, Role of complement in neurodegeneration and neuroinflammation, *Molecular Immunology*, Volume 44, p. 999–1010.

10. Bradford, B. M., and N. A., Mabbott, 2012, Prion Disease and the Innate Immune System, *Viruses*, Volume 4, p. 3389-3419.
11. Brandner, S., M. A., Klein, and A., Aguzzi, 1999, A crucial role for B cells in neuroinvasive scrapie, *Transfusion Clinique et Biologique*, Volume 6, p. 17-23.
12. Bueler, H., A., Aguzzi, A., Sailer, R. A., Greiner, P., Authenried, M., Aguet, and C., Weissmann, 1993, Mice devoid of PrP are resistant to Scrapie, *Cell*, Volume 73, p. 1339–1347.
13. Burwinkel, M., C., Riemer, A., Schwarz, J., Schultz, S., Neidhold, T., Bamme, and M., Baier, 2004, Role of cytokines and chemokines in prion infections of the central nervous system, *International Journal of Developmental Neuroscience*, Volume 22, p. 497–505.
14. Caughey, B., G. J., Raymond, and R. A., Bessen, 1998, Strain-dependent Differences in β -Sheet Conformations of Abnormal Prion Protein, *The Journal of Biological Chemistry*, Volume 273, p. 32230-32235.
15. Caughey, B., and G. S., Baron, 2006, Prions and their partners in crime, *Nature*, Volume 443, p. 803-810.
16. Cho, H. J., 1976, Is the scrapie agent a virus?, *Nature*, Volume 262, p. 411–412.
17. Clarke, M. C., and R. H., Kimberlin, 1984, Pathogenesis of mouse scrapie: distribution of agent in the pulp and stroma of infected spleens, *Veterinary Microbiology*, Volume 9, p. 215–225.
18. Collinge, J., and A. R., Clarke, 2007, A General Model of Prion Strains and Their Pathogenicity, *Science*, Volume 318, p. 930-936.

19. Combrinck, M. I., V. H., Perry, and C., Cunningham, 2002, Peripheral infection evokes exaggerated sickness behavior in pre-clinical murine prion disease, *Neuroscience*, Volume 112, p. 7–11.
20. Combs, C. K., J. C., Karlo, S. C., Kao, and G. E., Landreth, 2001, β -Amyloid stimulation of microglia and monocytes results in TNF α -dependent expression of inducible nitric oxide synthase and neuronal apoptosis, *Journal of Neuroscience*, Volume 21, p. 1179–1188.
21. Cunningham, C., D. C., Wilcockson, D., Boche, and V. H., Perry, 2005, Comparison of inflammatory and acute phase responses in the brain and peripheral organs of the ME7 model of prion disease, *Journal of Virology*, Volume 79, p. 5174–5184.
22. Cunningham, C., D. C., Wilcockson, D., Boche, K., Lunnon, and V. H., Perry, 2005a, Central and systemic endotoxin challenges exacerbate the local inflammatory response and increase neuronal death during chronic neurodegeneration, *Journal of Neuroscience*, Volume 25, p. 9275–9284.
23. Cunningham, C., S., Campion, K., Lunnon, C. L., Murray, J. F., Woods, R. M., Deacon, J. N., Rawlins, and V. H., Perry, 2009, Systemic inflammation induces acute behavioral and cognitive changes and accelerates neurodegenerative disease, *Biological Psychiatry*, Volume 65, p. 304–312.
24. Deleault, N. R., B. T., Harris, J. R., Rees, S., Supattapone, 2007, Formation of native prions from minimal components *in vitro*, *PNAS*, Volume 104, p. 9741-9746.
25. De Pablos, V., C., Barcia, J. E., Yuste-Jiménez, F., Ros-Bernal, M. A., Carrillo-de Sauvage, E., Fernández-Villalba, and M. T., Herrero, 2011, Acute Phase Protein's Levels as Potential Biomarkers for Early Diagnosis of Neurodegenerative Diseases, *Immunology, Allergology and Rheumatology*, Chapter 5.

26. Diaz-Espinoza, R., and C., Soto, 2010, Generation of prions in vitro and the protein-only hypothesis, *Landes Bioscience*, Volume 4, p. 53-59.
27. Dickinson, A. G., and G. W., Outram, 1988, Genetic aspects of unconventional virus infections: the basis of the virino hypothesis, *Ciba Foundation Symposium*, 135:63-83.
28. Dong, H., Y., Xiang, N., Farchi, W., Ju, Y., Wu, L., Chen, Y., Wang, B., Hochner, B., Yang, H., Soreq, and W., Lu, 2004, Excessive expression of acetylcholinesterase impairs glutamatergic synaptogenesis in hippocampal neurons, *Journal of Neuroscience*, Volume 24, p. 8950-8960.
29. Ferrero-Miliani, L., O. H., Nielsen, P. S., Andersen, and S. E., Girardin, 2007, Chronic inflammation: importance of NOD2 and NALP3 in interleukin-1b generation, *Clinical and Experimental Immunology*, Volume 147, p. 227-235.
30. Fontaine, V., S., Mohand-Said, N., Hanoteau, C., Fuchs, K., Pfizenmaier, and U., Eisel, 2002, Neurodegenerative and Neuroprotective Effects of Tumor Necrosis Factor (TNF) in Retinal Ischemia: Opposite Roles of TNF Receptor 1 and TNF Receptor 2, *Journal of Neuroscience*, Volume 23, p. 1-7.
31. Frank-Cannon, T. C., L. T., Alto, F. E., McAlpine, and M. G., Tansey, 2009, Does neuroinflammation fan the flame in neurodegenerative diseases?, *Molecular Neurodegeneration*, Volume 4, p. 47-60.
32. Fu, Y. X., and D. D., Chaplin, 1999, Development and maturation of secondary lymphoid tissues, *Annual Review Immunology*, Volume 17, p. 399-433.
33. Gao, H. M., J., Jiang, B., Wilson, W., Zhang, J. S., Hong, and B., Liu, 2002, Microglial activation-mediated delayed and progressive degeneration of rat nigral dopaminergic

- neurons: Relevance to Parkinson's disease, *Journal of Neurochemistry*, Volume 81, p. 1285–1297.
34. Glenner, G. G., and C. W., Wong, 1984, Alzheimer's disease: initial report of the purification and characterization of a novel cerebrovascular amyloid protein, *Biochemical and Biophysical Research Communications*, Volume 120, p. 885-90.
35. Gnanapavan, S., and G., Giovannoni, 2013, Neural cell adhesion molecules in brain plasticity and disease, *Multiple Sclerosis and Related Disorders*, Volume 2, p. 13-20.
36. Griffith, J. S., 1967, Self-replication and scrapie, *Nature*, Volume 215, p. 1043–1044.
37. Hachiya, N. S., M., Imagawa, and K., Kaneko, 2007, The possible role of protein X, a putative auxiliary factor in pathological prion replication, in regulating a physiological endoproteolytic cleavage of cellular prion protein, *Medical Hypotheses*, Volume 68, p. 670-673.
38. Haik, S., B. A., Faucheux, V., Sazdovitch, N., Privat, J. L., Kemeny, A., Perret-Liaudet, and J. J., Hauw, 2003, The sympathetic nervous system is involved in variant Creutzfeldt-Jakob disease, *Nature Medicine*, Volume 9, p. 1121–1122.
39. Hill, A. F., S., Joiner, J., Linehan, M., Desbruslais, P. L., Lantos, J., Collinge, 2000, Species-barrier-independent prion replication in apparently resistant species, *PNAS*, Volume 97, p. 10248-10253.
40. Honjo, K., S. E., Black, and N. P.L.G., Verhoeff, 2012, Alzheimer's Disease, Cerebrovascular Disease, and the β -amyloid Cascade, *The Canadian Journal of Neurological Sciences*, Volume 39, p. 712-728.

41. Hosseini, A., T., Lam, U. Farooq, S. M., Dunn, D., Vine, N., Daude, D., Westaway, D. S., Wishart, and B. N., Ametaj, 2011, Lipopolysaccharide affects permeation of prion protein through the gastrointestinal tract of rodents, Prion Congress, Montreal, Canada.
42. Isaacs, J. D., G. S., Jackson, and D. M., Altmann, 2006, The role of the cellular prion protein in the immune system, British Society for Immunology, Clinical and Experimental Immunology, Volume 146, p. 1–8.
43. Iwasaki, A., and R., Medzhitov, 2004, Toll-like receptor control of the adaptive immune responses, Nature Immunology, Volume 5, p. 987-995.
44. Kaeser, P. S., M. A., Klein, P., Schwarz, and A., Aguzzi, 2001, Efficient lymphoreticular prion propagation requires PrP^c in stromal and hematopoietic cells, Journal of Virology, Volume 75, p. 7097–7106.
45. Kawanokuchi, J., K., Shimizu, A., Nitta, K., Yamada, T., Mizuno, H., Takeuchi, A., Suzumura, 2008, Production and functions of IL-17 in microglia, Journal of Neuroimmunology, Volume 194, p. 54–61.
46. Keene, C. D., E., Cudaback, X., Li, K. S., Montine, and T. J., Montine, 2011, Apolipoprotein E isoforms and regulation of the innate immune response in brain of patients with Alzheimer's disease, Current Opinion in Neurobiology, Volume 21, p. 920–928.
47. Kim, J., J. M., Basak, and D. M., Holtzman, 2009, The Role of Apolipoprotein E in Alzheimer's Disease, Neuron, Volume 63, p. 287-303.
48. Klein, M. A., R., Frigg, E., Flechsig, A. J., Raeber, U., Kalinke, H., Bluethmann, F., Bootzk, M., Suter, R. M., Zinkernagel, and A., Aguzzi, 1997, A crucial role for B cells in neuroinvasive scrapie, Nature, Volume 390, p. 687-690.

49. Klein, M. A., P. S., Kaeser, P., Schwarz, H., Weyd, I., Xenarios, R. M., Zinkernagel, M. C., Carroll, J. S., Verbeek, M., Botto, M. J., Walport, H., Molina, U., Kalinke, H., Acha-Orbea, and A., Aguzzi, 2001, Complement facilitates early prion pathogenesis, *Nature Medicine*, Volume 7, p. 488–492.
50. Korth, C., B., Stierli, P., Streit, M., Moser, O., Schaller, R., Fischer, W., Schulz-Schaeffer, H., Kretzschmar, A., Raeberk, U., Braun, F., Ehrensperger, S., Hornemann, R., Glockshuber, R., Riek, M., Billeter, K., Wu¨thrich, and B., Oesch, 1997, Prion (PrPSc)-specific epitope defined by a monoclonal antibody, *Nature*, Volume 390, p. 74-77.
51. Kovacs, D.M., 2000, α 2-Macroglobulin in late-onset Alzheimer's disease, *Experimental Gerontology*, Volume 35, p. 473–479.
52. Lauer, D., A., Reichenbach, and G., Birkenmeier, 2001, Alpha 2-macroglobulin-mediated degradation of amyloid beta 1-42: a mechanism to enhance amyloid beta catabolism, *Experimental Neurology*, Volume 167, p. 385–392.
53. Lawson, V. A., J. B., Furness, H. M., Klemm, L., Pontell, E., Chan, A. F., Hill, and R., Chiocchetti, 2010, The brain to gut pathway: a possible route of prion transmission, *Gut*, Volume 59, p. 1643-1651.
54. Lee, J. W., Y. K., Lee, D. Y., Yuk, D. Y., Choi, S. B., Ban, K. W., Oh, and J. T., Hong, 2008, Neuro-inflammation induced by lipopolysaccharide causes cognitive impairment through enhancement of beta-amyloid generation, *Journal of Neuroinflammation*, Volume 5, p. 37-51.
55. Ligios, C., C. J., Sigurdson, C., Santucci, G., Carcassola, G., Manco, M., Basagni, C., Maestrale, M. G., Cancedda, L., Madau, and A., Aguzzi, 2005, PrPSc in mammary glands of sheep affected by scrapie and mastitis, *Nature Medicine*, Volume 11, p. 1137–1138.

56. Mabbott, N. A., A., Williams, C. F., Farquhar, M., Pasparakis, G., Kollias, and M. E. Bruce, 2000, Tumor Necrosis Factor Alpha-Deficient, but Not Interleukin-6-Deficient, Mice Resist Peripheral Infection with Scrapie, *Journal of Virology*, p. 3338-3344.
57. Mabbott, N. A., J., Young, I., McConnell, and M. E., Bruce, 2003, Follicular dendritic cell dedifferentiation by treatment with an inhibitor of the lymphotoxin pathway dramatically reduces scrapie susceptibility, *Journal of Virology*, Volume 77, p. 6845–6854.
58. Mabbott, N. A., 2004, The complement system in prion diseases, *Current Opinion in Immunology*, Volume 16, p. 587-593.
59. Magliozzi, R., S., Columba-Cabezas, B., Serafini, and F., Aloisi, 2004, Intracerebral expression of CXCL13 and BAFF is accompanied by formation of lymphoid folliclelike structures in the meninges of mice with relapsing experimental autoimmune encephalomyelitis, *Journal of Neuroimmunology*, Volume 148, p. 11–23.
60. McGeer, P. L., and E. G., McGeer, 2004, Inflammation and the Degenerative Diseases of Aging, *Annals of the New York Academy of Sciences*, Volume 1035, p. 104-116.
61. Murray, C. L., D. T., Skelly, and C., Cunningham, 2011, Exacerbation of CNS inflammation and neurodegeneration by systemic LPS treatment is independent of circulating IL-1b and IL-6, *Journal of Neuroinflammation*, Volume 8, p. 50-62.
62. Nguyen, M. D., J. P., Julien, and S., Rivest, 2002, Innate immunity: The missing link in neuroprotection and neurodegeneration?, *Nature Review*, Volume 3, p. 216–227.
63. Norrby, E., 2011, Prions and Protein Folding Diseases, *Journal of Internal Medicine*, Volume 270, p. 1-14.

64. Oesch, B., D., Westaway, M., Walchli, M. P., McKinley, S. B. H., Kent, R., Aebersold, R. A., Barry, P., Tempst, D. B., Teplow, L. E., Hood, S. B., Prusiner, and C., Weissmann, 1985, A cellular gene encodes scrapie PrP 27-30 protein, *Cell*, Volume 40, p. 735–746.
65. Pattison, I. H., and K. M., Jones, 1967, The possible nature of transmissible agent of scrapie, *Veterinary Record*, Volume 80, p. 2-9.
66. Peretz, D., R. A., Williamson, K., Kaneko, J., Vergara, E., Leclerc, G., Schmitt-Ulms, I. R., Mehlhorn, G., Legname, M. R., Wormald, P. M., Rudd, R. A., Dwek, D. R., Burton, and S. B., Prusiner, 2001, Antibodies inhibit prion propagation and clear cell cultures of prion infectivity, *Nature*, Volume 412, p. 739-743.
67. Perry, V. H., C., Cunningham, and C., Holmes, 2007, Systemic infections and inflammation affect chronic neurodegeneration, *Nature Reviews Immunology*, Volume 7, p. 161-167.
68. Prusiner, S. B., 1982, Novel proteinaceous infectious particles cause scrapie, *Science*, Volume 216, p. 136-144.
69. Qin, L., X., Wu, M. L., Block, Y., Liu, G. R., Breese, J. S., Hong, D. J., Knapp, and F. T., Crews, 2007, Systemic LPS causes chronic neuroinflammation and progressive neurodegeneration, *Glia*, Volume 55, p. 453–462.
70. Riemer, C., I., Queck, D., Simon, R., Kurth, and M., Baier, 2000, Identification of up-regulated genes in scrapie-infected brain tissue, *Journal of Virology*, Volume 74, p. 10245-10248.
71. Saborio, G. P., B., Permanne, and C., Soto, 2001, Sensitive detection of pathological prion protein by cyclic amplification of protein misfolding, *Nature*, Volume 411, p. 810-813.

72. Safar, J. G., K., Kellings, A., Serban, D., Groth, J. E., Cleaver, S. B., Prusiner, and D., Riesner, 2005, Search for a prion-specific nucleic acid, *Journal of Virology*, Volume 79, p. 10796-10806.
73. Sakudo, A., D., Lee, K., Saeki, Y., Matsumoto, S., Itohara, and T., Onodera, 2003, Tumor necrosis factor attenuates prion protein-deficient neuronal cell death by increases in anti-apoptotic Bcl-2 family proteins, *Biochemical and Biophysical Research Communications*, Volume 310, p. 725-729.
74. Sastre, M., J., Walter, and S. M., Gentleman, 2008, Interactions between APP secretases and inflammatory mediators, *Journal of Neuroinflammation*, Volume 5, p. 25-36.
75. Schmitt-Ulms, G., G., Legname, M. A., Baldwin, H. L., Ball, N., Bradon, P. J., Bosque, K. L., Crossin, G. M., Edelman, S. J., DeArmond, F. E., Cohen, and S. B., Prusiner, 2001, Binding of Neural Cell Adhesion Molecules (N-CAMs) to the Cellular Prion Protein, *Journal of Molecular Biology*, Volume 314, p. 1209-1225.
76. Seeger, H., M., Heikenwalder, N., Zeller, J., Kranich, P., Schwarz, A., Gaspert, B., Seifert, G., Miele, and A., Aguzzi, 2005, Coincident scrapie infection and nephritis lead to urinary prion excretion, *Science*, Volume 310, p. 324–326.
77. Senkova, O., O., Tikhobrazovac, and A., Dityatevb, 2012, PSA–NCAM: Synaptic functions mediated by its interactions with proteoglycans and glutamate receptors, *The international journal of biochemistry and cell biology*, Volume 44, p. 591-595.
78. Sisó, S., M., Jeffrey, and L., González, 2009, Neuroinvasion in sheep transmissible spongiform encephalopathies: the role of the haematogenous route, *Neuropathology and Applied Neurobiology*, Volume 35, p. 232–246.

79. Siso, S., L., Gonzalez, and M., Jeffrey, 2010, Neuroinvasion in Prion Diseases: The Roles of Ascending Neural Infection and Blood Dissemination, *Interdisciplinary Perspectives on Infectious Diseases*, Volume 2010, p. 1-17.
80. Smith, P. G., and R., Bradley, 2003, Bovine spongiform encephalopathy (BSE) and its epidemiology, *British Medical Bulletin*, Volume 66, p. 185-198.
81. Sorensen, G., S., Medina, D., Parchaliuk, C., Phillipson, C., Robertson, and S., A Booth, 2008, Comprehensive transcriptional profiling of prion infection in mouse models reveals networks of responsive genes, *Biomedical Genomics*, Volume 9, p. 1-14.
82. Soto, C., and J., Castilla, 2004, The controversial protein-only hypothesis of prion propagation, *Nature Medicine*, Volume 10, p. 63-67.
83. Spinner, D. S., I. S., Cho, S. Y., Park, J. I., Kim, H. C., Meeker, X., Ye, G., LaFauci, D. J., Kerr, M. J., Flory, B. S., Kim, R. B., Kascsak, T., Wisniewski, W. R., Levis, G. B., Schuller-Levis, R. I., Carp, E., Park, and R. J. Kascsak, 2008, Accelerated Prion Disease Pathogenesis in Toll-Like Receptor 4 Signaling-Mutant Mice, *Journal of Virology*, p. 10701–10708.
84. Tanzi, R. E., and L., Bertram, 2005, Twenty Years of the Alzheimer's Disease Amyloid Hypothesis: A Genetic Perspective, *Cell*, Volume 120, p. 545–555.
85. Tayebi, M., J., Collinge, and S., Hawke, 2009, Unswitched immunoglobulin M response prolongs mouse survival in prion disease, *Journal of General Virology*, Volume 90, p. 777-782.
86. Thackray, A. M., M. A., Klein, and R., Bujdoso, 2003, Subclinical Prion Disease Induced by Oral Inoculation, *Journal of Virology*, Vol. 77, p. 7991–7998.
87. Träger, U., and S. J., Tabrizi, 2013, Peripheral inflammation in neurodegeneration, *Journal of Molecular Medicine*, Volume 91, p. 673-681.

88. Van Amersfoort, E. S., T. J. C., Van Berkel, and J., Kuiper, 2003, Receptors, Mediators, and Mechanisms Involved in Bacterial Sepsis and Septic Shock, *Clinical Microbiology Reviews*, Volume 16, p. 379-414
89. Vella, L. J., R. A., Sharples, V. A., Lawson, C. L., Masters, R., Cappai, and A. F., Hill, 2007, Packaging of prions in exosomes is associated with a novel pathway of PrP processing, *Journal of pathology*, Volume 211, p. 582-590.
90. Wadsworth, J. D. F., and J., Collinge, 2012, Molecular Basis of Prion Disease (Book chapter), *Basic Neurochemistry*, Eighth Edition.
91. Wang, F., X., Wang, C., Yuan, and J., Ma, 2010, Generating a Prion with Bacterially Expressed Recombinant Prion Protein, *Science*, Volume 327, p. 1132-1135.
92. Wang, F., Z., Zhang, X., Wang, J., Li, L., Zha, C., Yuan, C., Weissmann, and J., Ma, 2011, Genetic informational RNA is not required for recombinant prion infectivity, *Journal of Virology*, p.1874-1876.
93. White, S. H., A. S., Ladokhin, S., Jayasinghe, and K., Hristova, 2001, How Membranes Shape Protein Structure, *The Journal of Biological Chemistry*, Volume 276, p. 32395–32398.
94. Wyss-Coray, T., and L., Mucke, 2002, Inflammation in Neurodegenerative Disease- A Double-Edged Sword, *Neuron*, Volume 35, p. 419-432.
95. Zimmerman, G., and H., Sorreq, 2006, Termination and beyond: acetylcholinesterase as a modulator of synaptic transmission, *Cell and Tissue Research*, Volume 326, p. 655-669.

**Chapter Two: Chronic subcutaneous administration of lipopolysaccharide
and LPS-converted mouse PrP^C induced neurodegeneration in FVB/N wild
type female mice**

Abstract

Since the outbreak of the “protein-only” hypothesis, a misfolded, partially proteinase K (PK) resistant, pathogenic proteinaceous particle, termed prion (PrP^{Sc}), has been considered as the causative agent of transmissible spongiform encephalopathies. Lipopolysaccharide (LPS), the major constituent of the cell wall of all Gram-negative bacteria, has been hypothesized to be a potential, widely available exogenous cofactor facilitating prion conversion and pathogenicity. Recently we showed that bacterial LPS is able to convert *in vitro* mouse recombinant PrP (moPrP) into a beta-rich isoform resistant to proteinase K ($\text{moPrP}^{\text{res}}$). The objectives of this research were to test whether injection of LPS-converted $\text{moPrP}^{\text{res}}$ alone or combined with LPS would be able to cause brain degeneration and prion-like disease in wild type FVB/N female mice. Ninety female FVB/N mice were randomly assigned to 6 groups (n=15 per group) and treated subcutaneously (sc) with: 1) 6wk sc administration of saline at 11 $\mu\text{L/hr}$, 2) 6wk sc injection of LPS at 0.1 $\mu\text{g/g BW}$ at 11 $\mu\text{L/hr}$, 3) one time sc injection of $\text{moPrP}^{\text{res}}$ at 45 $\mu\text{g/mouse}$, 4) 6wk sc injection of LPS at 0.1 $\mu\text{g/g BW}$ at 11 $\mu\text{L/hr}$ plus one time sc injection of $\text{moPrP}^{\text{res}}$ at 45 $\mu\text{g/mouse}$, 5) one time sc injection of RML at 10^7 ID 50 units of scrapie prions, and 6) 6wk sc administration of LPS plus one time sc injection of RML at 10^7 ID 50 units of scrapie prions. Brain samples were collected immediately after mice euthanasia or death. Results showed that $\text{moPrP}^{\text{res}}$ alone was able to exhibit 60% mortality rate in infected mice. Sagittal brain slices were stained to evaluate the degree of vacuolation, detect presence of PrP^{Sc} , amyloid plaques, and astrogliosis. Immunohistochemistry staining of saline control mice showed no vacuolation, PrP^{Sc} accumulation, amyloid plaques, or astrogliosis in target areas of the brain, whereas those treated with $\text{moPrP}^{\text{res}}$ showed vacuolation in various areas of the brain, astrogliosis in mid-brain and cerebellum, slight accumulation of PrP^{Sc} , and no deposits of

amyloid plaques. Moreover, all mice treated with RML or RML+LPS had widespread vacuolation, accumulation of PrP^{Sc}, and astrogliosis in different regions of the brain. Mice treated with moPrP^{res} or RML combined with LPS or LPS alone showed clinical signs of brain neurodegenerative disease. In addition, results demonstrated that chronic sc administration of LPS in conjunction with one time sc injection of RML scrapie strain aggravated prion disease as shown by histological differences and decreased incubation days in comparison to the positive controls (RML). Moreover, chronic sc administration of LPS over 6 wk led to 40% mortality rate and was associated with prion-like clinical symptoms, neurodegeneration, and amyloid plaque deposition in the cerebellum over long incubation days. In conclusion results of this study showed that sc administration of moPrP^{res} caused neurodegenerative disorder with vacuolation in various brain regions and expression of resistant PrP in various regions of the brain. More research is warranted to evaluate the ability to induce infectivity and pathogenicity in healthy mice by administering brain homogenate derived from moPrP^{res}-inoculated mice.

Key Words: Prion, Exogenous cofactor, Lipopolysaccharide, Spongiform vacuolation.

1. Introduction

Prion diseases, including Creutzfeldt-Jacob disease in humans, scrapie in sheep and goat, bovine spongiform encephalopathy (BSE) in cows, and chronic wasting disease (CWD) in elks and deers, are a group of neurodegenerative diseases affecting the central nervous system (CNS), which leads to typical spongiform vacuolation of the brain (Soto, 2011). As indicated in the ‘protein-only’ hypothesis, prion disease is believed to be majorly due to prion misfolding from the healthy cellular isoform (PrP^C) to a proteinase K resistant, self-propelling, rich in β -sheet pathogenic isoform (PrP^{Sc}) (Prusiner, 1982).

Mounting evidence indicates a potential role of endogenous and exogenous cofactors in prion conversion and pathogenicity. Currently, lipids and polyanions have been proven as two of the positive cofactors influencing prion conversion, propagation, and infectivity (Wang et al., 2010). Lately we proposed bacterial lipopolysaccharide (LPS) as a potential cofactor in conversion of PrP (Ametaj et al., 2010). Indeed LPS instantly converts mouse recombinant PrP (moPrP) to a proteinase K resistant isoform (moPrP^{res}), rich in β -sheet under normal conditions without the use of sonication (Protein Misfolding Cyclic Amplification - PMCA) (Ametaj et al., 2010). Most importantly, there is no published report up-to-date on the ability of any cofactor(s) being able to induce prion-like pathogenicity when administered by itself to healthy wild type animal models.

Bacterial LPS is the major constituent of the outer membrane of all Gram-negative bacteria (GNB) essential for their survival (Van Amersfoort et al., 2003). Different serotypes of LPS are widely available in the exogenous environment and highly present in the gastrointestinal tract (Wolfs et al., 2010). LPS has been implicated as an etiopathogenic and aggravating agent in various metabolic and neurodegenerative diseases in humans and animals alike (Lassenius et al.,

2011; Ametaj et al., 2012). Alzheimer's and Parkinson's disease, for instance, have both been reported to be exacerbated by LPS administration (Combrinck et al., 2002; Liu and Bing, 2011). LPS has been found to activate the immune system leading to microglial activation and subsequent neuroinflammation in the CNS, further aggravating brain degeneration (Qin et al., 2007). In addition chronic peripheral challenge of the immune system with LPS has shown to favor brain degeneration in various neurodegenerative diseases (Qin et al., 2007).

Surveillance of neuropathological changes in the brain contributes to diagnostic confirmation of prion diseases (Budka, 2003). Immunohistochemistry (IHC) has long been an indispensable methodology contributing to our understanding and confirmation of prion diseases. Hematoxylin and eosin (H&E) staining was developed as one of IHC detection methods for surveillance of spongiform vacuolation in the brain tissue (Safar et al., 2005). In addition, staining for intensity of PrP^{Sc} accumulation in various regions of the brain has been among the developed IHC methods of interest (Schulz-Schaeffer et al., 2000). Underlying histological alterations in the brain of infected murine models is accompanied by simultaneous clinical changes including but not limited to kyphosis, ataxia, dysmetria, tremor, head tilt, tail rigidity, bradykinesia, proprioceptive deficits, stupor, loss of deep pain sensation, and loss of weight.

The major route of experimentally infecting animal models with prion disease has been the intracerebral injection with shorter incubation days compared to other peripheral infection methods (Hunter et al., 2002). However, to mimic natural prion transmission, various peripheral infection methods such the subcutaneous (sc) route has been used in animal models. Subcutaneous administration of prion infectivity has been reported to have fairly long incubation time but as effective in transmitting the disease as other routes (Chianini et al., 2013).

In the current study, we hypothesized that LPS derived from *Escherichia coli* 0111:B4 would expedite and aggravate prion disease using a murine model. Also, we hypothesized that administration of LPS-converted recombinant mouse prion protein (moPrP^{res}) would induce prion-like pathogenicity accompanied by typical histological and clinical signs. The objectives were to study the role of LPS in aggravating prion disease when administered sc in a chronic manner, and the role of LPS-converted moPrP^{res} in induction of prion disease when administered sc, using FVB/N wild type female mice.

2. Materials and Methods

2.1. Experimental design and animals

Sixty FVB/N wild type female mice (Charles River Laboratories, Wilmington, USA) at 5 wk of age, were randomly allocated to 6 treatment groups (n=15 per group) as following: 1) saline (negative control), 2) LPS (*Escherichia coli* 0111:B4; Sigma-Aldrich, St. Louis, USA), 3) moPrP^{res} (29-232), 4) moPrP^{res}+LPS, 5) RML (Rocky Mountain Laboratory) +LPS, and 6) RML (positive control). Bacterial LPS (0.1µg/gram of body weight) and saline were administered sc at a rate of 0.11 µL/h using ALZET[®] osmotic mini pumps (ALZET, Cupertino, CA), which were implanted on their back for a period of 6 wk. A simultaneous one-time sc injection of moPrP^{res} (29-232; 45µg/mice) or RML (10⁷ ID 50 units of scrapie prions) was given at the time of minipump implantation to the designated treatment groups. Recombinant mouse prion protein was provided by Dr. David Wishart's lab at the University of Alberta.

2.2. Mouse recombinant prion protein

Lyophilized LPS (Sigma-Aldrich, St. Louis, USA) was reconstituted with mqH₂O to provide an initial working concentration of 5 mg/mL. This stock solution was diluted and used to

reconstitute lyophilized moPrP (29-232) to ~0.5 mg/mL (500 μ L in 1.5 mL), providing milligram (mg) ratios of moPrP:LPS of 1:1. Given that the average molecular weight of LPS is about 10 kDa or half that of the prion protein, this mg ratios equate to twice that of the molar ratio. Because an exact molecular weight does not exist for LPS, mg ratios were used in this study for comparison and consistency. The prion conversion reactions were followed using circular dichroism (CD) spectroscopy recorded in the far-UV region (190-260 nm) at 25 °C in a 0.02 cm path-length quartz cell on an Olis DSM 17 spectropolarimeter. Five scans were averaged for each CD spectrum collected. The protein concentrations were 0.5 mg/mL (~25 μ M). Reference spectra were collected in the same manner and subtracted from the measured prion spectra prior to molar ellipticity determination. Ellipticity values were calculated using an average amino acid molecular weight of 113.64 g/mol and the secondary structure content was calculated with CDPro using the CONTINLL algorithm and the SP22X reference set. The endpoint to β -sheet conversion was defined when the helical content (as measured by CD) dropped to 15% and the β -sheet content exceeded 25%. The endpoint to fibril propagation was defined when the helical content dropped to 10% and the β -sheet content exceeded 30%.

Lyophilized moPrP was reconstitution to 0.5 mg/mL with an equimolar amount of LPS to facilitate conversion. LPS was then removed from the LPS converted prion solution using polymyxin-B agarose resin (Sigma-Aldrich, St. Louis, USA). Five hundred microliters of resin was added to a 1.5 mL Eppendorf tube and equilibrated with 3 separate volumes of 500 μ L ammonium bicarbonate buffer (100 mM, pH 8.0, Sigma-Aldrich, St. Louis, USA). Subsequently, 250 μ L of the PrP:LPS sample was added and incubated at room temperature for 60 min allowing free LPS to bind to the resin. The resin was then pelleted by centrifugation (850 g for 5 minutes) and the supernatant removed. This procedure was repeated an additional 3 times by

applying the supernatant to freshly equilibrated resin. The supernatant was then analyzed using the pyrochrome Limulusamebocyte lysate assay (Associates of Cape Cod Inc., East Falmouth, MA), to determine the extent of residual LPS contamination while the secondary structure of moPrP^{res} was confirmed by CD.

2.3. Euthanasia

Animals were euthanized at two time points, at 11wk post infection (pi) and at terminal sickness. Five mice per treatment group were euthanized at 11 wk pi with no clinical signs of prion disease or any sort of abnormality and normal body weights. The remaining 10 mice per treatment group were euthanized at the terminal stage. All experimental procedures and animal care procedures were approved by the University of Alberta Animal Care and Use Committee for Health Sciences Laboratory Animal Services in accordance with the guidelines of the Canadian Council on Animal Care (reference no. 6).

2.4. Tissue preparation

Mice were anesthetized using isoflurane gas. After checking their reflexes making sure of the loss of pain sensation, blood samples were taken via cardiac puncture. Brain samples were then collected immediately and cut in a sagittal orientation and fixed in 10% buffered formalin phosphate (Sigma-Aldrich, St. Louis, USA) at 10 times the volume of the tissue for a minimum of 48 hr at room temperature. Thereafter, the brain samples were rinsed with tap water for 20 min and then stored in 70% ethanol (Commercial Alcohol, Winnipeg, Canada) at 4 °C to be processed for immunohistochemical (IHC) staining. The samples were then processed for a series of IHC stainings to distinguish the pattern and distribution of PrP^{Sc} and amyloid- β deposition in various regions of the brain as well as astrogliosis and spongiform vacuolation.

2.5. Hematoxylin and eosin staining

All brain tissues were collected on adhesive-treated slides, embedded in paraffin (formula “R” paraffin Surgipath[®], Leica Biosystem, Nussloch, Germany), and dried over night at 37 °C. Then, 4.5-6 µm thick slices of the brain sample were cut in a sagittal orientation and mounted on colorfrost plus slides (Fisher Scientific, Waltham, USA). Paraffin-embedded tissues were de-paraffinized and rehydrated by a graded series of ethanol and de-ionized water emerging. Slides were then incubated in filtered Mayer's Hematoxylin (Fisher Scientific, Waltham, USA) for 10 min, rinsed with tap water for 3 min, incubated in eosin Y working solution for 30 sec and dipped 2-3 times in distilled water. Subsequent to dehydration, slips were covered and mounted with cyto seal 60 (Fisher Scientific, Waltham, USA) and left at room temperature for 48 hr to dry. Thereafter, pictures were taken from each slide using digital slide scanner Nanozoomer XR (Hamamatsu, SZK, Japan).

Images were then evaluated with computer-based InCell Investigator software (GE Healthcare Life Sciences, Quebec, Canada) to quantify the vacuolation load in various regions of the brain in comparison to the controls. To do so, general description of typical vacuoles was defined to the software using software-specific formula. Selected H&E pictures (Figures 3 and 4) in all 4 brain regions (Cc, Th, Mb, Cr) were then automatically run in the software to quantify vacuole number and perimeter for each treatment group and corresponding brain region.

2.6. PrP^{Sc} staining

Samples were de-paraffinized and rehydrated as explained above. Thereafter, each brain slide was processed for maximum clearance of PrP^C from the tissues. A series of incubation with formic acid, 4M guanidine thiocyanate, 3% H₂O₂, mouse monoclonal SAF83 (1:500 dilution,

Cayman Chemical, Michigan, USA) antibody, streptavidin-peroxidase, diaminobenzidine substrate and Mayer's Hematoxylin (Fisher Scientific, Waltham, USA) was conducted. After dehydration using ethanol, slides were rinsed in xylene (Sigma-Aldrich, St. Louis, USA) for 10 min. Subsequently, slips were covered and mounted with cytooseal 60 to dry for 48 hr at room temperature. Once the pictures were taken from each slide, comparisons were made subjectively comparing various regions of the brain to the controls.

2.7. Amyloid plaque staining

After sample de-paraffinization and rehydration, as described previously, brain slices were incubated in thioflavine S (Sigma-Aldrich, St. Louis, USA) for 8 min. Samples were then differentiated in 80% alcohol for 2 x 3 min. Using 95% alcohol, brain slices were dehydrated for 3 min. Using ddH₂O, each sample was rinsed twice for 3 min each time. Brain samples were counterstained with propidium iodine (Sigma-Aldrich, St. Louis, USA) for 5 min. Slides were quickly rinsed with ddH₂O. Each brain slice was mounted on the slides allowing them to dry in the dark overnight. The samples were then observed for amyloid plaque (Ap) deposition using Nikon microscope (Eclipse 90i; Nikon Instruments Inc., Melville, USA).

2.8. Astrogliosis staining

After de-paraffinization and rehydration, brain slices were washed twice with PBS (Boston BioProducts, Ashland, USA) 0.05% Tween (Sigma-Aldrich, St. Louis, USA), each time for 5 min. The samples were then heated at 121 °C in 10 mM citrate buffer (Sigma-Aldrich, St. Louis, USA) for 2 min. Thereafter the samples were left to cool at room temperature for 10-20 min. Once again, brain slices were washed with PBS 0.05% Tween (2 x 5 min). Then brain slices were incubated in 3% H₂O₂ (Fisher Scientific, Waltham, USA) for 6 min with a subsequent wash

with PBS 0.05% Tween (2 x 5 min). The GFAP antibody (Sigma-Aldrich, St. Louis, USA and BD Pharmingen, Mississauga, Canada) was biotinylated (BD Pharmingen, Mississauga, Canada) according to the manufacturer protocol and blocked in 50 mM Tris-HCl (Sigma-Aldrich, St. Louis, USA) pH 7.4 with 1% BSA (OmniPur, Darmstadt, Germany). Then the samples were incubated overnight at 4 °C. Thereafter, brain slices were washed 4 times with PBS 0.05% Tween, 5 min each time, with an incubation with streptavidin-peroxidase (Invitrogen, Carlsbad, USA) for 16 min after the second wash. Then samples were incubated with DAB (BD Pharmingen, Mississauga, Canada) up to 20 min until the brown color showed up. After that 2 other washes with PBS 0.05% Tween, 5 min each, were conducted. A counterstaining with Mayer's hematoxylin (Fisher Scientific, Waltham, USA) was done for 2 min. Brain slices were then washed twice, each time for 3 min, in running tap water with 10 dips in sodium bicarbonate in between the wash. Then samples were treated with 95% and 100% ethanol (2 min each) and treated with xylene (2 x 5 min, Sigma-Aldrich, St. Louis, USA). Finally brain slices were mounted with cyto seal (Fisher Scientific, Waltham, USA) and left to dry for 48 hr at room temperature.

2.9. Western blot assay

Brain and spleen samples were cut to make 10% tissue homogenate in PBS (1X) (Bio-RAD, Hercules, USA). Using bicinchoninic acid protein assay (Thermo Fisher Scientific, Waltham, USA) the total amount of protein was quantitated. Sufficient amount of the tissue homogenate was taken to compensate 250 and 400 µg of brain and spleen protein content, respectively. This amount of protein was then put in 250 µL of RIPA (radioimmunoprecipitation assay buffer; Sigma-Aldrich, St. Louis, USA) final volume. 50 µg/mL of proteinase K (PK) was added to the tissue each homogenate. Then, 2 µL 0.02% bromophenol blue (Bio-RAD, Hercules, USA) was

added to the solution. Samples were vortexed briefly and let to be digested by PK for 1 hr at 37 °C. The reaction was then stopped with 25 uL PMSF (5mM final volume; Sigma-Aldrich, St. Louis, USA). After allowing the samples to cool down at room temperature for 5 min, they were then centrifuged at 20,000 g for 60 min at 4 °C. The supernatant was then discarded. Fifteen uL of SB (2X) was then added to the remaining pellet to boil for 10 min.

Each sample was loaded (20-25 µL) to its corresponding gel (NuPAGE Bis-Tris mini gels, Life Technologies, Carlsbad, USA) well. The samples were then electrophoresed (SDS-PAGE apparatus, Bio-RAD, Hercules, USA) at 200 volts for 50 min. Chemiluminescent molecular weight standards (Precision Plus Protein™ WesternC Standards, Bio-RAD, Hercules, USA) were included on each gel. The membranes were then transferred (wet Western blotting apparatus, Bio-RAD, Hercules, USA) overnight at 20 volts. The membranes were then rinsed quickly in 1X TBS-tween (0.5%, Sigma-Aldrich, St. Louis, USA) and incubated with prion protein monoclonal Sha31 antibody (1:30000, Bertin Pharma, Montigny le Bretonneux, France) in 1X TBS-tween (0.5%) overnight at 4 °C. The membranes were subsequently washed and incubated with secondary goat anti-mouse HRP conjugate antibody (1:10000, Bio-RAD, Hercules, USA) in 1X TBS-tween (0.1%) with 5% skim milk (Carnation-maker Smucker Foods of Canada, Ontario, Canada). Imaging was done using Pierce® ECL Plus Western Blotting Substrate (Thermo Fisher Scientific, Waltham, USA) using ImageQuant LAS (4000 series, GE Healthcare Life Sciences, Quebec, Canada).

2.10. Scrapie cell assay

To expose L929 (mouse fibroblast cell line, ATCC, Manassas, USA) cells to prion samples, 3 replicates of the brain homogenates (prepared in 1X PBS, 10%) and control samples (30 µL

each), including saline (negative control), *E. coli* 0111:B4 LPS, moPrP^{res}, moPrP^{res}+LPS, RML+LPS, and RML (positive control) treat were loaded to a 96 well plate (tissue culture plate, Corning Costar, Tewksbury, USA) with a dilution series of 0.1 to 0.0001% in 6 replicates. Twenty μ L of the cell volume containing 5,000 L929 cell was added to each well. The plate was then incubated at 37 °C for 3-5 minutes with subsequent addition of 150 μ L of media (DMEM containing 10% horse serum, Sigma, St. Louis, USA) volume. The plates were then incubated for 5 d at 37 °C. Thereafter, the cells were passaged twice (1:4 and 1:7) with an incubation interval of 5 d at 37 °C between each passage.

To activate the ELISPOT (96 well Elispot plates, Millipore, Billerica, USA) membranes, the plate was first washed with 70% ethanol (60 μ L for 3 minutes) (Commercial Alcohol, Winnipeg, Canada) and 1X TBS (3 times, Sigma-Aldrich, St. Louis, USA). Thirty μ L of TBS (1X) was then added to the membranes to keep them wet. Then, 20,000 cells were loaded to each well of the ELISPOT. Filtered cells on each plate were then vacuumed and dried at 50 °C for 1 h.

To digest with proteinase K (PK; Invitrogen, Carlsbad, USA) 60 μ L of RIPA lysis buffer containing 5 μ g/mL PK was added to each well. The plates were then incubated at 37 °C for 90 min. The lysis buffer was then removed and each well washed 3 times with TBS (1X). Then, 100 μ L of 2 mM phenylmethylsulfonyl fluoride (PMSF; Sigma-Aldrich, St. Louis, USA) (made in TBS) was added to each well and the plates were incubated on rocker (large 3-D rotator, model 4631, Thermo Scientific, Waltham, USA) at room temperature for 10 min. PMSF was then removed and the wells were washed 3 times with TBS (1X). 100 μ L of 3 M GdnSCN (Guanidine thiocyanate; Fisher Scientific, Waltham, USA) was added to each well with a subsequent incubation on rocker at room temperature for 10 min. Then, GdnSCN was removed and the wells were washed 4 times with TBS (1X). 100 μ L of 5% skim milk (prepared in 1X TBS; Carnation[®],

Alberta, Canada) was then added. The plate was once again incubated at room temperature for 60 min. After removing the milk and washing with TBS (1X for 3 times), the primary antibody (SAF83 at 1:1000 in 1X TBS, Cayman Chemical, Michigan, USA) was added and incubated on a rocker for 120 min at room temperature. SAF83 is washed away with TBS (1X for 3 times) and the secondary antibody (1:5,000, goat anti-mouse alkaline phosphatase, alkaline phosphatase conjugated, in TBS 1% milk; Bio-RAD, Hercules, USA) was added. Incubation was done for 90 min at room temperature on a rocker. The secondary antibody was then washed away with TBS (1X for 3 times). Then, 60 μ L of the alkaline phosphatase (Promega, Madison, USA) buffer (100 mM TrisHCl, 100 mM NaCl, 5 mM MgCl \cdot 6H $_2$ O; Sigma-Aldrich, St. Louis, USA) was added to each well with subsequent 10 min incubation on the rocker. Alkaline phosphatase buffer was then removed with BCIP (5-bromo-4-chloro-3-indolyl-phosphate)/NBT (nitro blue tetrazolium) (Promega, Madison, USA) followed by 20 min incubation. BCIP/NBT was then removed and the wells were washed 4 times with distilled water. The plates were finally dried overnight, in the dark.

2.11. Statistical analysis

Weight trends were analyzed using MIXED procedure of SAS (version 9.3, SAS Institute, Cary, NC, USA) with the following model:

$$Y_{ijkl} = \mu + t_i + p_j + tp_{ij} + \epsilon_{ijkl}$$

Y_{ij} represents the dependent variables, μ is the population mean, t_i is the fixed effect of treatment, p_j is the fixed effect of period (age in week), tp_{ij} counts for the interaction between treatment and period, and ϵ_{ij} accounts for the residual error which is assumed to be normally distributed. The degree of freedom was calculated using the Kenward-Roger method. Using SAS probability difference option, the results are shown using comparison of the least square means.

The cut off significance value used was set at $P < 0.05$. In addition, to obtain survival analysis results, the PRISM software (Prism Software Corporation) was used.

3. Results

3.1. Weight change

Animals from all treatment groups were weighed on a monthly basis, starting from initiation of the experiment (6 wk of age) until 74 wk, and then at 102nd and 110th wk (experiment termination), to monitor the weight trend over time in different treatment groups (Figure 2.1). Comparisons show statistical difference, with cut off value of $P < 0.05$, between the LPS and RML treatments (at 35, 39, 43, 48, 52, and 66 wk), LPS treatment vs saline negative treatment (48, 52, 56, 66 and 110 wk), LPS treatment vs RML+LPS treatment (35 and 39 wk), LPS treatment vs moPrP^{res} treatment (43, 48, 52, 56, 61, 66, 70 and 74 wk), LPS treatment vs moPrP^{res}+LPS treatment (39, 43, 48, 52, 56, 61, 66, 70, 74, 102 and 110 wk), moPrP^{res} treatment vs RML treatment (35 wk), moPrP^{res} treatment vs RML+LPS treatment (35 and 39 wk), moPrP^{res}+LPS treatment vs RML+LPS treatment (39 wk), moPrP^{res}+LPS treatment vs saline negative treatment (56 and 70 wk), RML treatment vs RML+LPS treatment (39 wk), RML+LPS treatment vs saline negative treatment (39 wk) (Figure 2.1).

The weight trend numerically distinguishes the LPS-treated animals from all other treatments starting 30 wk of age onward maintaining high body weight for the LPS treatment group (Figure 2.1). This difference is statistically valid in 48, 52, and 66 wk of age between the LPS treatment vs saline, moPrP^{res}, moPrP^{res}+LPS, and RML (Figure 2.1). The LPS treatment group also sets statistical difference in 61, 70, and 74wk of age with the moPrP^{res} and moPrP^{res}+LPS.

The LPS+RML treatment group had a sudden drop in weight starting from 30 wk until 39 wk (Figure 2.1). This was associated with early deaths observed with typical clinical signs of prion diseases of all animal replicates in this treatment group. Starting from 30wk onwards, the moPrP^{res} treated animal groups compared to the positive control group shows, on average, lower numerical weight value (Figure 2.1). This difference is statistically valid between moPrP^{res} vs RML and RML+LPS treatment groups in 35, and 35 and 39 wk of age, respectively. The moPrP^{res} treated animals also statistically differentiate from the LPS treatment group in 43, 48, 52, 56, 61, 66, 70 and 74 wk of age. This is while both the moPrP^{res} and RML treated animal groups exhibit, on average, lower numerical body weights than the saline negative control group beginning from 30 wk onwards (Figure 2.1).

3.2. Survival analysis

Five animals from each treatment group were randomly chosen to be euthanized at 11 wk pi with average body weights and showing no clinical signs or abnormality of any sort. The remaining 10 mice per treatment were left to be euthanized after developing typical clinical signs of prion disease such as kyphosis, ataxia, dysmetria, tremor, head tilt, tail rigidity, bradykinesia, proprioceptive deficits, stupor, loss of deep pain sensation, and loss of weight for over 72 hours.

The RML positive control group had a drop of 80% in survival rate after 200 dpi but 2 mice survived until termination of the experiment at 700 dpi with a 10% survival rate (Figure 2.1). The negative saline control group maintained 100% survival for over 600 dpi with a 40% mortality rate just 1 mo before the termination of the experiment (Figure 2.1).

The RML+LPS treatment group lost 30% of its experimental animals after 100 dpi with a sudden drop to 100% mortality rate at 200 dpi (Figure 2.1). Over the first 350 dpi the LPS-

treated mice had 10% mortality rate (Figure 2.1). Deaths in this treatment group increased to 40% after 650 dpi leaving the LPS treatment group with a survival rate of 60% at termination of the experiment (Figure 2.1). The moPrP^{res} treatment group had a 20% loss of animals at 200 dpi with a continuing decrease of up to 60% mortality rate until termination of the experiment (Figure 2.1). The remaining 40% of moPrP^{res}-treated animals survived up to 750 dpi (Figure 2.1). The moPrP^{res}+LPS treatment group lost 30% of its animals in the first 200 dpi and ending with a 50% survival rate at termination of the experiment (Figure 2.1).

3.3. Immunohistochemical stainings

Lipopolysaccharide-only treated animals. Five LPS-only treated animals euthanized at 11 wk pi, with no apparent clinical signs of disease showed mild vacuolation in the cerebral cortex (Cc), thalamus (Th), midbrain (Mb), and cerebellum (Cr) (Figure 2.3, e-h). Their corresponding PrP^{Sc} brain staining, in similar brain regions (Figure 2.5, e-f), showed little difference from the saline treated control group (Figure 2.5, a-d).

Interestingly, the LPS-only treated FVB/N mice, at terminal sickness, showed widespread vacuolation in different regions of their brain including the Cc, Th, Mb and specifically the Cr (Figure 2.4, e-h). These vacuoles had bigger size in comparison to similar brain regions of the RML positive controls (Figure 2.4, u-x). Vacuolation pattern of the LPS-only treated in terminally sick mice were comparable to the positive controls (i.e., RML) at terminal sickness in terms of vacuole distribution in different regions of the brain. Interestingly, even though vacuole abundance was lower in number in comparison to similar brain regions of terminally sick RML mice, vacuole size showed an increase in terminally sick LPS-only treated animals in comparison to the RML group.

The PrP^{Sc} staining results of terminally sick LPS-only treated mice (Figure 2.6, e-h) showed difference in PrP^{Sc} deposition in brain regions in comparison to the positive control (Figure 2.6, u-x). The LPS-treated animals showed mild deposits of the pathogenic prion protein in different regions of their brain; however, they were still different from the saline PrP^{Sc} staining results (Figure 2.6, a-d).

Terminally sick LPS-only treated mice had also aggravated astrogliosis only in the Cr region comparable to the positive control (Figure 2.7, h and x). This is while other brain regions, i.e., Cc, Th, Mb, did not have any difference in comparison to the negative control (Figure 2.7, a-g). This pattern was also observed in staining for Ap in which only the Cr of terminally sick LPS-treated mice showed amyloid- β plaques (Figure 2.8, h). This level of Ap accumulation in the Cr was unique as none of the other treatment groups and controls has similar Ap deposition in their Cr region (Figure 2.8, d, l, p and x).

Lipopolysaccharide-converted moPrP^{res} treated groups. Mice receiving recombinant moPrP^{res} and euthanized at 11 wk pi with no clinical abnormalities showed mild vacuolation in different brain regions including Cc, Th, Mb, and Cr (Figure 2.3, i-l). The negative controls (Figure 2.3, a-d) and the RML-treated groups (Figure 2.3, u-x) showed either lack of vacuolation or very little vacuolation in similar brain regions, respectively, at 11 wk pi. In addition, the PrP^{Sc} deposition in the brain of moPrP^{res} treated mice at 11 wk pi (Figure 2.5, i-l) showed mild PrP^{Sc} depositions as compared to the negative (Figure 2.5, a-d) and positive (Figure 2.5, u-x) controls at 11 wk pi.

H&E staining results obtained from terminally sick mice of the moPrP^{res}-treated group demonstrated intense vacuolation in different brain regions including the Cc, Th, Mb, and

specifically the Cr (Figure 2.4, i-l). Distribution of vacuolation in brains of terminally sick moPrP^{res}-treated mice showed similarity to terminally sick RML control mice with lower vacuole abundance, i.e., in the Cc, and bigger vacuole size in Cc, Th, Mb, and Cr brain regions (Figure 2.4, i-l).

In addition, results from the PrP^{Sc} staining of terminally sick moPrP^{res}-treated animals showed mild intensity of PrP^{Sc} accumulation in the Cc, Th, Mb, and Cr (Figure 2.6, i-l). Only slight subjective differences in terms of PrP^{Sc} staining were evidenced when compared to the negative control (Figure 2.6, a-d).

Furthermore, the moPrP^{res} treated animals had severe astrogliosis in their Cr (Figure 2.7, l) comparable to the positive control. Mild astrogliosis was also observed in the Mb of this treatment group (Figure 2.7, k) differentiating it from the negative control. This is while the Cc and Th brain regions of the moPrP^{res} treatment group did not show astrogliosis compared to similar brain regions of the negative control (Figure 2.7, i-j). In terms of Ap deposition, none of the brain regions showed Ap (Figure 2.8, i-l).

Lipopolysaccharide-converted moPrP^{res}+LPS treatment group. Five FVB/N female mice with no clinical signs of disease were randomly chosen and euthanized from this treatment group at 11 wk pi. H&E staining of their brain slides at this time showed mild vacuolation spread throughout different regions of the brain including Cc, Th, Mb, and Cr (Figure 2.3, m-p). Their corresponding PrP^{Sc} staining (Figure 2.5, m-p) showed subjectively little difference with the positive (Figure 2.5, u-x) and negative (Figure 2.5, a-d) controls, with no PrP^{Sc} accumulation in different regions of the brain.

Terminally sick moPrP^{res}+LPS-treated mice showed widespread vacuolation in different brain regions including the Cc, Th, Mb, and specifically the Cr (Figure 2.4, m-p) comparable to the terminally sick RML group (Figure 2.4, u-x). In terms of vacuole intensity they showed lesser intensity in comparable regions of the brain when compared to the terminally sick RML-treated animals. Similar to the LPS and moPrP^{res} treatment groups, terminally sick moPrP^{res}+LPS treated mice exhibited subjectively larger size vacuoles when compared to the RML treated animals. Moreover, terminally-sick mice treated with moPrP^{res}+LPS showed similar PrP^{Sc} accumulation (Figure 2.6, m-p) to the negative saline treated controls (Figure 2.6, a-d).

In this treatment group, IHC staining revealed mild astrogliosis in all brain regions with the Cr being more aggravated (Figure 2.7, m-p). In comparison to the negative control, the moPrP^{res}+LPS treated animals showed differences in their Cc, Th, and Mb with only few signs of astrogliosis (Figure 2.7, m-o). On the other hand positive controls showed highly aggravated astrogliosis in similar regions (Figure 2.7, u-w) when compared to the moPrP^{res}+LPS treatment group. In addition Cr showed more intense astrogliosis as compared to the other 3 regions of the moPrP^{res}+LPS treated animals but less aggravation when compared to positive controls (Figure 2.7, p and x). Furthermore, the Ap staining of the moPrP^{res}+LPS treatment group revealed only mild Ap deposition in the Th with the other regions of the brain showing no sign of Ap deposition (Figure 2.8, m-p).

Rocky Mountain Laboratory+LPS treatment group. Mice treated with RML+LPS and euthanized at 11 wk pi with no clinical signs of prion disease exhibited mild vacuolation in different brain regions including the Cc, Th, Mb, and Cr (Figure 2.3, q-t). Furthermore, PrP^{Sc} accumulation in similar brain regions of this treatment group showed subjective difference when

compared to 11 wk RML-treated mice (Figure 2.5, u-x) exhibiting greater intensity of PrP^{Sc} accumulation (Figure 2.5, q-t).

Terminally sick RML+LPS treated mice showed further widespread vacuolation in various brain regions including the Cc, Th, Mb, and specifically the Cr (Figure 2.4, q-t). Distribution of vacuolation was similar to terminally sick RML positive controls with subjective greater vacuolation intensity in comparable brain regions. Comparison between terminally sick RML+LPS treated animals (Figure 2.6, q-t) and the positive controls (Figure 2.6, u-x) showed distinct subjective difference of PrP^{Sc} accumulation, most specifically in the Cc, Th, and the Cr.

Astrogliosis staining of the RML+LPS treatment group (Figure 2.7, q-t) showed highly aggravated astrogliosis in all brain regions compared to the positive controls. Brains of RML+LPS treated mice seemed to have more intensified astrogliosis than the RML-alone treated mice (Figure 2.7, u-x). Meanwhile staining for Ap did not show any difference between the RML and RML+LPS treated mice (Figure 2.8, q-x) as they lacked Ap deposition in all brain regions except the Mb for the RML-treated mice (Figure 2.8, w).

LPS treated and non-LPS treated mice. Comparison of the LPS treated and non-LPS treated mice at 11 wk pi with no clinical signs of prion disease showed little difference compared to the RML treated mice. At this time point, comparison of the H&E staining between LPS+RML and RML treatment groups showed little subjective difference, if none, with both treatment groups exhibiting minimum vacuolation in several brain regions. This pattern was also valid at 11 wk pi in the moPrP^{res}-treated groups with minor subjective differences of vacuolation in the brain of moPrP^{res} and moPrP^{res}+LPS. A similar pattern was observed in terms of PrP^{Sc} deposition in the brains of LPS treated and non-LPS treated groups. However, both moPrP^{res}-treated groups were

closer to negative controls at 11 wk pi. On the other hand, both moPrP^{res} and RML treated groups showed differences from the negative saline treatment in the H&E slides at 11 wk pi.

Combination of LPS with RML seems to increase the abundance and distribution of brain vacuolation in terminally sick mice as compared to RML treatment group. Widespread vacuolation was observed in the H&E staining of terminally sick RML+LPS treatment group in all regions of the brain including the CC, corpus callosum, hippocampus, Th, hypothalamus, midbrain, and the Cr. On the other hand, terminally sick RML-treated mice showed lower vacuolation intensity in similar brain regions.

Similar patterns were observed from the PrP^{Sc} and astrogliosis staining results. Terminally sick RML+LPS treated mice had subjectively greater intensity of PrP^{Sc} accumulation in the Cc and Th, whereas the terminally sick RML-treated mice showed slightly lower PrP^{Sc} accumulation in similar brain regions (Figure 2.6, q-x). This was also the case with astrogliosis in all brain regions when comparing terminally sick RML+LPS to the RML treatment group (Figure 2.7, q-x). In addition, comparison of the Ap staining results showed that both treatment groups had similar Ap deposition with only the Mb region in the RML-treated animals being aggravated with Ap deposition (Figure 2.8, q-x)

Combination of LPS treatment with moPrP^{res} resulted in a different vacuolation pattern at terminal sickness. Terminally sick moPrP^{res}-treated mice exhibited greater abundance of vacuolation in their brain regions as compared to the moPrP^{res}+LPS treatment group. In addition, this difference was similarly observed in terms of distribution patterns of vacuoles in the brain regions of terminally sick mice with the moPrP^{res} treatment showing widespread vacuolation as

compared to the limited distribution of vacuoles in terminally sick moPrP^{res}+LPS treated mice (Figure 2.4, i-p).

The PrP^{Sc} accumulation pattern and intensity in moPrP^{res}-treated terminally-sick mice was slightly more intense than moPrP^{res}+LPS treatment group (Figure 2.6, i-p). However, both treatment groups did not differ greatly from the negative controls with regards to PrP^{Sc} staining and were subjectively different when compared to the terminally sick positive controls (Figure 2.6, a-d and u-x). Results from astrogliosis staining demonstrated slightly more intense astrocyte presence in the moPrP^{res}+LPS treatment group in the Cc, Th, and Mb in comparison to the moPrP^{res} treatment animals (Figure 2.7, i-k and m-o), whereas the Cr of the moPrP^{res}-treated mice had more intense astrocyte accumulation in comparison to the moPrP^{res}+LPS treatment group (Figure 2.7, l and p). In both PrPres-treated groups there were no signs of Ap deposition in the brain of terminally sick mice (Figure 2.8, i-o).

3.4. Western blot

Western blot analyses and PK treatment of brain homogenates and spleen samples were conducted to determine whether disease-associated PrP-res could be detected at 11 wk pi in both euthanized and terminally sick FVB/N female mice infected with LPS, moPrP^{res}, or RML (Figure 2.9). Results showed that both brain and spleen homogenates of saline-treated mice had no bands of PrP-res (Figure 2.9, lanes 1 and 11). In addition, the positive RML-treated controls showed no band at 11 wk pi and PrP-res band at terminal sickness in their corresponding brain homogenates (Figure 2.9A, lanes 9 and 10). Of note, early euthanasia of RML-treated mice at 11 wk pi with no clinical signs of prion disease exhibited detectable levels of PrP-res in their spleen homogenates (Figure 2.9B, lane 19). This was indeed accompanied by detectable levels of PrP-

res in the spleen homogenates of terminally sick mice of the RML treated group (Figure 2.9B, lane 20). The RML+LPS treated group showed similar results with the RML having intense levels of PrP-res in its brain homogenates of terminally sick mice (Figure 2.9A, lane 10) and detectable levels of PrP^{res} in the spleen homogenates at 11 wk pi and terminal sickness (Figure 2.9B, lanes 17 and 18). All groups treated with LPS and/or moPrP^{res} showed no detectable PrP^{res} in both brain and spleen homogenates at 11 wk pi or terminal sickness (Figure 2.9, lanes 2-7 and 12-16).

3.5. Scrapie cell assay

The L929 mouse fibroblast cell line was used to be infected with brain homogenates of terminally sick mice from each treatment group to visualize prion infected cells. Therefore, a number of cells were loaded onto plates of ELISPOT with subsequent treatment with PK digestion. All negative control wells including uninfected saline brain homogenates and L929 cells showed no positive signal. All positive RML controls together with the RML+LPS treatment group exhibited a PrP^{Sc}-positive signal (Figure 2.10). All other treatment groups administered LPS and/or moPrP^{res} showed a PrP^{Sc}-negative signal with lower values than the cut off value (Figure 2.10).

4. Discussion

4.1. Infectivity and pathogenicity of LPS-converted recombinant moPrP^{res}

We hypothesized that *in vitro* LPS-converted recombinant mouse PrP^{res} (29-232) would cause prion-like pathology in FVB/N wild type female mice. Indeed, results showed that moPrP^{res} developed under normal incubation protocol without seeding or PMCA treatment could lead to neurodegeneration when inoculated sc to healthy wild type FVB/N female mice

exhibiting typical prion clinical signs and brain vacuolation. Our data showed that moPrP^{res} does lead to widespread vacuolation (i.e., neuronal death) in different regions of the brain, comparable to the positive controls, with similar clinical signs of typical prion infected mice. This vacuolation pattern, however, had bigger sized vacuoles in comparison to RML inoculated mice. This is further supported by aggravated astrogliosis in the cerebellum of moPrP^{res}-treated mice together with mild astrogliosis of other brain regions in the moPrP^{res}+LPS treatment group. Another difference observed between the moPrP^{res} treatment and the positive controls (i.e., RML) was the incubation time needed for the prion isoform to propagate and reach the CNS together with the mortality rate. The difference consisted in the finding that 80% of the RML-treated animals were euthanized within the first 250 dpi, whereas only 20% died later. The moPrP^{res} treatment groups had 20-30% mortality rate between 100-250 dpi with another 40% dying after 500 dpi. This could be due to the dose of moPrP^{res}, and the fact that this treatment contained pure recombinant prion protein rather than a brain homogenate mixture (i.e., RML) containing various factors including multiple cytokines and immune cells that might influence development of inflammation and progression of brain disease. In addition, the subcutaneous route of inoculation used in this experiment requires longer incubation days for the prion agent to propagate to the CNS (Chianini et al., 2013). Sixty percent of the mice receiving subcutaneous moPrP^{res} inoculum developed clinical signs of prion-like disease accompanied with histological spongiform alterations in various brain regions similar to the RML-inoculated positive controls. On the other hand the moPrP^{res}+LPS treatment group had a mortality rate of 50% at termination of the experiment. This suggests that LPS did not aggravate brain neurodegeneration caused by moPrP^{res}.

It should be pointed out that the H&E staining of the brain slides from moPrP^{res}-treated mice showed comparable vacuolation with the RML-treated ones, whereas, the PrP^{Sc} staining did not show similar prion accumulation in comparison to the positive controls. The underlying concept of this histological staining is based on a specific antibody used to detect the target protein. Since moPrP^{res} is a newly developed recombinant prion protein, there is no specific antibody developed for its detection. Therefore, this might be an explanation for the low detectability of moPrP^{res} in PrP^{Sc}-staining results. Another explanation might be related to the dose of moPrP^{res} used. A random dose of the protein was chosen and warrants further investigation to determine the right amount of moPrP^{res} that needs to be inoculated. To the best of our knowledge, this is the first report of a recombinant prion protein developed *in vitro* without seeding factors or PMCA treatment that leads to clinical signs and brain spongiform vacuolation similar to prion pathogenesis. Also, the Western blot results showed no detectable bands of PrP^{Sc} in moPrP^{res}-treated groups. This could be related to the low levels of our recombinant PrP in specific brain regions of the infected mice, which was diluted by homogenization with other brain regions and therefore not in sufficient amount to be detected by Western blot analysis. The scrapie cell assay (SCA) using L929 mouse fibroblast cell line was also incapable of infecting the host cells. This again may be due to the same reasons related to low levels of moPrP^{res} in the brain homogenates derived from the infected mice or may be related to the fact that murine fibroblast cell line L929 is more prone to replicating the 22L, RML, and ME7 prion strains (Vorberg et al., 2004; Mahal et al., 2007) than this new strain of prion.

4.2. Prion-like pathogenesis induced by LPS-only inoculation

Increasing evidence has shown the role of polyanions, specifically RNA, and proteoglycans in the brain homogenate as potential cofactors promoting de novo prion conversion (Deleault et

al., 2012; Ma, 2012; Wang et al., 2012). Various trials using multiple cofactors including RNA or lipids have been attempted for in vitro development of pathogenic recombinant prion protein (Wang et al., 2010). However, most, if not all of these procedures require PMCA accompanied with brain homogenate as substrate, presumably containing various levels of bacterial contamination to form a recombinant pathogenic prion isoform (Wang et al., 2010; Deleault et al., 2012). In this study we showed the significance of LPS as a potential cofactor in converting mouse PrP (29-232) into a misfolded, β -sheet abundant, and PK-resistant isoform, which showed the ability to infect more than half of the healthy wild type FVB/N female mice through a sc route of inoculation. Others have also used highly purified *E. coli*-expressed PrP causing TSE in healthy wild type mice and hamsters (Kim et al., 2010; Makarava et al., 2010; Wang et al., 2011; Deleault et al., 2012; Deleaultb et al., 2012). *Escherichia coli* is a GNB with the outer membrane very rich in LPS molecules (Van Amersfoort et al., 2003). It is assumed that any purified recombinant prion protein derived from GNB would be amplified, presumably, under abundant presence of and in contact with LPS in the cytoplasm and cellular membrane of GNB (Wang and Quinn, 2010). To the best of our knowledge, there has been no direct report on the role of bacterial LPS as a cofactor in prion conversion. This investigation is the first to report the novel role of Gram-negative-derived bacterial LPS as a potential cofactor in prion conversion leading to prion-like infectivity, pathogenicity and brain degeneration in healthy wild type murine models.

Most importantly, none of the cofactors so far have been proven to induce prion infectivity directly without further inoculation of any infectious prion agent when inoculated to healthy wild type animal models. As part of the observations in this research, the LPS-only treated mice have shown increased weight values throughout majority of the experiment

maintaining high body weights (Figure 2.1). Previous reports (Cani et al., 2007) show that chronic subcutaneous administration (4 wk) of LPS has led to increased body weights and caused insulin resistance and obesity. The accumulated adipose tissue in the abdominal region of the LPS-treated mice has been denoted to be a reservoir of various inflammatory factors associating obesity with inflammatory markers and poor wound healing (Lawrence et al., 2012). In addition, chronic sc administration of LPS in female FVB/N mice for 6 wk led to 40% mortality rate with accompanied prion-like clinical signs. Further investigations in H&E brain slides showed widespread vacuolation in various regions of the brain specifically the Cc, Th, Mb, and Cr compared to the positive RML controls (Figure 2.4, e-h and u-x). Of note, vacuoles of the LPS-only treated mice had bigger size than the positive controls in similar brain regions at terminal sickness. On the other hand, the negative control group did not show spongiform vacuolation in comparable brain regions (Figure 2.4, a-d). Moreover, there was a substantial difference in the terminal sickness PrP^{Sc} staining between the LPS treatment group in comparison to the positive and negative controls with the RML treatment mice having more PrP^{Sc} accumulation and the saline-treated mice having no sign of PrP^{Sc} accumulation. In addition, the staining for astrogliosis and Ap of the LPS-only treated animals showed severe astrogliosis and Ap deposition in the cerebellum of this treatment group as compared to the RML-treated mice. Furthermore, the SCA analysis showed no signal of PrP^{Sc} in brain homogenates of terminally sick LPS-treated mice. However, the longer incubation days associated with chronic subcutaneous administration of LPS (Figure 2.2), nearly twice the positive control, together with less than half the mortality rate of the RML positive controls does implicate the time consuming procedure required to induce brain neurodegeneration when inoculating only LPS without using any prion agent. This finding supports other reports (Johansson et al., 2005; Qin et al., 2007;

Xing et al., 2011) on a potential role of bacterial LPS in induction of brain neurodegeneration without the need of horizontal transmission of prion agent. This is while LPS in our experiment has been administered in a chronic manner over 6 wk using the subcutaneous route whereas others may have used short-term or one time injection of LPS (Johansson et al., 2005; Qin et al., 2007; Xing et al., 2011).

4.3. Aggravation of prion pathogenesis in the presence of LPS in conjugation with RML

The level of prion infectivity has been associated with presence of available cofactors (Ma, 2012). In addition, in vitro developed cofactors known up-to-date have shown to enhance prion infectivity when administered to healthy animal models (Ma, 2012). Lipopolysaccharide has long been known as a major factor aggravating brain degeneration in most neurodegenerative disorders (Sly et al., 2001; Sheng et al., 2003; Nguyen et al., 2002; Qin et al., 2007). Existing disease conditions tend to accelerate sickness behavior after systemic administration of LPS (Murray et al., 2011). In the context of a progressing disease, systemic inflammatory challenge with LPS has shown, not only to expedite the disease, but also lead to a cognitive dysfunction and neuronal death (Murray et al., 2011). The effect of LPS has been mainly investigated with regards to immune activation of the host and effects of inflammatory orchestrated brain degeneration (Amor et al., 2010; De Pablos et al., 2011; Murray et al., 2011). Direct and indirect impact of LPS administration in cases of Alzheimer's or Parkinson's diseases has shown to alter amyloid- β processing, neurotoxicity, and further damage to the dopaminergic neurons (Sly et al., 2001; Gao et al., 2002; Qin et al., 2007; Block and Hong, 2005) specifically at times of LPS-induced chronic inflammation (Cunningham et al., 2005; Perry et al., 2007).

In our experiment, we showed that chronic sc administration of LPS over 6 wk in conjunction with a one-time sc injection of RML scrapie prion strain aggravated prion accumulation in different brain regions including the Cc, Th, Mb, and Cr in comparison to RML-only inoculated mice at terminal sickness. This difference is both in terms of vacuolation intensity and PrP^{Sc} accumulation and astrogliosis (Figure 2.4, and 6, and 7, q-x). This comparison is also valid at 11 wk euthanasia with the RML+LPS treated animals showing slightly more vacuolation pattern and PrP^{Sc} accumulation specifically in the Cc, Th, Mb, and Cr (Figure 2.3 and 5, q-x) compared to the RML-treated group. This was also accompanied with a lower numerical value of incubation days for the RML+LPS treatment in comparison to the RML-treated animals (Figure 2.2). The deaths from the RML+LPS treatment group started earlier with all the animals dying sooner and in a shorter time-length compared to the RML only treated animals (Figure 2.2). Deaths from the RML+LPS treatment group were accompanied with typical prion clinical signs, similar to observations from the RML treatment group. Furthermore, weight comparisons between the two treatment groups showed a sudden drop of weight during 30 to 39 wk of age in the RML+LPS treatment while the positive control group maintained its average weight throughout the experiment (Figure 2.1). Weight comparisons showed statistical difference between the RML+LPS treated group and both control groups (i.e., negative and positive) at 39 wk of age (Figure 2.1). Western blot results showed similarity in the RML and RML+LPS treatment groups, in the spleen and brain homogenates of terminally sick animals, with a detectable signal of PrP^{tes} (Figure 2.9 A and B, lanes 8, 10, 18, 20). Most interestingly, mice treated sc and euthanized at 11 wk pi with no clinical signs of prion disease exhibited a detectable band of PrP^{tes} in the spleen but not brain homogenates (Figure 2.9 A and

B, lanes 7, 9, 17, 19). The SCA results also showed a similar PrP^{Sc}-positive signal for both RML and RML+LPS treatment groups (Figure 2.10).

When sc administration of LPS over 6 wk was accompanied with a one-time sc injection of pure recombinant moPrP^{res}, the effects were not comparable to when LPS was accompanied with RML. For instance, moPrP^{res}+LPS treated animals showed a 50% survival rate while the moPrP^{res} treatment group had only 40% survival rate (Figure 2.2) with animals of both treatment groups exhibiting prion-like clinical signs. The weight trend comparison between the two moPrP^{res} treated groups showed similar trends throughout the experiment with no statistical difference between them (Figure 2.1). The IHC staining of both moPrP^{res} treated groups at 11 wk pi and terminal sickness showed similar vacuolation patterns and PrP^{Sc} accumulation while the staining for astrogliosis showed aggravation in the Cr region only in terminally sick mice (Figure 2.3-8 and 4, e-1). In addition, the major characteristic found in the H&E brain slides of terminally sick moPrP^{res}-inoculated mice was the bigger size of the vacuoles when compared to the positive controls (Figure 2.4, u-x). Both the Western blot and SCA results were negative for all moPrP^{res}-treated groups showing no bands of PrP^{res} (Figure 2.9 A and B, lanes 3-6 and 13-16) or PrP^{Sc}-positive signals (Figure 2.10).

5. Conclusions

This study was aimed to validate the role of chronic sc LPS treatment on brain neurodegeneration and the LPS-converted mouse recombinant PrP^{res} in development of prion-like disease. Results showed that chronic sc administration of LPS for 6 wk was successful in leading to brain spongiform degeneration reflected in clinical signs and histological analyses of the infected terminally sick murine models over extended incubation days and accumulation of A β and microglia in cerebellum. Moreover, the LPS-converted moPrP^{res} was successful in

inducing 60% mortality rate when inoculated sc to wild type female mice accompanied with prion-like clinical signs and histological spongiform vacuolation in the brain as well as astrogliosis in the cerebellum region. Bacterial LPS also showed the ability to aggravate prion disease by increasing the number of brain vacuoles and further accumulation of PrP^{Sc}, and astrogliosis in different brain regions when administered with RML scrapie prions. In addition, sc RML-treated mice euthanized at 11 wk pi showed PrP^{res} accumulation in the spleen but not in the brain samples confirming previous reports that spleen might be monitored for initiation of prion disease.

6. Acknowledgment

We are thankful for the technical support of the staff at the Centre for Prions and Protein Folding Diseases (CPPFD) at the University of Alberta, especially Mrs. Hristina Gapeshtina and Dr. Jacques Van der Merwe for conducting the IHC staining and SCA tests, respectively. We also thank the CPPFD staff for continuous help and care to the mice in the experiment. We acknowledge the financial support of the funding agencies including Alberta Livestock and Meat Agency Ltd. (ALMA), Alberta Prion Research Institute (APRI), and Natural Sciences and Engineering Research Council of Canada (NSERC) for this project. We are grateful to the technical staff of the Centre for Prions and Protein Folding Diseases, University of Alberta, for their routine checkup and care of the mice.

References

1. Aguzzi, A., F., Baumann, and J., Bremer, 2008, The prion's elusive reason for being, *Annual Review of Neuroscience*, Volume 31, p. 439-477.
2. Ametaj, B. N., F., Saleem, V., Semenchenko, C., Sobsey, and D. S., Wishart, 2010, Lipopolysaccharide interacts with prion protein and catalytically converts it into a protein resistant β -sheet-rich isoform, *Prion Congress*, Salzburg, Austria.
3. Ametaj, B. N., S., Sivaraman, S. M., Dunn, and Q., Zebeli, 2012, Repeated oral administration of lipopolysaccharide from *Escherichia coli* 0111:B4 modulated humoral immune responses in periparturient dairy cows, *Innate Immunity*, Volume 18, p. 638-647.
4. Amor, S., F., Puentes, D., Baker, and P., van der Valk, 2010, Inflammation in neurodegenerative diseases, *Immunology*, volume 129, p. 154-169.
5. Block, M. L., and J. S., Hong, 2005, Microglia and inflammation-mediated neurodegeneration: Multiple triggers with a common mechanism, *Progress in Neurobiology*, Volume 76, p. 77-98.
6. Budka, H., 2003, Neuropathology of Prion Diseases, *British Medical Bulletin*, Volume 66, p. 121-130.
7. Canadian Council on Animal Care, 1993, Guide to the care and use of experimental animals, Volume 1, 2nd edition, Ottawa, Ontario, CCAC.
8. Cani, P. D., J., Amar, M. A., Iglesias, M., Poggi, C., Knauf, D., Bastelica, A. M., Neyrinck, F., Fava, K. M., Tuohy, C., Chabo, A., Waget, E., Delmee, B., Cousin, T., Sulpice, B., Chamontin, J., Ferrieres, J., Tanti, G. R., Gibson, L., Casteilla, N. M., Delzenne, M. C., Alessi, and R., Burcelin, 2007, Metabolic Endotoxemia Initiates Obesity and Insulin Resistance, *Diabetes*, Volume 56, p. 1761-1772.

9. Chianinia, F., S., Sisób, E., Ricci, S. L., Eatona, J., Finlaysona, Y., Panga, S., Hamiltona, P., Steele, H. W., Reida, C., Cantilec, J., Salesd, M., Jeffrey, M. P., Dagleisha, L., González, 2013, Pathogenesis of scrapie in ARQ/ARQ sheep after subcutaneous infection: Effect of lymphadenectomy and immune cell subset changes in relation to prion protein accumulation, *Veterinary Immunology and Immunopathology*, Volume 152, p. 348-358.
10. Cohen, F. E., and S. B., Pruisner, 1998, Pathologic conformations of prion proteins, *Annual Review of Biochemistry*, Volume 67, p. 793-819.
11. Combrinck, M. I., V. H., Perry, and C., Cunningham, 2002, Peripheral Infection Evokes Exaggerated Sickness Behaviour In Pre-Clinical Murine Prion Disease, *Neuroscience*, Volume 112, p. 7-11.
12. Cunningham, C., D. C., Wilcockson, D., Boche, and V. H., Perry, 2005, Comparison of inflammatory and acute phase responses in the brain and peripheral organs of the ME7 model of prion disease, *Journal of Virology*, Volume 79, p. 5174–5184.
13. Deleault, N. R., D. J., Walsh, J. R., Piroa, F., Wang, X., Wang, J., Ma, J. R., Rees, and S., Supattapone, 2012, Cofactor molecules maintain infectious conformation and restrict strain properties in purified prions, *PNAS*, Volume 109, p. 1938-1946.
14. Deleault^b, N. R., J. R., Piroa, D. J., Walsh, F., Wang, J., Ma, J. C., Geoghegan, and S., Supattapone, 2012, Isolation of phosphatidylethanolamine as a solitary cofactor for prion formation in the absence of nucleic acids, *PNAS*, Volume 109, p. 8546-8551.
15. De Pablos, V., C., Barcia, J. E., Yuste-Jimenez, F., Ros-Bernal, M. A., Carrillo-de Sauvage, E., Fernandez-Villalba, and M. T., Herrero, 2011, Acute Phase Protein's Levels as Potential Biomarkers for Early Diagnosis of Neurodegenerative Diseases, *Immunology, Allergology and Rheumatology*, Chapter 5.

16. Gao, H. M., J., Jiang, B., Wilson, W., Zhang, J. S., Hong, and B., Liu, 2002, Microglial activation-mediated delayed and progressive degeneration of rat nigral dopaminergic neurons: Relevance to Parkinson's disease, *Journal of Neurochemistry*, Volume 81, p. 1285–1297.
17. Hunter, N., J., Foster, A., Chong, S., McCutcheon, D., Parnham, S., Eaton, C., MacKenzie, and F., Houston, 2002, Transmission of prion diseases by blood transfusion, *Journal of General Virology*, Volume 83, p. 2897–2905.
18. Johansson, S., S., Bohman, A., Radesater, C., Oberg, and J., Luthman, 2005, Salmonella Lipopolysaccharide (LPS) Mediated Neurodegeneration in Hippocampal Slice Cultures, *Neurotoxicity Research*, Volume 8, p. 207-220.
19. Lassenius, M. I., K. H., Pietilainen, K., Kaartinen, P. J., Pussinen, J., Syrjanen, C., Forsblom, I., Porsti, A., Rissanen, J., Kaprio, J., Mustonen, P., Groop, M., Lehto, 2011, Bacterial Endotoxin Activity in Human Serum Is Associated With Dyslipidemia, Insulin Resistance, Obesity, and Chronic Inflammation, *Diabetes Care*, Volume 34, p. 1809-1815.
20. Lawrence, C. B., D., Brough, and E. M., Knight, 2012, Obese mice exhibit an altered behavioural and inflammatory response to lipopolysaccharide, *Disease Models & Mechanisms*, Volume 5, p. 649-659.
21. Liu, M., and G., Bing, 2011, Lipopolysaccharide Animal Models of Parkinson's Disease, *Parkinson's Disease*, Volume 2011, p. 1-7.
22. Ma, J., 2012, The role of cofactors in prion propagation and infectivity, *PLoS Pathogens*, Volume 8, p. 1-3.
23. Mahal, S. P., C. A., Baker, C. A., Demczyk, E. W., Smith, C., Julius, C., Weissmann, 2007, Prion strain discrimination in cell culture: The cell panel assay, *PNAS*, Volume 104, p. 20908–20913.

24. Makarava, N., G. G., Kovacs, O., Bocharova, R., Savtchenko, I., Alexeeva, H., Budka, R. G., Rohwer, I. V., Baskakov, 2010, Recombinant prion protein induces a new transmissible prion disease in wild-type animals, *Acta Neuropathology*, Volume 119, p. 177-187.
25. Murray, C. L., D. T., Skelly, and C., Cunningham, 2011, Exacerbation of CNS inflammation and neurodegeneration by systemic LPS treatment is independent of circulating IL-1b and IL-6, *Journal of Neuroinflammation*, Volume 8, p. 50-62.
26. Nguyen, M. D., J. P., Julien, and S., Rivest, 2002, Innate immunity: The missing link in neuroprotection and neurodegeneration?, *Nature Review*, Volume 3, p. 216–227.
27. Perry, V. H., C., Cunningham, and C., Holmes, 2007, Systemic infections and inflammation affect chronic neurodegeneration, *Nature Reviews Immunology*, Volume 7, p. 161-167.
28. Prusiner, S. B., 1982, Novel Proteinaceous Infectious Particles Cause Scrapie, *Science*, Volume 216, p. 136-144.
29. Qin, L., X., Wu, M. L., Block, Y., Liu, G. R., Breese, J. S., Hong, D. J., Knapp, and F. T., Crews, 2007, Systemic LPS causes chronic neuroinflammation and progressive neurodegeneration, *Glia*, Volume 55, p. 453–462.
30. Safar, J. G., M. D., Geschwind, C., Deering, S., Didorenko, M., Sattavat, H., Sanchez, A., Serban, M., Vey, H., Baron, K., Giles, B. L., Miller, S. J., DeArmond, and S. B., Prusiner, 2005, Diagnosis of human prion disease, *Proceedings of the National Academy of Sciences of the United States of America*, Volume 102, p. 3501-3506.
31. Schulz-Schaeffer, W. J., S., Tschoke, N., Kranefuss, W., Drose, D., Hause-Reitner, A., Giese, M. H., Groschup, and H. A., Kretzschmar, 2000, The Paraffin-Embedded Tissue Blot Detects PrPSc Early in the Incubation Time in Prion Diseases, *American Journal of Pathology*, Volume 156, p. 51-56.

32. Sheng, J. G., S. H., Bora, G., Xu, D. R., Borchelt, D. L., Price, and V. E., Koliatsos, 2003, Lipopolysaccharide-induced-neuroinflammation increases intracellular accumulation of amyloid precursor protein and amyloid β peptide in APP^{swe} transgenic mice, *Neurobiology of Disease*, Volume 14, p. 133-145.
33. Sly, L. M., R. F., Krzesicki, J. R., Brashler, A. E., Buhl, D. D., McKinley, D. B., Carter, and J. E., Chin, 2001, Endogenous brain cytokine mRNA and inflammatory responses to lipopolysaccharide are elevated in the Tg2576 transgenic mouse model of Alzheimer's disease, *Brain Research Bulletin*, Volume 56, p. 581–588.
34. Soto, C., 2011, Prion Hypothesis: the end of controversy?, *Trends in Biochemical Sciences*, Volume 36, p. 151-158.
35. Van Amersfoort, E. S., T. J. C., Van Berkel, and J., Kuiper, 2003, Receptors, Mediators, and Mechanisms Involved in Bacterial Sepsis and Septic Shock, *Clin. Microbiol. Rev.*, Volume 16, p. 379-414.
36. Vorberg, I., A., Raines, B., Story, S. A., Priola, 2004, Susceptibility of common fibroblast cell lines to transmissible spongiform encephalopathy agents, *The Journal of Infectious Disease*, Volume 189, 431–439.
37. Wang, F., X., Wang, C., Yuan, and J., Ma, 2010, Generating a Prion with Bacterially Expressed Recombinant Prion Protein, *Science*, Volume 327, p. 1132-1135.
38. Wang, X., and P. J., Quinn, 2010, Lipopolysaccharide: Biosynthetic pathway and structure modification, *Progress in Lipid Research*, Volume 49, p. 97-107.
39. Wang, F., X., Wang, and J., Ma, 2011, Conversion of bacterially expressed recombinant prion protein, *Methods*, Volume 53, p. 208-213.

40. Wang, F., Z., Zhang, X., Wang, J., Li, L., Zha, C., Yuan, C., Weissmann, and J., Ma, 2012, Genetic Informational RNA Is Not Required for Recombinant Prion Infectivity, *Journal of Virology*, Volume , p. 1874-1876.
41. Wolfs, T. G. A. M., J. P. M., Derikx, C. M. I. M., Hodin, J., Vanderlocht, A., Driessen, A. P., de Bruine, C. L., Bevins, F., Lasitschka, N., Gassler, W. G., van Gemert, and W. A., Buurman, 2010, Localization of the Lipopolysaccharide Recognition Complex in the Human Healthy and Inflamed Premature and Adult Gut, *Inflammatory Bowel Disease*, Volume 16, p. 68-75.
42. Xing, B., A. D., Bachstetter, and L. J., Van Eldik, 2011, Microglial p38 α MAPK is critical for LPS-induced neuron degeneration, through a mechanism involving TNF α , *Molecular Neurodegeneration*, Volume 6, p. 84-96.

Figure Captions

Figure 2.1. Weight comparison of FVB/N female mice. Monthly weights of different treatment groups including: 1) saline (negative control), 2) bacterial lipopolysaccharide (LPS), 3) moPrP^{res}, 4) moPrP^{res}+LPS, 5) RML+LPS, or 6) RML (positive control). Lipopolysaccharide or saline were administered for 6 wk through ALZET[®] osmotic mini pumps (ALZET, Cupertino, CA) implanted subcutaneously (sc). A one-time injection of moPrP^{res} or RML was given at the time of minipump implantation through a sc route. Comparisons show statistical differences between the LPS vs RML (at 35, 39, 43, 48, 52, and 66 wk), LPS vs saline (48, 52, 56, 66 and 110 wk; marked with a star), LPS vs RML+LPS (35 and 39 wks), LPS vs moPrP^{res} (43, 48, 52, 56, 61, 66, 70 and 74 wks), LPS vs moPrP^{res}+LPS (at 39, 43, 48, 52, 56, 61, 66, 70, 74, 102 and 110 wks), moPrP^{res} vs RML (35 wk), moPrP^{res} vs RML+LPS (at 35 and 39 wks), moPrP^{res}+LPS vs RML+LPS (at 39 wk), moPrP^{res}+LPS vs saline (56 and 70 wks), RML vs RML+LPS (39 wk), RML+LPS vs saline (39 wk).

Figure 2.2. Survival analysis of terminally sick FVB/N female mice. All mice were kept until 750 days post inoculation to monitor for clinical signs of prion disease and then euthanized/found dead after maintaining clinical signs for a minimum of 72 h. None of the negative controls (saline treated animals) showed clinical signs of prion disease with all but one (euthanized due to ear rupture and bleeding) found dead in the cage without any prior abnormalities. Most other treated animals were euthanized/found dead with prior clinical signs similar to prion disease. Twenty per cent of the RML positive controls maintained their survival up to experiment termination. Combination of RML with bacterial lipopolysaccharide (LPS) caused death sooner (before 150 days) and terminated with all mice dead before 250 days. Sixty percent of the moPrP^{res} treated mice died before termination of the experiment with 4 mice showing clinical signs. The moPrP^{res}+LPS had a mortality rate of 50%, with 3 mice showing clinical signs. Moreover, 40% of the LPS-treated animals showed clinical signs and euthanized subsequently.

Figure 2.3. Early demonstration of minor prion-like vacuolation in the Hematoxylin and Eosine staining of the brain of FVB/N wild type female mice (10X magnification). Mice treated with subcutaneous administration of bacterial lipopolysaccharide (LPS) from *Escherichia coli* 0111:B4 for 6 wk (e-h), mouse recombinant PrP resistant (moPrP^{res}) (i-l), moPrP^{res}+LPS (m-p), and RML+LPS (q-t) and euthanized at 11wk post inoculation show minor vacuolation in comparison to the positive (u-x) and negative (a-d) controls (RML and saline treatment groups, respectively), in various brain regions including cerebral cortex (Cc), thalamus (Th), midbrain (Mb), and cerebellum (Cr). Yellow arrows point to representative vacuoles in each picture.

Figure 2.4. Prion-like vacuolation profile in brain Hematoxylin and Eosine staining of terminally sick FVB/N wild type female mice (10X magnification). Mice euthanized/found dead with terminal prion-like clinical signs and sickness treated with subcutaneous lipopolysaccharide (LPS) from *Escherichia coli* 0111:B4 (e-h), mouse recombinant PrP resistant (moPrP^{res}) (i-l), moPrP^{res}+LPS (m-p), and RML+LPS (q-t) show major vacuolation in comparison to the positive (u-x) and negative (a-d) controls (RML and saline treatment groups, respectively), in various brain regions including cerebral cortex (Cc), thalamus (Th), midbrain (Mb), and cerebellum (Cr). moPrP^{res}-containing and LPS treatment groups show bigger sized

vacuoles compared to the RML-containing groups. Yellow arrows point to representative vacuoles in each picture.

Figure 2.5. PrP^{Sc} deposition in brains of FVB/N wild type female mice at 11wk post inoculation (10X magnification). Mice euthanized at 11wk post inoculation treated with subcutaneous administration of bacterial lipopolysaccharide (LPS) from *Escherichia coli* 0111:B4 (e-h), mouse recombinant PrP resistant (moPrP^{res}) (i-l), moPrP^{res}+LPS (m-p), showed minor PrP^{Sc} deposition, whereas the RML+LPS treatment (q-t) showed more PrP^{Sc} accumulation in comparison to the positive (u-x) and negative (a-d) controls (RML and saline treatment groups, respectively), in various brain regions including cerebral cortex (Cc), thalamus (Th), midbrain (Mb), and cerebellum (Cr).

Figure 2.6. PrP^{Sc} deposition in brains of FVB/N wild type female mice at terminal sickness (10X magnification). Mice euthanized at terminal sickness treated with subcutaneous administration of lipopolysaccharide (LPS) from *Escherichia coli* 0111:B4 (e-h), mouse recombinant PrP resistant (moPrP^{res}) (i-l), moPrP^{res}+LPS (m-p) show minor PrP^{Sc} deposition, whereas the RML+LPS treatment (q-t) shows aggravated PrP^{Sc} accumulation in comparison to the positive (u-x) and negative (a-d) controls (RML and saline treatment groups, respectively), in various brain regions including cerebral cortex (Cc), thalamus (Th), midbrain (Mb), and cerebellum (Cr).

Figure 2.7. Astrogliosis in brains of FVB/N wild type female mice. Mice euthanized at terminal sickness treated with subcutaneous administration of lipopolysaccharide (LPS) from *Escherichia coli* 0111:B4 (e-h), mouse recombinant PrP resistant (moPrP^{res}) (i-l), moPrP^{res}+LPS (m-p) show minor astrogliosis with only the cerebellum (Cr) region in moPrP^{res}-treated groups being aggravated, whereas the RML+LPS treatment (q-t) shows aggravated astrogliosis in comparison to the positive (u-x) and negative (a-d) controls (RML and saline treatment groups, respectively), in various brain regions including cerebral cortex (Cc), thalamus (Th), midbrain (Mb), and Cr.

Figure 2.8. Staining for amyloid plaque in brains of FVB/N wild type female mice. Mice euthanized at terminal sickness treated with subcutaneous administration of lipopolysaccharide (LPS) from *Escherichia coli* 0111:B4 (e-h), mouse recombinant PrP resistant (moPrP^{res}) (i-l), moPrP^{res}+LPS (m-p) show no Ap deposition with only the cerebellum (Cr) region in the LPS-treated group being accumulated. A similar pattern was also observed in the RML+LPS treatment (q-t) and the RML treatment group (u-x) in various brain regions including cerebral cortex (Cc), thalamus (Th), midbrain (Mb), and Cr with the only Ap deposition in the Cr of RML-treated mice.

Figure 2.9. Western blot of brain (A) and spleen (B) homogenates. FVB/N female mice were inoculated subcutaneously with saline (negative control) (lanes 1 and 11), lipopolysaccharide (LPS) from *Escherichia coli* 0111:B4 (lanes 2 and 12), mouse recombinant PrP resistant (moPrP^{res}) (lanes 3-4 and 13-14), moPrP^{res}+LPS (lanes 5-6 and 15-16), RML+LPS (lanes 7-8 and 17-18), and RML (positive control) (lanes 9-10 and 19-20). All samples were treated with 50 µg/mL proteinase K. All moPrP^{res}- and RML-containing treatment groups (lanes 3-10 and 13-20)

contain both 11 wk (lanes 3, 5, 7, 9, 13, 15, 17, and 19) and terminally sick (at 4, 6, 8, 10, 14, 16, 18, and 20) euthanized/found dead mice. Lane 0 contains the ladder.

Figure 2.10. Scrapie cell assay using L929 mouse fibroblast cell line and brain homogenates of terminally sick FVB/N female mice. Three brain homogenates collected from each of the terminally sick LPS, moPrP^{res} (PrPb), moPrP^{res}+LPS, RML+LPS and RML treatment groups were exposed to L929 (mouse fibroblast cell line, ATCC) cells in with a dilution series of 0.1 to 0.0001% in 6 replicates. Cut off value is 150 spots/20000 cells.

Figure 2.1.

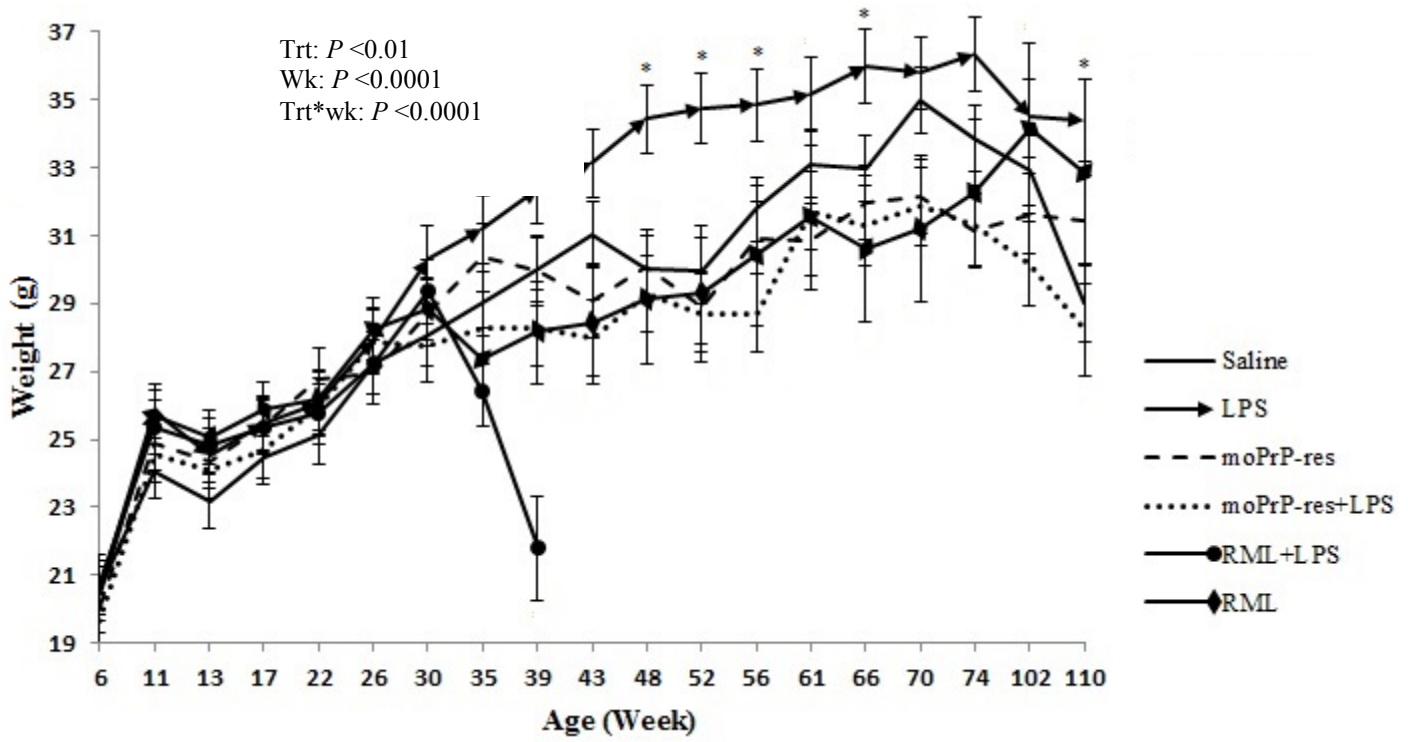


Figure 2.2.

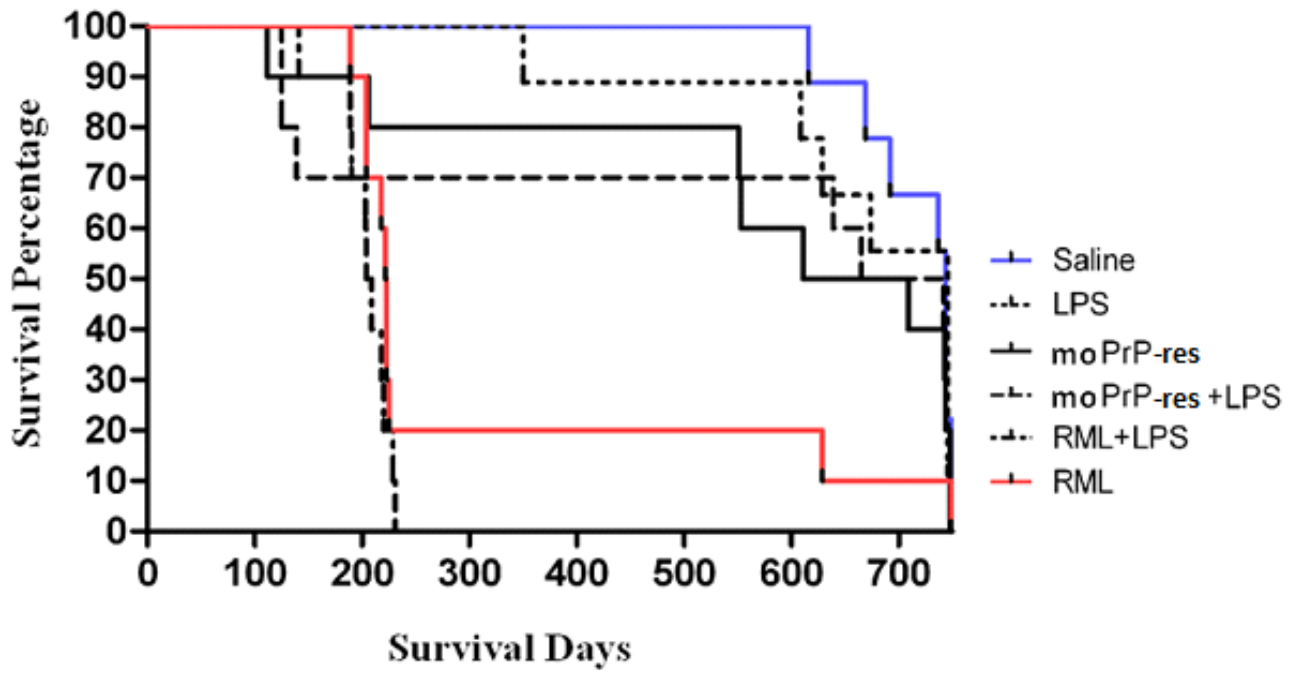


Figure 2.3.

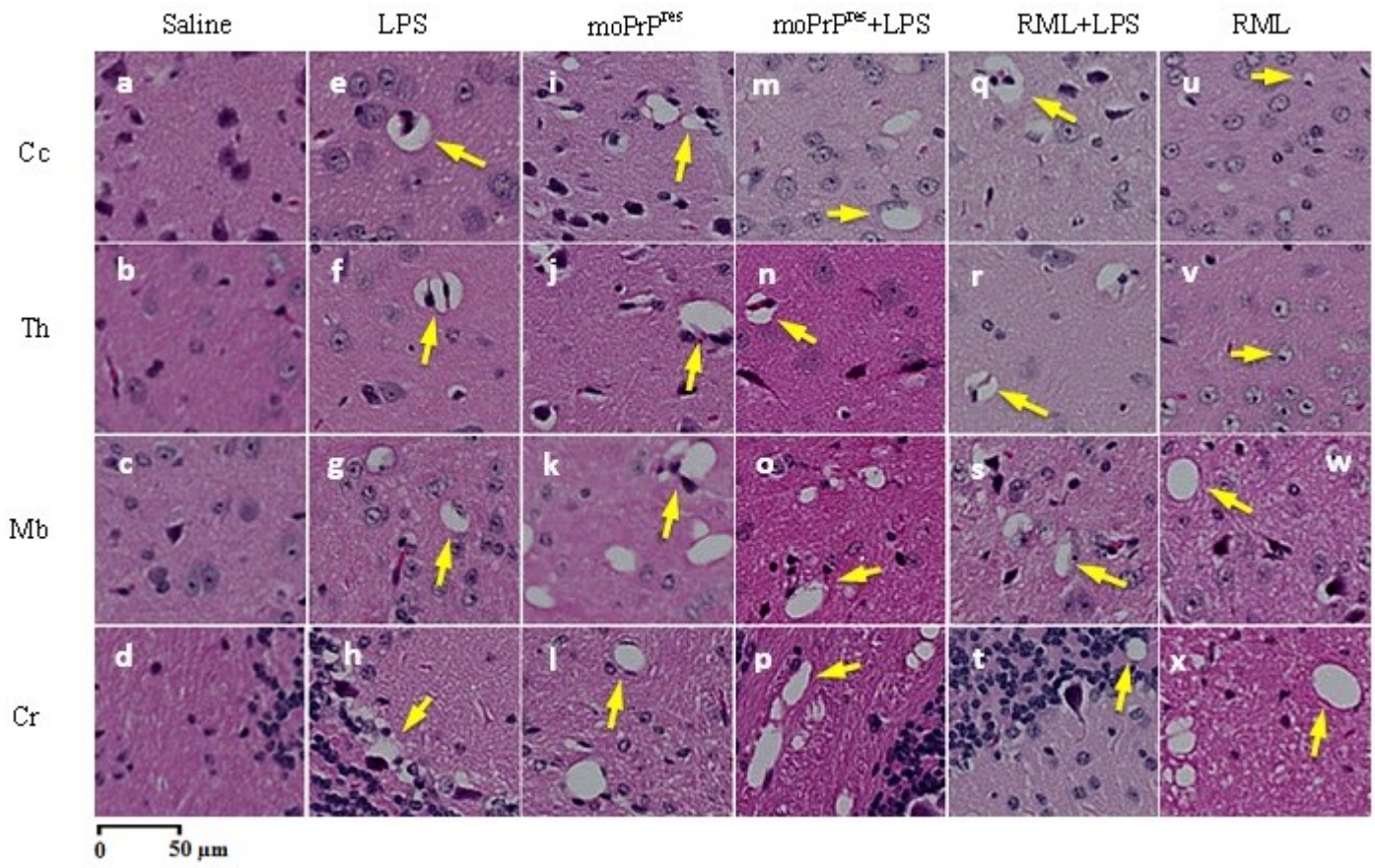


Figure 2.4.

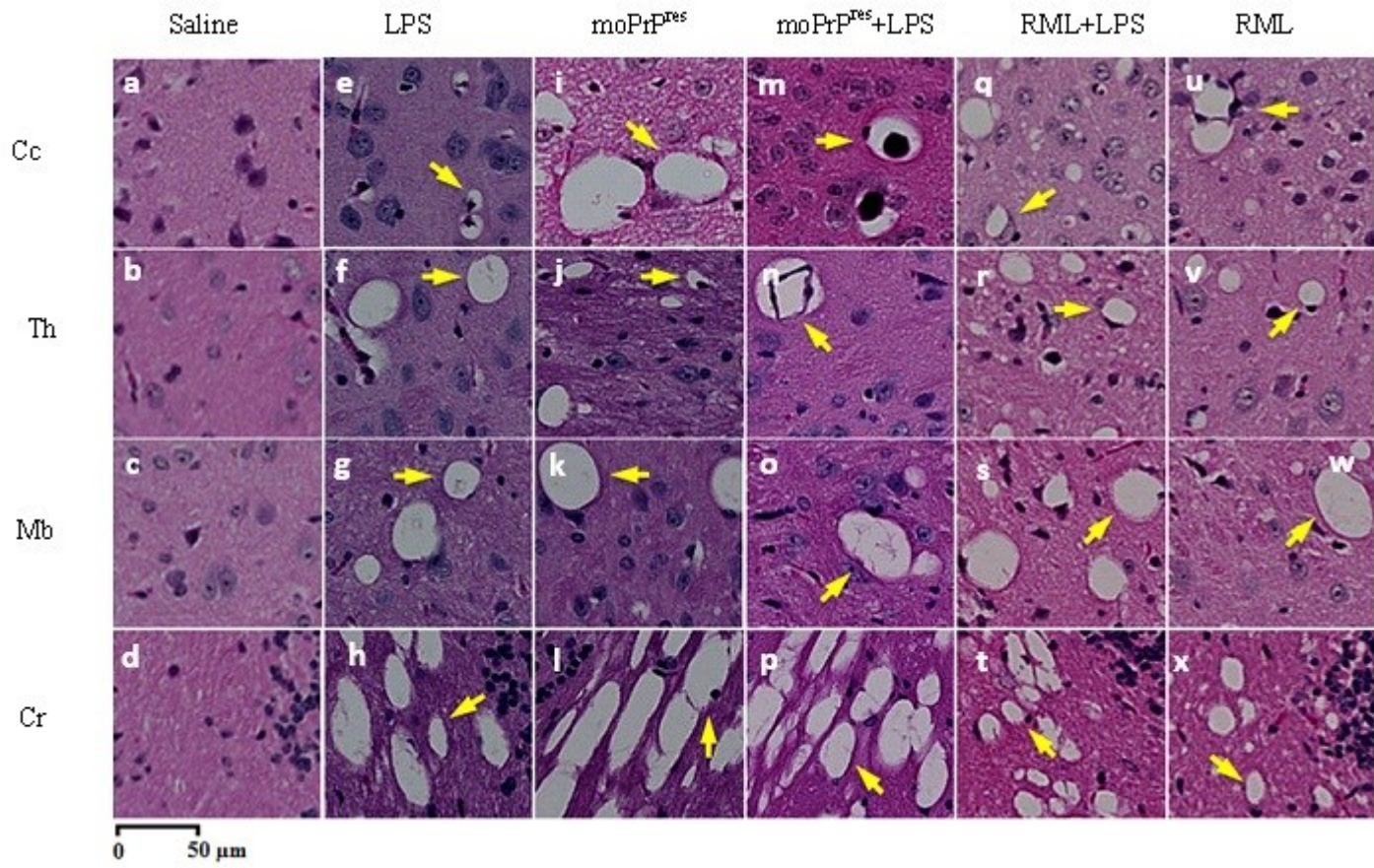


Figure 2.5.

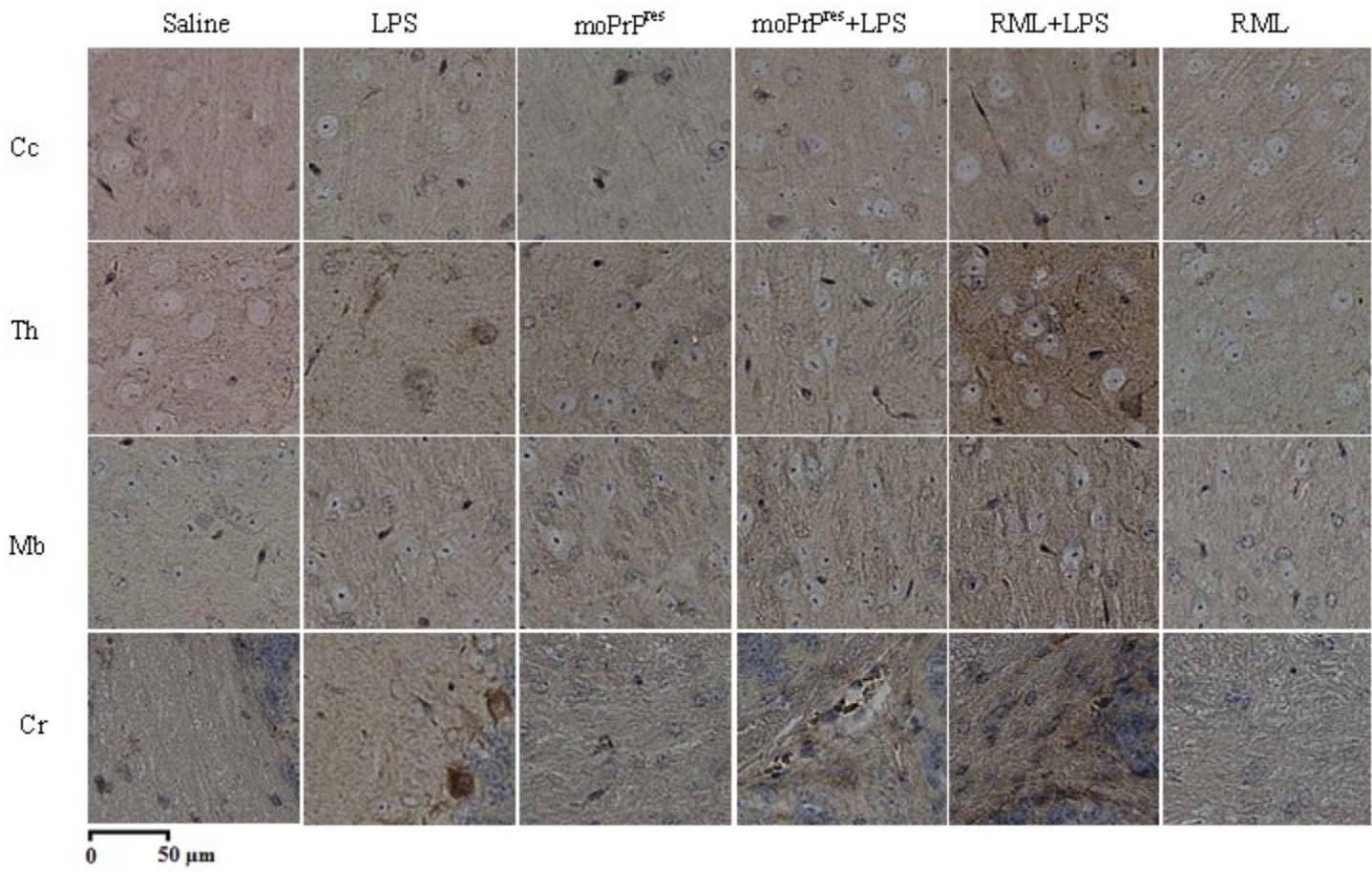


Figure 2.6.

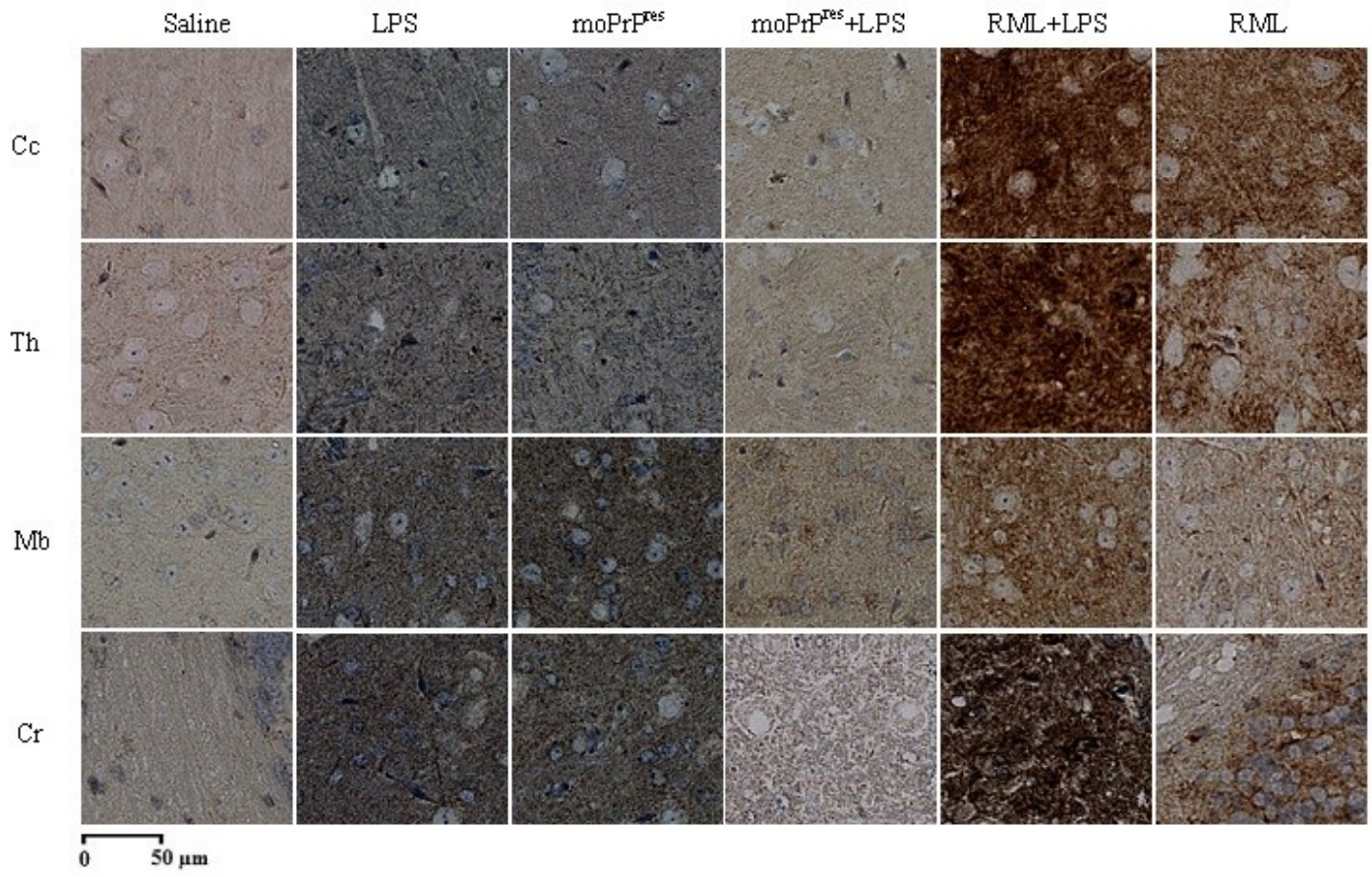


Figure 2.7.

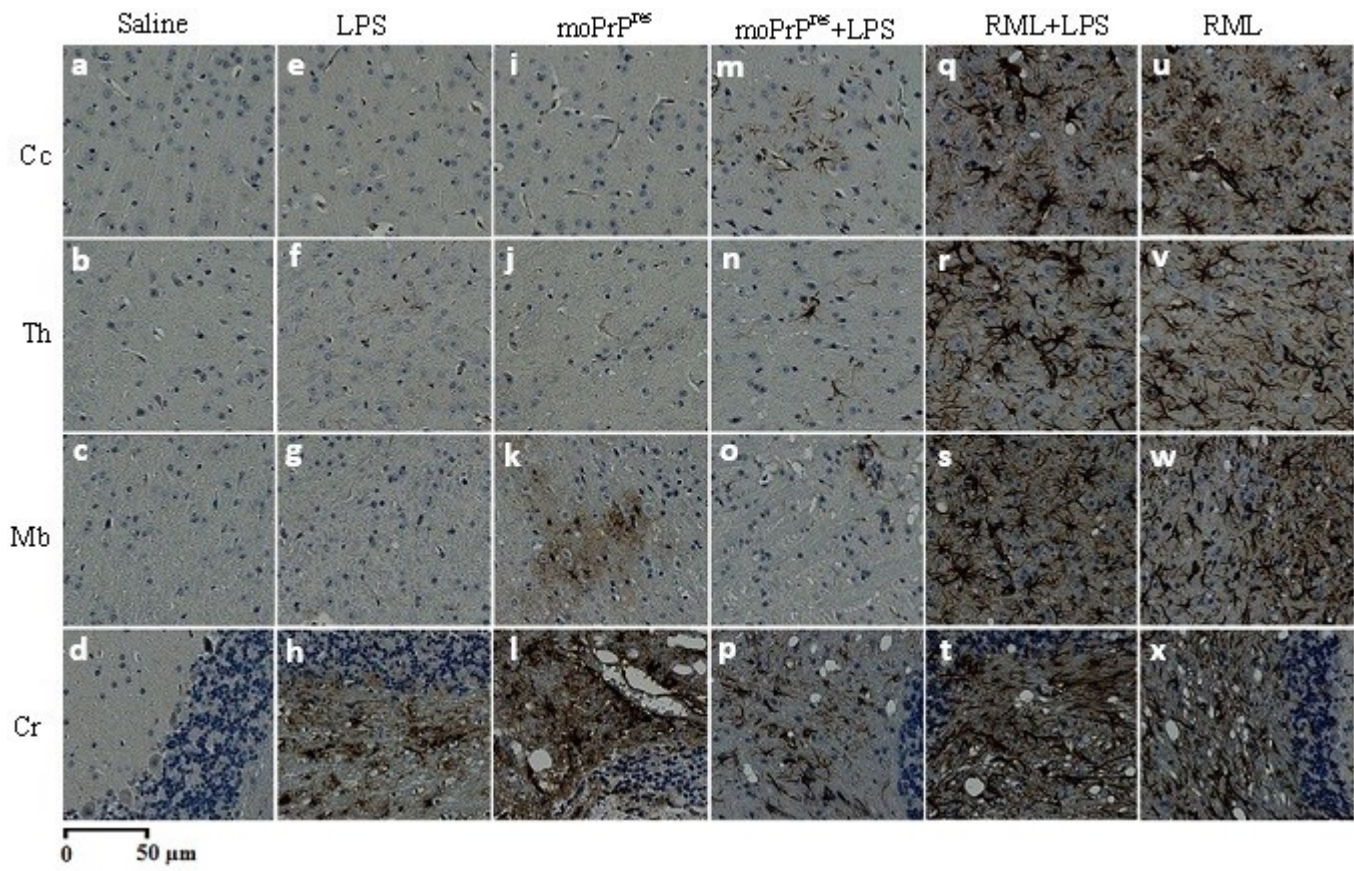


Figure 2.8.

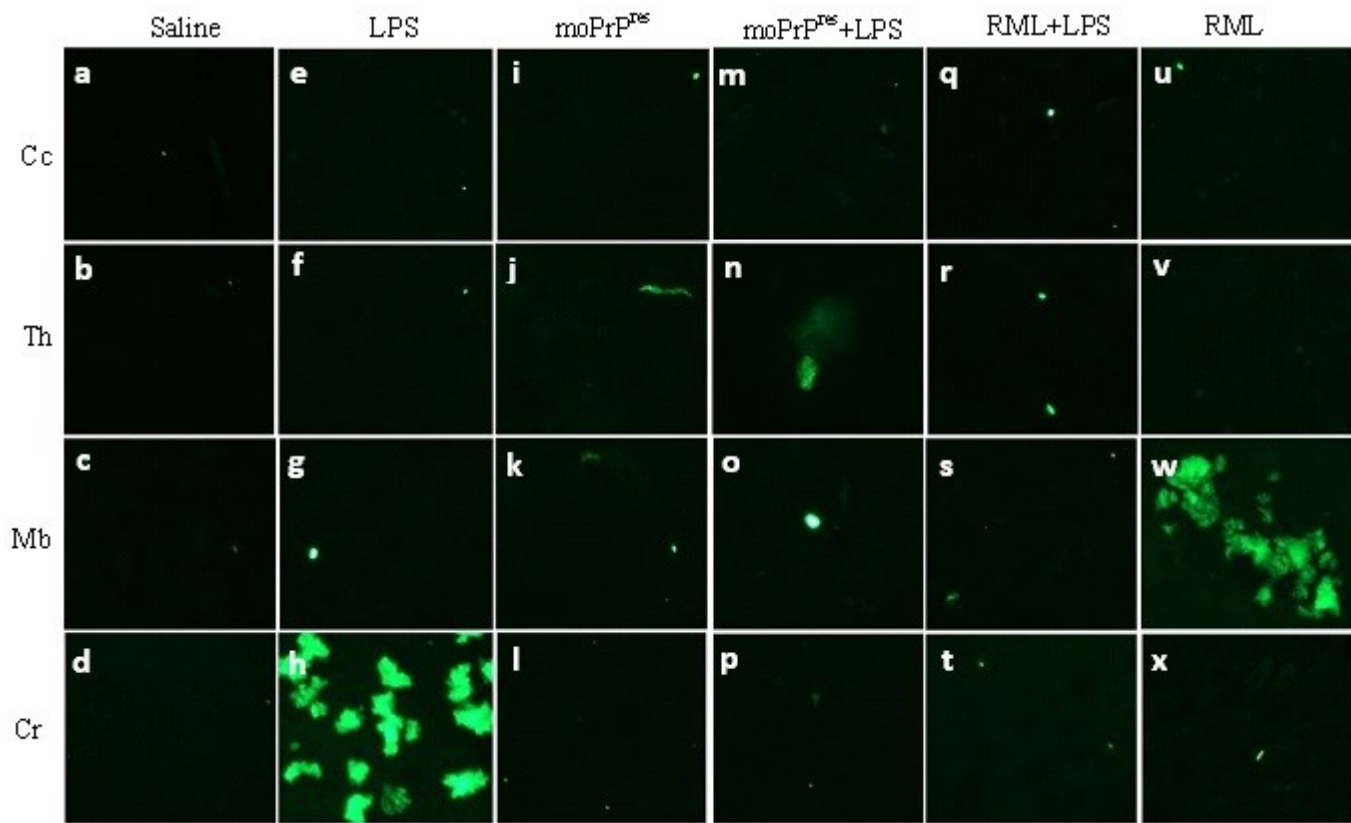


Figure 2.9.

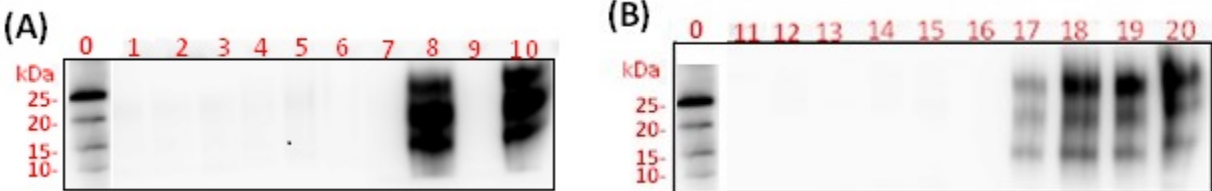
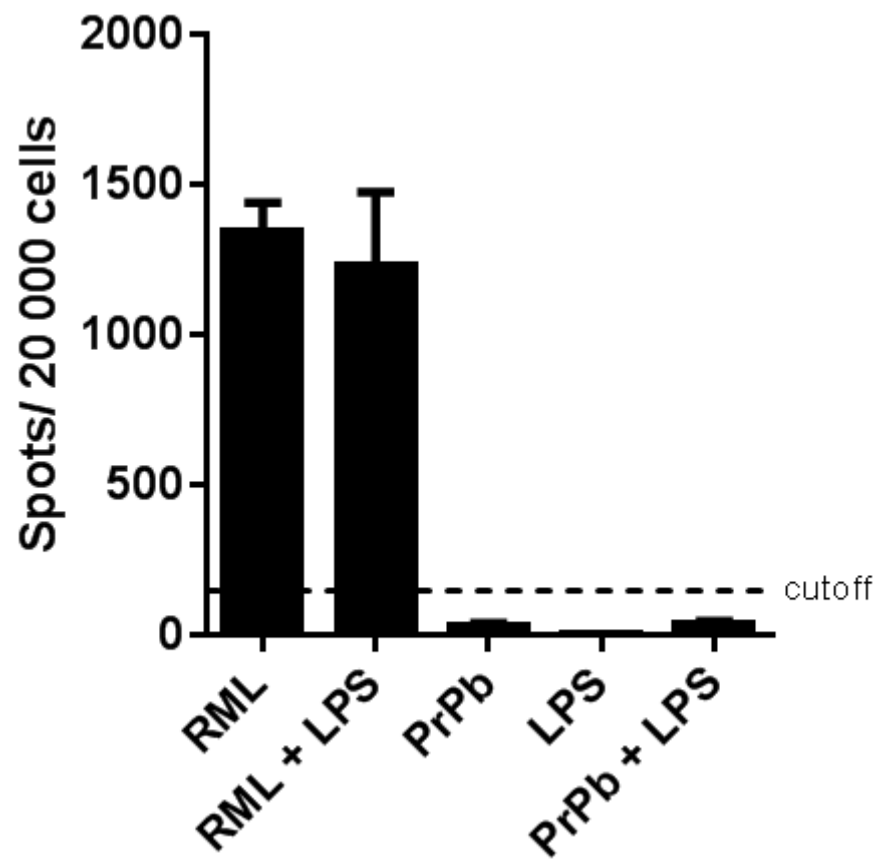


Figure 2.10.



**Chapter Three: Subcutaneous injection of lipopolysaccharide (LPS)-
converted mouse PrP^{res} or LPS alone are associated with brain gene
expression signatures typical of prion pathology**

Abstract

Transmissible Spongiform Encephalopathies (TSEs) or prion diseases are characterized by various alterations in the brain tissue of affected animals. Moreover, various strains of scrapie might affect different regions of the brain. The objective of this study was to evaluate whether subcutaneous (sc) injection of LPS-converted mouse (mo)PrP^{res} alone or combined with chronic sc administration of LPS, or chronic LPS-alone would be able to affect the expression of 84 brain tissue genes related to prion disease and inflammation in wild type FVB/N female mice. Ninety female FVB/N mice were randomly assigned to 6 groups (n=15 per group) and treated sc with: 1) 6-wk sc administration of saline at 11 μ L/hr, 2) 6-wk sc injection of LPS at 0.1 μ g/g BW at 11 μ L/hr, 3) 1 time sc injection of moPrP^{res} at 45 μ g/mouse, 4) 6-wk sc injection of LPS at 0.1 μ g/g BW at 11 μ L/hr plus 1 time sc injection of moPrP^{res} at 45 μ g/mouse, 5) 1 time sc injection of RML at 10^7 ID 50 units of scrapie prions, and 6) 6-wk sc administration of LPS plus 1 time sc injection of RML at 10^7 ID 50 units of scrapie prions. Five mice without clinical signs of illness were euthanized at 11 wk post-inoculation (pi), whereas the rest of the mice were allowed to develop disease and or were euthanized at terminal stage or at the end of the experiment. All brain samples were collected immediately after euthanization and frozen at -86 °C until analyses. A custom profiler RT PCR array was used to determine the expression of 84 genes related to prion pathology and inflammation. Results of this study showed that all treatments involved affected various genes related to prion disease and neuroinflammation starting at 11 wk pi and more profoundly at the terminal stage. Most importantly sc administration of de novo generated moPrP^{res} at terminal stage down-regulated expression of *Prnp* and *Sprn* but had no effect on *Prnd* indicating that moPrP^{res} induced a prion-like signature of genes in the treated mice.

Intriguingly LPS also down-regulated *Sprn* and up-regulated *Prnd* suggesting a potential role of LPS as co-factor in the etiopathology of prion disease. Moreover combination of moPrP^{res} with LPS, RML alone, or RML+LPS down-regulated both *Sprn* and *Prnp* and up-regulated *Prnd*. Several other genes related to brain neurodegeneration like *ApoE*, *Bax*, *Fyn* and other genes related to inflammation, apoptosis or anti-apoptosis, chemokines, neuron functions, oxidation processes and anti-oxidation were affected by various treatments. In conclusion, data from this study showed that sc administration of de novo generated moPrP^{res}, LPS, and combination of moPrP^{res} with LPS were able to cause differential expression of multiple genes typical of prion pathology and inflammation. More research is warranted to understand the role of bacterial LPS in the etiopathology of prion diseases.

Key words: mice, prion, lipopolysaccharide, brain genes, RML

1. Introduction

Transmissible spongiform encephalopathies (TSEs), or prion diseases are a group of fatal neurodegenerative disorders that are characterized by misfolding of cellular prion protein (PrP^C) into a pathogenic form, the scrapie prion protein (PrP^{Sc}). The scrapie or the misfolded form of the protein is commonly found in the brain tissue of affected animals and humans. This led Prusiner (1998) to the prion only hypothesis. The main challenge before the scientific community was to prove that indeed the misfolded protein (PrP^{Sc}) was the real causal agent of prion disease. Although there was very high scepticism about the potential role of a misfolded protein in the etiology of prion diseases several reports during the last decade proved that brain homogenates coming from sick animals or an *in vitro* generated misfolded protein might indeed cause typical prion disease in experimental animal models (Legname et al., 2004; Deleault et al., 2007; Barria et al., 2009; Makarava et al., 2010; Wang et al., 2010; Ma et al., 2013). Is this the end of our long search for the agent of prion disease? Not yet! There is still one drawback of all the reported investigations: they have used un-natural conditions to generate the infectious prions like serial rounds of protein misfolding cyclic amplification (PMCA) and long incubations periods, presence of RNA or other synthetic forms like polyriboadenylic acid, poly-anions like glucosaminoglycans (GAGs), denaturing acidic conditions, and synthetic lipids like 1-palmitoyl-2-oleoylphosphatidylglycerol (POPG) or phosphatidylethanolamine (Castilla et al., 2005; Wang et al., 2010; Deleault et al., 2012a, 2012b; Wang et al., 2012). The main issue with all these successful *in vitro* investigations is that the odds of these co-factors being present in the brain microenvironment is almost null. It is difficult to bring together sonication, free lipids, free nucleic acids, and extremely low pH or un-naturally high concentrations of urea in the brain microenvironment to cause prion disease. Therefore the search for potential and natural co-

factors that might be involved in prion disease is open. In addition there is a need to better understand what is happening in the brain at the beginning of the prion disease and at the end stage. More research is warranted with regards to using 'omics' sciences to reveal gene signatures in the central nervous system (CNS) or other tissues as early in the disease process as possible and use those data as potential indicators or biomarkers of disease.

Indeed, various studies during the last decade have identified numerous genes differentially expressed in the brain tissue of experimental animals infected with various scrapie strain isolates. Reimer et al. (2000) reported up-regulation of 19 genes in hamsters infected intraperitoneally with scrapie strain 263K. A considerable number of these genes including encoding interferon-inducible protein 10 (IP-10), 2',5'-oligo(A) synthetase, Mx protein, IIGP protein, major histocompatibility complex classes I and II, complement, and β 2-microglobulin were inducible by interferons (IFNs), suggesting that an IFN response is a possible mechanism of gene activation in scrapie. Xiang et al. (2004) also showed that mice infected with ME7 and RML differentially expressed genes encoding proteins involved in proteolysis, protease inhibition, cell growth and maintenance, immune response, signal transduction, cell adhesion, and molecular metabolism. Moreover Booth et al. (2004) found that intracerebral infection of C57BL/6 mice with mouse-adapted scrapie, ME7 and 79a, affected 158 genes in the brain tissue related to protease/peptidolysis, lysosomal functions, lipid-binding, defence- and immune-responses, cell communication, apoptosis, cell differentiation, regulation of cell growth and organization, hormone metabolism as well as ion and oxygen transport. Additionally Skinner et al. (2006) identified genes involved in cellular processes including protein folding, endosome/lysosome function, immunity, synapse function, metal ion binding, calcium regulation, and cytoskeletal function in experimental mice. In another study conducted by

Sawiris et al. (2007) in male mice, infected intraperitoneally with 301V BSE-infected mouse brain, 25 genes were differentially expressed including those involved in ubiquitin-mediated protein degradation, lysosomal function, protein folding, apoptosis, and calcium ion binding, transport and homeostasis in the brain tissue. It should be pointed out that three most important and signature genes that characterize prion disease and that have been reported to be affected by scrapie infection are *Prnp* and *Srpn* that decrease during prion disease and *Prnd* that increases during neurodegeneration (Westaway et al., 2011a, 2011b; Watts et al., 2011).

Recently, we showed that lipopolysaccharide (LPS) from *Escherichia coli* 0111:B4 is able to convert instantly and under normal pH, temperature, and natural conditions the Syrian hamster (Sh) PrP protein into a beta-rich isoform and resistant to proteinase K (ShPrP^{res}), very similar in physical characteristic with a prion (Ametaj et al., 2010). Lipopolysaccharide also similarly converted recombinant mouse PrP into a β -rich protein (moPrP^{res}; data not published) with the same physical features. We hypothesized that the in vitro generated moPrP^{res} might be infectious and cause neurodegenerative disease in FVB/N female mice and is associated with gene-expression signature typical of prion disease. Therefore the objectives of this study were to evaluate the effects of sc administration of moPrP^{res} alone or combined with chronic sc administration of LPS or chronic sc LPS alone in female FVB/N mice on the expression of 84 brain tissue genes related to prion disease and inflammation. We also wanted to test whether chronic sc LPS would exacerbate prion disease in Rocky Mountain Laboratory (RML)-infected mice.

2. Materials and Methods

2.1. Animals and experimental design

The FVB/N mice were housed in groups of 5 per cage under a 12 hour light/dark cycle where food and water were provided ad libitum. All the protocols used during the study were in accordance with the Canadian Council on Animal Care (1993) and were approved by Animal Care and Use Committee, Health Sciences at University of Alberta.

After one week of adaptation time, FVB/N mice at 5 weeks of age were randomly assigned to 6 treatment groups: 1) six wk sc administration of saline at 11 $\mu\text{L/hr}$, 2) six wk sc injection of lipopolysaccharide from *Escherichia coli* 0111:B4 LPS at 0.1 $\mu\text{g/g BW}$ at 11 $\mu\text{L/hr}$, 3) one time sc injection of de novo generated mouse recombinant prion protein (moPrP; 29-232) rich in β -sheet by incubation with LPS (moPrP^{res}) at 45 $\mu\text{g/mouse}$, 4) six wk sc injection of LPS at 0.1 $\mu\text{g/g BW}$ at 11 $\mu\text{L/hr}$ plus 1 time sc injection of moPrP^{res} at 45 $\mu\text{g/mouse}$, 5) one time sc injection of brain homogenate from Rocky Mountain Laboratory (RML) scrapie strain at 10^7 ID 50 units of scrapie prions, and 6) six wk sc administration of LPS plus 1 time sc injection of RML at 10^7 ID 50 units of scrapie prions. For the groups that involve saline or LPS sc administration, ALZET[®] osmotic mini pumps (ALZET, Cupertino, CA) were used, whereas the rest of the treatment groups. moPrP^{res} and RML were subcutaneously injected at the time of ALZET[®] osmotic mini pumps implantation, at the start of the experiment.

The ALZET[®] mini-osmotic pumps were implanted sc to mimic the continuous but minimal access of LPS to the body through the oral route. The sc infusion with ALZET[®] mini-osmotic pumps was done for six weeks continuously to eliminate the need for frequent animal handling and repetitive injection schedules. The sc infusion was performed according to the

manufacturers' procedure. Briefly, mice were anaesthetised by isoflurane (Baxter Corporation, Mississauga, Canada) and once the mouse was not responsive to tail pinch, a low and continuous isoflurane and oxygen was supplied using the anaesthetic machine (Matrx by Midmark corporation, Versailles, OH, USA). After shaving the hair and disinfection, a cut was made at the back of the mice using sterile surgical scissors. The ALZET[®] mini-osmotic pumps were inserted and the opening was closed with sutures (ALZET Osmotic Pumps, Cupertino, CA, USA). After 6 wk, the same procedure was repeated to take the empty pumps out and close the skin opening with sutures.

2.2.Euthanasia at 11 wk post inoculation (pi) and terminal stage

A total of 30 FVB/N female mice, 5 from each treatment groups were euthanized at 11 wk of age. Mice were euthanized by overdose inhalation of isoflurane. Using sterile scalpel, the brain tissue was sagittally cut in to two symmetrical halves where one half was snap frozen and stored in -86 °C until RNA purification while the other half was processed for immunohistochemistry staining.

The euthanasia of terminal stage mice was conducted at different time points. During the entire experimental period, mice were checked on a daily basis for the onset and progression of prion disease. Mice were euthanized when the clinical signs were consistent and progressive. Terminal stage sickness was characterized by kyphosis, ataxia, dysmetria, tremor, head tilt, tail rigidity, bradykinesia, proprioceptive deficits, stupor, loss of deep pain sensation, and loss of weight. The euthanasia and brain samples processing procedures were same as the described for euthanasia at 11 wk.

2.3.Total RNA isolation

Total RNA was isolated from brain and spleen tissues (n=3) using SV total RNA Isolation System (Promega Corporation, Madison, USA) following manufacturer's protocol. Briefly, brain and spleen samples were thawed at room temperature and 30 mg was taken for RNA isolation. Then after samples were lysed in 175 μ L RNA lysis buffer (RLA + BME) in autoclaved tube. After adding 350 μ L RNA dilution buffer (RDA), samples were heated at 70 $^{\circ}$ C for 3 min. Samples were then centrifuged for 10 min at 14,000xg (model 5430R, Eppendorf, Hamburg, Germany). The clear lysate was collected to a new collection 5 mL tube (Promega, Madison, USA) and 200 μ L (95%) ethanol (Commercial Alcohol, Winnipeg, Canada) was added. After transferring the lysate to spin basket assembly (Promega, Madison, USA) and centrifuged for 1 min, the lysate was washed with RNA wash solution. On-column DNA digestion was subsequently done using DNase I to remove any DNA contamination. After subsequent washing with washing buffers, total RNA was eluted with 100 μ L nuclease free water.

2.4.Custom-made PCR array

Custom profiler RT² PCR array was designed to investigate the expression of 84 genes in 96-genes in 1 sample per plate PCR array format. The 96 wells of the PCR array consisted of specific primers for 84 genes, genomic DNA contamination control (GDC), reverse transcription control (RTC) and positive PCR control. Genes related to prion pathology and inflammation was selected from literature. The gene symbol and ResSeq number for mouse was listed in Excel sheet and submitted to SABioscience (SABiosciences, Frederick, MD). The custom profiler RT²

PCR array was manufactured by SABioscience (SABiosciences, Frederick, MD) and run in StepOnePlus Real Time PCR System (Applied Biosystems, Foster City, USA).

2.5. First strand cDNA synthesis and quantitative PCR (qPCR) assay

All RNA samples were checked for their concentration and purity (based on 260/280 nm measurement) using Nanodrop 8000 instrument (peqLab Biotechnologies GmbH, Erlangen, Germany). Equal amount of RNAs (0.65 µg) from all the treatment groups were used for first strand cDNA synthesis using RT² miRNA first Strand kit (SABiosciences, Frederick, MD) following manufacturer's protocol. First genomic DNA elimination mix was prepared by combining 0.65 µg total RNA and 2 µL of 5x gDNA elimination buffer. Then, ddH₂O was added to a final volume of 10 µL. After gently mixing the contents with a pipette (Eppendorf, Hamburg, Germany) followed by brief centrifugation (Eppendorf, Hamburg, Germany), the mix was incubated at 42 °C for 5 min. Next, the RT cocktail was prepared by combining 4 µL of 5x RT buffer 3 (BC3), 1 µL of primer and external control mix (P2), 2 µL of RT enzyme mix 3 (RE3) and 3 µL of ddH₂O to a total volume of 10 µL reaction for each sample. Then, 10 µL of RT cocktail was added to each 10 µL of genomic DNA elimination mixture. After mixing gently with pipettor, the mix was incubated at 42 °C for 15 min and immediately heated at 95 °C for 5 min to stop the reaction. Finally, 91 µL of ddH₂O to each 20 µL cDNA synthesis reaction and stored at -20 °C until analysis.

Expression profiling of 84 genes in mice brain tissue was conducted using a custom RT²-PCR array (SABioscience, Frederic, USA) following manufacturers protocol. The 96-well custom RT²-PCR array was designed to quantify a total of 84 genes related to prion pathology and inflammation. Five housekeeping genes (*B2M*, *Actb*, *Gapdh*, *Gusb*, and *HSP90ab1*), 3

reverse transcription controls (RTC), 3 positive PCR controls, and mouse genomic DNA contamination controls were included in the 96-well plate. Prior to real time PCR profiling 91 μ L DNase/RNase-free water was added to each of the 20 μ L first strand cDNA product from each biological replicates in the treatment and the negative control groups. A PCR master mix was prepared using the 102 μ L diluted cDNA template, 1,350 μ L RT² SYBR Green PCR master mix and 1,248 μ L DNase/RNase-free water. Twenty-five μ L of this mix was distributed to each well of the 96-well plate containing sequence specific primer sets for each gene and the respective controls. Following brief centrifugation (Eppendorf, Hamburg, Germany), the plate was loaded onto StepOnePlus Real Time PCR System (Applied Biosystems, Darmstadt, Germany) and run with a thermal program of initial heating at 95 °C for 10 min followed by 40 cycles of 95 °C for 15 sec and 60 °C for 1 min. The specificity of amplification was controlled using a melting curve generated at the end of the PCR protocol.

2.6. Protein expression and purification

The expression and purification of mouse recombinant moPrP (29-232) was prepared as previously described in detail by Bjorndahl et al. (2011). Shortly, a synthetic gene including a 22-residue N-terminal fusion tag containing 6 x His and a thrombin cleavage site (MGSSHHHHHSSGLVPRGSHML) was synthesized by DNA 2.0 (Menlo Park, USA). The gene was cloned into a pET15b expression vector between *XhoI* and *EcoRI* restriction sites and heat shock transformed into *Escherichia coli* strain BL21 (DE3). For expression, the transformed cells were grown in 100 mL Luria–Bertani broth plus 100 μ g/mL ampicillin overnight to generate a starter culture. Between 1% and 2% of this starter culture was then used to inoculate 1 L of Luria–Bertani media (giving a starting D_{600} of 0.1). The cells were allowed to reach a D_{600} between 0.6 and 1.0 before induction with 1 mM isopropyl thiogalactoside. Twelve to eighteen

hours later, the cells were harvested by centrifugation at 1600 g for 25 min at 4 C. In addition, ^{15}N -labeled moPrP (90–232) was also expressed and purified from M9 media (1.0 g/L $^{15}\text{NH}_4\text{Cl}$) for collection of heteronuclear NMR data. The inclusion of the 6x His tag afforded a standardized nickel affinity purification strategy for the protein construct.

2.7. Statistical analysis

The mRNA expression of selected genes included in the custom PCR array was analyzed using $\Delta\Delta\text{CT}$ method from the PCR array data analysis web portal (<http://www.sabiosciences.com/pcrarraydataanalysis.php>). The software calculates average threshold cycle values for the biological replicates from both the treatment and control group for all the genes in the custom PCR array. Those genes having >35 ct values and undetected ones were removed from the analysis. Data was normalized by correcting all comparative threshold (CT) values for the average ct value of endogenous controls present in the array. After sequential computations, the software calculates fold regulation and associated t-test P value. Thus, fold change value >1.5 and $P \leq 0.05$ were taken as cutoff values to identify genes that are differentially expressed in the treatment groups as compared to the saline treated negative control group.

3. Results

3.1. Differentially expressed genes in the brains of mice treated at 11 wk postinfection

Brain tissues from mice euthanized at 11 wk pi were analyzed for genes related to prion disease and inflammation. Brains of mice treated with moPrP^{res} showed up-regulation of 2 genes (*Ifi2912a* and *Nos2*) and down-regulation of 3 genes (*ApoE*, *Sprn*, and *C1qb*) at 11 wk pi (Table 1). Results also indicated that treatment with LPS subcutaneously for a period of 6 wk down-

regulated 6 genes including *ApoE*, *Gbp4*, *Grn*, *Sod1*, *Bax*, and *Ccl17*. Combination of moPrP^{res} and LPS up-regulated 5 genes (*Tlr3*, *Tlr6*, *Nos2*, *Il1a*, and *Il1f10*) and down-regulated *C4b*. On the other hand RML down-regulated 5 genes (*C1qb*, *C4b*, *Grn*, *Anp32a*, and *Sod1*), whereas combination of RML with LPS down-regulated 3 genes (*C1qb*, *Rtp4*, and *Sod1*) and up-regulated *H2-T23* and *Ccl25*.

3.2. Differentially expressed genes in the brains of mice treated with moPrP^{res} and moPrP^{res}+LPS at terminal stage

The mRNA expression of Apolipoprotein E (*ApoE*), Shadow of prion protein (*Sprn*), Interferon induced transmembrane protein 3 (*Ifitm3*), Myeloid differentiation primary response gene 88 (*Myd88*), Bcl2-associated X protein (*Bax*), Fyn proto-oncogene (*Fyn*), Toll-like receptor 4 (*Tlr4*), Chemokine (C-C motif) ligand 5 (*Ccl5*) and Tumor necrosis factor (*Tnf*) was differentially regulated in the brains of mice treated with LPS converted moPrP as compared to saline treated negative control group (Table 2). Whereas 5 genes showed tendencies of differential expression ($0.05 < P < 0.1$) in the moPrP^{res} treated group. Among the differentially expressed genes six were up regulated (*Ifitm3*, *Myd88*, *Fyn*, *Tlr4*, *Ccl5*, and *Tnf*) and the remaining three were down regulated (*ApoE*, *Sprn* and *Bax*). *Ifitm3* showed the highest magnitude of up regulation with 4.2-fold change while *ApoE* and *Bax* were the most down regulated with -3.8 fold change. The magnitude of up regulation for genes that showed tendencies of differential regulation varies from 1.7 to 6.99 fold changes for *Lyz2* and *Tlr1*, respectively.

Importantly, the mRNA expression level of Apolipoprotein E (*ApoE*), Shadow of prion protein (*Sprn*), Glial fibrillary acidic protein (*Gfap*), ATPase, Na⁺/K⁺ transporting, beta 1 polypeptide (*Atp1b1*), Protein kinase, cAMP dependent, catalytic, alpha (*Prkaca*) was significantly reduced in the brain tissue of mice injected with moPrP^{res}+LPS. Moreover, seven genes (*Ncam1*, *Sod1*, *Bax*, *Fyn*, *Il18*, *Adam9*, and *Ache*) showed tendency reduced mRNA expression in moPrP^{res}+LPS as compared to the saline injected group (Table 1). *ApoE*, *Sprn*, and *Bax* were consistently down regulated in both moPrP^{res} and moPrP^{res}+LPS injected groups. The magnitude of *ApoE* mRNA down-regulation was 10-fold changes in moPrP^{res}+LPS injected group while, 3.77 fold change in moPrP^{res} alone treated group. The down-regulation of *Sprn* and *Bax* was comparable between the two groups.

3.3. Differentially expressed genes in the brains of mice treated with LPS

Subcutaneous chronic administration of LPS differentially expressed 19 genes as shown in Table 2. The most interesting genes are those related to *Sprn* and *Prnd*, which were down-regulated 3.20 fold or up-regulated >29 fold, respectively. Down-regulation of *Sprn* is a typical finding during prion disease. Also, up-regulation of *Prnd* has been associated with brain neurodegeneration. No effect of LPS was evidenced on *Prnp* expression. Lipopolysaccharide significantly down-regulated 8 genes including *ApoE*, *Ache*, *Sprn*, *Fcgr2b*, *Grn*, *Gfap*, *Bax*, and *Ccl19* (Table 2). On the other hand LPS up-regulated *Prnd*, *Iftm3*, *Fcgr3*, *H2-T23*, *Ly86*, *Anp32a*, *Ncam1*, *Mdk*, *Ccl17*, *Ccl25*, and *Tlr3* (Table).

3.4. Differentially expressed genes in the brains of mice treated with RML and RML+LPS

Brain samples from mice treated with RML+LPS showed 11 differentially expressed genes. Among those *Prnd*, *Clqb*, *Ly86*, *Lyz2*, and *H2-K1* were up-regulated while *Sprn*, *Prnp*, *Atp1b*, *Anp32a*, *Ncam1*, *Sod1*, *Prkaca*, and *Erg1* were down-regulated. *Atp1b1* showed the maximum down-regulation with 19-fold change, whereas *Lyz2* displayed the maximum up-regulation with 5.18-fold change. Three genes including *C4b*, *Ifi27i2a*, and *A2m* showed tendencies of up-regulation in the RML+LPS treated mice with 6.5, 8.2, and 6.5 fold changes, respectively.

Injection of RML alone increased significantly the expression of *Prnd*, *Lyz2*, and *Tlr3* and decreased the expression of *Sprn*, *Prnp*, *Atp1b1*, *Ncam1*, *Prkaca*, and *Erg1*. Among the down-regulated genes *Atp1b1* and *Erg1* showed relatively greater magnitude of down-regulation with -6.2 fold change. Moreover *Ache*, *Anp32a*, *Sod1*, and *Bax* showed tendencies of down-regulation, whereas *Fcgr3* and *Ly86* showed tendencies of up-regulation in the RML-injected mice as compared to the saline treated ones.

The expression of *ApoE* was significantly decreased in moPrP^{res} and moPrP^{res}+LPS treated groups whereas the expression of *Sprn* was universally decreased in mice treated with moPrP^{res}, moPrP^{res}+LPS, LPS, RML+LPS, and RML alone.

4. Discussion

Previously we showed that LPS from *E. coli* 0111:B4 instantly converted recombinant hamster and mouse PrP into a β -rich isoform PrP^{res} resistant to proteinase K (Ametaj et al., 2010). In the present study we tested the hypothesis that the moPrP^{res}, administered once sc,

would cause prion disease in FVB/N female mice and affect genes related to prion disease and inflammation in the brain of mice infected sc with moPrP^{res} at 11 wk pi as well as at terminally sick state. Indeed moPrP^{res} caused sickness and death in 60% of the experimental mice with clinical signs similar with prion disease (see previous article) and affected various brain genes at 11 wk pi as well as at the terminal stage. Moreover combinations of moPrP^{res} with LPS or treatment with RML, RML+LPS, and LPS alone also affected multiple genes at 11 wk pi and at terminal stage as will be discussed in more detail below.

Brain tissues from mice euthanized at 11 wk pi and after showing clinical signs of prion disease and terminated within a short period of time were tested for differential expression of 84 genes related to prion disease and inflammation. Although mice had no clinical sign of disease at 11 wk pi they were euthanized to explore gene expression in the brain for early effects of the treatments. Treatment with moPrP^{res} was the only one that down-regulated *Sprn* (shadow of prion protein) in the treated mice at this stage. The product of this gene, Sho, is typically decreased during scrapie disease and down-regulation of this gene at 11 wk pi is of interest and shows that moPrP^{res} is initiating prion disease very early in the infected mice.

Another gene (*C1qb*) was down-regulated by moPrP^{res}, RML, and RML+LPS at 11 wk pi. The complement protein C1qb binds to a very wide range of non-self and altered-self-materials. For instance, amyloid proteins are a group of altered-self-materials to which C1qb binds. Mabbott et al. (2001) showed that mice deficient in C1qb, or temporarily depleted of complement component C3 by treatment with cobra venom factor show longer survival

following scrapie infection, confirming that interactions between prion and complement at the very early stages of infection affects the course of neurodegeneration.

Nos2, which transcribes nitric oxide synthase, was up-regulated by moPrP^{res} and moPrP^{res}+LPS treatments at 11 wk pi. This enzyme is important because it affects production of nitric oxide (NO) and its overproduction may compromise energy production in neurons and initiate the process of neurodegeneration (Moncada and Bolanos, 2006).

Subcutaneous administration of LPS, RML, and RML+LPS down-regulated expression of *Sod1*, the gene that encodes transcription of the copper-zinc superoxide dismutase. The latter is a copper-dependent enzyme that catalyzes the conversion of superoxide radicals to hydrogen peroxide and water. Previous research work has demonstrated lack of neurodegeneration in *Sod1* knockout animals. Moreover, the generation of transgenic animals expressing mutant *Sod1* leads to motor neuron degeneration without reduction in *Sod1* activity (Haldano et al., 2001; Bruijn et al., 2004). Therefore down-regulation of this gene by several treatments in our study might be a protective response of the host to development of neurodegeneration.

Lipopolysaccharide and moPrP^{res} down-regulated expression of *ApoE*. Apolipoprotein E (apoE) has been involved in the development, remodeling, and regeneration of the nervous system. In the central nervous system (CNS), apoE is primarily synthesized and secreted by astrocytes (Pitas et al., 1987) and macrophages (Tedla et al., 2004) and its synthesis is increased after brain injury. Non-esterified cholesterol released after injury is esterified and transported by apoE to neurons undergoing reinnervation. It is not clear how *ApoE* was down-regulated during

these treatments; however, it is obvious that this might be one of the mechanisms of development of neurodegeneration observed in those groups of mice.

Lipopolysaccharide down-regulated *Gbp4* in the brain at 11 wk pi. Guanylate binding protein (GBP) 4 belongs to a group of IFN inducible GTPase families (Martens and Howard, 2006). The GBP family has 13 members, GBP1 to GBP13, sharing common structural features including an N terminal GTP binding domain and the common biochemical property of oligomerization-dependent GTPase activity (Shenoy et al., 2007). The functions of GBP4 are not clear yet. In a recent study Hu et al. (2011) showed that knockdown of endogenous *Gbp4* increased interferon regulatory factor (IRF7)-mediated interferon (IFN)- α production, whereas overexpression of *Gbp4* had the opposite effect. Atypical production of IFN is associated with many types of disease, such as cancers, immune disorders, and multiple sclerosis (Stetson and Medzhitov, 2006).

Mouse recombinant PrP^{res} and moPrP^{res}+LPS up-regulated *Il1a* and *Il1f10* at 11 wk pi. The interleukin 1 family includes 10 members (Dunn et al., 2001). Recent studies have uncovered some of the actions of the newer members of the IL-1 family (IL-1F5-10). For example IL-1F10 binds to the soluble IL-1 receptor (Lin et al. 2001) although the biological importance of these interactions is not fully understood. On the other hand IL-1 has been identified to have numerous actions in the CNS. Interleukin-1 is a polypeptide that exists in two different isoforms, IL-1 α and IL-1 β (Allan et al., 2005), known for their pro-inflammatory activities. Its elevation has been reported within brain lesions from patients with Alzheimer's disease (AD), Multiple Sclerosis (MS), Down's Syndrome, and HIV-associated dementia (Griffin et al., 1989; McGuinness et al., 1997; Stanley et al., 1994). Furthermore, increased IL-1 has been

detected in cerebral spinal fluid samples in MS, Parkinson's (PD) and Creutzfeldt-Jakob disease (CJD) (Hauser et al., 1990; Mogi et al., 1996; Van Everbroeck et al., 2002).

Several other genes that were differentially expressed by various treatments at 11 wk pi like *Grn*, *Bax*, *Ccl17*, *Ccl25*, *Tlr3*, *H2-T23*, *C4b*, and *Anp32a* and also at end stage of disease will be discussed in more detail below.

Interestingly the results showed that only one gene (i.e., *Sprn* - Shadoo (Sho) of prion protein) was differentially expressed by all treatments (moPrP^{res}, LPS, moPrP^{res}+LPS, RML, and RML+LPS) applied in this study at terminal sickness. Down-regulation of *Sprn* was more pronounced in the group of mice treated with moPrP^{res}+LPS (-3.46 fold) versus -3.20 fold in the LPS-treated mice, -3.13 fold in RML-treated mice as well as -2.39 and -1.94 fold in mice treated with moPrP^{res} or RML+LPS, respectively. Previously Premzl et al. (2003) showed that Sho is a neuronal glycoprotein and a member of the mammalian prion protein family, including PrP^C and Doppel (Dpl). Recently it was shown that there is a strong decrease of Sho protein in the brain of mice clinically ill with prion disease and that Sho has protective effects against prion disease (Watts et al., 2007; Westaway et al., 2011a). Additionally, lowered levels of endogenous Sho have been shown to trace an early response of PrP^{Sc} buildup in the CNS and that Sho down-regulation is a common and typical event in much of the prion strain isolates in vivo (Westaway et al., 2011a). Moreover, Westaway et al. (2011b) demonstrated a relationship whereby the degree of down-regulation of the mature Sho protein is inversely related to concentrations of PrP^{Sc}. Our data are the first to show down-regulation of *Sprn* in mice treated with moPrP^{res}, RML, LPS, and combinations of moPrP^{res} and RML with LPS and supports our hypothesis that

moPrP^{res} and other treatments caused prion-like disease in the infected mice. Intriguing was the down-regulation of *Sprn* by chronic subcutaneous LPS treatment. To our best knowledge this the first report that implicates LPS in the etiopathology of prion diseases and warrants further inquiry.

In a series of articles published recently by Westaway and associates (Watts et al., 2007; Westaway et al., 2011a; Westaway et al., 2011b; Daude and Westaway, 2012; Mays et al., 2014) and Prusiner and associates (Watts et al., 2011) it is indicated that a typical finding during prion disease is decreased Sho and PrP^C in the brain of animals or humans affected by prion disease. Decrease of Sho and PrP^C proteins are typical findings of prion disease and not present in other misfolding disorders like cytoplasmic accumulation of Tau in Tg(P301L)23027 mice (Murakami et al., 2006), and parenchymal and vascular accumulation of A β and Bri peptide in TgCRND8 and TgADanPP7 mice, respectively (Chishti et al., 2001; Watts et al., 2009; Coomaraswamy et al., 2010). Indeed expression of *Prnp* also was decreased by moPrP^{res}, moPrP^{res}+LPS, RML, and RML+LPS treatments. These findings strongly support clinical observations of prion-like disease in mice under those treatments. Of note is the lack of effect of LPS on *Prnp* gene, although LPS treatment decreased expression of *Sprn*.

Another important gene related to the prion family and involved in neurodegeneration in transgenic mice is *Prnd*. Unexpectedly all treatments involving LPS, moPrP^{res}+LPS, RML, and RML+LPS up-regulated *Prnd* more than 2-fold with LPS and RML+LPS at the top of the list (>29- and 10 fold, respectively). moPrP^{res} was the only treatment that did not have an effect on expression of *Prnd*. The latter gene encodes the protein Dpl which when ectopically up-regulated

has been shown to cause late-onset ataxia and apoptosis of Purkinje and granule cells in the cerebellum of experimental transgenic mice (Rossi et al., 2001; Moore et al., 2001). Although it is known that in healthy subjects Dpl is expressed mainly in testis and minimally in brain (Moore et al., 1999), recent research has demonstrated overexpression of *Prnd* in people with astrocytoma (Comincini et al., 2006). Of interest is that not only the RML treatments affected expression of Dpl but also treatments involving LPS and the combination of moPrP^{res} with LPS up-regulated *Prnd* expression. Further research is needed to define the precise role of moPrP^{res} and LPS in neurodegenerative processes in the brain and in the etiopathology of prion disease.

Two other important genes that are known to be associated with prion disease (i.e., *ApoE* and *Bax*) also were differentially expressed in 3 treatments involving moPrP^{res}, moPrP^{res}+LPS, and LPS compared with control mice. The gene encoding apoE was down-regulated 2.53 fold by LPS, more than 3 fold by moPrP^{res}, and more than 10 fold by moPrP^{res}+LPS treatment. It has been widely documented that apoE is present in high concentrations in neurons following brain injury (Horsburgh et al., 1997, 1999). Moreover, some studies have shown that increased *ApoE* expression leads to synaptic regeneration (White et al., 2001). In contrast, in *ApoE*-deficient mice, synaptic plasticity and regeneration are impaired (Krugers et al., 1997). Down-regulation of *ApoE* in our experiment suggests contribution of *ApoE* down-regulation in development of brain neurodegenerative disease in terminally ill mice treated with moPrP^{res}, LPS, and moPrP^{res}+LPS. The mechanism by which *ApoE* gene is affected during brain neurodegeneration warrants further investigation.

Another important protein that has been shown consistently to participate in prion disease is Bax. *Bax* was down-regulated by moPrP^{res}, moPrP^{res}+LPS, LPS, and RML scrapie isolate treatments in our study. In a recent study Gong et al. (2007) showed that *Bax* deletion in Tg(PrP Δ 32-134) mice delays the development of clinical illness and slows down the apoptosis of cerebellar granule cells. The Bax molecule resides in the cytoplasm and responds to various stimuli by migration to the mitochondria (Wolter et al., 1997) where it is capable of causing cytochrome C release (Jurgensmeier et al., 1998), thereby activating apoptotic protease activating factor (Apaf)-1 dimerization and the apoptotic cascade. Bax is a powerful executioner of neurons and PrP has been shown to protect neurons from Bax-mediated cell death (Bounhar et al., 2001). Our data suggest that down-regulation of Bax by these treatments might be a host response to slow down the process of neuronal cell death.

An additional gene that was differentially expressed in both moPrP^{res} and moPrP^{res}+LPS treatments was *Fyn*. Intriguingly *Fyn* was up-regulated by moPrP^{res} and down-regulated by moPrP^{res}+LPS treatment. *Fyn* encodes a membrane-associated tyrosine kinase that is implicated in cell growth. Recently it was shown that Fyn kinase functions to mediate signal transduction from amyloid(A) β -PrP^C complexes (Um et al., 2012). In terms of signaling, PrP^C is coupled to Fyn kinase, a key player in a cascade of events that ultimately leads to NMDA (N-methyl-D-aspartate) receptor mediated excitotoxicity and hyperphosphorylation of tau (Wang et al., 2013). Recent studies also define an A β oligomer signal transduction pathway that requires PrP^C and Fyn to alter synaptic function, and that is relevant to Alzheimer's Disease (AD; Um et al., 2012). Chen et al. (2003) also showed that PrP^C activates *Fyn* and induces neurite outgrowth that is important for neuronal survival.

Other genes up-regulated by moPrP^{res} treatment were *Ifitm3*, *Myd88*, *Tlr4*, *Ccl5*, *Tnf*, *Fcgr3*, *Lyz2*, *Mdk*, *Tlr1*, and *Il1ra*. The interferon-induced transmembrane (*Ifitm3*) protein is a small (17 kDa) antiproliferative protein that is deregulated in cells that are interferon resistant and therefore cannot exert its antiproliferative properties (Deblandre, Marinx et al. 1995). Additionally, studies have shown that overexpression of recombinant *Ifitm3* leads to inhibition of proliferation in IFN- α -sensitive cell lines (Brem et al. 2003). Moreover *Ifitm3* is considered a marker for interferon resistance and it has also been identified as an early biomarker of colon tumors (Fan et al., 2008; Peng et al. 2008). Several IFN response genes (*Ifit1*, *Ifit3*, *Ifitm3*, and *Igip30*) were reported to be increased significantly during progression of amyotrophic lateral sclerosis (ALS) in SOD1^{G93A} microglia (Chlu et al., 2013). It is not clear why this gene was up-regulated by moPrP^{res} treatment and if there is a function in neuroprotection or neurodegeneration.

Up-regulation of genes related to innate immunity like *Tlr4*, *Myd88*, *Tnf*, *Tlr1*, and *Il1rn* were characteristic for the moPrP^{res} treatment only. Interestingly mutations in TLR4 have been shown to expedite prion disease (Spinner et al., 2008). Moreover, Prinz et al. (2003) showed that *Myd88*^{-/-} mice were fully affected by scrapie as wild-type mice, suggesting that protective effects of activation of TLR4 signaling does not results from direct interaction with prions. On the other hand, MyD88 is a cytoplasmic adapter protein that associates as an obligate functional partner with all members of the TLR including TLR4 and interleukin (IL)-1 receptor (IL-1R) family (Muzio et al., 1997; Medzhitov et al., 1998). Moreover, overexpression of *Tnf* is important because TNF stimulates NF- κ B transcription factor, which induces the expression of proinflammatory cytokines, and promotes the synthesis of neuronal survival factors such as

calbindin, manganese superoxide dismutase, and anti-apoptotic Bcl-2 protein (Sakudo et al., 2003; Wajant et al., 2003; Kamata et al., 2005). This cytokine also can stimulate microglia glutaminase to release glutamate, thus generating excitotoxicity (Takeuchi et al., 2006) and promoting the development of neurodegenerative diseases.

moPrP^{res} up-regulated *Ccl5*, a gene that has been implicated in neurodegenerative diseases including AD. Elevated expression of *Ccl5* in the cerebral microcirculation is associated with recruitment of immune cells (Lumpkins et al., 2008). It has also been demonstrated in cell culture models that *Ccl5* can stimulate chemotaxis, increase nitric oxide (NO) secretion, and attenuate IL-10 and insulin growth factor (IGF)-1 production in activated microglia (Skuljec et al., 2011). Moreover Skuljec et al. (2011) reported that, in addition to its chemoattractant function, *Ccl5* also has a modulatory effect on microglia activation. Treatment of neurons with *Ccl5* has resulted in an increase in cell survival and a neuroprotective effect against the toxicity of thrombin and sodium nitroprusside (Lee et al., 2012). It is obvious that mice treated with moPrP^{res} are responding to infection with enhanced *Ccl5* gene expression to attract and activate microglia at the site of inflammation.

Of note was the overexpression of *Mdk* (Midkine) by moPrP^{res}, which encodes a protein that is important in attraction of immune cells to the site of inflammation. Sato et al (2001) reported that *Mdk*^{-/-} mice show significantly suppressed recruitment of inflammatory cells (Sato et al., 2001). Midkine also plays a significant role as an anti-apoptotic factor for neuronal cells during apoptosis induced by serum starvation of neurons (Horiba et al., 2000).

Although the role of *Lyz2* in brain neurodegenerative disease is not clear yet it is interesting to note that a recent report indicates that human lysozyme was able to prevent amyloid aggregation of the A β peptides (Luo et al., 2013). Therefore, it is tempting to speculate that up-regulation of *Lyz2* in moPrP^{res}-treated mice in our experiment might provide more lysozyme to the host to counteract establishment of prion fibrils. However, this warrants further investigation.

Subcutaneous treatment with moPrP^{res} also up-regulated *Fcgr3*. Our results are in agreement with previous research demonstrating up-regulation of this gene in scrapie infected animals (Manuelidis et al., 2003; Xiang et al., 2004). Fc γ receptors (Fc γ Rs) for IgG are expressed on a wide variety of immune cells, linking cellular and humoral immunity. Engagement of activating Fc γ Rs, associated with the common γ -chain, triggers effector cell responses, such as antibody-dependent cell-mediated cytotoxicity, phagocytosis, reactive oxygen production, and release of inflammatory mediators (Nimmerjahn and Ravetch, 2008). During inflammation, Fc γ Rs play important roles in leukocyte recruitment and activation. More specifically Fc γ R3 mediates neutrophil tethering and adhesion in response to immune complexes during inflammation (Coxon et al., 2001; Tsuboi et al., 2008). Up-regulation of *Fcgr3* gene in the brain of mice treated with moPrP^{res} in our experiment suggests host responses to increase recruitment of leukocytes to the site of inflammation.

The other two genes up-regulated by moPrP^{res} treatment were *Tlr1* and *Ilr1a*. Tlr1 and Tlr2 have been shown to be primary receptors for A β and activation of inflammatory processes (Liu et al., 2012). In addition, genetic deletion of *IL1ra* (also known as *IL-1rn*) in mice increases

microglia activation and reduces neuronal survival in response to intracerebroventricular infusion of A β in human subjects (Craft et al., 2005).

There were 5 genes that were commonly down-regulated by moPrP^{res}+LPS, RML, and RML+LPS treatments (i.e., *Sprn*, *Atp1b1*, *Prkaca*, *Ncam1*, and *Sod1*), whereas a total of 9 genes were commonly affected by RML and RML+LPS treatments, 7 of them were down-regulated (i.e., *Sprn*, *Atp1b1*, *Ncam1*, *Prkaca*, *Egr1*, *Anp32a*, and *Sod1*) and 2 of them were up-regulated (i.e., *Lyz2* and *Ly86*).

Down-regulation of *Atp1b1* gene by moPrP^{res}+LPS, RML, and RML+LPS treatments is in agreement with previous research indicating that failure of Na⁺/K⁺-ATPase (i.e., sodium/potassium pump) is implicated in the pathogenesis of several neurodegenerative disorders (Manczak et al., 2006). *Atp1b1* encodes the β 1 unit of Na⁺/K⁺-ATPase, which is important in repolarization of neuronal plasma membrane after excitatory depolarization, transmission of action potentials in neurons, and also it is associated with caveolae and intracellular signal transduction events (Wong-Riley, 2012).

The neural cell adhesion molecule (Ncam), encoded by *Ncam1*, is a cell membrane constituent with three isoforms. Ncam1 plays significant roles in interneuronal and glia-neuronal adhesion phenomena, cell-cell recognition, development of the nervous system, synaptic plasticity, memory and learning as well as re-myelination and post-injury regeneration (Edelman, et al., 1986; Cioffi et al., 1986; Ronn et al., 1998; Nait-Oumesmar et al., 1995). Therefore down-regulation of this gene by moPrP^{res}+LPS, RML, and RML+LPS suggests multiple neuronal functions might have been affected by these treatments.

These 3 treatments also differentially expressed *Prkaca* (Protein kinase, cAMP dependent, catalytic, alpha), which is suggestive of apoptotic processes occurring in the brain. The protein kinase encoded by this gene binds cAMP and initiates phosphorylation of various downstream substrates, and has been shown to function as a neuroprotective molecule with anti-apoptotic activity (Pedersen et al., 2001; 2002).

moPrP^{res}, RML, and RML+LPS also decreased expression of *Sod1*. Decreased superoxide dismutase (Sod) activity has been shown previously in prion protein knockout mice and cell cultures (Brown et al., 1997; Brown and Besinger, 1998; Klamt et al., 2001; Sakudo et al., 2005), and a loss of Sod function is one proposed mechanism of prion disease pathogenesis. Alterations in activity and redistribution to mitochondria is reported for *Sod1* mutants associated with genetic amyotrophic lateral sclerosis (ALS) in humans and mice (Carri and Cozzolino, 2011; Goldsteine et al., 2008) indicating that mislocalization and altered activity of the Sod enzymes can have deleterious consequences for neurons. Sod activity was lowered in 4 neurodegenerative diseases including AD, PD, ALS, and Downer's syndrome (Jóhannesson et al., 2003).

Our results related to RML and RML+LPS treatments are in line with those of Koldamova et al. (2013) who reported decreased *Egr1* expression in AD mice models. Similar down-regulation of *Egr1* was demonstrated also by Dickey et al. (2004), in another AD model mice, at the time when mice exhibited cognitive deficits. *Egr1* has established roles in synaptic transmission, plasticity, learning and long-term memory (Davis et al., 2003; Jones et al., 2001). Recently, Koldamova et al. (2013) reported that *Egr1* regulates the expression of genes involved in clathrin-mediated endocytosis, vesicular transport, and synaptic transmission.

The Anp32a proteins have been implicated in a broad array of biological processes, including cell differentiation, proliferation, and apoptosis (Sun et al., 2006; Kular et al., 2009; Pan et al., 2009). Anp32a is thought to function in signal transduction and interacts with the cytoskeleton (Opal et al 2003; Matilla and Radrizzani 2005), and has been implicated in various neurodegenerative diseases. For instance, its expression is decreased in spinocerebellar ataxia type 3 (Evert et al 2003) and it binds to and colocalizes with mutant ataxin-1, the protein that causes spinocerebellar ataxia type 1 (Matilla et al 1997). Other investigators have reported both up-regulation and down-regulation of *Anpr32* in neurodegenerative diseases (Kim et al., 2008). This gene was down-regulated by RML and RML+LPS treatments; however, it was up-regulated by the LPS treatment.

Up-regulation of lymphocyte antigen 86 (Ly86) and *Lyz2* is a common finding in prion diseases (Moody et al., 2009). Ly86 is a microglial marker and *Lyz2* is an anti-fibrillar molecule. Three treatments including RML, RML+LPS, and LPS affected *Ly86* and only RML and RML+LPS affected *Lyz2*.

Additionally, moPrP^{res}+LPS, LPS, and RML treatments down-regulated mRNA expression of *Ache*, which encodes the enzyme acetylcholinesterase (AChE), expressed in cholinergic neurons. The primary function of AChE is to hydrolyze acetylcholine (Ach) and thus terminate cholinergic neurotransmission. Acetylcholinesterase is also believed to play a critical role in the pathogenesis of neurodegenerative diseases such as AD (Conway, 1998). AChE inhibitors, (Loizzo et al., 2008), such as tacrine (Conway, 1998), have been shown to slow down the development of AD. Moreover Park et al. (2004) showed that silencing of the *Ache* gene

inhibits the interaction between Apaf-1 and cytochrome c and that AChE plays an important role in apoptosome formation.

Subcutaneous treatment with moPrP^{res}+LPS down-regulated two other important genes *Ili8* and *Adam9*. Interleukin-18 is a pro-inflammatory cytokine produced by antigen presenting cells. It is a cytokine that has been shown to be essential for IFN- γ and TNF production (Pasquali et al., 2006). Therefore down-regulation of this gene in this treatment is essential for downsizing of inflammatory responses in the brain. It is interesting to note the down-regulation of *Adam9*, because this protease is involved in cleavage of PrP^C and generation of N1 (N-terminal fragment of PrP^C) (Cissé et al., 2005). It had been shown that expression of the N-terminal fragment truncated PrP in the mouse leads to ataxia and specific cerebellar lesions (Shmerling et al., 1998; Flechsig et al., 2003). It seems like the host is responding to moPrP^{res}+LPS treatment by lowering the proteolysis of PrP^C and generation of N-terminal fragment.

Five genes were uniquely up-regulated by RML+LPS including *Clqb*, *C4b*, *H2-k1*, *Ifi27i2a*, and *A2m*. Many reports describe the presence of early complement components like Clqb, C4b, and C3 and to a lesser extent late components of A β plaques in AD brain (Veerhuis et al., 2005). C1q protein has been involved in activation of microglia (Fonseca et al., 2004), whereas C4b may provide protection against excessive complement activation induced by dead cells and DNA in the brain (Trouw et al., 2008). *H2-k1* has been previously indicated to be associated with prion disease (Daude and Westaway, 2011; Bradford et al., 2012). Up-regulation of interferon alpha-inducible protein 27 like 2a gene (*Ifi27i2a*) is of interest because previous in vitro studies with microglia derived from CJD brain have demonstrated induction of various interferon-sensitive genes including interferon-induced protein 202 (IFI202) and 204 (IFI204)

(Baker and Manuelidis, 2003; Baker et al, 2002). Baker et al. (2004) also reported up-regulation of 10 interferon-sensitive transcripts at more than 10-fold in the brain of CD-1 mice inoculated with the FU strain of CJD and a continuous increase in the IFI202 and IFI204 expression. The reason for up-regulation of *Ifi27i2a* by RML+LPS is not understood completely and deserves further inquiry.

Of interest is up-regulation of *A2m* by RML+LPS. Alpha-2-macroglobulin (α 2M; encoded by the gene *A2m*) is a serum protease inhibitor that has been implicated in AD based on its ability to mediate the clearance and degradation of A β , the major component of β -amyloid deposits. Moreover, α 2M was found to co-localize with A β plaques in AD patients (Strauss et al., 1992), and is supposed to mediate the internalization and the clearance of α 2M-A β complexes, possibly by interaction with one of its major neuronal receptors, the low-density lipoprotein receptor-related protein (LRP) (Kounnas et al., 1995). Interestingly, α 2M was found to facilitate, at least in vitro, PrP^C-PrP^{Sc} conversion (Adler et al., 2007). Recently, it was also shown that binding of α 2M to Dpl protein initiates neurodegeneration in experimental rats (Benvengu et al., 2009).

Both moPrP^{res}+LPS and LPS treatments down-regulated *Gfap*. This gene encodes glial fibrillary acidic protein (Gfap) in astrocytes and is important for astrocyte-neuronal interactions and modulates synaptic efficacy in the CNS. Astrocytes are known to respond rapidly, after any degenerative injury or insult, by producing more Gfap, leading to vigorous astrogliosis (Yu et al., 1993; Sriram et al., 2004). During AD, PD, HIV-dementia, and prion disease there is loss of neurons associated or followed by massive activation of astrocytes (Prusiner, 1998). Once astrocytes are activated, during neurodegeneration, detrimental effects exceed beneficial effects

(Yu et al., 1993). Therefore down-regulation of *Gfap* in our experiment might protect the host from detrimental effects of overactivation of astrocytes. Staining for astrogliosis is directed at detection of the protein encoded by this gene (*Gfap*).

RML and LPS treatments differentially expressed (i.e., up-regulated) *Tlr3* gene. Activation of TLR3 has been shown to exacerbate neurodegenerative diseases (Field et al., 2010). TLR3 is involved in sensing viral infections and initiating the appropriate immune responses. However, recently it was shown that LPS was able to up-regulate the expression of TLR3 in human peripheral monocytes (Pan et al., 2011). It is known that TLR3 stimulates production of pro-inflammatory cytokines and antiviral immunity. The reason for overexpression of TLR3 by RML and LPS is not understood at present.

Subcutaneous chronic infusion of LPS differentially expressed 19 genes. Out of these genes only 6 were uniquely differentially expressed by LPS treatment including *Fcgr2b*, *Ccl17*, *Ccl19*, *Ccl25*, *Grn*, and *H2-T23*. Down-regulation of *Fcgr2b* gene is in alignment with previous reports that *Fcgr2b* knockout mice are protected from neurodegeneration in AD (Kam et al., 2013). Also, it has been reported that the FcγRIIb is a receptor of Aβ₁₋₄₂. Recently Kam et al. (2013) demonstrated that FcγRIIb is significantly up-regulated in the hippocampus area of the AD brains and in neuronal cells exposed to synthetic Aβ and that genetic depletion of *Fcgr2b* rescues memory impairments in an AD mouse model. Mice treated with LPS in our experiment are responding with down-regulation of *Fcgr2b* in order to prevent neurodegenerative processes in the brain.

It is interesting to observe that 2 chemokine genes (*Ccl17* and *Ccl25*) were up-regulated, whereas *Ccl19* was down-regulated by LPS. The function of chemokines is to regulate leukocyte

trafficking at the site of inflammation. Recently it was shown that mice deficient in *Ccl17* lowered deposition of A β in the brain, and were protected against neuronal loss and cognitive deficits. In addition in absence of *Ccl17* there is accelerated uptake and degradation of A β (Neitzert et al., 2013). Interestingly, receptors for both *Ccl17* and *Ccl25* are located in the hippocampal neurons, the part of the brain that is related to learning and memory (Cartier et al., 2005; Meucci et al., 1998; Mu and Gage, 2011). On the other hand *Ccl19* was reported to be constitutively transcribed in the normal human CNS and that its transcription was elevated in MS patients. The locally produced *Ccl19* might be involved in the maintenance of different types of immune cells in the brain. Therefore subcutaneous treatment with LPS apparently affected expression of brain chemokines to invite immune cells to the sites of inflammation.

Another gene down-regulated by LPS was *Grn*. This gene encodes the protein granulin. Granulin is expressed in neurons and microglia (Almeida et al., 2011). Mutations in the *Grn* have been shown to give rise to frontotemporal lobar degeneration (FTLD) (Baker et al. 2006; Cruts et al. 2006). Granulin inhibits TNF and promotes the up-regulation of Th2 cytokines such as IL-4, IL-10, and IL-5 (Okura et al. 2010). Granulin also has a function during wound healing, where it increases the accumulation of neutrophils, macrophages, blood vessels, and fibroblasts (He et al., 2003). Therefore down-regulation of *Grn* by LPS has influenced the etiopathology of neurodegeneration in the treated animals.

It is interesting to note that LPS and RML commonly affected 8 genes (*Sprn*, *Ncam1*, *Tlr3*, *Ache*, *Fcgr3*, *Ly86*, *Anp32a*, and *Bax*). Intriguingly, LPS differentially expressed 8 genes that have been previously reported in experimental scrapie disease in rodents (Kim et al., 2008). This implicates LPS as a potential co-factor in prion disease and suggests that the effects of LPS

on the etipathogenesis of neurodegeneration involve similar pathogenic mechanisms with scrapie agents.

It should be noted that although most of the genes identified in this study showed greater than 2-fold alteration in the expression relative to control mice, a few other genes showed less than 2-fold change. Moreover, because our study used RNA from the whole brain tissue, it is assumed that gene expression that occurred in a cell type or in a particular region of the brain has shown lower fold change in this analysis due to dilution by mRNA from surrounding cells or brain regions in which the particular gene alteration was not happening. Therefore, during analyses of gene expression related to tissues such as brain, low fold changes in gene expression might be misleading because changes in a subset of cells or cells in a particular region of the tissue should not be overlooked.

5. Conclusions

In conclusion, data from this study indicate that moPrP^{res} generated in vitro by incubation with LPS was able to cause a gene expression signature typical of prion disease. For instance moPrP down-regulated two genes typically related to development of prion disease like *Sprn* and *Prnp*. Combination of moPrP^{res} with LPS also differentially expressed genes typically related to prion disease especially *Sprn*, *Prnp*, and *Prnd*. Of interest is the signature of genes differentially expressed by chronic subcutaneous administration of LPS that commonly expressed 8 genes with RML, typical of prion disease like down-regulation of *Sprn* and up-regulation of *Prnd*. RML and combination of RML with LPS also affected a variety of genes that are involved in scrapie and that have been reported previously by other investigators. More

research is warranted to study the potential role of chronic LPS and LPS-converted PrP^{res} in development of neurodegenerative diseases in humans and animals.

6. Acknowledgement

The authors acknowledge the financial support of this study by Alberta Livestock and Meat Agency Ltd. (ALMA), Alberta Prion Research Institute (APRI), and Natural Sciences and Engineering Research Council of Canada (NSERC). The authors thank Fozia Saleem and Ashenafi Abera for preparation of the mouse recombinant prion protein and generation of LPS-converted moPrP^{res}. Also, our appreciation goes to all the staff at Centre for Prions and Protein Folding Disease at University of Alberta for the care and daily monitoring of the mice.

References

1. Allan, S. M., P. J., Tyrrell, and N. J., Rothwell, 2005, Interleukin-1 and neuronal injury, *Nature Reviews*, Volume 5, p. 629-640.
2. Ametaj, B. N., F., Saleem, V., Semenchenko, C., Sobsey, and D. S., Wishart, 2010, Lipopolysaccharide interacts with prion protein and catalytically converts it into a protein resistant β -sheet-rich isoform, *Prion Congress*, Salzburg, Austria.
3. Almeida, S., L., Zhou, and F. B., Gao, 2011, Progranulin, a glycoprotein deficient in frontotemporal dementia, is a novel substrate of several protein disulfide isomerase family proteins, *PLoS One*, Volume 6, p. 1-8.
4. Baker, C. A., D., Martin, and L., Manuelidis, 2002, Microglia from CJD brain are infectious and show specific mRNA activation profiles, *Journal of Virology*, Volume 76, p. 10905-10913.
5. Baker, C. A., and L., Manuelidis, 2003, Unique inflammatory profiles of microglia in Creutzfeldt-Jakob disease, *PNAS*, Volume 100, p. 675-679.
6. Baker, C. A., Z. Y., Lu, and L., Manuelidis, 2004, Early induction of interferon-responsive mRNAs in Creutzfeldt-Jakob disease, *Journal of Neurovirology*, Volume 10, p. 29-40.
7. Barria, M. A., A., Mukherjee, D., Gonzalez-Romero, R., Morales, and C., Soto, 2009, De novo generation of infectious prions in vitro produces a new disease phenotype, *PLoS Pathogens*, Volume 5, p. e1000421.
8. Bjorndahl, T. C., G. P., Zhou, X. H., Liu, R., Perez-Pineiro, V., Semenchenko, F., Saleem, S., Acharya, A., Bujold, C., Sobsey, and D. S., Wishart, 2011, Detailed biophysical

- characterization of the acid-induced PrP^C to PrP^B conversion process, *Biochemistry*, Volume 50, p. 1162-1173.
9. Bounhar, Y., Y., Zhang, C. G., Goodyer, and A., LeBlanc, 2001, Prion protein protects human neurons against Bax-mediated apoptosis, *The Journal of Biological Chemistry*, Volume 276, p. 39145-39149.
 10. Booth, S., C., Bowman, R., Baumgartner, G., Sorensen, C., Robertson, M., Coulthart, C., Phillipson, and R. L., Somorjai, 2004, Identification of central nervous system genes involved in the host response to the scrapie agent during preclinical and clinical infection, *The Journal of General Virology*, Volume 85, p. 3459-3471.
 11. Brem, R., K., Oraszlan-Szovik, S., Foser, B., Bohrmann, and U., Certa, 2003, Inhibition of proliferation by 1-8U in interferon-alpha-responsive and non-responsive cell lines, *Cellular and Molecular Life Sciences*, Volume 60, p. 1235-1248.
 12. Brown, D. R., W. J., Schulz-Schaeffer, B., Schmidt, and H. A., Kretzschmar, 1997, Prion protein-deficient cells show altered response to oxidative stress due to decreased SOD-1 activity, *Experimental Neurology*, Volume 146, p. 104-112.
 13. Brown, D. R., and A., Besinger, 1998, Prion protein expression and superoxide dismutase activity, *The Biochemical Journal*, Volume 334, p. 423-429.
 14. Bruijn, L. I., T. M., Miller, and D. W., Cleveland, 2004, Unraveling the mechanisms involved in motor neuron degeneration in ALS, *Annual Review of Neuroscience*, Volume 27, p. 723-749.

15. Canadian Council on Animal Care, 1993, Guide to the care and use of experimental animals, Volume 1, 2nd edition, CCAC, Ottawa, Ontario, Canada.
16. Castilla, J., P., Saá, C., Hetz, and C., Soto, 2005, In vitro generation of infectious scrapie prions, *Cell*, Volume 121, p. 195-206.
17. Chen, S., A., Mange, L., Dong, S., Lehmann, and M., Schachner, 2003, Prion protein as trans-interacting partner for neurons is involved in neurite outgrowth and neuronal survival, *Molecular and Cellular Neurosciences*, Volume 22, p. 2270-233.
18. Chishti, M. A., D. S., Yang, C., Janus, A. L., Phinney, P., Horne, J., Pearson, R., Strome, N., Zuker, J., Loukides, J., French, S., Turner, G., Lozza, M., Grilli, S., Kunicki, C., Morissette, J., Paquette, F., Gervais, C., Bergeron, P. E., Fraser, G. A., Carlson, P. S., George-Hyslop, and D., Westaway, 2001, Early-onset amyloid deposition and cognitive deficits in transgenic mice expressing a double mutant form of amyloid precursor protein 695, *The Journal of Biological Chemistry*, Volume 276, p. 21562-21570.
19. Cioffi, R. P., G., Carbone, and A. R., Massaro, 1986, Alcuni aspetti neurobiologici della N-CAM, *Archivio di Psicologia, Neurologia e Psichiatria*, Volume 47, p. 191-208.
20. Cissé, M. A., C., Sunyach, S., Lefranc-Jullien, R., Postina, B., Vincent, and F., Checler, 2005, The disintegrin ADAM9 indirectly contributes to the physiological processing of cellular prion by modulating ADAM10 activity, *The Journal of Biological Chemistry*, Volume 280, p. 40624-40631.
21. Coomaraswamy, J., E., Kilger, H., Wolfing, C., Schafer, S. A., Kaeser, B. M., Wegenast-Braun, J. K., Hefendehl, H., Wolburg, M., Mazzella, J., Ghiso, M., Goedert, H., Akiyama, F.,

- Garcia-Sierra, D. P., Wolfer, P. M., Mathews, and M., Jucker, 2010, Modeling familial Danish dementia in mice supports the concept of the amyloid hypothesis of Alzheimer's disease, PNAS, Volume 107, p. 7969-7974.
22. Comincini, S., L. R., Chiareli, P., Zelini, I., Del Vecchio, A., Azzalin, A., Arias, V., Ferrara, P., Rognoni, A., Dipoto, R., Nano, G., Valentini, and L. Ferreti, 2006, Nuclear mRNA retention and aberrant doppel protein expression in human astrocytic tumor cells, Oncology Reports, Volume 16, p. 1325-1332.
23. Conway, E. L., 1998, A review of the randomized controlled trials of tacrine in the treatment of Alzheimer's disease: methodologic considerations, Clinical Neuropharmacology, Volume 21, p. 8-17.
24. Coxon, A., X., Cullere, S., Knight, S., Sethi, M. W., Wakelin, G., Stavrakis, F. W., Luscinskas, and T. N., Mayadas, 2001, Fc gamma riii mediates neutrophil recruitment to immune complexes, A mechanism for neutrophil accumulation in immune-mediated inflammation, Immunity, Volume 14, p. 693-704.
25. Craft, J. M., D. M., Watterson, E., Hirsch, and L. J., Van Eldik, 2005, Interleukin 1 receptor antagonist knockout mice show enhanced microglial activation and neuronal damage induced by intracerebroventricular infusion of human β -amyloid, Journal of Neuroinflammation, Volume 2, p. 15.
26. Daude, N., and D., Westaway, 2011, Biological properties of the PrP-like Shadoo protein, Frontiers in Bioscience, Volume 16, p. 1505-1516.

27. Daude, N., and D. Westaway, 2012, Shadoo/PrP (Sprn(0/0) /Prnp(0/0)) double knockout mice: more than zeroes, *Prion*, Volume 6, p. 420-424.
28. Deleault, N. R., B. T., Harris, J. R., Rees, and S., Supattapone, 2007, Formation of native prions from minimal components in vitro, *PNAS*, Volume 104, p. 9741-9746.
29. Deleault, N. R., J. R., Piro, D. J., Walsh, F., Wang, J., Ma, J. C., Geoghegan, and S., Supattapone, 2012a, Isolation of phosphatidylethanolamine as a solitary cofactor for prion formation in the absence of nucleic acids, *PNAS*, Volume 109, p. 8546-8551.
30. Deleault, N. R., D. J., Walsh, J. R., Piro, F., Wang, X., Wang, J., Ma, J. R., Rees, and S., Supattapone, 2012b, Cofactor molecules maintain infectious conformation and restrict strain properties in purified prions, *PNAS*, Volume 109, p. 1938-1946.
31. Edelman, G. M., 1986, Cell adhesion molecules in the regulation of animal form and tissue pattern, *Annual Reviews Cell and Development Biology*, Volume 2, p. 81-116.
32. Evert, B. O., I. R., Vogt, A. M., Vieira-Saecker, L., Ozimek, R. A., de Vos, E. R., Brunt, T., Klockgether, and U., Wüllner, 2003, Gene expression profiling in ataxin-3 expressing cell lines reveals distinct effects of normal and mutant ataxin-3, *Journal of Neuropathology Experimental Neurology*, Volume 62, p. 1006-10018.
33. Fan, J., Z., Peng, C., Zhou, G., Qiu, H., Tang, Y., Sun, X., Wang, Q., Li, X., Le, and K., Xie, 2008, Gene-expression profiling in Chinese patients with colon cancer by coupling experimental and bioinformatic genome wide gene expression analyses: identification and validation of IFITM3 as a biomarker of early colon carcinogenesis, *Cancer*, Volume 113, p. 266-75.

34. Field, R., S., Campion, C., Warren, C., Murray, and C., Cunningham, 2010, Systemic challenge with the TLR3 agonist poly I:C induces amplified IFN α /beta and IL-1beta responses in the diseased brain and exacerbates chronic neurodegeneration, *Brain, Behavior, and Immunity*, Volume 24, p. 996-1007.
35. Flechsig, E., I., Hegyi, R., Leimeroth, A., Zuniga, D., Rossi, A., Cozzio, P., Schwarz, T., Rulicke, J., Gotz, A., Aguzzi, and C., Weissmann, 2003, Expression of truncated PrP targeted to Purkinje cells of PrP knockout mice causes Purkinje cell death and ataxia, *EMBO Journal*, Volume 22, p. 3095-3101.
36. Fonseca, M. I., J., Zhou, M., Botto, and A. J., Tenner, 2004, Absence of C1q leads to less neuropathology in transgenic mouse models of Alzheimer's disease, *The Journal of Neuroscience*, Volume 24, p. 6457-6465.
37. Gong, J., A., Jellali, V., Forster, J., Mutterer, E., Dubus, W. D., Altmann, J. A., Sahel, A., Rendon, and S., Picaud, 2007, The toxicity of the PrP106-126 prion peptide on cultured photoreceptors correlates with the prion protein distribution in the mammalian and human retina, *The American Journal of Pathology*, Volume 170, p. 1314-1324.
38. Griffin, W. S., L. C., Stanley, C., Ling, L., White, V., MacLeod, L. J., Perrot, C. L., White, and C., Araoz, 1989, Brain interleukin 1 and S-100 immunoreactivity are elevated in Down syndrome and Alzheimer disease, *PNAS*, Volume 86, p. 7611-7615.
39. Hauser, S. L., T. H., Doolittle, R., Lincoln, R. H., Brown, and C. A., Dinarello, 1990, Cytokine accumulations in CSF of multiple sclerosis patients: frequent detection of interleukin-1 and tumor necrosis factor but not interleukin-6, *Neurology*, Volume 40, p. 1735-1739.

40. He, Z., C. H., Ong, J., Halper, and A., Bateman, 2003, Progranulin is a mediator of the wound response, *Nature Medicine*, Volume 9, p. 225-229.
41. Horiba, M., K., Kadomatsu, E., Nakamura, H., Muramatsu, S., Ikematsu, S., Sakuma, K., Hayashi, Y., Yuzawa, S., Matsuo, M., Kuzuya, T., Kaname, M., Hirai, H., Saito, T., Muramatsu, 2000, Neointima formation in a restenosis model is suppressed in midkine-deficient mice, *The Journal of Clinical Investigations*, Volume 105, p. 489-495.
42. Hu, Y., J., Wang, B., Yang, N., Zheng, M., Qin, Y., Ji, G., Lin, L., Tian, X., Wu, L., Wu, and B., Sun, 2011, Guanylate binding protein 4 negatively regulates virus-induced type I IFN and antiviral response by targeting IFN regulatory factor 7, *Journal of Immunology*, Volume 187, p. 6456-6462.
43. Jurgensmeier, J. M., Z., Xie, D., Quinn, L., Ellerby, D., Bredesen, and J. C., Reed, 1998, *PNAS*, Volume 95, p. 4997-5002.
44. Kam, T. I., S., Song, Y., Gwon, H., Park, J. J., Yan, I., Im, J. W., Choi, T. Y., Choi, J., Kim, D. K., Song, T., Takai, Y. C., Kim, K. S., Kim, S. Y., Choi, S., Choi, W. L., Klein, J., Yuan, and Y. K., Jung, 2013, Fc γ RIIb mediates amyloid- β neurotoxicity and memory impairment in Alzheimer's disease, *The Journal of Clinical Investigations*, Volume 3, p. 2791-802.
45. Kim, H. O., G. P., Snyder, T. M., Blazey, R. E., Race, B., Chesebro, and P. J., Skinner, 2008, Prion disease induced alterations in gene expression in spleen and brain prior to clinical symptoms, *AABC*, Volume 1, p. 29-50.
46. Klamt, F., F., Dal-Pizzol, M. L., Jr Conte da Frota, R., Walz, M. E., Andrades, E. G., da Silva, R. R., Brentani, I., Izquierdo, and J. C., Fonseca Moreira, 2001, Imbalance of

- antioxidant defense in mice lacking cellular prion protein, *Free Radical Biology and Medicine*, Volume 10, p. 1137-1144.
47. Krugers, H. J., M., Mulder, J., Korf, L., Havekes, E. R., de Kloet, and M., Joëls, 1997, Altered synaptic plasticity in hippocampal CA1 area of apolipoprotein E deficient mice, *Neuroreport*, Volume 8, p. 2505-2510.
48. Kular, R. K., M., Cvetanovic, S., Siferd, A. R., Kini, and P., Opal, 2009, Neuronal differentiation is regulated by leucine-rich acidic nuclear protein (LANP), a member of the inhibitor of histone acetyltransferase complex, *The Journal of Biological Chemistry*, Volume 284, p. 7783-7792.
49. Lee, J. K., E. H., Schuchman, H. K., Jin, and J. S., Bae, 2012, Soluble CCL5 derived from bone marrow-derived mesenchymal stem cells and activated by amyloid beta ameliorates Alzheimer's disease in mice by recruiting bone marrow-induced microglia immune responses, *Stem Cells*, Volume 30, p. 1544-1555.
50. Legname, G., I. V., Baskakov, H. O., Nguyen, D., Riesner, F. E., Cohen, S. J., DeArmond, and S. B., Prusiner, 2004, Synthetic mammalian prions, *Science*, Volume 305, p. 673-676.
51. Liu, S., Y., Liu, W., Hao, L., Wolf, A. J., Kiliaan, B., Penke, C. E., Rube, J., Walter, M. T., Heneka, T., Hartmann, M. D., Menger, and K., Fassbender, 2012, TLR2 is a primary receptor for Alzheimer's amyloid β peptide to trigger neuroinflammatory activation, *Journal of Immunology*, Volume 188, p. 1098-107.

52. Loizzo, M. R., R., Tundis, F., Menichini, and F., Menichini, 2008, Natural Products and their Derivatives as Cholinesterase Inhibitors in the Treatment of Neurodegenerative Disorders: An Update, *Current Medicinal Chemistry* Volume 15, p. 1209-1228.
53. Lumpkins, K., G. V., Bochicchio, B., Zagol, K., Ulloa, J. M., Simard, S., Schaub, W., Meyer, and T., Scalea, 2008, Plasma levels of the beta chemokine regulated upon activation, normal T cell expressed, and secreted (RANTES) correlate with severe brain injury, *The Journal of Trauma*, Volume 64, p. 358-361.
54. Luo, J., S. K. T. S., Wärmländer, A., Gräslund, and J. P., Abrahams, 2013, Human lysozyme inhibits the *in vitro* aggregation of A β peptides, which *in vivo* are associated with Alzheimer's disease, *Chemical Communications*, Volume 49, p. 6507-6509.
55. Manczak, M., T. S., Anekonda, E., Henson, B. S., Park, J., Quinn, and P. H., Reddy, 2006, Mitochondria are a direct site of A beta accumulation in Alzheimer's disease neurons: implications for free radical generation and oxidative damage in disease progression, *Human Molecular Genetics*, Volume 15, p. 1437-1449.
56. Makarava, N., G. G., Kovacs, O., Bocharova, R., Savtchenko, I., Alexeeva, H., Budka, R. G., Rohwer, and I. V., Baskakov, 2010, Recombinant prion protein induces a new transmissible prion disease in wild-type animals, *Acta Neuropathologica*, Volume 119, p. 177-187.
57. Manuelidis, L., D. M., Tesin, T., Sklaviadis, and E. E., Manuelidis, 1987, Astrocyte gene expression in Creutzfeldt-Jakob disease, *PNAS*, Volume 84, p. 5937-5941.
58. Martens, S., and J., Howard, 2006, The interferon-inducible GTPases, *Annual Review of Cell and Developmental Biology*, Volume 22, p. 559-589.

59. Matilla, A., B. T., Koshy, C. J., Cummings, T., Isobe, H. T., Orr, and H. Y., Zoghbi, 1997, The cerebellar leucine-rich acidic nuclear protein interacts with ataxin-1, *Nature*, Volume 389, p. 974-978.
60. Matilla, A., and M., Radrizzani, 2005, The Anp32 family of proteins containing leucine-rich repeats, *Cerebellum*, Volume 4, p. 7-18.
61. Mays, C. E., C., Kim, T., Haldiman, J., van der Merwe, A., Lau, J., Yang, J., Grams, M. A., Di Bari, R., Nonno, G. C., Telling, Q., Kong, J., Langeveld, D., McKenzie, D., Westaway, and J. G., Safar, 2014, Prion disease tempo determined by host-dependent substrate reduction, *The Journal of Clinical Investigations*, Volume 124, p. 847-858.
62. McGuinness, M. C., J. M., Powers, W. B., Bias, B. J., Schmeckpeper, A. H., Segal, V. C., Gowda, S. L., Wesselingh, J., Berger, D. E., Griffin, and K. D., Smith, 1997, Human leukocyte antigens and cytokine expression in cerebral inflammatory demyelinating lesions of X-linked adrenoleukodystrophy and multiple sclerosis, *Journal of Neuroimmunology*, Volume 75, p. 174-182.
63. Medzhitov, R., P., Preston-Hurlburt, E., Kopp, A., Stadlen, C., Chen, S., Ghosh, and C. A. Jr., Janeway, 1998, MyD88 is an adaptor protein in the hToll/IL-1 receptor family signaling pathways, *Molecular Cell*, Volume 2, p. 253-258.
64. Meucci, O., A., Fatatis, A. A., Simen, T. J., Bushell, P. W., Gray, and R. J., Miller, 1998, Chemokines regulate hippocampal neuronal signaling and gp120 neurotoxicity, *PNAS*, Volume 95, p. 14500-14505.

65. Mogi, M., M., Harada, H., Narabayashi, H., Inagaki, M., Minami, and T., Nagatsu, 1996, Interleukin (IL)-1 beta, IL-2, IL-4, IL-6 and transforming growth factor-alpha levels are elevated in ventricular cerebrospinal fluid in juvenile parkinsonism and Parkinson's disease, *Neuroscience Letters*, Volume 211, p. 13-16.
66. Moore, R. C., I. Y., Lee, G. L., Silverman, P. M., Harrison, R., Strome, C., Heinrich, A., Karunaratne, S. H., Pasternak, M. A., Chishti, Y., Liang, P., Mastrangelo, K., Wang, A. F. A., Smit, S., Katamine, G. A., Carlson, F. E. Cohen, S. B. Prusiner, D. W., Melton, P. Treblay, L. E. Hood, and D. Westaway, 1999, Ataxia in prion protein(PrP)-deficient mice is associated with upregulation of the novel PrP-like protein doppel, *Journal of Molecular Biology*, Volume 229, p. 797-817.
67. Moore, R. C., P., Mastrangelo, E., Bouzamondo, C., Heinrich, G., Legname, S. B., Prusiner, L., Hood, D., Westaway, S. J., DeArmond, and P., Tremblay, 2001, Doppel-induced cerebellar degeneration in transgenic mice, *PNAS*, Volume 98, p. 15288-15293.
68. Murakami, T., E., Paitel, T., Kawarabayashi, M., Ikeda, M. A., Chishti, C., Janus, E., Matsubara, A., Sasaki, T., Kawarai, A. L., Phinney, Y., Harigaya, P., Horne, N., Egashira, K., Mishima, A., Hanna, J., Yang, K., Iwasaki, M., Takahashi, M., Fujiwara, K., Ishiguro, C., Bergeron, G. A., Carlson, K., Abe, D., Westaway, P., St George-Hyslop, and M., Shoji, 2006, Cortical neuronal and glial pathology in TgTauP301L transgenic mice: neuronal degeneration, memory disturbance, and phenotypic variation, *The American Journal of Pathology*, Volume 169, p. 1365-1375.
69. Muzio, M., J., Ni, P., Feng, and V. M., Dixit, 1997, IRAK (Pelle) family member IRAK-2 and MyD88 as proximal mediators of IL-1 signaling, *Science*, Volume 278, p. 1612-1615.

70. Nait-Oumesmar, B., L., Vignais, E., Duhamel-Clérin, V., Avellana Adalid, G., Rougon, A., Baron-Van Evercooren, 1995, Expression of the highly polysialylated neural cell adhesion molecule during postnatal and following chemically induced demyelination of the adult mouse spinal cord, *The European Journal of Neuroscience*, Volume 7, p. 480-491.
71. Neitzert, K., Ö., Albayram, R., Göhrs, C., Müller, I., Karaca, S., Kumar, M., Cron, J., Walter, I., Förster, A., Bilkei-Gorzo, W. Maier, A., Zimmer, and J., Alferink, 2013, CCL17 deficiency is associated with beneficial CNS immune responses and prevents cognitive decline in a mouse model of Alzheimer's disease, *Brain, Behavior, and Immunity*, Volume 29, p. S20-S22.
72. Nimmerjahn, F., and J. V., Ravetch, 2008, Fcγ receptors as regulators of immune responses, *Nature reviews Immunology*, Volume 8, p. 34-47.
73. Okura, H., S., Yamashita, T., Ohama, A., Saga, A., Yamamoto-Kakuta, Y., Hamada, N., Sougawa, R., Ohyama, Y., Sawa, and A., Matsuyama, 2010, HDL/apolipoprotein A-I binds to macrophage-derived progranulin and suppresses its conversion into pro-inflammatory granulins, *Journal of Atherosclerosis and Thrombosis*, Volume 17, p. 568-577.
74. Opal, P., J. J., Garcia, F., Propst, A., Matilla, H. T., Orr, and H. Y., Zoghbi, 2003, Mapmodulin/leucine-rich acidic nuclear protein binds the light chain of microtubule-associated protein 1B and modulates neuritogenesis, *The Journal of Biological Chemistry*, Volume 278, p. 34691-34699.
75. Pan, W, L. S., da Graca, Y., Shao, Q., Yin, H., Wu, and X., Jiang, 2009, PHAPI/pp32 suppresses tumorigenesis by stimulating apoptosis, *The Journal of Biological Chemistry*, Volume 284, p. 6946-6954.

76. Pan, Z. K., C., Fisher, J. D., Li, Y., Jiang, S., Huang, and L. Y., Chen, 2011, Bacterial LPS up-regulated TLR3 expression is critical for antiviral response in human monocytes: evidence for negative regulation by CYLD, *International Immunology*, Volume 23, p. 357-364.
77. Pasquali, P., R. Nonno, M. T. Mandara, M. A. Di Bari, G. Ricci, P. Petrucci, S. Capuccini, C. Cartoni, A. Macrì, and U. Agrimi. 2006. Intracerebral administration of interleukin-12 (IL-12) and IL-18 modifies the course of mouse scrapie. *BMC Vet. Res.* 2:37.
78. Pedersen, W. A., D., McCullers, C., Culmsee, N. J., Haughey, J. P., Herman, and M. P., Mattson, 2001, Corticotropin-releasing hormone protects neurons against insults relevant to the pathogenesis of Alzheimer's disease, *Neurobiology of Disease*, Volume 8, p. 492-503.
79. Pedersen, W. A., R., Wan, P., Zhang, and M. P., Mattson, 2002, Urocortin, but not urocortin II, protects cultured hippocampal neurons from oxidative and excitotoxic cell death via corticotropin-releasing hormone receptor type I, *The Journal of Neuroscience*, Volume 22, p. 404-412.
80. Peng, L., J., Wang, P. J., Malloy, and D., Feldman, 2008, The role of insulin-like growth factor binding protein-3 in the growth inhibitory actions of androgens in LNCaP human prostate cancer cells, *International Journal of Cancer*, Volume 122, p. 558-566.
81. Pitas, R. E., J. K., Boyles, S. H., Lee, D., Foss, and R. W., Mahley, 1987, Astrocytes synthesize apolipoprotein E and metabolize apolipoprotein E-containing lipoproteins, *Biochimica et Biophysica Acta*, Volume 917, p. 148-61.

82. Prinz, M., M., Heikenwalder, P., Schwarz, K., Takeda, S., Akira, and A., Aguzzi, 2003, Prion pathogenesis in the absence of Toll-like receptor signalling, *EMBO Reports*, Volume 42, p. 195-199.
83. Prusiner, S. B., 1998, Prions, *PNAS*, Volume 95, p. 13363-13383.
84. Riemer, C., I., Queck, D., Simon, R., Kurth, and M., Baier, 2000, Identification of up-regulated genes in scrapie-infected brain tissue, *Journal of Virology*, Volume 7421, p. 10245-10248.
85. Ronn, L. C., B. P., Hartz, and E., Bock, 1998, The neural cell adhesion molecule (NCAM) in development and plasticity of the nervous system, *Experimental Gerontology*, Volume 33, p. 853-864.
86. Sato, W., K., Kadomatsu, Y., Yuzawa, H., Muramatsu, N., Hotta, S., Matsuo, and T., Muramatsu, 2001, Midkine is involved in neutrophil infiltration into the tubulointerstitium in ischemic renal injury, *Journal of Immunology*, Volume 167, p. 3463-3469.
87. Sakudo, A., D. C., Lee, K., Saeki, Y., Matsumoto, S., Itohara, and T., Onodera, 2003, Tumor necrosis factor attenuates prion protein-deficient neuronal cell death by increases in anti-apoptotic Bcl-2 family proteins, *Biochemical and Biophysical Research Communications*, Volume 313, p. 725-729.
88. Sakudo, A., D. C., Lee, S., Li, T., Nakamura, Y., Matsumoto, K., Saeki, S., Itohara, K., Ikuta, T., Onodera, 2005, PrP cooperates with STII to regulate SOD activity in PrP-deficient neuronal cell line, *Biochemical and Biophysical Research Communications*, Volume 3281, p. 14-19.

89. Sawiris, G. P., K. G., Becker, E. J., Elliott, R., Moulden, and R. G., Rohwer, 2007, Molecular analysis of bovine spongiform encephalopathy infection by cDNA arrays, *The Journal of General Virology*, Volume 88, p. 1356-1362.
90. Shenoy, A. R., B. H., Kim, H. P., Choi, T., Matsuzawa, S., Tiwari, and J. D., MacMicking, 2007, Emerging themes in IFN-gamma-induced macrophage immunity by the p47 and p65 GTPase families, *Immunobiology*, Volume 212, p. 771-784.
91. Shmerling, D., I., Hegyi, M., Fischer, T., Blattler, S., Brandner, J., Gotz, T., Rulicke, E., Flechsig, A., Cozzio, C., von Mering, A., Aguzzi, C., Weissmann. 1998, Expression of amino-terminally truncated PrP in the mouse leading to ataxia and specific cerebellar lesions. *Cell* 93, p. 203-214.
92. Skinner, P. J., H., Abbassi, B., Chesebro, R. E., Race, C., Reilly, A. T., Haase, 2006, Gene expression alterations in brains of mice infected with three strains of scrapie, *BMC Genomics*, Volume 7, p. 114-126.
93. Skuljec, J., H., Sun, R., Pul, K., Bénardais, D., Ragancokova, D., Moharreggh-Khiabani, A., Kotsiari, C., Trebst, and M., Stangel, 2011, CCL5 induces a pro-inflammatory profile in microglia in vitro, *Cellular Immunology*, Volume 270, p. 164-171.
94. Spinner, D. S., I. S., Cho, S. Y., Park, J. I., Kim, H. C., Meeker, X., Ye, G., Lafauci, D. J., Kerr, M. J., Flory, B. S., Kim, R. B., Kascsak, T., Wisniewski, W. R., Levis, G. B., Schuller-Levis, R. I., Carp, E., Park, and R. J., Kascsak, 2008, Accelerated prion disease pathogenesis in Toll-like receptor 4 signaling-mutant mice, *Journal of Virology*, Volume 82, p. 10701-10708.

95. Sriram, K., S. A., Benkovic, M. A., Hebert, D. B., Miller, and J. P., O'Callaghan, 2004, Induction of gp130-related cytokines and activation of JAK2/STAT3 pathway in astrocytes precedes up-regulation of glial fibrillary acidic protein in the 1-methyl-4-phenyl-1,2,3,6-tetrahydropyridine model of neurodegeneration: key signaling pathway for astrogliosis in vivo?, *The Journal of Biological Chemistry*, Volume 279, p. 19936-19947.
96. Stanley, L. C., R. E., Mrazek, R. C., Woody, L. J., Perrot, S., Zhang, D. R., Marshak, S. J., Nelson, and W. S., Griffin, 1994, Glial cytokines as neuropathogenic factors in HIV infection: pathogenic similarities to Alzheimer's disease, *Journal of Neuropathology and Experimental Neurology*, Volume 53, p. 231-238.
97. Stetson, D. B., and R., Medzhitov, 2006, Type I interferons in host defense, *Immunity*, Volume 25, p. 373-381.
98. Sun, W., H., Kimura, N., Hattori, S., Tanaka, S., Matsuyama, and K., Shiota, 2006, Proliferation related acidic leucine-rich protein PAL31 functions as a caspase-3 inhibitor, *Biochemical and Biophysical Research Communications*, Volume 342, p. 817-823.
99. Tamgüney, G., K., Giles, D. V., Glidden, P., Lessard, H. Wille, P., Tremblay, D. F., Groth, F., Yehiely, C., Korth, R. C., Moore, J., Tatzelt, E., Rubinstein, C., Boucheix, X., Yang, P., Stanley, M. P., Lisanti, R. A., Dwek, P. M., Rudd, J., Moskovitz, C. J., Epstein, T. D., Cruz, W. A., Kuziel, N., Maeda, J., Sap, K. H., Ashe, G. A., Carlson, I., Tesseur, T., Wyss-Coray, L., Mucke, K. H., Weisgraber, R. W., Mahley, F. E., Cohen, and S. B., Prusiner, 2008, Genes contributing to prion pathogenesis, *The Journal of General Virology*, Volume 89, p. 1777-1788.

100. Tedla, N. E. N., Glaros, U. T., Brunk, W., Jessup, and B., Garner, 2004, Heterogeneous expression of apolipoprotein-E by human macrophages, *Immunology*, Volume 113, p. 338-347.
101. Telling, G. C., M., Scott, J., Mastrianni, R., Gabizon, M., Torchia, F. E., Cohen, S. J., DeArmond, and S. B., Prusiner, 1995, Prion propagation in mice expressing human and chimeric PrP transgenes implicates the interaction of cellular PrP with another protein, *Cell*, Volume 83, p. 79-90.
102. Trouw, L. A., H. M., Nielsen, L., Minthon, E., Londos, G., Landberg, R., Veerhuis, S., Janciauskiene, and A. M., Blom, 2008, C4b-binding protein in Alzheimer's disease: binding to Abeta1-42 and to dead cells, *Molecular Immunology*, Volume 45, p. 3649-3660.
103. Tsuboi, N., K., Asano, M., Lauterbach, and T. M., Mayadas, 2008, Human neutrophil fcgamma receptors initiate and play specialized nonredundant roles in antibody-mediated inflammatory diseases, *Immunity*, Volume 28, p. 833-846.
104. Um, J. W., H. B., Nygaard, J. K., Heiss, M. A., Kostylev, M., Stagi, A., Vortmeyer, T., Wisniewski, E. C., Gunther, and S. M., Strittmatter, 2012, Alzheimer amyloid- β oligomer bound to postsynaptic prion protein activates Fyn to impair neurons, *Nature Neuroscience*, Volume 15, p. 1227-1235.
105. Van Everbroeck, B., E., Dewulf, P., Pals, U., Lubke, J. J., Martin, and P., Cras, 2002, The role of cytokines, astrocytes, microglia and apoptosis in Creutzfeldt-Jakob disease, *Neurobiology of Aging*, Volume 23, p. 59-64.

106. Veerhuis, R., R. S., Boshuizen, and A., Familian, 2005, Amyloid associated proteins in Alzheimer's and prion disease, *Current Drug Targets CNS and Neurological Disorders*, Volume 4, p. 235-248.
107. Wang, F., X., Wang, C. G., Yuan, and J., Ma, 2010, Generating a prion with bacterially expressed recombinant prion protein, *Science*, Volume 327, p. 1132–1135.
108. Wang, F., Z., Zhang, X., Wang, J., Li, L., Zha, C. G., Yuan, C., Weissmann, and J., Ma, 2012, Genetic informational RNA is not required for recombinant prion infectivity, *Journal of Virology*, Volume 86, p. 1874-1876.
109. Watts, J. C., B., Drisaldi, V., Ng, J., Yang, B., Strome, P., Horne, M. S., Sy, L., Yoong, R., Young, P., Mastrangelo, C., Bergeron, P. E., Fraser, G. A., Carlson, H. T., Mount, G., Schmitt-Ulms, and D., Westaway, 2007, The CNS glycoprotein Shadoo has PrP(C)-like protective properties and displays reduced levels in prion infections, *The EMBO Journal*, Volume 26, p. 4038-4050.
110. Watts, J. C., H., Huo, Y., Bai, S., Ehsani, A. H., Jeon, T., Shi, N., Daude, A., Lau, R., Young, L., Xu, G. A., Carlson, D., Williams, D., Westaway, and G., Schmitt-Ulms, 2009, Interactome analyses identify ties of PrP and its mammalian paralogs to oligomannosidic N-glycans and endoplasmic reticulum-derived chaperones, *PLoS Pathogens*, Volume 5, p. e1000608.
111. Watts, J. C., K., Giles, S. K., Grillo, A., Lemus, S. J., DeArmond, and S. B., Prusiner, 2011, Bioluminescence imaging of Aβ deposition in bigenic mouse models of Alzheimer's disease, *PNAS*, Volume 108, p. 2528-2533.

112. Westaway, D., S., Genovesi, N., Daude, R., Brown, A., Lau, I., Lee, C. E., Mays, J., Coomaraswamy, B., Canine, R., Pitstick, A., Herbst, J., Yang, K. W., Ko, G., Schmitt-Ulms, S. J., Dearmond, D., McKenzie, L., Hood, and G. A., Carlson, 2011a, Down-regulation of Shadoo in prion infections traces a pre-clinical event inversely related to PrP(Sc) accumulation, *PLoS Pathogens*, Volume 7, p. e1002391.
113. Westaway, D., N., Daude, S., Wohlgemuth, and P., Harrison, 2011b, The PrP-like proteins Shadoo and Doppel, *Topic in Current Chemistry*, Volume 305, p. 225-256.
114. White, F., J. A., Nicoll, A. D., Roses, and K., Horsburgh, 2001, Impaired neuronal plasticity in transgenic mice expressing human apolipoprotein E4 compared to E3 in a model of entorhinal cortex lesion, *Neurobiology of Disease*, Volume 8, p. 611-625.
115. Wolter, K. G., Y. T., Hsu, C. L., Smith, A., Nechushtan, X. G., Xi, and R. J., Youle, 1997, Movement of Bax from the cytosol to mitochondria during apoptosis, *The Journal of Cell Biology*, Volume 139, p. 1281-1292.
116. Wong-Riley, M. T. T., 2012, Bigenomic regulation of cytochrome c oxidase in neurons and the tight coupling between neuronal activity and energy metabolism, In Kadenbach, B. (Ed.), *Mitochondrial Oxidative Phosphorylation: Nuclear-Encoded Genes, Enzyme Regulation, and Pathophysiology*, Springer, New York, p. 283-304.
117. Xiang, W., O., Windl, G., Wunsch, M., Dugas, A., Kohlmann, N., Dierkes, I. M., Westner, and H. A., Kretzschmar, 2004, Identification of differentially expressed genes in scrapie-infected mouse brains by using global gene expression technology, *Journal of Virology*, Volume 78, p. 11051-11060.

118. Yu, A. C., Y. L., Lee, and L. F., Eng, 1993, Astrogliosis in culture: I. The model and the effect of antisense oligonucleotides on glial fibrillary acidic protein synthesis, *Journal of Neuroscience Research*, Volume 34, p. 295-303.

Figure Captions

Table 3.1. List of differentially expressed genes in the brains of mice treated with LPS, moPrP^{res}, moPrP^{res}+LPS, RML+LPS and RML at 11 weeks of post inoculation.

Table 3.2. List of differentially expressed genes in the brains of FVB/N mice treated with LPS at terminal stage.

Table 3.3. List of differentially expressed genes in the brain tissue of terminally sick mice after subcutaneous injection of LPS-converted resistant mouse recombinant prion protein (moPrP^{res}) and moPrP^{res}+LPS injection.

Table 3.4. List of differentially expressed genes in brain tissue of terminally sick mice after RML and RML+LPS injection.

Figure 3.1. Genes differentially expressed in the brain of mice terminally sick that were euthanized after treatment with: 1) resistant mouse recombinant prion protein (moPrP^{res}); 2) moPrP^{res}+LPS; 3) RML; and 4) RML+LPS.

Table 3.1.

Gene symbol	Gene name	Fold change	P-value
DE Genes in LPS vs saline			
ApoE	Apolipoprotein E	-7.6	0.001
GbP4	Guanylate binding protein 4	-2.4	0.05
Grn	Granulin	-2.4	0.05
Sod1	Superoxide dismutase 1, soluble	-3.0	0.001
Bax	BCL2-associated X protein	-3.8	0.01
Ccl17	Chemokine (C-C motif) ligand 17	-1.5	0.05
DE genes in moPrP^{res} vs saline			
ApoE	Apolipoprotein E	-2.8	0.05
Sprn	Shadow of prion protein	-2.2	0.01
C1qb	Complement component 1, q subcomponent, beta polypeptide	-1.7	0.01
Ifi2712a	Interferon, alpha-inducible protein 27 like 2A	1.8	0.01
Nos2	Nitric oxide synthase 2, inducible	1.5	0.05
DE genes in moPrP^{res} + LPS vs saline			
Tlr6	Toll-like receptor 6	2.1	0.001
Tlr3	Toll-like receptor 3	2.8	0.05
C4b	Complement component 4B (Chido blood group)	-1.9	0.07
Nos2	Nitric oxide synthase 2, inducible	1.4	0.08
Il1a	Interleukin 1 alpha	2.2	0.06
Il1f10	Interleukin 1 family, member 10	1.4	0.08
DE genes in RML + LPS vs saline			
H2-T23	Histocompatibility 2, T region locus 23	1.8	0.05
C1qb	Complement component 1, q subcomponent, beta polypeptide	-1.8	0.09
Rtp4	Receptor transporter protein 4	-2.2	0.09
Sod1	Superoxide dismutase 1, soluble	-1.2	0.08
Ccl25	Chemokine (C-C motif) ligand 25	2.3	0.01
DE genes in RML vs LPS			
C1qb	Complement component 1, q subcomponent, beta polypeptide	-1.8	0.01
C4b	Complement component 4B (Chido blood group)	-2.2	0.08
Grn	Granulin	-1.4	0.05
Anp32a	Acidic (leucine-rich) nuclear phosphoprotein 32 family, member	-1.9	0.05
Sod1	Superoxide dismutase 1, soluble	-1.5	0.01
Bax	BCL2-associated X protein	-1.9	0.05

Table 3.2.

Gene Symbol	Gene name	Fold change	P-Value
ApoE	Apolipoprotein E	-2.53	0.01
Ache	Acetylcholinesterase	-3.19	0.08
Sprn	Shadow of prion protein	-3.21	0.01
Iftm3	Interferon induced transmembrane protein 3	2.50	0.09
Fcgr2b	Fc receptor, IgG, low affinity IIb	-2.50	0.08
Fcgr3	Fc receptor, IgG, low affinity III	1.60	0.05
Grn	Granulin	-3.19	0.01
H2-T23	Histocompatibility 2, T region locus 23	1.98	0.05
Ly86	Lymphocyte antigen 86	1.59	0.05
Gfap	Glial fibrillary acidic protein	-2.02	0.05
Anp32a	Acidic (leucine-rich) nuclear phosphoprotein 32 family, member A	1.59	0.07
Ncam1	Neural cell adhesion molecule 1	3.10	0.07
Bax	BCL2-associated X protein	-2.00	0.05
Ccl17	Chemokine (C-C motif) ligand 17	-1.97	0.05
Ccl19	Chemokine (C-C motif) ligand 19	-2.53	0.05
Mdk	Midkine	4.99	0.05
Ccl25	Chemokine (C-C motif) ligand 25	2.49	0.05
Tlr3	Toll-like receptor 3	2.52	0.01
Prnp	Prion protein	1.27	0.5
Prnd	Prion protein dublet	3.15	0.06

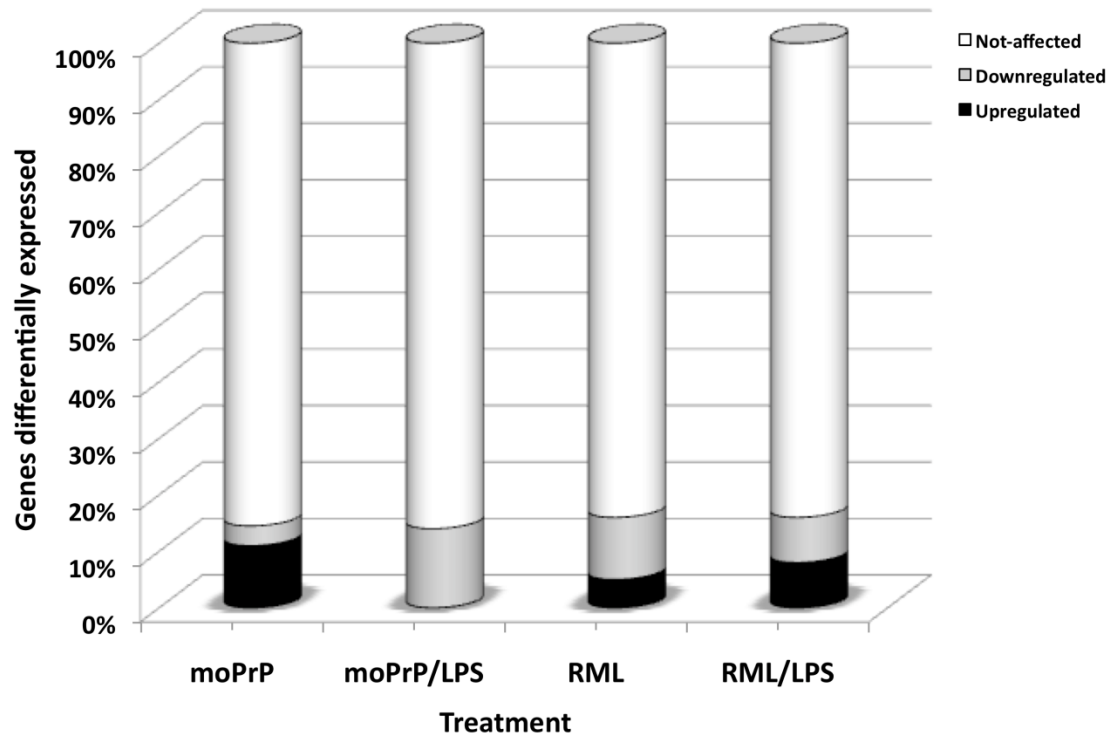
Table 3.3.

Gene	Gene name	Fold change	P-Value
DE genes in moPrP^{res} vs saline			
ApoE	Apolipoprotein E	-3.77	0.01
Sprn	Shadow of prion protein	-2.39	0.02
Ifitm3	Interferon induced transmembrane protein 3	4.23	0.01
Myd88	Myeloid differentiation primary response gene 88	1.70	0.02
Bax	Bcl2-associated X protein	-3.78	0.01
Fyn	Fyn proto-oncogene	1.69	0.02
Tlr4	Toll-like receptor 4	1.68	0.02
Ccl5	Chemokine (C-C motif) ligand 5	3.33	0.01
Tnf	Tumor necrosis factor	1.75	0.01
Fcgr3	Fc receptor, IgG, low affinity III	2.13	0.05
Lyz2	Lysozyme 2	1.68	0.09
Mdk	Midkine	2.11	0.08
Tlr1	Toll-like receptor 1	6.99	0.05
Il1rn	Interleukin 1 receptor antagonist	3.48	0.09
Prnp	Prion protein	-2.99	0.25
Prnd	Prion protein dublet	-1.17	0.98
DE genes in moPrP^{res}+LPS vs saline			
ApoE	Apolipoprotein E	-10.98	0.01
Sprn	Shadow of prion protein	-3.46	0.01
Gfap	Glial fibrillary acidic protein	-3.45	0.03
Atp1b1	ATPase, Na ⁺ /K ⁺ transporting, beta 1 polypeptide	-8.68	0.01
Prkaca	Protein kinase, cAMP dependent, catalytic, alpha	-3.42	0.03
Ncam1	Neural cell adhesion molecule 1	-4.33	0.05
Sod1	Superoxide dismutase 1, soluble	-3.46	0.06
Bax	Bcl2-associated X protein	-2.73	0.05
Fyn	Fyn proto-oncogene	-2.75	0.05
Il18	Interleukin 18	-4.35	0.06
Adam9	A disintegrin and metallopeptidase domain 9	-3.48	0.05
Ache	Acetylcholinesterase	-4.34	0.08
Prnp	Prion protein	-2.74	0.12
Prnd	Prion protein dublet	2.36	0.39

Table 3.4.

Gene	Gene name	Fold change	P-Value
DE genes in RML vs saline			
Sprn	Shadow of prion protein	-3.13	0.01
Lyz2	Lysozyme 2	4.08	0.001
Atp1b1	ATPase, Na ⁺ /K ⁺ transporting, beta 1 polypeptide	-6.20	0.01
Ncam1	Neural cell adhesion molecule 1	-3.90	0.02
Prkaca	Protein kinase, cAMP dependent, catalytic, alpha	-3.89	0.01
Egr1	Early growth response 1	-6.20	0.001
Tlr3	Toll-like receptor 3	2.56	0.03
Ache	Acetylcholinesterase	-3.90	0.08
Fcgr3	Fc receptor, IgG, low affinity III	2.59	0.09
Ly86	Lymphocyte antigen 86	4.08	0.06
Anp32a	Acidic (leucine-rich) nuclear phosphoprotein 32 family, member A	-1.95	0.08
Sod1	Superoxide dismutase 1, soluble	-3.12	0.06
Bax	Bcl2-associated X protein	-2.46	0.06
Prnp	Prion protein	-1.933	0.18
Prnd	Prion protein dublet	10.829	0.14
DE genes in RML+LPS vs saline			
Sprn	Shadow of prion protein	-1.94	0.01
C1qb	complement component 1, q subcomponent, beta polypeptide	2.61	0.03
Ly86	Lymphocyte antigen 86	2.05	0.02
Lyz2	Lysozyme 2	5.18	0.01
Atp1b1	ATPase, Na ⁺ /K ⁺ transporting, beta 1 polypeptide	-19.46	0.01
Anp32a	Acidic (leucine-rich) nuclear phosphoprotein 32 family, member A	-3.07	0.03
Ncam1	Neural cell adhesion molecule 1	-7.76	0.01
Sod1	Superoxide dismutase 1, soluble	-4.87	0.01
Prkaca	Protein kinase, cAMP dependent, catalytic, alpha	-3.84	0.03
Egr1	Early growth response 1	-4.85	0.001
H2-k1	Histocompatibility 2, K1, K region	2.58	0.02
C4b	Complement component 4B (Childo blood group)	6.51	0.09
Ifi27i2a	Interferon, alpha-inducible protein 27 like 2A	8.24	0.08
A2m	Alpha-2-macroglobulin	6.53	0.09
Prnp	Prion protein	-2.47	0.10
Prnd	Prion protein dublet	3.29	0.38

Figure 3.1.



**Chapter Four: Metabolomics approach reveals alterations in the urine and
serum of FVB/N female mice infected with RML**

Abstract

Preclinical detection of disease biomarkers in readily available biofluids such as blood and urine is a promising strategy in curing various diseases before clinical manifestation and further understanding the underlying mechanism of the disease. Prion disease is a category of neurodegenerative diseases with absolutely no therapeutic or preventional strategy up-to-date. The objectives of this research were to identify candidate molecules to be used as biomarkers of preclinical prion disease in the urine and serum of prion infected murine models in a longitudinal study from preclinical up to clinical stages of disease manifestation. For this purpose, two treatment groups, RML and RML+LPS, were selected using FVB/N female mice (n=15) for metabolomics analyses. Urine and serum samples were collected at multiple time points after treatment until terminal sickness. Non-targeted metabolomics technologies, direct injection mass spectrometry and nuclear magnetic resonance, were used to detect alterations in the body fluids. Results indicate alterations in various urine and serum metabolites detected from early stages of disease initiation. In conclusion, multiple urine and serum lipid and amino acid metabolites identified seem to be the most promising candidate metabolites for preclinical diagnosis of prion diseases.

Key words: biomarkers, prion diseases, RML, urine, serum

1. Introduction

Transmissible spongiform encephalopathies (TSEs) or prion diseases are a group of fatal neurodegenerative diseases that affect both humans and animals. Prion diseases are believed to be caused by conversion of a host-encoded protein (PrP^C) into an infectious form (Prusiner 1998). The pathogenic form of the protein is known as prion or scrapie (PrP^{Sc}) and is found in abundance in the affected brains. The disease has a long incubation time and when it shows up clinically the brain neurodegeneration process is very advanced and there is not very much to be done to reverse the pathological process except for palliative treatments. Prion disease can be definitively diagnosed after death by brain staining techniques. However, it would be of utmost importance to be able to identify potential predictive metabolites and diagnostic biomarkers of disease in a non-invasive way through blood or urine samples. Although presently there is no medication available for prion disease, early detection of illness might help to slow down the degeneration process and potentially stop progression of disease in the brain. In addition it would be of great interest to study the link between metabolic processes and brain pathology to better understand the disease process.

One of the most current and promising technologies used for identification of predictive and diagnostic biomarkers of disease is metabolomics. Metabolomics is a global approach that enables us to study the metabolome, which is the repertoire of small molecules present in cells and tissue. These metabolites represent metabolic processes in various tissues and are final products of a complex interaction involving genes and their enzymes as well as the cellular environment. Metabolomics tools have been used to characterize metabolic signatures for several diseases including Chronic Wasting Disease (CWD) in elks (Pushie et al., 2014), Parkinson's disease (Bogdanov et al., 2008), and Alzheimer's Disease (Kaddurah-Daouk et al., 2010).

In the current study, we hypothesized that female mice infected with Rocky Mountain Laboratory (RML) scrapie strain alone or RML plus chronic subcutaneous (sc) administration of Lipopolysaccharide (RML+LPS) would show serum or urine candidate metabolite that might be identified and measured through metabolomics tools. Therefore the objectives of the study were to identify and measure various metabolites present in the serum and urine of RML- and RML+LPS-infected FVB/N female mice through Direct Flow Injection Mass Spectrometry (DI-MS) and Nuclear Magnetic Resonance ($^1\text{H-NMR}$).

2. Materials and Methods

2.1. Experimental Design

Forty five FVB/N female wild type mice (Charles River Laboratories) at 5 wk of age with an approximate weight of 20 grams were randomly allocated to three treatment groups (n=15 per group): 1) saline (negative control), 2) LPS+RML (Rocky Mountain Laboratory), and 3) RML (positive control). LPS (0.1 μg /gram of body weight) and saline were administered sc using ALZET[®] osmotic mini pumps (ALZET, Cupertino, CA) which were implanted on their back, for a period of 6 wk. A simultaneous one-time sc injection of RML (10^7 ID 50 units of scrapie prions) was given at the time of minipump implantation to their designated treatment groups. Animals were fed pelleted feed (containing 20% protein, 10.6% total fat, 4.7% crude fiber, 52.9% carbohydrates, in addition to minerals and vitamins) *ad libitum* formulated for mice (PicoLab[®] Rodent Diet 20, LabDiet, ST. Louis, USA) and had free access to water at all times.

2.2. Euthanasia

Animals were euthanized at two time points: 1) at 11wk post infection (pi) and 2) at terminal sickness after observing typical prion clinical signs including kyphosis, ataxia, dysmetria,

tremor, head tilt, tail rigidity, bradykinesia, proprioceptive deficits, stupor, loss of deep pain sensation, and loss of weight. Five mice per treatment group were euthanized at 11 wk pi with no clinical signs of prion disease or any sort of abnormality and normal body weights. The remaining 10 mice per treatment group were euthanized at the terminal stage in which they developed clinical signs of scrapie. All experimental procedures and animal care procedures were approved by the University of Alberta Animal Care and Use Committee for Health Sciences Laboratory Animal Services in accordance with the guidelines of the Canadian Council on Animal Care (6).

2.3. Sample Collection

Urine samples were taken at 4 time points, 11 wk pi, 2 months prior to euthanasia (D-2), 1 month prior to euthanasia (D-1), and at clinical or end stage prior to being euthanized (D). Upon sample collection, urine samples were snap-frozen on dry ice and stored at -86 °C for future analysis.

Serum samples were collected at two time points, before 11 wk pi and at the time of euthanasia because of terminal sickness. Prior to blood collection, animals were anesthetized using isoflurane gas. After checking their reflexes to make sure of the loss of pain sensation, blood samples were taken via cardiac puncture. The blood was then kept at +4 °C overnight and then centrifuged (at 1500 rpm for 10 min) for better separation of the serum and blood cells.

2.4. Direct flow injection mass spectrometry (DI-MS)

Urine samples were analyzed by DI-MS. Pooled samples from 3 individual mice per each treatment group and each time point (11 wk pi, D-1, and D) were analyzed. Urine samples were thawed on ice in the biosafety cabinets. 100 µL of each sample were aliquoted in Eppendorf

tubes (Eppendorf, Hamburg, Germany). Using phosphoric acid (Sigma-Aldrich, St. Louis, USA) and pH-paper (Whatman pH Indicator, Sigma-Aldrich, St. Louis, USA), sample pH was adjusted to 5.0. 300 μ L of cold isopropanol was then slowly added to each sample while keeping the samples on ice. The samples were left for 1h on ice with occasional shaking. 150 μ L of cold chloroform (Sigma-Aldrich, St. Louis, USA) was subsequently added to the solution. The solutions were thoroughly mixed and left for another hour to allow protein denaturation and precipitation. The samples were then centrifuged at 10,000 rpm for 20 min at 4 °C (Eppendorf, Hamburg, Germany). The solution then separates into three phases, protein pellet at the bottom, chloroform layer in the middle and the water layer on top. Using a 1 mL syringe (Becton Dickinson Company, Franklin Lakes, USA) with an 18-gauge needle, the chloroform layer is extracted into a glass tube (Fisher Scientific, Waltham, USA). The protein-free chloroform layer is then checked with coomassie (Bio-RAD, Hercules, USA) staining method to be devoid of any protein. After confirmation of uncontaminated chloroform extract, the glass screw vials are disinfected and transferred out of the prion facility for DI-MS analysis.

A targeted quantitative metabolomics approach was used to analyze the urine samples using direct flow injection mass spectrometry (Absolute*IDQ*TM Kit, BIOCRATES Life Sciences AG, Austria). This kit assay in combination with a 4000 QTrap (Applied Biosystems/MDS Sciex) mass spectrometer was used for targeted identification and quantification of a large number of endogenous metabolites including amino acids, acylcarnitines, glycerophospholipids, sphingolipids, and sugars. The method used combines the derivatization and extraction of analytes, and the selective mass-spectrometric detection using multiple reaction monitoring (MRM) pairs. Isotope-labeled internal standards are integrated in the kit plate filter for metabolite quantification.

The Absolute*IDQ* kit contains a 96 deep-well plate with a filter plate attached with sealing tape, and reagents and solvents used to prepare the plate assay. The first eight wells of the plate were used as blank wells. Samples were prepared for the assay as described in the User Manual. Samples were vortexed and centrifuged at 13,000 g for 3 min. Ten μL of the supernatant of each urine sample were loaded on the filter paper of the plate and dried in a stream of nitrogen gas (Praxai, Danbury, USA). Extraction of metabolites is then achieved using methanol (Fisher Scientific, Waltham, USA) containing 5 mM ammonium acetate (BDH, Toronto, Canada). The extracts were analyzed using a 4000 QTrap (Applied Biosystems/MDS Sciex, Framingham, USA) mass spectrometer. A standard flow injection protocol consisting of two 20 μL injections (one for the positive and one for the negative ion detection mode) was applied for all measurements. MRM detection was used for quantification. Met/*Q* software (Biocrates, Life Sciences AG, Eduard-Bodem-Gasse, Austria) provided with the kit controls the entire assay workflow, i.e., sample registration, automated calculation of metabolite concentrations, export of data into other data analysis programs. Quantified metabolite concentrations were then analyzed using MetaboAnalyst 2.0 (<http://www.metaboanalyst.ca/MetaboAnalyst/faces/Home.jsp>).

2.5. Nuclear Magnetic Resonance (^1H -NMR)

Urine analysis. Urine samples were thawed on ice in the biosafety cabinets. Due to limited volume of urine samples per individual, samples from various replicates within each treatment group at a given time point were pooled to make 32.8 μL of total sample volume. 0.7 μL of 1M NaPO_4 (pH=7.0; Sigma-Aldrich, St. Louis, USA) were added to each pooled sample. In addition, 1.5 μL of a standard buffer solution (11.667 mM DSS [disodium-2,2-dimethyl-2-silapentane-5-sulphonate], 730 mM imidazole, and 0.47% NaN_3 in H_2O ; Sigma-Aldrich, St. Louis, USA) was added to the solution. The final 35 μL volume were then injected into capillary tubes (size/cap

0.8-1.1x90mm, Kimble Chase, Vineland, USA) using Hamilton syringe (7000 series, Modified Microlitre™ Syringe, Hamilton, USA). Capillary tubes were then sealed with wax and transferred within a standard 5 mm thin-walled glass NMR tube (Wilmad-LabGlass, Vineland, USA). NMR tubes were filled with sufficient amount of D₂O to cover up to the urine level within the capillary tubes (tube in tube method).

All ¹H-NMR spectra were collected on a 500 MHz (Varian Inc. Palo Alto, California, USA) spectrometer equipped with a 4 mm pulsed-field gradient (PFG) indirect detection nanoprobe. ¹H-NMR spectra were acquired at 25 °C using the first transient of the Varian tnoesy-presaturation pulse sequence, which was chosen for its high degree of quantitative accuracy. Spectra were collected with 128 transients and 8 steady-state scans using a 4 sec acquisition time and 1 sec recycle delay. Prior to spectral analysis, all FIDs (free induction decays) were zero-filled to 64,000 data points and line broadened 0.5 Hz. The singlet produced by the DSS methyl groups was used as an internal standard for chemical shift referencing (set to 0 ppm) and for quantification. The ¹H-NMR spectra were processed and analyzed using the Chenomx NMR Suite Professional Software package version 7.1 (Chenomx Inc, Edmonton, Alberta, CA). The Chenomx NMR Suite software allows qualitative and quantitative analysis of the ¹H-NMR spectrum by manually fitting spectral signatures from the standard Chenomx 500 MHz metabolite library. To minimize compound misidentification and misquantification, each spectrum was processed and analyzed.

Serum analyses. A significant concentration of proteins and lipoproteins are present in the serum. In using ¹H-NMR spectroscopy these large molecular weight particles tend to affect identification of small molecular weight metabolites. Therefore, serum samples undertake a deproteinization step which involves ultra-filtration of the samples. Serum samples were thawed

on ice in the biosafety cabinets. Due to limited serum sample volume per individual, samples from various replicates within each treatment group at a given time point were pooled to make 400 μL of total sample volume. Aliquots of pooled serum samples were transferred to 3 KDa cut-off filter units (Amicon Microcon YM-3, EMD Millipore, Billerica, USA) and centrifuged for >50 minutes at 12,000 rpm (Eppendorf, Hamburg, Germany). The centrifugal filter units are rinsed five times with dH_2O (0.5 mL, 10 minutes at 10,000 rpm) prior to filtration in order to remove residual glycerol bound to filter membranes. The filtered serum is then checked subjectively for any evidence of membrane damage or compromised. If membrane damage is observed, those samples were repeated with a different filter unit. 300 μL of the normal serum filtrates are then collected and added to 30 μL of D_2O and 15 μL of the standard buffer solution (11.667 mM DSS [disodium-2, 2-dimethyl-2-silcepentane-5-sulphonate], 730 mM imidazole, and 0.47% NaN_3 in ddH_2O).

The final 345 μL volume was then transferred to a standard SHIGEMI tube (Shigemi Co., Hachioji-City, Japan) for subsequent spectral analysis. All ^1H -NMR spectra were collected on a 500 MHz (Varian Inc. Palo Alto, California, USA) spectrometer equipped with a 4 mm PFG indirect detection nanoprobe. ^1H -NMR spectra were acquired at 25 $^\circ\text{C}$ using the first transient of the NOESY- pre-saturation pulse sequence, chosen for its high degree of quantitative accuracy. All FIDs were zero-filled to 64 K data points and subjected to line broadening of 0.5 Hz. The singlet produced by the DSS methyl groups was used as an internal standard for chemical shift referencing (set to 0 ppm) and for quantification. The ^1H -NMR spectra were processed and analyzed using the Chenomx NMR Suite Professional Software package version 7.1 (Chenomx Inc, Edmonton, Alberta, CA). The Chenomx NMR Suite software allows qualitative and quantitative analysis of the NMR spectrum by manually fitting spectral signatures from the

standard Chenomx 500 MHz metabolite library. To minimize compound misidentification and misquantification, each spectrum was processed and analyzed by 2 NMR spectroscopists.

2.6. Statistical analysis

To determine the alterations in concentration of various metabolites detected by DI-MS, multivariate analysis a partial least squares regression analysis (PLSDA) was conducted using MetaboAnalyst 2.0 (<http://www.metaboanalyst.ca/MetaboAnalyst/faces/Home.jsp>). The NMR spectra analysis was conducted using Chenomx NMR Suite 7.1 (CHENOMX, Canada) accompanied with statistical analysis method using Mann-Whitney-Wilcoxon and Kruskal-Wallis tests. $P \leq 0.05$ was chosen to denote significant difference.

3. Results

3.1. Direct Injection-Mass Spectrometry

RML versus the control group (urine metabolites). The metabolic profile of urine samples collected from RML and RML+LPS treatment groups at 11 wk, D-1, and D were quantified using DI-MS. The partial least square discriminant analysis (PLSDA) of the saline control group versus the RML treatment group at 11 wk pi identified 2 separate groups with differentiable metabolite patterns (Figure 4.1). This comparison shows significant alterations in 16 metabolites including carnitine ($P < 0.005$), phosphatidylcholine diacyl (PC aa) C34:3 ($P < 0.01$), sphingomyeline (SM) C18:1 ($P < 0.01$), PC aa C36:1 ($P < 0.011$), hydroxyvalerylcarnitine ($P < 0.01$), PC aa C36:2 ($P < 0.01$), malonylcarnitine 3-hydroxybutyrylcarnitine (C3-DC(C4-OH)) ($P < 0.01$), PC aa C36:3 ($P < 0.02$), PC aa C34:1 ($P < 0.03$), sphingomyeline (SM) C24:1 ($P < 0.03$), PC aa C38:3 ($P < 0.03$), phosphatidylcholine acyl-alkyl (PC ae) C42:2 ($P < 0.03$), PC aa C38:5 ($P < 0.03$), acetylcarnitine ($P < 0.03$), methylglutarylcarnitine ($P < 0.03$), and PC aa C38:4 ($P < 0.03$).

As the prion incubation time increased in RML-treated FVB/N mice, at one month prior to euthanasia (D-1) when animals were about to initiate developing typical clinical signs of prion disease, the PLSDA plot differentiates clearly between the urine metabolites of the control group versus the RML treatment group (Figure 4.2). Statistical comparisons show that RML-treated mice have significant alterations in their urine carnitine ($P<0.03$), lysophosphatidylcholine acyl (lysoPC a) C20:3 ($P<0.04$), and PC aa C36:3 ($P<0.04$) when compared to the controls. At terminal stage, where the animals have sustained various prion clinical signs for over 72 hours, comparisons between the urine samples of the healthy controls versus the RML treatment group clearly separated these two groups (Figure 4.3). Metabolite alterations at D between the RML and control group showed significant differences in concentrations of urine carnitine ($P<0.01$), PC aa C34:3 ($P<0.01$), PC aa C42:4 ($P<0.01$), PC aa C36:3 ($P<0.02$), PC aa C34:2 ($P<0.02$), PC aa C38:5 ($P<0.02$), lysoPC a C18:0 ($P<0.02$), PC aa C36:4 ($P<0.03$), PC aa C34:4 ($P<0.035$), PC aa C34:1 ($P<0.04$), PC aa C36:2 ($P<0.044$), PC aa C38:4 ($P<0.049$), and PC aa C36:5 ($P<0.05$).

RML group over time (urine metabolites). Over the period of 11 wk, D-1, and D when the animals were euthanized, quantification of metabolites in the RML inoculated animal's revealed various metabolic signatures that tended to change significantly over the period of 11 wk until death (D). Even though the comparisons do not show clear separation of the metabolic profile at 11 wk, D-1, and D (Figure 4.10), 2 of the urine metabolites show significant alterations over time from 11 wk until D. These include hexadecanoylcarnitine ($P<0.01$), which is significantly different at 11 wk in comparison to D, and at D-1 compared to D, and C3-DC(C4-OH) ($P<0.02$), which significantly different at 11 wk in comparison to D and D-1.

RML+LPS versus control (urine metabolites). With regards to the RML+LPS treatment group, the PLSDA plot showed separation versus control group at 11 wk pi (Figure 4.4). Statistical analysis also showed significant differences in the concentration of 24 RML+LPS urine metabolites including glutaconylcarnitine ($P<0.001$), PC aa C36:3 ($P<0.01$), PC aa C36:2 ($P<0.01$), PC aa C38:4 ($P<0.01$), acetylcarnitine ($P<0.01$), butyrylcarnitine ($P<0.0071$), carnitine ($P<0.009$), C3-DC(C4-OH) ($P<0.01$), PC aa C34:3 ($P<0.01$), SM C24:1 ($P<0.01$), PC aa C34:2 ($P<0.02$), PC aa C36:1 ($P<0.02$), PC aa C34:1 ($P<0.02$), methylglutaryl carnitine ($P<0.02$), lysoPC a C20:3 ($P<0.02$), PC aa C36:4 ($P<0.02$), PC aa C38:3 ($P<0.03$), hydroxyhexadecanoylcarnitine ($P<0.032$), hydroxyvalerylcarnitine ($P<0.03$), hydroxysphingomyeline (SM(OH)) C22:1 ($P<0.03$), SM C18:1 ($P<0.04$), SM C16:1 ($P<0.04$), PC ae C34:1 ($P<0.04$), and SM C16:0 ($P<0.05$) when compared to the saline-treated control group at 11 wk pi. At D-1, the PLSDA plot for the RML+LPS treated animals versus the controls also showed a distinguishable difference between the 2 treatment groups (Figure 4.5). Alterations in 11 urine metabolites, PC aa C34:1 ($P<0.01$), PC aa C36:3 ($P<0.01$), PC aa C34:2 ($P<0.012$), lysoPC a C18:0 ($P<0.01$), PC aa C34:3 ($P<0.017$), PC aa C36:2 ($P<0.02$), methylglutaryl carnitine ($P<0.03$), PC aa C36:4 ($P<0.03$), PC aa C34:4 ($P<0.03$), PC aa C38:4 ($P<0.03$), tetradecanoylcarnitine ($P<0.05$), were identified versus saline-treated mice. RML+LPS treated animals at D, with clinical signs of prion disease, also had distinguished urine metabolites from the control mice (Figure 4.5). Statistical analysis showed significant alterations in 8 urine metabolites of the RML+LPS treatment group at D; PC aa C36:3 ($P<0.02$), PC aa C34:2 ($P<0.02$), PC aa C34:3 ($P<0.02$), lysoPC a C18:0 ($P<0.02$), PC ae C42:2 ($P<0.03$), PC aa C38:4 ($P<0.03$), PC aa C36:2 ($P<0.03$), PC aa C34:1 ($P<0.04$).

RML+LPS treatment group over time (urine metabolites). The PLSDA plot showing the comparisons of the RML+LPS treatment group at 11 wk, D-1, and D (Figure 4.10) revealed separation of urine metabolites at 11 wk pi from both the D-1 and D samples. This was also accompanied by 15 different urine metabolites that showed significant differences from 11 wk pi until D. These metabolites included hydroxyhexadecanoylcarnitine ($P<0.0012$), C3-DC(C4-OH) ($P<0.01$), lysoPC a C20:3 ($P<0.01$), hexose ($P<0.01$), all having significant difference between all 3 timelines, carnitine ($P<0.01$) and methylglutaryl carnitine ($P<0.01$) with both having significant difference at 11 wk pi in comparison to D-1 and D, lysoPC a C18:0 ($P<0.01$) with significant difference at 11 wk pi versus D and D-1 versus D, hydroxyvalerylcarnitine ($P<0.01$) significantly different at 11 wk pi in comparison to D-1 and D, hexadecanoylcarnitine ($P<0.01$) with significant difference at 11 wk pi versus D, and D-1 versus D, butyrylcarnitine ($P<0.01$) and PC ae C34:1 ($P<0.01$) both significantly different at 11 wk pi in comparison to D-1 and D, hydroxytetradecenoylcarnitine ($P<0.02$) and tetradecadienyl carnitine ($P<0.02$) both significantly different at 11 wk pi versus D and D-1 versus D, PC aa C42:2 ($P<0.04$) significantly different at 11 wk pi in comparison to D-1 and D, and SM C24:1 ($P<0.04$) significantly different at 11 wk pi in comparison to D-1.

RML versus RML+LPS treatment groups over time (urine metabolites). The RML and RML+LPS treatment groups were compared at 11 wk, D-1, and D to verify metabolite differences at each time point. At 11 wk pi, D-1, and D the metabolites of both treatment groups differentiate from each other as shown by PLSDA plots (Figures 7, 8, and 9 respectively). At 11 wk pi, the 2 treatment groups showed significant differences only in one metabolite, PC aa C34:2 ($P<0.01$). This was also valid at D-1 with only PC ae C44:3 ($P<0.03$) showing significant difference between the urine samples of both treatment groups. At terminal sickness, D, 3 urine

metabolites showed significant differences including C3-DC(C4-OH) ($P<0.01$), lysoPC a C18:0 ($P<0.01$), and carnitine ($P<0.03$).

3.2. Nuclear Magnetic Resonance ($^1\text{H-NMR}$)

Increasing urine metabolites. NMR Spectra revealed various alterations in the urine metabolic profile of RML and RML+LPS-treated FVB/N female mice from 11 wk pi until terminal sickness. The RML treatment group showed a significant ($P<0.01$) increase in the level of urine acetoacetate from 11 wk up to D while only being significantly different from the negative control at 11 wk ($P<0.01$), D-2 ($P<0.05$), and D-1 ($P<0.05$). In the RML+LPS-treated group, a significant ($P<0.01$) increase in urine 3-methyl-2-oxovalerate from 11 wk up to D is observed with only 11 wk ($P<0.01$) and D-2 ($P<0.03$) showing significant difference from the negative control.

Decreasing urine metabolites. Various different urine metabolites showed decreasing trends over time, from 11 wk until D, in both the RML and RML+LPS treatment urine samples. The RML treatment group exhibits significant decreasing pattern in urine 3-indoxylsulfate ($P\leq 0.001$), arginine ($P\leq 0.001$), carnitine ($P<0.03$), dimethylamine ($P<0.03$), ethanol ($P\leq 0.001$), and lactate ($P<0.02$) over 11wk to D. This is while 3-indoxylsulfate and lactate showed significant differences from the negative control at D-2 ($P<0.04$ and $P<0.05$, respectively), D-1 ($P\leq 0.0001$ and $P<0.04$, respectively), and D ($P<0.0001$ and $P<0.01$, respectively), ethanol was significantly different from the negative control at D-2 ($P<0.03$) and D ($P<0.01$), arginine and dimethylamine were different from the negative control at D-1 ($P<0.01$ and $P<0.01$, respectively) and D ($P<0.01$ and $P<0.03$, respectively), and carnitine was different at D-1 ($P<0.04$) when compared to the saline treated animals. The RML+LPS treatment group showed only 3 urine metabolites

with decreasing trends from 11 wk to D; betaine ($P<0.001$), O-acetylcarnitine ($P<0.0001$), and scyllitol ($P<0.001$), which were different from the negative control at D ($P\leq 0.0001$), 11 wk ($P<0.02$), D-1 ($P<0.02$), D ($P<0.0001$), D-2 ($P<0.04$), D-1 ($P<0.01$), and D ($P<0.0001$), respectively.

Increasing serum metabolites. Serum metabolites were quantified at 2 time points, 11 wk pi and D. RML-treated animals had 9 increasing metabolites including 3-hydroxybutyrate ($P<0.001$), acetoacetate ($P<0.02$), acetone ($P<0.0001$), carnitine ($P<0.03$), choline ($P<0.01$), malonate ($P<0.02$), ornithine ($P<0.001$), pyruvate ($P<0.0001$), and succinate ($P<0.001$). All increasing serum metabolites of the RML group, except 3-hydroxybutyrate and acetone, were significant ($P<0.05$) both at 11 wk and D when compared to the negative saline controls while 3-hydroxybutyrate and acetone were different ($P<0.02$) only at D. On the other hand, the RML+LPS treatment group had increasing urine 3-hydroxybutyrate ($P<0.03$), acetate ($P<0.02$), acetoacetate ($P<0.001$), acetone ($P<0.0001$), choline ($P<0.0001$), creatine ($P<0.007$), glutamate ($P<0.0001$), ornithine ($P<0.005$), pyruvate ($P<0.0001$), and succinate ($P<0.002$) from 11 wk pi to D. These metabolites showed difference ($P<0.05$) from negative controls both at 11 wk pi and at D with the exception of acetoacetate being different ($P<0.01$) only at 11 wk, glutamate and pyruvate being different ($P<0.01$) only at D, and 3-hydroxybutyrate showed no difference from the saline-treated animals.

Decreasing serum metabolites. Fourteen metabolites in the serum of the RML treatment group were detected decreasing from 11 wk pi until terminal sickness stage including alanine ($P<0.03$), arginine ($P<0.01$), aspartate ($P<0.01$), betaine ($P<0.0001$), creatine ($P<0.01$), glucose ($P<0.001$), isobutyrate ($P<0.0006$), isoleucine ($P<0.001$), methanol ($P<0.02$), methionine ($P<0.001$), serine ($P<0.01$), valine ($P<0.04$), sn-glycero-3-phosphocholine ($P<0.01$), and 3-

methylhistidine ($P<0.001$). All decreasing serum metabolites were different ($P<0.05$) from the negative controls with the exception of creatine and 3-methylhistidine which were different ($P<0.02$) at 11 wk pi, arginine, aspartate, glucose, isoleucine, and serine different ($P<0.02$) at D, and alanine and valine were no different from the negative controls. The serum samples collected from the RML+LPS treatment group from 11 wk pi to D exhibited various metabolites with a decreasing trend including alanine ($P<0.01$), arginine ($P<0.05$), aspartate ($P<0.001$), betaine ($P<0.02$), citrate ($P<0.02$), ($P<0.02$), hypoxanthine ($P<0.0001$), leucine ($P<0.01$), methanol ($P<0.002$), methionine ($P<0.0001$), and serine ($P<0.001$). These metabolites showed difference ($P<0.05$) when compared to the negative controls at both 11 wk and D, except glycine, leucine, methanol, and methionine which were different ($P<0.01$) only at 11 wk compared to the negative controls; aspartate was different ($P<0.01$) from the negative controls only at D, and alanine was not different from the negative controls.

RML versus RML+LPS (serum metabolites). Statistical comparisons showed differences between the metabolic profiles of the RML versus RML+LPS treatment groups in concentrations of 3-methyl-2-oxovalerate ($P\leq 0.0001$), 3-indoxylsulfate ($P<0.03$), dimethylamine ($P<0.04$), ethanol ($P\leq 0.0001$), and scyllitol ($P\leq 0.0001$). Comparisons between the serum metabolic profile of the RML versus RML+LPS treatment groups showed differences in concentrations of 3-hydroxybutyrate ($P<0.001$), acetone ($P<0.01$), ornithine ($P<0.0001$), pyruvate ($P<0.0001$), and succinate ($P<0.02$).

4. Discussion

4.1. Common RML and RML+LPS predictive metabolites

In this study we sought to identify potential predictive and diagnostic metabolites and biomarkers of scrapie in the serum and urine of mice infected sc with RML or RML+LPS. Indeed results of this study showed changes of various metabolites in both urine and serum of infected animals. Among the common altered serum metabolites of the RML and RML+LPS treatment groups that showed significant difference in comparison to the control mice at different time points, several have been detected with a linear increasing or decreasing trend over time, from 11 wk pi up to terminal sickness.

Choline was one of the organic compounds and essential vitamins that increased in the serum of both RML and RML+LPS treatment groups. Choline performs an important role as component of neurotransmitter acetylcholine (ACh; Freeman and Jenden, 1976). Choline cannot be synthesized *de novo* within the brain or by the host, and therefore depends on the diet and blood supply to provide substantial levels to the cholinergic neurons in the brain (Cohen and Wurtman, 1975). Evidence indicates that loss of cholinergic neurotransmission and function in the CNS is associated with cognitive impairments observed in Alzheimer's and Parkinson's diseases (AD and PD, respectively) (Hall et al., 2013). Therefore, substantial supply of blood choline must be provided to meet the needs of an infected brain during the process of neurodegeneration, as confirmed by our ¹H-NMR data. Another possibility for increased levels of choline in the serum of RML and RML+LPS infected mice in comparison to the controls, from 11 wk pi up to terminal sickness, could be related to its release as a result of ACh hydrolysis. It has been reported that during both AD and PD administration of acetylcholinesterase inhibitors restores cholinergic neurotransmission (Keowkase et al., 2010; Hall et al., 2013). The excess choline may be removed from the brain via the blood elsewhere in

the body. Another source of choline are choline-containing phospholipids, i.e., phosphatidylcholine, which make up about 40% of phospholipids of the cellular membranes in eukaryotic cells (Kelin, 2000). During neurodegenerative diseases there is a breakdown of neuronal cell membranes and the released phosphatidylcholine is hydrolyzed into free choline. Therefore, the increased concentrations of choline in the serum of RML- and RML+LPS-infected mice from 11 wk to terminal sickness might also reflect breakdown of cell membranes during scrapie. Elevated levels of choline-containing compounds have been reported also in cases of AD (Klein, 2000). Choline also helps in maintaining high carnitine concentrations in the blood (Dodson and Sachan, 1996).

Ketone bodies were the other category of organic compounds detected by $^1\text{H-NMR}$ analysis to be altered in the urine and serum sample of RML and RML+LPS inoculated mice. Acetoacetate and 3-hydroxybutyrate are ketone bodies produced by the liver, which is taken from the blood to be used as a source of energy in the brain (Nehlig, 2004; Pifferi et al., 2011; Nugent et al., 2013). In neurodegenerative pathologies, compensation for brain energy, which under normal conditions is majorly provided through glucose consumption from the blood, becomes a major concern (Pifferi et al., 2011). Due to decreased feed consumption, possible starvation, and drop of body weight in the context of progressing neurodegenerative disorder, alternative methods of energy production such as ketone bodies become crucial. At times of deficient glucose supply in the blood, up to 70% of brain energy can be supplied from ketone bodies (Cahill et al., 2006). Ketone bodies also play an important role in the process of autophagy (self-eating) especially in neuronal cells (Martinez-Vicente et al., 2007). Autophagy is not limited to starvation conditions and may function under normal conditions to rid cells of damaged or accumulated proteins. Autophagy may be an important mechanism of neurons to

clear axonal obstructions such as those that occur in AD or other prion diseases (Stokin et al., 2006). This might explain the high concentration of acetoacetate and 3-hydroxybutyrate in serum samples of RML and RML+LPS infected mice from 11 wk pi until terminal sickness detected by ¹H-NMR spectroscopy in our experiment. In alignment with that, increased levels of blood ketone bodies have been proven to improve short-term cognitive function at times of brain neurodegeneration such as AD (Henderson, 2008). Furthermore, ketones are reported to have neuroprotective activity as well as being precursors of lipid and amino acids synthesis in the body (Buckley and Williamson, 1973; DeVivo et al., 1975; Webber and Edmond, 1977; Kashiwaya et al., 2000; Noh et al., 2006). On the other hand, ketones are not bound to any compound in the blood and thus are freely available (Comstock and Garber, 1990). This allows free filtration of the ketones in the kidney of the host. This can explain increased concentration of urinary acetoacetate from 11 wk pi to D. In addition, increased presence of ketone bodies such as acetoacetate from 11 wk until D in the urine of RML- and RML+LPS-infected mice is an indicator of metabolic and physiological disorders in the host, which is insignificant at normal healthy conditions (Klocker et al., 2013).

L-Arginine (Arg) is one of the interesting compounds that was found to decrease in both urine and serum of RML- and RML+LPS-inoculated mice detected by ¹H-NMR spectroscopy from 11 wk pi until terminal sickness. Arginine depletion has been shown to be neuroprotective (Esch et al., 1998). Arginine is an amino acid required for production of nitric oxide (NO) (Harry et al., 2001). The latter is an atypical messenger molecule biosynthesized from Arg and molecular oxygen by NO synthase (NOS). NO plays an important role as vasodilator and neurotransmitter, and is involved in cellular immune responses. In addition, NO can react with superoxide to produce reactive peroxynitrite that causes oxidative damage to proteins by

nitration of tyrosine residues and may lead to cellular injury (Wiesinger, 2001). Several reports indicate that excess production of peroxynitrite plays a crucial role in neuronal cell death (Radi, 2013; Neniskyte and Brown, 2013). NO also plays a protective role in the brain because neurons that express NOS are resistant to various types of neurotoxic insults including NMDA mediated toxicity (Nitsch et al., 1991), ischemic hypotoxic insults (Noh et al., 2006), and the degenerative processes of HD (Nugent et al., 2013). Therefore, greater amounts of Arg are probably required locally to produce NO molecules. This might explain lower quantities of Arg in the blood and urine of treated mice.

Decreasing concentrations of betaine in the serum of RML treated mice at 11 wk pi until D might contribute to enhanced NO production from microglial cells. Betaine has been shown to inhibit inducible NOS (Go et al., 2005). Inhibitory effects of betaine on production and release of NO from activated microglia serves as an anti-inflammatory mechanism in maintaining the level of neurotoxic factors in the CNS (Go et al., 2005; Amiraslani et al., 2012). It has been noted that supplementation of betaine could play an important role in prevention of chronic diseases (Craig, 2004; Feng et al., 2006; Fernandez-Figares et al., 2009) including chronic neuroinflammation at times of neurodegenerative disorders. The mechanism by which betaine protects against neurodegeneration also is related to its suppression of activation of nuclear factor-kB (NF-kB) with oxidative stress, and expression of pro-inflammatory molecules such as cyclooxygenase-2 (COX-2), and tumor necrosis factor (TNF) (Go et al., 2005). Betaine is also precursor to methionine, creatine, and carnitine and is indirectly associated with other neurodegenerative disease such as AD, PD, and dementia by manipulating levels of homocysteine (Craig, 2004; Ratriyanto et al., 2009; Amiraslani et al., 2012). Interestingly, even though betaine has shown a decreasing trend over time, RML administration to our animal models was associated with

decreased serum methionine levels from preclinical stages at 11 wk pi until exhibition of typical prion clinical signs and terminal sickness, whereas serum choline increased during the same period of time by both RML and RML+LPS treatments.

In our $^1\text{H-NMR}$ analysis of urine obtained from RML- and RML+LPS-infected mice, decreased concentrations of dimethylamine were detected from 11 wk to terminal sickness. Although small amounts of dimethylamine are ingested directly, the major dietary source is believed to be via dietary choline (Tsikas et al., 2007; Mitchel et al., 2008). Another source of dimethylamine is asymmetric dimethylarginine (ADMA) a product of protein methylation (arginine methylation), which is hydrolysed by dimethylarginine dimethylaminohydrolase (DDAH) into dimethylamine and citrulline (Vallance, 2001). Lower urinary dimethylamine in our mice infected with RML and that developed scrapie might be related to lowered feed intake and as a result lowered dimethylamine intake and elimination in the urine.

$^1\text{H-NMR}$ analysis indicated that another amino acid to be increased in the serum of mice from the RML- and RML+LPS-treated group was ornithine. Ornithine is an amino acid important for generation of polyamines. The latter play important roles for growth and division of all mammalian cells (Slotkin and Bartolome, 1986). The initial step in polyamine biosynthesis involves the decarboxylation of ornithine by the enzyme ornithine decarboxylase (ODC) (Pegg and McCann, 1982). Polyamines may play a role in the response to neuronal injury and stress (Gilad and Gilad, 1992), in regulation of ionic flux and neuronal ion channels (Lopatin et al., 1994), and in neurodegenerative conditions including AD (Greenamyre and Young, 1989). Recent reports indicate that alterations in brain polyamine metabolism may be critical for nerve cell survival after free radical initiated neurodegenerative processes. For example, elevated protein levels of the enzyme ODC were observed in neocortical neurons (Bernstein et al., 1995),

and altered polyamine levels were observed in AD frontal cortex (Seidl et al., 1996). Recent research also demonstrated that amyloid- β , associated with AD, up-regulates polyamine uptake and the activity of ODC (Yatin et al., 1999). It is possible that increased serum ornithine in RML-treated mice in our experiment might be related to enhanced availability of ornithine to help brain cells to survive the oxidative stress and death.

Among the many energy building blocks is pyruvate, an end product of cytosolic glycolysis, breakdown of carbohydrates including glucose, with mitochondrial oxidation of fatty acids and amino acids (Schell and Rutter, 2013). Pyruvate flow from the mitochondria has been denoted important in tuning cancer cells to meet their rapid growth demands (Schell and Rutter, 2013). Increasing amounts of pyruvate detected in the serum of RML and RML+LPS administered mice from 11 wk pi up to terminal sickness suggest potential utilization of this metabolite by the host physiological and immune system to protect, repair, and support the damaged and existing neurons during the course of brain degeneration for energy production. As brain degeneration progresses, the need to sustain the energy balance required by the damaged areas of the brain is compromised (Mattson et al., 1999). Of more interest, pyruvate and pyruvate derivative compounds have shown to induce immune functions in the host. Through induction of antioxidant and anti-inflammatory functions, pyruvate has proven to be cytoprotective in the CNS (Ryou et al., 2012). Pyruvate derivatives including ethyl pyruvate, the aliphatic ester of pyruvic acid, have been proposed to inhibit reactive oxygen specie (ROS)-dependent signaling pathways in microglia due to their antioxidant activities and thus inhibiting production of pro-inflammatory molecules such as inducible NOS and cytokines (Yang et al., 2002; Varma et al., 2006; Hollenbach et al., 2008). Furthermore, ethyl pyruvate has shown to suppress transcription of pro-inflammatory genes including IL-1 β , IL-6, and TNF (Song et al., 2004; Kim et al., 2008).

Interestingly, pyruvate and lactate derivatives have shown to suppress production of pro-inflammatory mediators evoked by administration of LPS to the animal model (Hollenbach et al., 2008). In this regard, increasing levels of pyruvate in serum of RML- and RML+LPS-infected mice from 11 wk until terminal sickness could also be contributing to modulating the level of neuroinflammation by altering expression and production of pro-inflammatory mediators in their brain.

Central to ATP production in the body are the mitochondria. Mitochondrial activity is responsible for more than 90% of the cellular ATP production (Protti et al., 2007). For ATP to be produced in the mitochondria the electron transport chain is necessary containing 4 complexes (Brand, 2005; Protti et al., 2007). The complexes have specific electron donors that tend to release an electron into the transfer chain. Succinate is a metabolite that serves as a specific electron donor to complex 2 of the electron transport chain (Protti et al., 2007; Ohlenbusch et al., 2012). Therefore, presence of succinate is vital for the electron chain to function and production of sufficient ATP. Our RML- and RML+LPS-inoculated mice showed increasing amounts of succinate in their blood from 11 wk pi until exhibition of terminal clinical signs of prion disease. This increased level of succinate could serve as the substrate required for increased ATP production needed at times of brain degeneration.

4.2.RML specific metabolites

Among the various urine metabolites of the RML-treated group that showed significant difference versus controls several have shown a decreasing trend detected by DI-MS analysis. One of the categories of metabolites included in our experiment were carnitines and acylcarnitines. Carnitines are compounds that are absorbed mainly from the diet or produced *de novo* and are essential for metabolism of fatty acids (Vaz and Wanders, 2002; Schooneman et al.,

2013). In this process acylcarnitines are produced to transport activated fatty acids to the mitochondria for fatty acid oxidation (Rinaldo et al., 2008; Schooneman et al., 2013). Although lipids are not the major source of energy consumption in the brain, one of the sites of carnitine synthesis is the brain itself (Jones et al., 2010). After being produced, only 20% of it is used within the brain and the rest is distributed in the body, (i.e., to the skeletal muscles and heart) through systemic circulation (Vaz and Wanders, 2002). Supplementation of carnitines and acylcarnitines have been shown to positively affect neurological disorders, perform neuroprotective and antioxidant activities, influence composition of cell membranes as well as gene regulation and protein synthesis (Jones et al., 2010). In our experiment, C3-DC(C4-OH) belonging to the acylcarnitine family showed a decreasing trend from 11 wk pi to terminal sickness with statistical difference compared to the control only at 11 wk pi. In fact carnitine itself exhibits a decreasing trend from 11 wk pi to D-1 and then maintains almost a constant concentration from D-1 up to the terminal sickness, with significant difference from control mice at 11 wk, D-1, and D. The same decreasing pattern was also observed in concentration of carnitine in the urine detected by ¹H-NMR analysis over time. Meanwhile, ¹H-NMR analysis of the serum of RML-infected mice showed increased levels carnitine maintained in the blood from 11 wk pi up to the terminal sickness. In addition, increased amounts of choline in the serum of RML- and RML+LPS-treated mice might contribute to maintaining high carnitine levels in the blood (Dodson and Sachan, 1996). Decreasing amounts of carnitine in the urine samples of RML-infected mice from 11 wk pi until D-1 together with high levels of serum carnitine could be related to increased consumption of carnitine in lipid metabolism and energy production for the body as a whole and the brain in particular. Considering the degeneration process during prion disease, the host would try to compensate the energy loss (Pifferi et al., 2011) and repair

the damaged membranes. In both scenarios carnitine metabolites might be held back from being excreted in the urine to be used by the host.

Glucose has been recognized as the main source of energy for the brain at normal conditions specifically for neural cells and is continuously supplied from the blood indirectly through astrocytes (Howarth et al., 2012). Glucose in the brain is then transformed into ATP to fuel the physiological functions related to neural and non-neural cell functions and provide precursors for neurotransmitter synthesis (Harris et al., 2012; Dienel, 2012). Of these physiological functions the most important ones include synaptic activity and action potentials which tend to consume most of the brain energy (Alle et al., 2009; Liotta et al., 2012). Disruption of glucose metabolism has been associated with neuronal cell death and brain disorders (Mergenthaler et al., 2013). Glucose was a differentiating metabolite detected to be decreasing in the serum of only RML-inoculated mice over time. Insufficient amounts of glucose supply to the brain, based on aforementioned biological contribution of glucose to the brain, would alter brain cognitive functions, synaptic functionality, and malfunctions in propagation of action potentials, and alterations in synthesis of neurotransmitters. Furthermore, apoptosis and neural death has been associated with the metabolic rate of the nerve cells. Glucose reduction in the systemic circulation can be one of the causes of pathophysiological mechanisms in the CNS and similarly, could also be the result of neurodegeneration (Mergenthaler et al., 2013). Degeneration of brain neural networks that regulate energy metabolism and glucose homeostasis (Grayson et al., 2013) could also contribute to the decreasing trend of serum glucose observed in the RML-infected mice.

Urinary lactate decreased in the RML-infected mice in our experiment from 11 wk pi up to the end stage. The mammalian brain depends on glucose and lactate as its two main sources of

energy. However, neurons do not have direct access to glucose or lactate and are not able to save energy in the form of glycogen. Both glucose and lactate are provided to neurons by astrocytes and the latter also are able to store glycogen. Astrocytes hydrolyze both glucose and glycogen into lactate available for neurons. A specific role for glycogen-derived lactate has been suggested from the observation that pharmacological inhibition of glycogen phosphorylase in rat hippocampus impairs the formation of long-term memory, an effect that could be rescued by exogenous lactate (Newman et al., 2011; Suzuki et al., 2011). In addition genetic knockdown of the lactate transporters of astrocytes (MCT4), oligodendrocytes (MCT1), and neurons (MCT2) induces amnesia. Exogenous lactate rescues memory formation in MCT4 and MCT1 knockdowns but not in MCT2 knockdown, emphasizing the relevance of lactate transfer between glial cells and neurons (Suzuki et al., 2011). The decrease in urine lactate in our mice treated with RML might be a result of high demand and utilization of lactate by neurons and also by all other brain cells in the sick mice.

One of the interesting compounds found to be increasing from 11 wk pi until terminal sickness in the serum of RML treated animals and related to mitochondrial function was malonate. Malonate has been used as a neurodegenerative agent in various research models (Greene and Greenamyre, 1996; Schulz et al., 1998; Van Westerlaak et al., 2001). Previous research indicates that malonate has the ability to function as trigger of apoptosis leading to depletion of antioxidant systems and overproduction of reactive oxygen species (ROS) in the cell from mitochondria (Ehrhart and Zeevalk, 2003; Fernandez-Gomez et al., 2005). Furthermore, malonate is categorized as mitochondrial complex inhibitor and has been used to study important brain degeneration pathways in neurodegenerative disorder such as PD and HD (Browne and Beal, 2002). Both *in vitro* and *in vivo* studies have revealed a dose-dependent effect of malonate

on neural toxicity, ATP depletion, neural depolarization, delayed caspase activation and finally apoptosis (Greene and Greenamyre, 1996; Schulz et al., 1998; Van Westerlaak et al., 2001). Interconnection of malonate to mitochondrial alterations can lead to deleterious impressions within the cell (Fernandez-Gomez et al., 2005). Increased amount of blood malonate in the RML-inoculated animals from 11 wk to terminal sickness might reflect high brain malonate content and an effort of the host to eliminate malonate from the system. However, high malonate could lead to decreased antioxidant activity within the neuronal cells leading to free production and release of ROS from mitochondria and resultant oxidative stress of the neurons. In this regard, mitochondrial alterations have been reported to release various factors within the cell leading to neuronal death (Jordan et al., 2003). At times of neurodegeneration, mitochondrial dysfunction has been suggested to play a pivotal role. Postmortem evaluation of the brain of PD models has shown dopaminergic degeneration in the substantia nigra region of the brain due to mitochondrial impairment and resultant oxidative stress (Gautier et al., 2013). Similarly, in AD and HD as well as PD, mitochondrial impairment has been found to lead to elevated concentrations of free radicals and increased production of NO (Cardinali et al., 2013). Above all, malonate-related mitochondrial dysfunction will affect the metabolic functionalities of mitochondria, i.e., calcium ion homeostasis regulation within the cell, heme and non-heme iron biosynthesis and urea production (Jordan et al., 2003).

Among the amino acids, isoleucine (Ile) and valine (Val), were the only ones found to be decreasing over time in the serum of RML-infected mice. Isoleucine and Val are categorized as branched chain amino acids (BCAA) (Korman, 2006). The latter are closely associated with lipid and glucose metabolism, both of which are highly important for energy supply of the brain (Doi et al. 2005; Layman and Walker 2006). BCAA deficiency has shown to increase fat mobilization

(Cheng et al., 2010; Du et al., 2012) leading to decreased body weight, which was the case in our experimental animals. Alterations in the level of Ile, specifically related to degradation of this amino acid, have been associated with cognitive impairment (Yang et al., 2007). Inborn errors of Ile metabolism have been reported to alter mitochondrial functionality in the CNS leading to mental and motor skill disabilities and brain degeneration (Perez-Cerda et al., 2005). On the other hand, accumulation of BCAA and their derivatives in the brain has also shown to contribute to neural death and apoptosis (Jouvet et al., 2000). This is in alignment with our data suggesting malfunctioning of the mitochondria in the CNS as detected by various aforementioned serum metabolites and decreased levels of Val and Ile in the serum of RML-infected mice over time.

Scrapie is associated with major loss of body weight, especially muscle mass. This was the case in both RML+LPS- and RML-treated mice in our experiment. Skeletal muscle is predominantly composed of structural proteins, i.e., myofibrils, and the major mechanism to maintain muscle mass is through the regulation of protein synthesis and degradation. A change in the normal balance between protein synthesis and protein degradation, i.e., a diminished protein synthesis and/or enhanced proteolysis, can lead to loss of muscle mass. There was a decrease over time in the concentrations of 3-methylhistidine (3MH) in the urine of mice treated with RML in our study. Our results are in agreement with other research reporting similar finding in an HD mouse model (She et al., 2011). Decreased 3MH in the urine and the ratio between 3MH/creatinine are indexes of proteolysis in the muscle (She et al., 2011). The same authors reported elevated apoptotic signals in muscle cells as well as in T and B lymphocytes and monocytes of HD patients (She et al., 2011; Almeida et al., 2008).

4.3. RML plus lipopolysaccharide specific metabolites

Among the many specific metabolites of the RML+LPS treatment group, some glycerophospholipids detected in the urine of infected mice showed significant differences in comparison to the controls with a decreasing trend over time. Glycerophospholipid composition of neural membranes greatly impacts their functional efficacy in modulating various membrane-related activities. This category of lipids largely impact membrane stability, accumulation of lipid peroxides, and energy metabolism disorders contributing to neural membrane alterations and resultant brain degeneration (Farooqui et al., 2000). Interestingly, at times of apoptosis, the glycerophospholipid neural plasma membrane loses its asymmetric distribution contributing to the process of neural death (Emoto et al., 1997). This change of membrane asymmetry is required in order to allow specialized molecules to tag the corresponding cell as a dying cell so that the immune cells take the required action upon it (Fadok et al., 1992). Furthermore, neurodegenerative diseases such as prion disease have been closely associated with loss of glycerophospholipids detected by change in their composition and stimulation of their degrading enzymes (Farooqui and Horrocks, 1994; Farooqui et al., 2000). In AD, alterations in glycerophospholipids have been detected to occur before manifestation of any clinical signs (Pettegrew et al., 1995). Even though it is not well understood whether alterations in brain lipid composition, including glycerophospholipids, cause or are a consequence of neural degeneration, it has been pointed out, in some neurodegenerative disorders, perturbed lipid signaling would exacerbate pathological conditions of the disease (Frisardi et al., 2011). Brain autopsies from AD patients have also shown decreased levels of glycerophospholipids as a result of lipid degradation during brain degeneration (Nitsch et al., 1991).

Scyllitol (known also as scyllo-inositol), one of the isomers of inositol, is another compound detected to be decreasing solely in urine of RML+LPS treated mice over time. Derivatives of this cyclic alcohol have shown to inhibit neuropathological symptoms in animal models of AD regardless of time of inoculation (McLaurin et al., 2006). Others have detected elevated levels of scyllitol-derivatives in degenerating brains (Griffith et al., 2007), most possibly explaining lowered levels of this compound in the urine of RML+LPS animal models.

Of the other category of metabolites detected uniquely in the serum of RML+LPS treatment group are the organic acids including citrate and acetate. Not much could be understood on the role of citrate in the context of our experiment. Derivatives of acetate have been successful in mediating an immune response in animal models of neurodegenerative disease after immunization (Bakalash et al., 2011). In AD, inoculation of acetate-derived polymers has shown effective reduction in neural loss, neurotoxic molecules, and mediating the detrimental local inflammation (Kipnis and Schwartz, 2002; Frenkel et al., 2005; Butovsky et al., 2006). Most interestingly, acetate supplementation has shown to have anti-inflammatory effects at times of LPS-induced neuroinflammation by reducing the release of pro-inflammatory cytokines and microglial activation in the brain (Brissette et al., 2012). This could explain why acetate has been uniquely detected in the RML+LPS treatment group further emphasizing the role of LPS-induced neuroinflammation. Furthermore, acetate treatment has shown to release anti-inflammatory cytokines as well (Soliman et al., 2012). Therefore, increased levels of acetate in the RML+LPS treated mice over time could be correlated to the anti-inflammatory response and mediation of microglial aggravation in the CNS. Acetate also serves as an alternative to glucose in supplying energy to the brain (Patel et al., 2010). Acetate in the brain is oxidized minimally by neurons and majorly by astrocytes (Waniewski and Martin, 1998). As brain degeneration progresses, glucose

consumption by the brain tends to decrease (as previously explained) and the need for new energy sources rise. Along with other sources, acetate seems to have a share in brain energy supply.

Another metabolite of the BCAAs specifically detected in the serum of RML+LPS treatment group only to be decreasing over time is Leu. Aside from the characteristics of BCAA and their possible contribution to brain degeneration mentioned previously, Leu plays a crucial role in glutamate (Glu) metabolism in the CNS. Glutamate is also an amino acid, which functions as a neurotransmitter. Excess amount of Glu would exacerbate postsynaptic stimulation leading to excitotoxicity (Nicholls et al., 1999; Yudkoff et al., 2005). Leucine, on the other hand, is capable of crossing from blood into the brain and entering the astrocytes (Yudkoff et al., 2005). Within the astrocytes, Leu undergoes a series of events giving rise to Glu production (Meldrum, 2000; Hutson et al., 2001). Glutamate (Glu) is then released to the neurons to be used as excitatory neurotransmitter. Low levels of Leu detected in the serum of RML+LPS treatment group could implicate lower production of the excitatory neurotransmitter, Glu, in the brain. This interpretation fits the clinical observations in our study as the animals would lose their activity, mobility, and interaction during the course of disease progression. Furthermore, BCAAs have been proposed to facilitate neurodegeneration by manipulating microglial functionality. It has been suggested that high levels of BCAAs, including Leu, would trigger production of neurotoxic factors including ROS from microglia (De Simone et al., 2013). Meanwhile, high levels of BCAAs have been associated with lower expression of pro-inflammatory microglial molecules and NOS (De Simone et al., 2013). Therefore, quite contrary and in the context of our experiment, low levels of BCAA, in this case being Leu, would lead to further expression of

microglial pro-inflammatory mediators including TNF, IL-1, and NOS facilitating neurodegeneration.

Taking into consideration the effect of reduced Leu in the blood on Glu production in the brain, high concentration of serum Glu, as detected in our experiment in the RML+LPS treatment group, would sound contradictory. However, elevated levels of blood Glu does not reflect high concentrations in the brain as little or no Glu can be transported from the blood into the brain (Yudkoff et al., 2005). While the mechanism is not yet well established, high extracellular fluid, including blood Glu levels have been observed after several acute brain degenerations leading to further neural disorders (Zauner et al., 1996; Koura et al., 1998).

4.4. Creatine

Creatine is the only metabolite detected in the serum of infected mice that has shown diverse behaviors when comparing RML and RML+LPS treatment groups. Serum of RML-inoculated mice showed decreasing values for creatine concentrations from 11 wk pi until terminal sickness, whereas this metabolite was found to be increasing in the serum of RML+LPS-inoculated mice during the same time frame. Creatine supplementation has been successfully implicated in neurological diseases by buffering the cytosolic and mitochondrial environment, which is important in energy homeostasis of the brain (Rae et al., 2003). Besides its function in boosting brain performance by influencing brain energy supply, it has been shown that creatine also performs neuroprotective functions in degenerating brains by majorly targeting ROS production in the CNS (Wyss and Schulze, 2002; Lawler et al., 2002). Creatine is found to have antiapoptotic, antiexcitotoxic, and antioxidant characteristics together with enhancing neural growth and cognitive functions of the brain (Klopstock et al., 2011). In PD mitochondrial dysfunction and oxidative stress of the dopaminergic neurons have been denoted pivotal in

inducing brain degeneration, both of which are modulated by creatine levels (Schapira, 2008; Klopstock et al., 2011). Therapeutic strategies, which include creatine in their combination have shown to provide additional neuroprotective effects in cases of PD by modulating bioenergetic balance of the CNS and enhancing cellular energy charge (Klivenyi et al., 2003; Yang et al., 2009; Genius et al., 2012). Therefore, decreased concentrations of creatine in the serum of RML-administered mice from 11 wk pi until terminal sickness could contribute to higher susceptibility of neurons in the CNS to apoptosis, excitotoxicity, and neurotoxicity of ROS produced. On the other hand, interesting reports indicate that creatine derivatives, i.e., creatine kinase, exhibit an important role in the host immunity contributing to recognition and inhibition of the growth of highly abundant LPS-containing Gram-negative bacteria, *E. coli* (Gao et al., 2007; An et al., 2009). This could explain the controversy of why creatine is increasing in the RML+LPS treatment from preclinical stages up to terminal sickness elucidating the role and interaction between bacterial LPS and creatine. Taking into consideration that in our experiment LPS has been administered in a chronic manner, over a 6-wk period, detection of this highly immunogenic bacterial compound by the host immune system could lead to further release of creatine into blood which could also potentially benefit the CNS at times of neurodegeneration.

5. Conclusions

Detection of predictive candidate biomarkers in readily accessible biofluids has become a necessity. In neurodegenerative disease, including prion disease, detection of these predictive biomarkers could help in better understanding the disease process and most importantly, serve as potential indicators of disease onset at preclinical stages. With scientific breakthroughs and discovery of various treatments, it could be promising to treat prion disease in early stages. Development of various preclinical biomarker detection strategies of prion diseases in wild life

and livestock animals could also serve in preventing the spread of disease within and between various species. In this paper, using non-targeted and non-invasive metabolomics technologies, we have detected various lipids, amino acids, and other compounds related to energy metabolism in readily accessible fluids, blood and urine, that could serve as potential biomarkers of prion disease. Further research with higher number of replicates is required to validate these results.

6. Acknowledgments

We like to thank Dr. Rupasri Mandal, Dr. Trent Bjorndahl, Dr. BeomSoo Han, Ying Dong, Philip Liu, and Dr. Farid Aziat, at the Faculty of Science at University of Alberta in contributing to the metabolomics analysis. The authors also acknowledge the Alberta Livestock and Meat Agency Ltd. (ALMA), Alberta Prion Research Institute (APRI), and the Natural Sciences and Engineering Research Council (NSERC) of Canada for funding of this project. We also thank the technical staff at Centre for Prions and Protein Folding Diseases, Edmonton, University of Alberta for their daily monitoring and care for the mice.

References

1. Aguzzi, A., M., Nuvolone, and C., Zhu, 2013, The immunobiology of prion diseases, *Nature Reviews Immunology*, Volume 13, p. 888-902.
2. Alle, H., A., Roth, and J. R., Geiger, 2009, Energy-efficient action potentials in hippocampal mossy fibers, *Science*, Volume 325, p. 1405–1408.
3. Almeida, S., A. B., Sarmiento-Ribeiro, C., Januario, A. C., Rego, and C. R., Oliveira, 2008, Evidence of apoptosis and mitochondrial abnormalities in peripheral blood cells of Huntington's disease patients, *Biochemical and Biophysical Research Communications*, Volume 374, p. 599–603.
4. Ametaj, B. N., S., Sivaraman, S. M., Dunn, and Q., Zebeli, 2012, Repeated oral administration of lipopolysaccharide from *Escherichia coli* 0111:B4 modulated humoral immune responses in periparturient dairy cows, *Innate Immunity*, Volume 18, p. 638-647.
5. Amiraslani, B., F., Sabouni, S., Abbasi, H., Nazem, and M., Sabet, 2012, Recognition of Betaine as an Inhibitor of Lipopolysaccharide-Induced Nitric Oxide Production in Activated Microglial Cells, *Iranian Biomedical Journal*, Volume 16, p. 84-89.
6. An, Y., N., Fan, and S., Zhang, 2009, Creatine kinase is a bacteriostatic factor with a lectin-like activity, *Molecular Immunology*, Volume 46, p. 2666-2670.
7. Andrievskaia, O., J., Algire, A., Balachandran, and K., Nielsen, 2008, Prion protein in sheep urine, *Journal of Veterinary Diagnostic Investigation*, Volume 20, p. 141-148.
8. Bakalash, S., M., Pham, Y., Koronyo, B. C., Salumbides, A., Kramerov, H., Seidenberg, D., Berel, K. L., Black, and M., Koronyo-Hamaoui, 2011, Egr1 Expression Is Induced Following Glatiramer Acetate Immunotherapy in Rodent Models of Glaucoma and Alzheimer's Disease, *Investigative Ophthalmology and Visual Science*, Volume 52, p. 9033-9046.

9. Brissette, C. A., H. M., Houdek, A. M., Floden, and T. A., Rosenberger, 2012, Acetate supplementation reduces microglia activation and brain interleukin-1 β levels in a rat model of Lyme neuroborreliosis, *Journal of Neuroinflammation*, Volume 9, p. 249-259.
10. Brand, M. D., 2005, The efficiency and plasticity of mitochondrial energy transduction, *Biochemical Society Transactions*, Volume 33, p. 897–904.
11. Browne, S. E., and M. F., Beal, 2002, Toxin-induced mitochondrial dysfunction, *International Review of Neurobiology*, Volume 53, p. 243–279.
12. Buckley, B. M., and D. H., Williaamson, 1973, Acetoacetate and Brain Lipogenesis: Developmental Pattern of Acetoacetyl-Coenzyme A Synthetase in the Soluble Fraction of Rat Brain, *Biochemical Journal*, Volume 132, p. 653-656.
13. Butovsky, O., M., Koronyo-Hamaoui, G., Kunis, E., Ophir, G., Landa, H., Cohen, and M., Schwartz, 2006, Glatiramer acetate fights against Alzheimer's disease by inducing dendriticlike microglia expressing insulin-like growth factor 1, *PNAS*, Volume 103, p. 11784–11789.
14. Cahill, G. F., 2006, Fuel metabolism in starvation. *Annual Review of Nutrion*, Volume 26, p. 1-22.
15. Cardinali, D. P., E. S., Pagano, P. A. S., Bernasconi, R., Reynoso, and P., Scacchi, 2013, Melatonin and mitochondrial dysfunction in the central nervous system, *Hormones and Behavior*, Volume 63, p. 322-330.
16. Chang, B., X., Cheng, S., Yin, T., Pan, H., Zhang, P., Wong, S. C., Kang, F., Xiao, H., Yan, C., Li, L. L., Wolfe, M. W., Miller, T., Wisniewski, M. I., Greene, and M. S., Sy, 2007, Test for detection of disease-associated prion aggregate in the blood of infected but asymptomatic animals, *Clinical and Vaccine Immunology*, Volume 14, p. 36–43.

17. Cheng, Y., Q., Meng, C., Wang, H., Li, Z., Huang, S., Chen, F., Xiao, and F., Guo, 2010, Leucine deprivation decreases fat mass by stimulation of lipolysis in white adipose tissue and up-regulation of uncoupling protein 1 (UCP1) in brown adipose tissue, *Diabetes*, Volume 59, p. 17–25.
18. Cohen, E. L., and R. J., Wurtman, 1975, Brain acetylcholine: Increase after systemic choline administration, *Life Sciences*, Volume 16, p. 1095-1102.
19. Combrinck, M. I., V. H., Perry, and C., Cunningham, 2002, Peripheral Infection Evokes Exaggerated Sickness Behaviour In Pre-Clinical Murine Prion Disease, *Neuroscience*, Volume 112, p. 7-11.
20. Comstock, J. P., and A. J., Garber, 1990, *Clinical Methods: The History, Physical, and Laboratory Examinations*, 3rd edition, Chapter 140, p. 658-661.
21. Conlay, L. A., L. A., Sabounjian, and R. J., Wurtman, 1992, Exercise and neuromodulators: choline and acetylcholine in marathon runners, *International Journal of Sport Medicine*, Volume 13, p. 141-142.
22. Craig, S. A., 2004, Betaine in human nutrition, *The American Journal of Clinical Nutrition*, Volume 80, p. 539-549.
23. Dagdanova, A., S., Ilchenko, S., Notari, Q., Yang, M. E., Obrenovich, K., Hatcher, P., McAnulty, L., Huang, W., Zou, Q., Kong, P., Gambetti, and S. G., Chen, 2010, Characterization of the Prion Protein in Human Urine, *The Journal of Biological Chemistry*, Volume 285, p. 30489-30495.
24. DeVivo, D. C., M. P., Leckie, and H. C., Agrawal, 1975, D-beta-hydroxybutyrate: a major precursor of amino acids in developing rat brain, *Journal of Neurochemistry*, Volume 25, p. 161–70.

25. Diemel, G. A., 2012, Fueling and imaging brain activation, *ASN Neuro*, Volume 4, p. 267-321.
26. Dodson, W. L., and D. S., Sachan, 1996, Choline supplementation reduces urinary carnitine excretion in humans, *The American Journal of Clinical Nutrition*, Volume 63, p. 904-910.
27. Doi, M., I., Yamaoka, M., Nakayama, S., Mochizuki, K., Sugahara, and F., Yoshizawa, 2005, Isoleucine, a blood glucose-lowering amino acid, increases glucose uptake in rat skeletal muscle in the absence of increases in AMP-activated protein kinase activity, *The Journal of Nutrition*, Volume 135, p. 2103–2108.
28. Du, Y., Q., Meng, Q., Zhang, and F., Guo, 2012, Isoleucine or valine deprivation stimulates fat loss via increasing energy expenditure and regulating lipid metabolism in WAT, *Amino Acids*, Volume 43, p. 725-734.
29. Ehrhart, J., and G. D., Zeevalk, 2003, Cooperative interaction between ascorbate and glutathione during mitochondrial impairment in mesencephalic cultures, *Journal of Neurochemistry*, Volume 86, p. 1487–1497.
30. Eklund, M., E., Bauer, J., Wamatu, and R., Mosenthin, 2005, Potential nutritional and physiological functions of betaine in livestock, *Nutrition Research Reviews*, Volume 18, p. 31-48.
31. Emoto, K., N., Toyama-Sorimachi, H., Karasuyama, K., Inoue, and M., Umeda, 1997, Exposure of phosphatidylethanolamine on the surface of apoptotic cells, *Experimental Cell Research*, Volume 232, p. 430–434.
32. Fadok, V. A., D. R., Voelker, P. A., Campbell, J. J., Cohen, D. L., Bratton, P. M., Henson, 1992, Exposure of phosphatidylserine on the surface of apoptotic lymphocytes triggers

- specific recognition and removal by macrophages, *Journal of Immunology*, Volume 148, p. 2207–2216.
33. Farooqui, A. A., L. A., Horrocks, and T., Farooqui, 2000, Glycerophospholipids in brain: their metabolism, incorporation into membranes, functions, and involvement in neurological disorders, *Chemistry and Physics of Lipids*, Volume 106, p. 1-29.
34. Farooqui, A. A., and L. A., Horrocks, 1994, Excitotoxicity and neurological disorders: involvement of membrane phospholipids, *International Review of Neurobiology*, Volume 36, p. 267–323.
35. Feng, J., X., Liu, Y. Z., Wang, and Z. R., Xu, 2006, Effects of betaine on performance, carcass characteristics and hepatic betainehomocysteine methyltransferase activity in finishing barrows, *Asian-Australian Journal of Animal Science*, Volume 19, p. 402-405.
36. Fernandez-Figares, I., J. A., Conde-Aguilera, R., Nieto, M., Lachica, and J. F., Aguilera, 2008, Synergistic effects of betaine and conjugated linoleic acid on growth and carcass composition of growing Iberian pigs, *Journal of Animal Science*, Volume 86, p. 102-111.
37. Fernandez-Gomez, F. J., M. F., Galindo, M., Gomez-Lazaro, V. J., Yuste, J. X., Comella, N., Aguirre, and J., Jordan, 2005, Malonate induces cell death via mitochondrial potential collapse and delayed swelling through an ROS-dependent pathway, *British Journal of Pharmacology*, Volume 144, p. 528-537.
38. Franscini, N., A., El Gedaily, U., Matthey, S., Franitza, M., Sy, A., Burkle, M., Groschup, U., Braun, and R., Zahn, 2006, Prion Protein in Milk, *PLoS ONE*, Volume 1, p. 1-5.
39. Freeman, J. J., and D. J., Jenden, 1976, The source of choline for acetylcholine synthesis in brain, *Life Sciences*, Volume 19, p. 949-962.

40. Frenkel, D., R., Maron, D. S., Burt, and H. L., Weiner, 2005, Nasal vaccination with a proteosome-based adjuvant and glatiramer acetate clears beta amyloid in a mouse model of Alzheimer disease, *The Journal of Clinical Investigations*, Volume 115, p. 2423–2433.
41. Frisardi, V., F., Panza, D., Seripa, T., Farooqui, and A. A. Farooqui, 2011, Glycerophospholipids and glycerophospholipid-derived lipid mediators: A complex meshwork in Alzheimer's disease pathology, *Progress in Lipid Research*, Volume 50, p. 313-330.
42. Gao, Y. Y., D. F., Zhang, H., Li, R., Liu, Z. H., Zhuang, Q. F., Li, S. Y., Wang, and X. X., Peng, 2007, Proteomic approach for caudal trauma-induced acute phase proteins reveals that creatine kinase is a key acute phase protein in amphioxus humoral fluid, *Journal of Proteome Research*, Volume 6, p. 4321–4329.
43. Gautier, C. A., O., Corti, and A. Brice, 2013, Mitochondrial dysfunctions in Parkinson's disease, *Revue Neurologique*, Volume 1162, p. 1-5.
44. Genius, J., J., Geiger, A., Bender, H., Moller, T., Klopstock, and D., Rujescu, 2012, Creatine Protects against Excitotoxicity in an In Vitro Model of Neurodegeneration, *PLoS One*, Volume 7, p. 1-8.
45. Gibbs, M. E., Z., Gibbs, and L., Hertz, 2009, Rescue of A β (1-42)- induced memory impairment in day-old chick by facilitation of astrocytes oxidative metabolism: implications for Alzheimer's disease, *Journal Neurochemistry* 109, p. 230–236.
46. Gold, P. E., and D. L., Korol, 2012, Making memories matter, *Frontiers in Integrative Neuroscience*, Volume 6, p. 116-127.
47. Go, E. K., K. J., Jung, J. Y., Kim, B. P., Yu, and H. Y., Chung, 2005, Betaine suppresses pro-inflammatory signaling during aging: the involvement of nuclear factor- κ B via nuclear

- factor-inducing kinase/I κ B kinase and mitogen-activated protein kinases, *The Journals of Gerontology, Series A Biological Sciences and Medical Sciences*, Volume 60, p. 1252-1264.
48. Gordon, P. M., E., Schütz, J., Beck, H. B., Urnovitz, C., Graham, R., Clark, S., Dudas, S., Czub, M., Sensen, B., Brenig, M. H., Groschup, R. B., Church, and C. W., Sensen, 2009, Disease-specific motifs can be identified in circulating nucleic acids from live elk and cattle infected with transmissible spongiform encephalopathies, *Nucleic Acids Research*, Volume 37, p. 550–56.
49. Grayson, B. E., R. J., Seeley, and D. A., Sandoval, 2013, Wired on sugar: the role of the CNS in the regulation of glucose homeostasis, *Nature Reviews Neuroscience*, Volume 14, p. 24–37.
50. Greene, J. G., and J. T., Greenamyre, 1996, Manipulation of membrane potential modulates malonate-induced striatal excitotoxicity in vivo, *Journal of Neurochemistry*, Volume 66, p. 637–643.
51. Griffith, H. R., J. A., den Hollander, C. C., Stewart, W. T., Evanochko, S. D., Buchthal, L. E., Harrell, E. Y., Zamrini, J. C., Brockington, and D. C., Marson, 2007, Elevated brain scyllo-inositol concentrations in patients with Alzheimer's disease, *NMR in Biomedicine*, Volume 20, p.709-716.
52. Gropman, A. L., M., Summar, and J. V., Leonard, 2007, Neurological implications of urea cycle disorders, *Journal of Inherited Metabolic Disease*, Volume 30, p. 865-879.
53. Hall, H., S., Cuellar-Baena, V., Denisov, and D., Kirik, 2013, Development of NMR spectroscopic methods for dynamic detection of acetylcholine synthesis by choline acetyltransferase in hippocampal tissue, *Journal of Neurochemistry*, Volume 124, p. 336-346.

54. Harris, J. J., R., Jolivet, and D., Attwell, 2012, Synaptic energy use and supply, *Neuron*, Volume 75, p. 762–777.
55. Harry, G. J. , R., Sills, M. J., Schlosser, and W. E., Maier, 2001, Neurodegeneration and Glia ResponSe in Rat Hippocampus Following Nitro-L-Arginine Methyl Ester (L-NAME), *Neurotoxicity Research*, Volume 3, p. 307-319.
56. Henderson, S. T., 2008, Ketone Bodies as a Therapeutic for Alzheimer’s Disease, *The American Society for Experimental NeuroTherapeutics*, Volume 5, p. 470–480.
57. Henderson, S. T., and J., Poirier, 2011, Pharmacogenetic analysis of the effects of polymorphisms in APOE, IDE and IL1B on a ketone body based therapeutic on cognition in mild to moderate Alzheimer’s disease; a randomized , double-blind, placebo-controlled study, *BMC Medical Genetics*, Volume 12, p. 137-150.
58. Hertz, L., J., Xu, D., Song, T., Du , E., Yan, and L., Peng, 2009, Brainglycogenolysis, adrenoceptors, pyruvate carboxylase, Na^+,K^+ -ATPase and Marie E. Gibbs’ pioneering learning studies, *Frontiers in Integrative Neuroscience*, Volume 7, p. 1-7.
59. Hollenbach, M., A., Hintersdorf, K., Huse, U., Sack, M., Bigl, M., Groth, T., Santel, M., Buchold, I., Lindner, A., Otto, D., Sicker, W., Schellenberger, J., Almendinger, B., Pustowitz, C., Birkemeyer, M., Platzer, I., Oerlecke, N., Hemdan, and G., Birkenmeier, 2008, Ethyl pyruvate and ethyl lactate down-regulate the production of pro-inflammatory cytokines and modulate expression of immune receptors, *Biochemical Pharmacology*, Volume 76, p. 631-644.
60. Howarth, C., P., Gleeson, and D., Attwell, 2012, Updated energy budgets for neural computation in the neocortex and cerebellum, *Journal of Cerebral Blood Flow and Metabolism*, Volume 32, p. 1222–1232

61. Hutson, S. M., E., Lieth, and K. F., LaNoue, 2001, Function of leucine in excitatory neurotransmitter Metabolism in the central nervous system, *The Journal of Nutrition*, Volume 131, p. 846S–850S.
62. Jordan, J., V., Cella, and J. H. M., Prehn, 2003, Mitochondrial control of neuron death and its role in neurodegenerative disorders, *Journal of Physiology and Biochemistry*, Volume 59, p. 129-141.
63. Kashiwaya, Y., T., Takeshima, N., Mori, K., Nakashima, K., Clarke, and R. L., Veech, 2000, D-beta-hydroxybutyrate protects neurons in models of Alzheimer's and Parkinson's disease, *PNAS*, Volume 97, p. 5440–5444.
64. Kim, H. S., I. H., Cho, J. E., Kim, Y. J., Shin, J., Jeon, Y., Kim, Y. M., Yang, K., Lee, J. W., Lee, W., Lee, S., Ye, and M., Chung, 2008, Ethyl pyruvate has an anti-inflammatory effect by inhibiting ROS-dependent STAT signaling in activated microglia, *Free Radical Biology and Medicine*, Volume 45, p. 950-963.
65. Kim, J. H., B. S., Choi, C., Jung, Y., Chang, and S., Kim, 2011, Diffusion-weighted imaging and magnetic resonance spectroscopy of sporadic Creutzfeldt–Jakob disease: correlation with clinical course, *Neuroradiology*, Volume 53, p. 939-945.
66. Kipnis, J., and M., Schwartz, 2002, Dual action of glatiramer acetate (Cop-1) in the treatment of CNS autoimmune and neurodegenerative disorders, *Trends in Molecular Medicine*, Volume 8, p.319 –323.
67. Klivenyi, P., G., Gardian, N. Y., Calingasan, L., Yang, and M. F., Beal, 2003, Additive neuroprotective effects of creatine and a cyclooxygenase 2 inhibitor against dopamine depletion in the 1-methyl-4-phenyl-1, 2, 3, 6-tetrahydropyridine (MPTP) mouse model of Parkinson's disease, *Journal of Molecular Neuroscience*, Volume 21, p. 191–198.

68. Klocker, A. A., H., Phelan, S. M., Twigg, and M. E., Craig, 2013, Blood b-hydroxybutyrate vs. urine acetoacetate testing for the prevention and management of ketoacidosis in Type 1 diabetes: a systematic review, *Diabetic Medicine*, Volume 30, p. 818-824.
69. Klopstock, T., M., Elstner, and A., Bender, 2011, Creatine in mouse models of neurodegeneration and aging, *Amino Acids*, Volume 40, p. 1297-1303.
70. Korman, S. H., 2006, Inborn errors of isoleucine degradation: A review, *Molecular Genetics and Metabolism*, Volume 89, p. 289–299.
71. Koura, S. S., E. M., Doppenberg, A., Marmarou, S., Choi, H. F., Young, and R., Bullock, 1998, Relationship between excitatory amino acid release and outcome after severe human head injury, *Acta Neurochirurgica Supplement*, Volume 71, p. 244-246.
72. Lacroux, C., S., Simon, S. L., Benestad, S., Maillet, J., Mathey, S., Lugan, F., Corbiere, H., Cassard, P., Costes, D., Bergonier, J., Weisbecker, T., Moldal, H., Simmons, F., Lantier, C., Feraudet-Tarisse, N., Morel, F., Schelcher, J., Grassi, O., Andreoletti, 2008, Prions in Milk from Ewes Incubating Natural Scrapie, *PLoS Pathogens*, Volume 4, p. 1-12.
73. Lassenius, M. I., K. H., Pietilainen, K., Kaartinen, P. J., Pussinen, J., Syrjanen, C., Forsblom, I., Porsti, A., Rissanen, J., Kaprio, J., Mustonen, P., Groop, M., Lehto, 2011, Bacterial Endotoxin Activity in Human Serum Is Associated With Dyslipidemia, Insulin Resistance, Obesity, and Chronic Inflammation, *Diabetes Care*, Volume 34, p. 1809-1815.
74. Lawler, J. M., W. S., Barnes, G., Wu, W., Song, and S., Demaree, 2002, Direct antioxidant properties of creatine, *Biochemical and Biophysical Research Communications*, Volume 290, p. 47–52.
75. Layman, D. K., and D. A., Walker, 2006, Potential importance of leucine in treatment of obesity and the metabolic syndrome, *The Journal of Nutrition*, Volume 136, p. 319–323.

76. Liotta, A., J., Rösner, C., Huchzermeyer, A., Wojtowicz, O., Kann, D., Schmitz, U., Heinemann, and R., Kovács, 2012, Energy demand of synaptic transmission at the hippocampal Schaffer-collateral synapse, *Journal of Cerebral Blood Flow and Metabolism*, Volume 32, p. 2076–2083.
77. Liu, M., and G., Bing, 2011, Lipopolysaccharide Animal Models of Parkinson's Disease, *Parkinson's Disease*, Volume 2011, p. 1-7.
78. Mattson, M. P., W. A., Pedersen, W., Duan, C., Culmsee, S., Camandola, 1999, Cellular and molecular mechanisms underlying perturbed energy metabolism and neuronal degeneration in Alzheimer's and Parkinson's diseases, *Annals of the New York Academy of Sciences*, Volume 893, p. 154-175.
79. McLaurin, J., M. E., Kierstead, M. E., Brown, C. A., Hawkes, M. H. L., Lambermon, A. L., Phinney, A. A., Darabie, J. E., Cousins, J. E., French, M. F., Lan, F., Chen, S. S. N., Wong, H. T. J., Mount, P. E., Fraser, D., Westaway, and P., St George-Hyslop, 2006, Cyclohexanehexol inhibitors of Ab aggregation prevent and reverse Alzheimer phenotype in a mouse model, *Nature Medicine*, Volume 12, p. 801-808.
80. Meldrum, B. S., 2000, Glutamate as a neurotransmitter in the brain: review of physiology and pathology, *The Journal of Nutrition*, Volume 130, p. 1007S–1015S.
81. Mergenthaler, P., A., Kahl, A., Kamitz, V., van Laak, K., Stohlmann, S., Thomsen, H., Klawitter, I., Przesdzing, L., Neeb, D., Freyer, J., Priller, T. J., Collins, D., Megow, U., Dirnagl, D. W., Andrews, and A., Meisel, 2012, Mitochondrial hexokinase II (HKII) and phosphoprotein enriched in astrocytes (PEA15) form a molecular switch governing cellular fate depending on the metabolic state, *PNAS*, Volume 109, p. 1518–1523.

82. Mergenthaler, P., U., Lindauer, G. A., Dienel, and A., Meisel, 2013, Sugar for the brain: the role of glucose in physiological and pathological brain function, *Cell Press*, Volume 36, p. 587-597.
83. Mouille, B., V., Robert, and F., Blachier, 2004, Adaptive increase of ornithine production and decrease of ammonia metabolism in rat colonocytes after hyperproteic diet ingestion, *American Journal of Physiology, Gastrointestinal and Liver Physiology*, Volume 287, p. 344-351.
84. Nehlig, A., 2004, Brain uptake and metabolism of ketone bodies in animal models, *Prostaglandins Leukotrienes and Essential Fatty Acids*, Volume 70, p. 265-275.
85. Neniskyte, U., and G. C., Brown, 2013, Analysis of Microglial Production of Reactive Oxygen and Nitrogen Species, *Methods in Molecular Biology*, Volume 1041, p. 103-111.
86. Nicholls, D. G., S. L., Budd, M. W., Ward, and R. F., Castilho, 1999, Excitotoxicity and mitochondria, *Biochemical Society Symposium*, Volume 66, p. 55–67.
87. Nitsch, R., A., Pittas, J. K., Blusztajn, B. E., Slack, J. H., Growdon, and R. J., Wurtman, 1991, Alterations of phospholipid metabolites in postmortem brain from patients with Alzheimer's disease, *Annals of the New York Academy Sciences*, Volume 640, p. 110–113.
88. Noh, H. S., Y. S., Hah, R., Nilufar, J., Han, J. H., Bong, S. S., Kang, G. J., Cho, and W. S., Choi, 2006, Acetoacetate protects neuronal cells from oxidative glutamate toxicity, *Journal of Neuroscience Research* Volume 83, p. 702–709.
89. Nugent, S., S., Tremblay, K. W., Chen, N., Ayutyanont, A., Roontiva, C., Castellano, M., Fortier, M., Roy, A., Courchesne-Loyer, C., Bocti, M., Lepage, E., Turcotte, T., Fulop, E. M., and S. C., Reiman, 2013, Cunnane, Brain glucose and acetoacetate metabolism: a comparison of young and older adults, *Neurobiology of Aging*, p. 1-10.

90. Obeid, R., and W., Herrmann, 2005, Mechanisms of homocysteine neurotoxicity in neurodegenerative diseases with special reference to dementia, *FEBS Letters.*, Volume 580, p. 2994-3005.
91. Ohlenbusch, A., S., Edvardson, J., Skorpen, A., Bjornstad, A., Saada, O., Elpeleg, J., Gärtner, and K., Brockmann, 2012, Leukoencephalopathy with accumulated succinate is indicative of SDHAF1 related complex II deficiency, *Orphanet Journal of Rare Diseases*, Volume 7, p. 69-74.
92. Patel, A. B., R. A., de Graaf, D. L., Rothman, K. L., Behar, and G. F., Mason, 2010, Evaluation of cerebral acetate transport and metabolic rates in the rat brain in vivo using ¹H-¹³C-NMR, *Journal of Cerebral Blood Flow and Metabolism*, Volume 30, p. 1200-1213.
93. Perez-Cerda, C., J., García-Villoria, R., Ofman, P. R., Sala, B., Merinero, J., Ramos, M. T., García-Silva, B., Beseler, J., Dalmau, R. J., Wanders, M., Ugarte, and A., Ribes, 2005, 2-Methyl-3-hydroxybutyryl-CoA dehydrogenase (MHBD) deficiency: an X-linked inborn error of isoleucine metabolism that may mimic a mitochondrial disease, *Pediatric Research*, Volume 58, p. 488-491.
94. Pettegrew, J. W., W. E., Klunk, E., Kanal, K., Panchalingam, and R. L., McClure, 1995, Changes in brain membrane phospholipid and high-energy phosphate metabolism precede dementia, *Neurobiology of Aging*, Volume 16, p. 973–975.
95. Pifferi, F., S., Tremblay, E., Croteau, M., Fortier, J., Tremblay-Mercier, R., Lecomte, and S. C., Cunnane, 2011, Mild experimental ketosis increases brain uptake of ¹¹C-acetoacetate and ¹⁸F-fluorodeoxyglucose: a dual-tracer PET imaging study in rats, *Nutritional Neuroscience*, Volume 14, p. 51-58.

96. Protti, A., J., Carré, M. T., Frost, V., Taylor, R., Stidwill, A., Rudiger, and M., Singer, 2007, Succinate recovers mitochondrial oxygen consumption in septic rat skeletal muscle, *Critical Care Medicine*, Volume 35, p. 2150-2155.
97. Prusiner, S. B., 1982, Novel Proteinaceous Infectious Particles Cause Scrapie, *Science*, Volume 216, p. 136-144.
98. Pushie, M. J., R., Shaykhutdinov, A., Nazyrova, C., Graham, and H. J., Vogel, 2011, An NMR Metabolomics Study of Elk Inoculated with Chronic Wasting Disease, *Journal of Toxicology and Environmental Health*, Volume 77, p. 1476-1492.
99. Qin, L., X., Wu, M. L., Block, Y., Liu, G. R., Breese, J. S., Hong, D. J., Knapp, and F. T., Crews, 2007, Systemic LPS causes chronic neuroinflammation and progressive neurodegeneration, *Glia*, Volume 55, p. 453–462.
100. Raabe, W., 1990, Effects of NH_4^+ on the function of CNS, *Advances in Experimental Medicine and Biology*, Volume 272, p. 99-120.
101. Rachakonda, V., T. H., Pan, and W. D., Le, 2004, Biomarkers of neurodegenerative disorders: How good are they?, *Cell Research*, Volume 14, p. 349-360.
102. Rae, C., A. L., Digney, S. R., McEwan, and T. C., Bates, 2003, Oral creatine monohydrate supplementation improves brain performance: a double-blind, placebo-controlled, cross-over trial, *Proceedings of The Royal Society*, Volume 270, p. 2147-2150.
103. Ratriyanto, A., R., Mosenthin, E., Bauer, and M., Eklund, 2009, Metabolic, Osmoregulatory and Nutritional Functions of Betaine in Monogastric Animals, *Asian-Australian Journal of Animal Science*, Volume 22, p. 1461-1476.

104. Ryou, M., R., Liu, M., Ren, J., Sun, R. T., Mallet and S., Yang, 2012, Pyruvate Protects the Brain Against Ischemia–Reperfusion Injury by Activating the Erythropoietin Signaling Pathway, *Journal of the American Heart Association*, Volume 43, p. 1101-1107.
105. Sachdev, P. S., 2005, Homocysteine and brain atrophy, *Progress in Neuropsychopharmacology & Biological Psychiatry*, Volume 29, p. 1152-61.
106. Schapira, A. H., 2008, Mitochondria in the aetiology and pathogenesis of Parkinson's disease, *Lancet Neurology*, Volume 7, p. 97–109.
107. Schell, J. C., and J., Rutter, 2013, The long and winding road to the mitochondrial pyruvate carrier, *Cancer and Metabolism*, Volume 1, p. 6-15.
108. Schon, E. A., and G., Manfredi, 2003, Neuronal degeneration and mitochondrial dysfunction, *The Journal of Clinical Investigations*, Volume 111, p. 303–312.
109. Schoots, A. C., P. M., De Vries, R., Thiemann, W. A., Hazejager, S. L., Visser, and P. L., Oe, 1989, Biochemical and neurophysiological parameters in hemodialyzed patients with chronic renal failure, *Clinica Chimica Acta*, Volume 185, p. 91–107.
110. Schulz, J. B., M., Weller, R. T., Matthews, M. T., Heneka, P., Groscurth, J. C., Martinou, J., Lommatzsch, R., Von Coelln, U., Wullner, P. A., Loschmann, M. F., Beal, J., Dichgans, and T., Klockgether, 1998, Extended therapeutic window for caspase inhibition and synergy with MK-801 in the treatment of cerebral histotoxic hypoxia, *Cell Death and Differentiation*, Volume 5, p. 847–857.
111. She, P., Z., Zhang, D., Marchionini, W. C., Diaz, T. J., Jetton, S. R., Kimball, T. C., Vary, C. H., Lang, and C. J., Lynch, 2011, Molecular characterization of skeletal muscle atrophy in the R6/2 mouse model of Huntington's disease, *American Journal of Physiology Endocrinology and Metabolism*, Volume 301, p. 49-61.

112. Shirahata, M., A., Balbir, T., Otsubo, and R. S., Fitzgerald, 2007, Role of acetylcholine in neurotransmission of the carotid body, *Respiratory Physiology & Neurobiology*, Volume 157, p. 93-105.
113. Soliman, M. L., K. L., Puig, C. K., Combs, and T. A., Rosenberger, 2012, Acetate reduces microglia inflammatory signaling in vitro, *Journal of Neurochemistry*, Volume 123, p. 555–567.
114. Song, M., J. A., Kellum, H., Kaldas, and M. P., Fink, 2004, Evidence that glutathione depletion is a mechanism responsible for the anti-inflammatory effects of ethyl pyruvate in cultured lipopolysaccharide-stimulated RAW 264.7 cells, *Journal of Pharmacology and Experimental Therapeutics*, Volume 308, p. 307–316.
115. Soto, C., and N., Satani, 2011, The intricate mechanisms of neurodegeneration in prion diseases, *Trends in Molecular Medicine*, Volume 17, p. 14-24.
116. Suzuki, A., S. A., Stern, O., Bozdagi, G. W., Huntley, R. H., Walker, P. J., Magistretti, C. M., Alberini, 2011, Astrocyte-neuron lactate transport is required for long-term memory formation, *Cell*, Volume 144, p. 810–823.
117. Taylor, D. R., E. T., Parkin, S. L., Cocklin, J. R., Ault, A. E., Ashcroft, A. J., Turner, and N. M., Hooper, 2009, Role of ADAMs in the Ectodomain Shedding and Conformational Conversion of the Prion Protein, *The Journal of Biological Chemistry*, Volume 284, p. 22590-22600.
118. Theoharides, T. C., S., Asadi, and A. B., Patel, 2013, Focal brain inflammation and autism, *Journal of Neuroinflammation*, Volume 10, p. 46-53.
119. Tsikas, D., T., Thum, T., Becker, V. V., Pham, K., Chobanyan, A., Mitschke, B., Beckmann, F., Gutzki, J., Bauersachs, and D. O., Stichtenoth, 2007, Accurate quantification

- of dimethylamine (DMA) in human urine by gas chromatography–mass spectrometry as pentafluorobenzamide derivative: Evaluation of the relationship between DMA and its precursor asymmetric dimethylarginine (ADMA) in health and disease, *Journal of Chromatography*, Volume 851, p. 229-239.
120. Van Amersfoort, E. S., T. J. C., Van Berkel, and J., Kuiper, 2003, Receptors, Mediators, and Mechanisms Involved in Bacterial Sepsis and Septic Shock, *Clin. Microbiol. Rev.*, Volume 16, p. 379-414.
121. Van Westerlaak, M. G., E. A., Joosten, A. A., Gribnau, A. R., Cools, and P. R., Bar, 2001, Differential cortico-motoneuron vulnerability after chronic mitochondrial inhibition in vitro and the role of glutamate receptors, *Brain Research*, Volume 922, p. 243–249.
122. Varma, S. D., K. R., Hegde, S., Kovtun, 2006, Oxidative damage to lens in culture: reversibility by pyruvate and ethyl pyruvate, *Ophthalmologica*, Volume 220, p. 52–57.
123. Virtanen, E., 1995, Piecing together the betaine puzzle, *Feed Mix*, Volume 3, p. 12–7.
124. Wang, G., and W. A., Korfmacher, 2009, Development of a biomarker assay for 3-indoxyl sulfate in mouse plasma and brain by liquid chromatography/ tandem mass spectrometry, *Rapid Communications in Mass Spectrometry*, Volume 23, p. 2061-2069.
125. Waniewski, R. A., and D. L., Martin, 1998, Preferential utilization of acetate by astrocytes is attributable to transport, *Journal of Neuroscience*, Volume 18, p. 5225–5233.
126. Watson, G. G., and S., Craft, 2004, Modulation of memory by insulin and glucose: neuropsychological observations in Alzheimer’s disease, *European Journal of Pharmacology*, Volume 490, p. 97–113.

127. Webber, R. J., and J., Edmond, 1977, The in vivo utilization of acetoacetate, D(-)-3-hydroxybutyrate, and glucose for lipid synthesis in brain in the 18-day-old rat, *Journal of Biological Chemistry*, Volume 252, p. 5222–5226.
128. Williams, E. S., 2005, Chronic wasting disease, *Veterinary Pathology*, Volume 42, p. 530–49.
129. Wishart, D. S., C., Knox, A. C., Guo, R., Eisner, N., Young, B., Gautam, D. D., Hau, N., Psychogios, E., Dong, S., Bouatra, R., Mandal, I., Sinelnikov, J., Xia, L., Jia, J. A., Cruz, E., Lim, C. A., Sobsey, S., Shrivastava, P., Huang, P., Liu, L., Fang, J., Peng, R., Fradette, Dean Cheng, D., Tzur, M., Clements, A., Lewis, A. D., Souza, A., Zuniga, M., Dawe, Y., Xiong, D., Clive, R., Greiner, A., Nazyrova, R., Shaykhutdinov, L., Li, H. J., Vogel, and I., Forsythe, 2009, HMDB: a knowledgebase for the human metabolome, *Nucleic Acids Research*, Volume 37, p. D603-D610.
130. Wyss-Coray, T., and L., Mucke, 2002, Inflammation in Neurodegenerative Disease—A Double-Edged Sword, *Neuron*, Volume 35, p. 419-432.
131. Wyss, M., and A., Schulze, 2002, Health implications of creatine: can oral creatine supplementation protect against neurological and atherosclerotic disease?, *Neuroscience*, Volume 112, p. 243–260.
132. Yang, R., D. J., Gallo, J. J., Baust, T., Uchiyama, S. K., Watkins, R. L., Delude, and M. P., Fink, 2002, Ethyl pyruvate modulates inflammatory gene expression in mice subjected to hemorrhagic shock, *American Journal of Physiology*, Volume 283, p. 212–221.
133. Yang, S., X., He, and D., Miller, 2007, HSD17B10: A gene involved in cognitive function through metabolism of isoleucine and neuroactive steroids, *Molecular Genetics and Metabolism*, Volume 92, p. 36–42.

134. Yang, L., N. Y., Calingasan, E. J., Wille, K., Cormier, K., Smith, R. J., Ferrante, and M. F., Beal, 2009, Combination therapy with coenzyme Q10 and creatine produces additive neuroprotective effects in models of Parkinson's and Huntington's diseases, *Journal of Neurochemistry*, Volume 109, p. 1427–1439.
135. Yudkoff, M., Y., Daikhin, I., Nissim, O., Horyn, B., Luhovyy, A., Lazarow, and I., Nissim, 2005, Brain Amino Acid Requirements and Toxicity: The Example of Leucine, *The Journal of Nutrition*, Volume 135, p. 15315-15385.
136. Zauner, A., R., Bullock, A. J., Kuta, J., Woodward, and H. F., Young, 1996, Glutamate release and cerebral blood flow after severe human head injury, *Acta Neurochirurgica Supplement*, Volume 67, p. 40-44.
137. Zgoda-Pols, J. R., S., Chowdhury, M., Wirth, M. V., Milburn, D. C., Alexander, K. B., Alton, 2011, Metabolomics analysis reveals elevation of 3-indoxyl sulfate in plasma and brain during chemically-induced acute kidney injury in mice: Investigation of nicotinic acid receptor agonists, *Toxicology and Applied Pharmacology*, Volume 255, p. 48-56.

Figure Captions

Table 4.1. RML urine metabolite profile alteration over time. Table showing significant (p-value) of linearly decreasing/increasing urine metabolite profile collected from subcutaneously (sc) RML inoculated FVB/N female mice in comparison to the control at 11wk post inoculation (pi), two month prior to exhibition of prion clinical signs and euthanasia (D-2), D-1, and at terminal sickness with clinical signs of prion disease (D). Samples were analyzed using untargeted invasive metabolomics approach, nuclear magnetic resonance (NMR) and direct injection mass spectrometry (DI-MS), to detect metabolite alterations associated with disease progression over time. DI-MS analysis was conducted only at 11wk, D-1 and D while NMR analysis was done on D-2 as well. NS; not significant, NA: not available.

Table 4.2. RML serum metabolite profile alteration over time. Table showing significant (p-value) of linearly decreasing/increasing urine metabolite profile collected from sc RML inoculated FVB/N female mice in comparison to the control at 11wk pi and D. Samples were analyzed using untargeted invasive metabolomics approach, NMR, to detect metabolite alterations associated with disease progression over time. NS: not significant.

Table 4.3. RML+LPS urine metabolite profile alteration over time. Table showing significant (p-value) of linearly decreasing/increasing urine metabolite profile collected from sc RML+LPS inoculated FVB/N female mice in comparison to the control at 11wk pi, D-2, D-1, and at D. Samples were analyzed using untargeted invasive metabolomics approach, NMR and DI-MS, to detect metabolite alterations associated with disease progression over time. DI-MS analysis was conducted only at 11wk, D-1 and D while NMR analysis was done on D-2 as well. NS; not significant, NA: not available.

Table 4.4. RML+LPS serum metabolite profile alteration over time. Table showing significant (p-value) of linearly decreasing/increasing urine metabolite profile collected from sc RML+LPS inoculated FVB/N female mice in comparison to the control at 11wk pi and D. Samples were analyzed using untargeted invasive metabolomics approach, NMR, to detect metabolite alterations associated with disease progression over time. NS: not significant.

Figure 4.1. Partial least squares Discriminant Analysis (PLSDA) of urine metabolite profile data for the RML treatment group at 11wk post inoculation. Urine samples were collected at 11wk pi from sc RML-infected FVB/N female mice and analyzed using DI-MS in comparison to the saline-treated control mice. The PLSDA scores plots discriminates the metabolic urine profile of the control group from the RML treatment group at 11wk pi.

Figure 4.2. Partial least squares Discriminant Analysis (PLSDA) of urine metabolite profile data for the RML treatment group one month prior to death. Urine samples were collected one month prior to manifestation of clinical signs and death (Dm1) from sc RML-infected FVB/N female mice and analyzed using DI-MS in comparison to the saline-treated control mice. The PLSDA scores plots discriminates the metabolic urine profile of the control group from the RML treatment group at Dm1 pi.

Figure 4.3. Partial least squares Discriminant Analysis (PLSDA) of urine metabolite profile data for the RML treatment group at death. Urine samples were collected at terminal sickness prior to euthanasia (D) from sc RML-infected FVB/N female mice and analyzed using DI-MS in comparison to the saline-treated control mice. The PLSDA scores plots discriminates the metabolic urine profile of the control group from the RML treatment group at D pi.

Figure 4.4. Partial least squares Discriminant Analysis (PLSDA) of urine metabolite profile data for the RML+LPS treatment group at 11wk post inoculation. Urine samples were collected at 11wk pi from sc RML+LPS-infected FVB/N female mice and analyzed using DI-MS in comparison to the saline-treated control mice. The PLSDA scores plots discriminates the metabolic urine profile of the control group from the RML+LPS treatment group at 11wk pi.

Figure 4.5. Partial least squares Discriminant Analysis (PLSDA) of urine metabolite profile data for the RML+LPS treatment group one month prior to death. Urine samples were collected one month prior to manifestation of clinical signs and death (Dm1) from sc RML+LPS-infected FVB/N female mice and analyzed using DI-MS in comparison to the saline-treated control mice. The PLSDA scores plots discriminates the metabolic urine profile of the control group from the RML+LPS treatment group at Dm1 pi.

Figure 4.6. Partial least squares Discriminant Analysis (PLSDA) of urine metabolite profile data for the RML+LPS treatment group at death. Urine samples were collected at terminal sickness prior to euthanasia (D) from sc RML+LPS-infected FVB/N female mice and analyzed using DI-MS in comparison to the saline-treated control mice. The PLSDA scores plots discriminates the metabolic urine profile of the control group from the RML treatment group at D pi.

Figure 4.7. Partial least squares Discriminant Analysis (PLSDA) of urine metabolite profile data comparing the RML and RML+LPS treatment groups at 11wk post inoculation. Urine samples were collected at 11wk pi from sc RML- and RML+LPS-infected FVB/N female mice and analyzed using DI-MS. The PLSDA scores plots discriminates the metabolic urine profile of the RML treatment group in comparison to the RML+LPS treatment at 11wk pi.

Figure 4.8. Partial least squares Discriminant Analysis (PLSDA) of urine metabolite profile data comparing the RML and RML+LPS treatment groups one month prior to death. Urine samples were collected one month prior to manifestation of clinical signs and death (Dm1) from sc RML- and RML+LPS-infected FVB/N female mice and analyzed using DI-MS. The PLSDA scores plots discriminates the metabolic urine profile of the RML treatment group in comparison to the RML+LPS treatment at Dm1.

Figure 4.9. Partial least squares Discriminant Analysis (PLSDA) of urine metabolite profile data comparing the RML and RML+LPS treatment groups at death. Urine samples were collected at terminal sickness prior to euthanasia (D) from sc RML- and RML+LPS-infected FVB/N female mice and analyzed using DI-MS. The PLSDA scores plots discriminates the metabolic urine profile of the RML treatment group in comparison to the RML+LPS treatment at Dm1.

Figure 4.10. Partial least squares Discriminant Analysis (PLSDA) of urine metabolite profile data comparing the RML treatment group at 11wk post inoculation, one month prior to death and at death. Urine samples were collected at 11wk pi, one month prior to manifestation of clinical signs and death (Dm1), and at terminal sickness prior to euthanasia (D) from sc RML-infected FVB/N female mice and analyzed using DI-MS. The PLSDA scores plots discriminates the metabolic urine profile of RML treatment group at 11wk pi, Dm1, and D.

Figure 4.11. Partial least squares Discriminant Analysis (PLSDA) of urine metabolite profile data comparing the RML+LPS treatment group at 11wk post inoculation, one month prior to death and at death. Urine samples were collected at 11wk pi, one month prior to manifestation of clinical signs and death (Dm1), and at terminal sickness prior to euthanasia (D) from sc RML+LPS-infected FVB/N female mice and analyzed using DI-MS. The PLSDA scores plots discriminates the metabolic urine profile of RML+LPS treatment group at 11wk pi, Dm1, and D.

Table 4.1.

Metabolite	Control vs RML				Linearity
	11wk	D-2	D-1	D	
3-Indoxylsulfate	NS	0.0360	< 0.0001	< 0.0001	Down
Arginine	NS	NS	0.0034	0.0058	
Carnitine	NS	NS	0.0352	NS	
Dimethylamine	NS	NS	0.0077	0.0236	
Ethanol	NS	0.0242	NS	0.0048	
Lactate	NS	0.0445	0.0341	0.0095	
Carnitine	0.0060791	NA	0.03775	0.0044811	
Phosphatidylcholine diacyl C36:3	0.021802	NA	0.043243	0.019077	
Methylglutarylcarnitine	0.037811	NA	NS	NS	
lysoPC a C20:3	NS	NA	0.040394	NS	
Phosphatidylcholine diacyl C34:2	NS	NA	NS	0.023539	
Lysophosphatidylcholine acyl C18:0	NS	NA	NS	0.025266	
Phosphatidylcholine diacyl C34:4	NS	NA	NS	0.034678	
Acetoacetate	0.0057	0.0448	0.0448	NS	
Acetylcarnitine	0.033501	NA	NS	NS	

Table 4.2.

Metabolite	Control vs RML		Linearity
	11wk	D	
Alanine	NS	NS	Down
Arginine	NS	0.0143	
Aspartate	NS	0.0143	
Betaine	0.0143	0.0300	
Creatine	0.0143	NS	
Glucose	NS	0.0143	
Isobutyrate	0.0423	0.0209	
Isoleucine	NS	0.0143	
Methanol	0.0209	0.0300	
Methionine	0.0143	0.0209	
Serine	NS	0.0143	
Valine	NS	NS	
sn-Glycero-3-phosphocholine	0.0143	0.0143	
3-Methylhistidine	0.0143	NS	
3-Hydroxybutyrate	NS	0.0143	Up
Acetoacetate	0.0141	0.0141	
Acetone	NS	0.0143	
Carnitine	0.0143	0.0143	
Choline	0.0143	0.0143	
Malonate	0.0143	0.0143	
Ornithine	0.0141	0.0143	
Pyruvate	0.0423	0.0143	
Succinate	0.0143	0.0143	

Table 4.3.

Metabolite	Control vs RML+LPS				Linearity
	11wk	D-2	D-1	D	
Betaine	NS	NS	NS	0.0001	Down
O-Acetylcarnitine	0.0128	NS	0.0194	< 0.0001	
Scyllitol	NS	0.0357	0.0035	< 0.0001	
lysoPC a C18:0	NS	NA	0.012365	0.028423	
Methylglutaryl carnitine	0.024028	NA	0.029854	NS	
Phosphatidylcholine diacyl C34:4	NS	NA	0.037595	NS	
Glutaconyl carnitine	0.0009532	NA	NS	NS	
Acetylcarnitine	0.0054913	NA	NS	NS	
Butyryl carnitine	0.0070824	NA	NS	NS	
Carnitine	0.0089291	NA	NS	NS	
C3-DC (C4-OH)	0.011463	NA	NS	NS	
Lysophosphatidylcholine acyl C20:3	0.026002	NA	NS	NS	
Hydroxyhexadecanoyl carnitine	0.031811	NA	NS	NS	
Hydroxyvaleryl carnitine	0.032058	NA	NS	NS	
Phosphatidylcholine acyl-alkyl C34:1	0.047717	NA	NS	NS	
3-Methyl-2-oxovalerate	0.0039	0.0245	NS	NS	Up
Sphingomyeline C18:1	0.039306	NA	NS	NS	

Table 4.4.

Metabolite	Control vs RML+LPS		Linearity
	11wk	D	
Alanine	NS	NS	Down
Arginine	0.0092	0.0092	
Aspartate	NS	0.0092	
Betaine	0.0092	0.0092	
Citrate	0.0129	0.0092	
Glycine	0.0092	NS	
Hypoxanthine	0.0092	0.0438	
Leucine	0.0092	NS	
Methanol	0.0092	NS	
Methionine	0.0091	NS	
Serine	0.0092	0.0129	
3-Hydroxybutyrate	NS	NS	
Acetate	0.0440	0.0178	
Acetoacetate	0.0091	NS	
Acetone	0.0089	0.0129	
Choline	0.0092	0.0092	
Creatinine	0.0330	0.0092	
Glutamate	NS	0.0092	
Ornithine	0.0092	0.0092	
Pyruvate	NS	0.0092	
Succinate	0.0092	0.0092	

Figure 4.1.

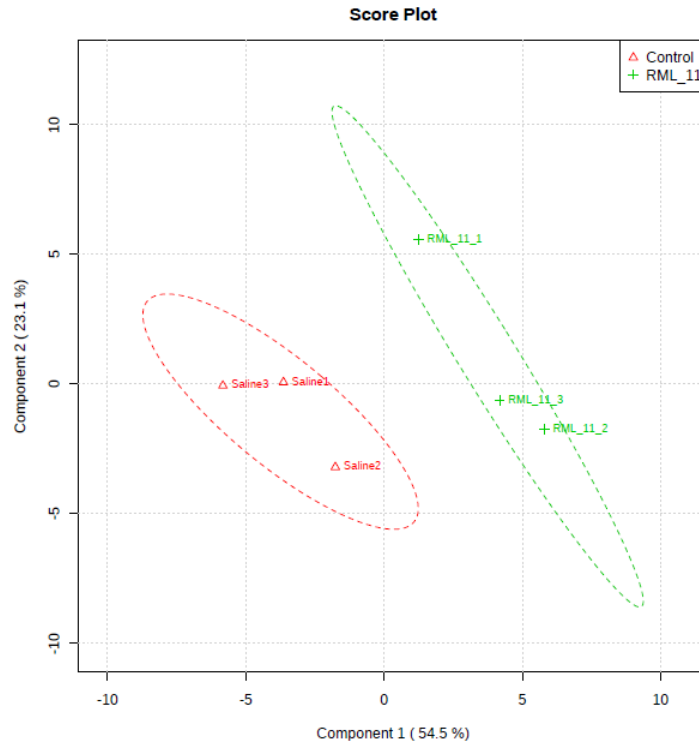


Figure 4.2.

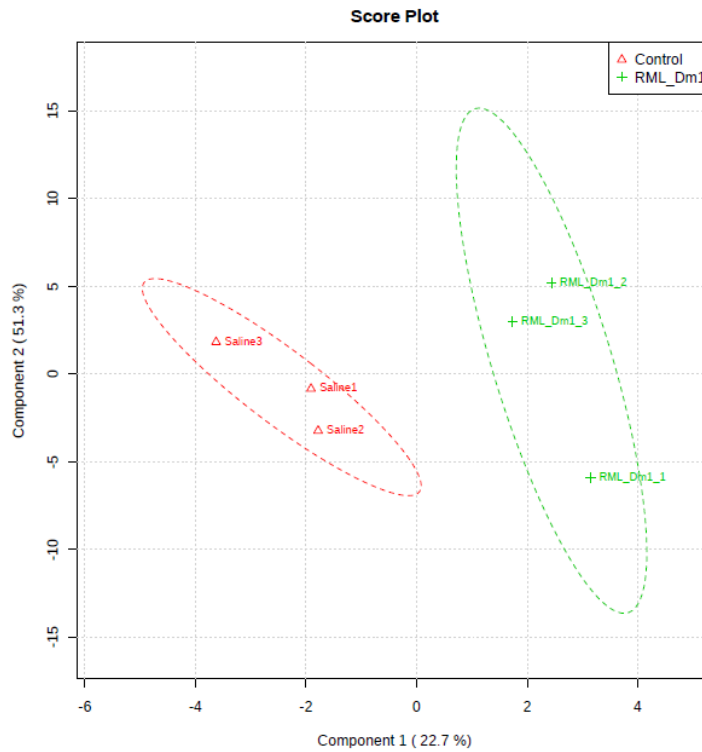


Figure 4.3.

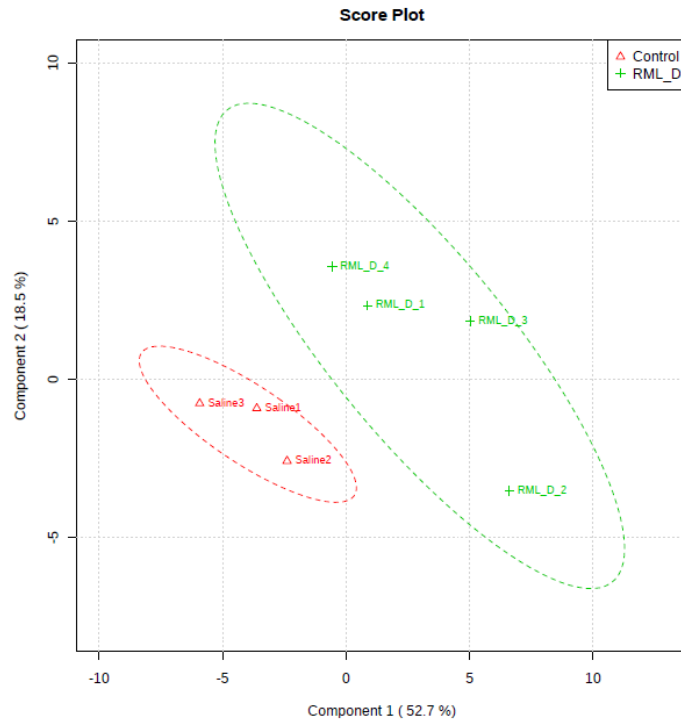


Figure 4.4.

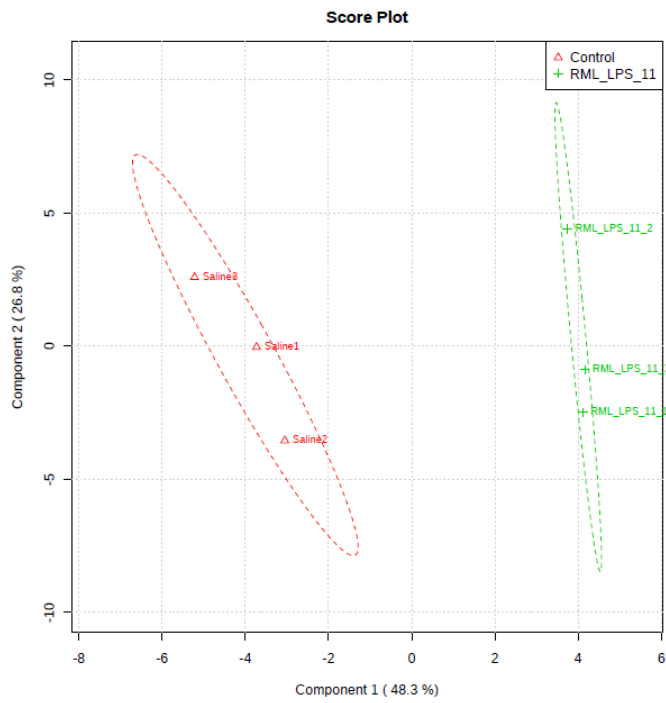


Figure 4.5.

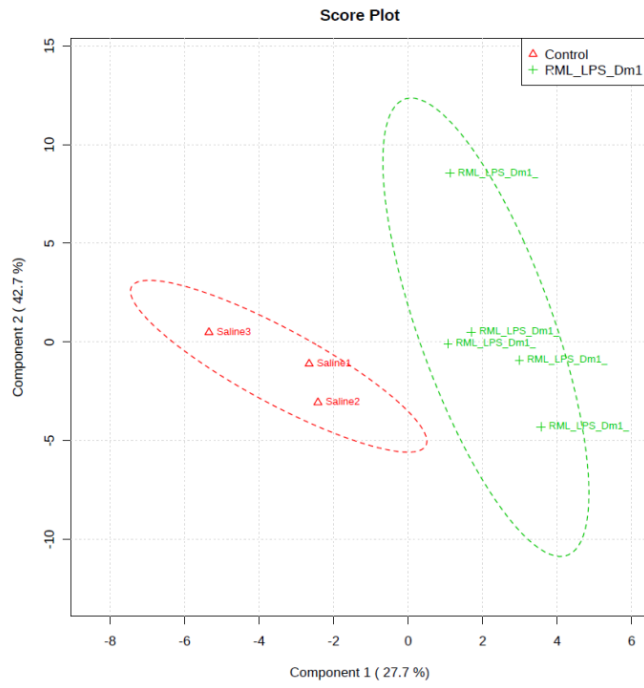


Figure 4.6.

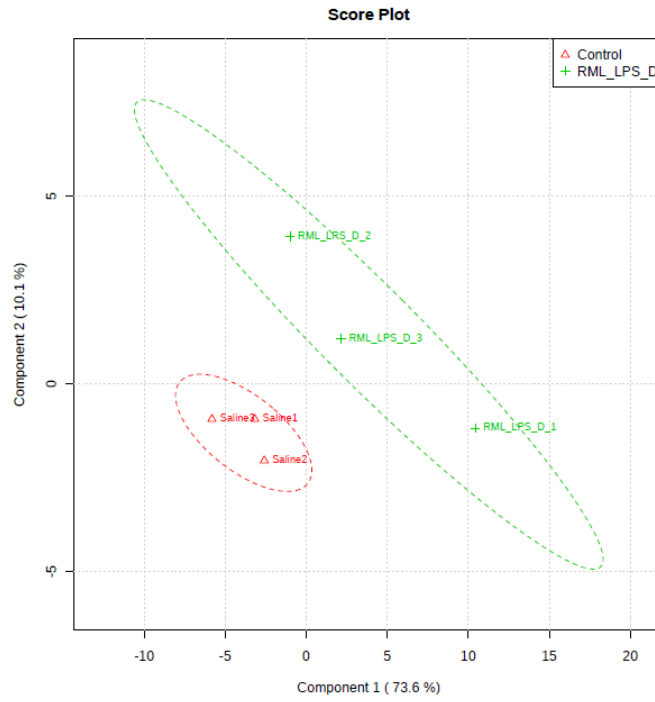


Figure 4.7.

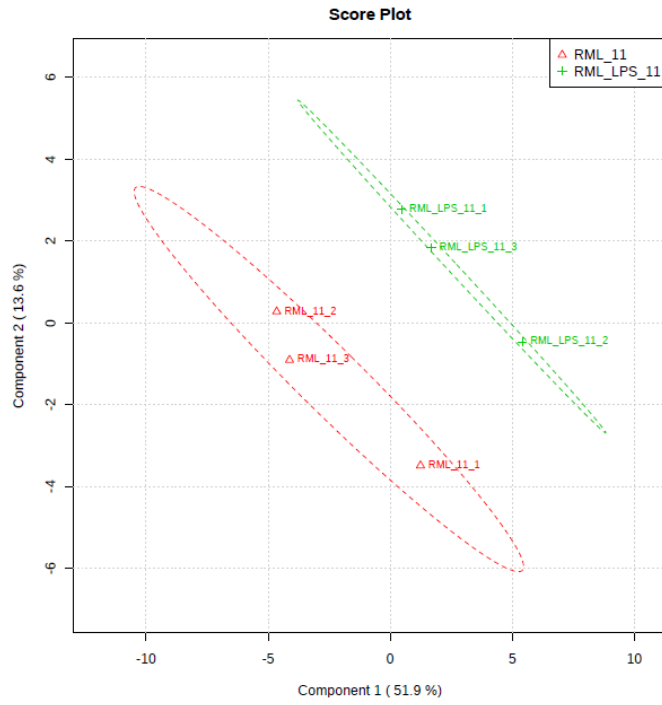


Figure 4.8.

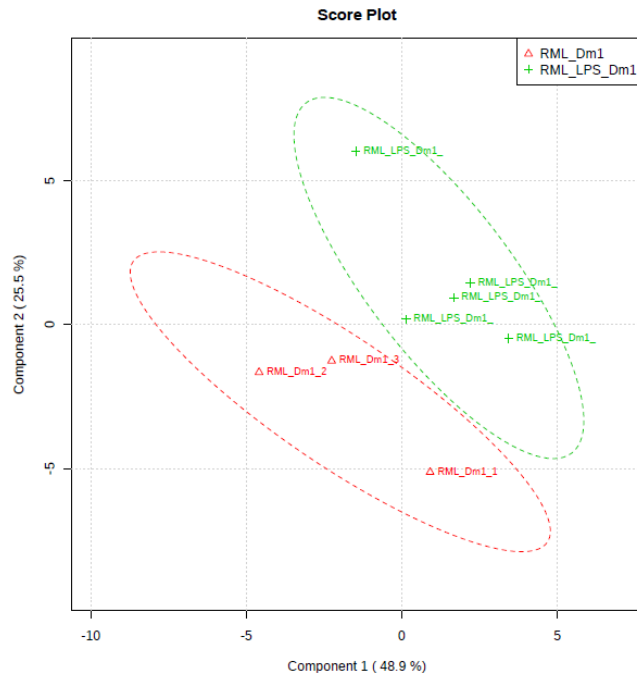


Figure 4.9.

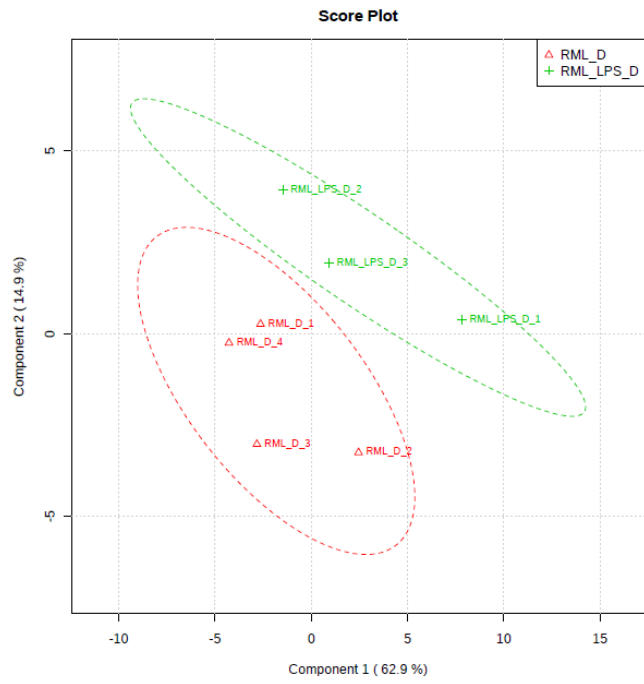


Figure 4.10.

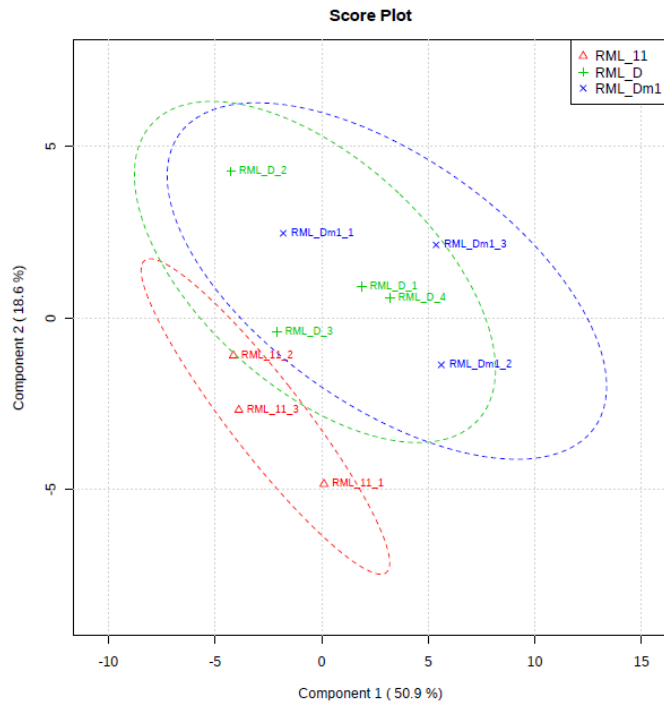
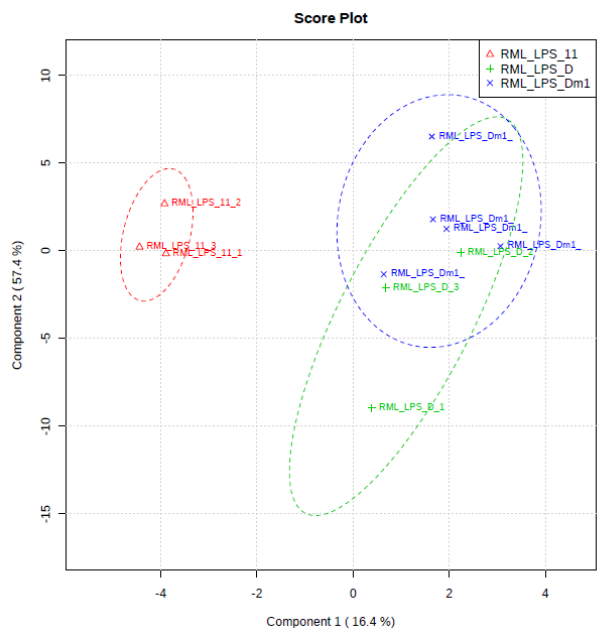


Figure 4.11.



Chapter Five: Overall Discussion

The main hypothesis of this research investigation was to test whether mouse recombinant PrP, converted *in vitro* into a beta-rich isoform resistant to proteinase K digestion (moPrP^{res}) through incubation with bacterial LPS (Ametaj et al., 2010), can cause prion-like disease in experimental FVB/N wt female mice. Generally, TSEs have been diagnosed by their most observable hallmarks including the histological features of spongiform changes (vacuolation), astrogliosis, and amyloid plaque formation, although the latter has not been consistently seen in all TSEs (Prusiner, 1998). Indeed multiple data generated from our study support our hypothesis that de novo generated moPrP^{res} caused prion-like disease in the infected mice as will be discussed in more detail below.

The first finding that supports our hypothesis comes from the clinical signs observed and the high death rate in moPrP^{res}-infected mice. Sixty percent of mice in this group died from prion-like disease within 750 days from infection. This group lost 20% of the mice between 100-250 dpi and another 40% within 500-750 dpi. Clinical monitoring of mice showed that mice displayed typical signs of prion disease including kyphosis, ataxia, tremor, head tilt, tail rigidity, bradykinesia, proprioceptive deficits, stupor, loss of deep pain sensation, and loss of weight and were euthanized for welfare purposes. The reason for shorter incubation time for 20% of the mice (i.e., 100-250 days), from this group, and longer ones (i.e., 750 days) for the rest might be related to potential conformational differences in strains of moPrP^{res} induced by LPS (Safar et al., 1998). Studying conformation structures induced by interaction of LPS with of moPrP or cellular prion protein from other species deserves further investigation in the future.

The other important observation that supports our hypothesis was the degree of vacuolation observed by H&E staining in moPrP^{res}-treated mice. Histology slides showed that mice infected with moPrP^{res} developed neuronal death with typical spongiform vacuolation and

larger size in various brain areas. Minor vacuolation was present during preclinical disease stages in the cerebral cortex (Cc), thalamus (Th), midbrain (Mb), and cerebellum (Cr) regions of the brain starting at 11 wk pi. At terminal stage of the disease the number of vacuoles increased substantially and so did their size in the same brain regions. In addition vacuoles in mice infected with the moPrP^{res} were larger in size compared with vacuoles in the RML-infected mice. Is brain vacuolation a typical sign of prion disease? Indeed, Prusiner (1998) indicated brain vacuolation among the determining pathological features of prion disease. However, it should be pointed out in some combinations of prion strains with different hosts there is accumulation of PrP^{Sc} after scrapie infection without vacuolation in their brain tissue (Orge et al., 2004; Iwata et al., 2006).

Immunohistochemical (IHC) staining indicated that moPrP^{res} caused mild astrocytosis in the Mb and a greater degree of accumulation of astrocytes in the Cr area. Astrogliosis is the second most important hallmark of prion disease (Prusiner, 1998). However, it should be noted that astrocytosis is not always suggestive of specific changes typical of prion disease because most neurodegenerative alterations are accompanied by proliferation of astrocytes. These changes are usually a result of damage to or death of neurons. DeArmond et al. (1992) and Giese et al. (1998) have reported that gliosis occurs before neurodegeneration in prion disease. It is known that astrocytes are the cell type in which the abnormal form of the prion protein, PrP^{Sc}, is first replicated in the CNS (Diedrich et al., 1991). Indeed, Raeber et al., 1997, demonstrated that only animals that express PrP in astrocytes are susceptible to prion disease. Also a recent in vitro study showed that presence of large numbers of astrocytes can accelerate the rate at which neurons are killed by the neurotoxic peptide PrP106-126 (Brown, 1999). Therefore, presence of astrogliosis in several brain areas in mice treated with moPrP^{res} at terminal stage supports our hypothesis that moPrP^{res} caused neurodegeneration and prion-like disease in the treated mice.

Brain histology data also showed that mice infected with de novo-generated moPrP^{res} had mild expression of PrP^{Sc} in the Mb and Cr areas. Does presence of PrP^{Sc} in the brain indicate prion disease? Indeed this is the golden standard for diagnosis of prion disease (Prusiner, 1998). Of note, PrP^{Sc} was not detected in Western blot analyses in the brain samples or L929 test; however, presence of PrP^{Sc} in the Mb and Cr areas is suggestive of prion-like disease in infected mice. One reason for not detecting PrP^{Sc} by Western blot analysis might be related to the fact that homogenization of the whole brain tissue have diluted the amount of PrP^{Sc} in our samples. We also did not use PMCA procedure to increase the amount of PrP^{Sc} in our samples. Recently PMCA has been used widely to increase concentration of PrP^{Sc} in the brain samples (Soto et al., 2001). There are several other factors that might have affected the amount of PrP^{Sc} in the brain. For instance the dose of the infective moPrP^{res} administered. We randomly chose to inject mice with the original moPrP^{res} solution (at 45 µg of protein per mouse). Is this the correct lethal dose of moPrP^{res} to be used sc? In fact we do not know the exact amount of moPrP^{res} to be administered sc to cause prion disease because no end-point titration bioassay was conducted in our study. Therefore a dose study is warranted to determine the right quantity of moPrP^{res} to be used for causing expedited neurodegeneration in the near future. In addition, the route of administration plays a significant role with regards to the incubation time. We used sc route, which is known for long incubation time in developing prion disease. Another important issue is that moPrP^{res} is a new de novo generated strain of prion produced by incubation of recombinant moPrP with LPS and there are no available specific antibodies to detect this strain by Western blot analysis yet.

We also conducted a customer designed 84-gene expression array to identify genes differentially expressed in the brain at different times after infection. Several other studies before

us have reported various proteins and genes differentially expressed in the brain as related to scrapie or other neurodegenerative diseases. These studies have identified a specific gene expression signature that is typical for prion disease. For instance evidence from two prominent labs (Prusiner's and Westaway's) suggest that two main proteins including prion protein (PrP^C) and shadoo of prion protein (Sho) decrease in the brain tissue of experimental animals infected with scrapie (Watts et al., 2011; Westaway et al., 2011). Indeed results of our study showed that the genes encoding *Prnp* and *Sprn* were down-regulated by moPrP^{res} treatment. Westaway et al. (2011) pointed out the post-translational reduction of Sho protein level and suggested a key role for proteolysis in decreasing the Sho concentrations. To our best knowledge, our data are the first to show that the *Sprn* gene was downregulated during development of scrapie in our experimental mice and that might be a key player in decreasing concentrations of Sho. Suggestion of Westaway's et al. (2011) with regards to posttranslational proteolysis of the mRNA for Sho cannot be ruled out because they reported a 90% decrease in Sho levels during prion infection under their experimental conditions. The same aforementioned labs have also indicated that concurrently with decreasing levels of PrP^C and Sho there is also an increase in the accumulation of PrP^{Sc} in the brain. Indeed our data showed that presence of PrP^{Sc} in several brain regions, including the Mb and Cr, increased in mice infected with moPrP^{res}.

The second hypothesis of this study was that simulation of chronic endotoxemia by sc administration of LPS might also cause neurodegeneration and prion-like disease in mice chronically treated with LPS for a 6-wk period. Previous research has shown that even a single administration of LPS intraperitoneally (i.p.) in wt mice, at 5 mg/kg, initiates inflammation in the brain that persists for 10 months with progressive loss of dopaminergic neurons in the substantia nigra (Qin et al., 2007). Our data showed that chronic infusion of LPS was deadly to 50% of the

mice involved in the experiment. Interestingly these mice showed a different type of disease. For instance, during the experiment and prior to development of clinical signs, mice increased their body weight and adipose tissue fat mass, which is in agreement with previous research indicating that 4-wk sc infusion of LPS induces obesity and insulin resistance in C57b16 mice (Cani et al., 2007).

Clinical monitoring data from our experiment also support the hypothesis that LPS caused brain neurodegeneration of a specific type. Mice infused for 6 wk with a moderate dose of LPS showed typical clinical signs of brain neurodegenerative disease similar to prion disease including kyphosis, lack of movement, ataxia, tremor, head tilt, tail rigidity, bradykinesia, proprioceptive deficits, loss of deep pain sensation, and loss of weight.

Histology data showed that mice infused with LPS displayed vacuoles in various regions of the brain including Cc, Th, Mb, and Cr starting at 11 wk pi and in a more intensive mode at terminal stage of disease. Interestingly LPS caused astrocytosis and accumulation of A β only in the Cr area. Noh et al. (2014) reported that ip administration of LPS in mice was associated with overexpression of mRNAs of TLR2 and TLR4 in prefrontal cortex and cerebellum. An increasing line of evidence has demonstrated that one time or short-term administration of LPS is associated with accumulation of A β in specific brain areas including cerebellum, hippocampus, and cerebral cortex (Sheng et al., 2003; Lee et al., 2008; Zhu et al., 2014). The reason why LPS differently affected accumulation of A β in specific areas of the brain might have to do with the serotype of LPS administered, species and gender of the animals used, and the frequency of LPS administration used by different investigators. For instance both Sheng et al. (2003) and Lee et al. (2008) used LPS from *E. coli* 055:B5 in their experiments. Moreover Lee et al. (2008) used male ICR mice and male Sprague-Dawley rats; whereas Sheng et al. (2003) used both female

and male transgenic mice overexpressing amyloid protein precursor. Meanwhile Zhu et al. (2014) used male Wistar rats but did not specify the serotype of the LPS used. In our experiment female FVB/N wt mice were used as animal models. The dose, the route of administration, and the number of LPS treatments in those three investigations is different with ours. For instance Sheng et al. (2003) used 10 μ L/g of BW i.p. once a week for 12 weeks, Lee et al. (2008) and Zhu et al. (2014) administered 250 μ g/kg of LPS i.p. for 3-7 days consecutively. We administered LPS sc at 100 μ g/kg of BW for 6 wk. All these factors should be kept in mind in future experimentations to account for different effects of LPS in various studies.

To our surprise brain gene expression data showed that LPS lowered expression of *Sprn*. Decrease in the concentration of Sho or down-regulation of its gene (i.e., *Sprn*) have been indicated as typical findings of prion disease (Westaway et al., 2011). Lipopolysaccharide, in our study, had no effect on expression of *Prnp*; however, treatment with LPS increased by more than 29-fold the expression of *Prnd* in the brain tissue. Increased concentrations of Dpl protein has been reported to cause ataxia and granule cell degeneration in the cerebellum of PrP knock-out mice (Anderson et al., 2004). Overall our data are in agreement with previous research and implicate chronic endotoxemia in the etiopathology of brain neurodegeneration.

It was intriguing to find out that LPS and RML in our study commonly affected expression of 8 genes (out of 13 genes significantly affected by LPS and 15 by RML). Furthermore, LPS altered expression of 8 genes that were previously reported to be differentially expressed during scrapie disease in murine models (Kim et al., 2008). These data support our hypothesis for a potential role of LPS as a co-factor in prion disease and warrants further research to better understand what is the precise role of LPS in the etiopathogenesis of TSEs.

The third hypothesis of this study was that 6-wk infusion of LPS would aggravate prion disease in mice treated once sc with RML or moPrP^{res}, at the beginning of LPS administration. Indeed mice treated with RML+LPS died at a 100% death rate within 230 dpi (30% of mice died within 150 dpi) compared with 80% of mice treated with RML that died within 250 dpi. Twenty percent of mice from the RML group survived for more than 630 days pi and 10% survived the whole experimental period of 749 days. The delayed death of 20% of the mice treated with RML only might be related to route of administration (i.e., sc) of the scrapie in this study. Chronic treatment with LPS had no effect on the death rate of mice infected with moPrP^{res} in our experiment. Thirty and 20% of mice from moPrP^{res}+LPS and moPrP^{res} groups, respectively, died within 250 dpi. The death rates at the time of termination of the experiment were 60 and 50%, respectively, for moPrP^{res} and moPrP^{res}+LPS groups. Our findings are in agreement with other research indicating that treatment of mice with LPS aggravates prion disease in mice. For instance Cunningham et al. (2009) reported that one time ip injection of LPS (100 µg/kg body weight) from *Salmonella Equine abortus*, in female C₅₇BL/6 mice at 12 wk post inoculation with ME₇ strain of scrapie, increased cytokine production (IL-1β, TNF, and interferon-γ transcription) and exaggerated sickness behavior (inducing acute cognitive impairment). Moreover, Murray et al. (2012) demonstrated that inoculation of female C₅₇BL/6 mice i.p. with a high dose (500 µg/kg) of LPS from *Salmonella Equine abortus*, 18-19 wk post intracerebral infection with ME₇ scrapie strain, exacerbated existing pathology by increasing apoptotic cell death in the brain tissue.

Histology data showed that LPS increased the number of vacuoles in all brain areas (Cc, Th, Mb, and Cr) in mice treated with RML+LPS versus RML-treated mice, at terminal stage but not at 11 wk pi; however, LPS had no effect on the number of vacuoles in moPrP^{res}+LPS versus

those treated with moPrP^{res}-only at 11 wk pi or at death. PrP^{Sc} staining data of RML+LPS-treated mice showed that sc administration of LPS caused a mild increase in the PrP^{Sc} level in Th and Mb of the infected mice at 11 wk pi and exacerbated presence of PrP^{Sc} in all brain areas studied (Cc, Th, Mb, and Cr) at terminal stage. Moreover, astrocytosis data obtained from clinical stage mice treated with RML+LPS showed greater accumulation of astrocytes in all brain regions in comparison to the RML-only infected mice.

With regards to gene expression data mice treated with RML+LPS or RML only commonly shared expression of 11 genes (*Sprn*, *Prnp*, *Prnd*, *Lyz2*, *Ly86*, *Atp1b1*, *Ncam1*, *Prkaca*, *Egr1*, *Anp32a*, *Sod1*) out of a total of 16 or 15 genes significantly affected by these treatments, respectively. The 3 main genes related to prion disease *Sprn*, *Prnp*, and *Prnd* were similarly affected by the two treatments. moPrP^{res} or moPrP^{res}+LPS showed similarities in expression of 6 genes in the brain that are strongly related to prion disease including *Sprn*, *Prnp*, *Prnd*, *ApoE*, *Bax*, *Fyn*, *Fcgr3*, and *Lyz2*. On the other hand it was observed that the group of mice treated with moPrP^{res}+LPS displayed similarity in expression of 8 genes reported in the literature to be affected by scrapie (Kim et al., 2008), out of a total of 14 genes significantly expressed by moPrP^{res}+LPS.

Lipopolysaccharide had no effect on A β accumulation in mice treated with RML+LPS or moPrP^{res}+LPS versus LPS-only. Lipopolysaccharide alone induced A β accumulation only in the cerebellum. The reason for this difference is not understood at present and deserves further inquiry.

The fourth hypothesis of this study was that experimental mice infected with RML or RML+LPS would show typical metabolite signatures that can be used for preclinical diagnosis of

prion disease or as predictive candidate biomarkers of disease. Indeed our study identified various metabolites in both urine and serum related to scrapie at 11 wk pi up to terminal sickness, important for early diagnosis of scrapie in both DI-MS and $^1\text{H-NMR}$ analyses. Mice infected with RML showed alterations in a total of 23 urine and serum metabolites measured with DI-MS and $^1\text{H-NMR}$. Most of the metabolites identified and measured are related to carnitine, phosphatidylcholine, and sphingomyelin families. On the other hand, a total of 25 metabolites were identified, as significantly different by DI-MS and $^1\text{H-NMR}$, in the urine and serum of mice treated with RML+LPS.

Comparison between RML and RML+LPS from 11 wk pi up to terminal sickness indicated difference in only 2 category of urine metabolites related to the carnitine family and glycerophospholipids detected by DI-MS approach.

All metabolites detected in this investigation using non-targeted invasive analytical metabolomics approach need to be validated for their potential role as predictive biomarkers of prion disease using a larger cohort of animals and a greater number of replicates in future studies.

References

1. Ametaj, B. N., F., Saleem, V., Semenchenko, C., Sobsey, and D. S., Wishart, 2010, Lipopolysaccharide interacts with prion protein and catalytically converts it into a protein resistant β -sheet-rich isoform, Prion Congress, Salzburg, Austria.
2. Anderson, L. D., Rossi, J., Linehan, S., Brandner, and C., Weissmann, 2004, Transgene-driven expression of the Doppel protein in Purkinje cells causes Purkinje cell degeneration and motor impairment, PNAS, Volume 101, p. 3644-3649.
3. Brown, D. R., 1999, Prion Protein Peptide Neurotoxicity Can Be Mediated by Astrocytes, Journal of Neurochemistry, Volume 73, p. 1105–1113.
4. Cani, P. D., A., Jacques, M. A., Iglesias, M., Poggi, C., Knauf, D., Bastelica, A. M., Neyrinck, F., Fava, K. M., Tuohy, C., Chabo, A., Waget, E., Delmée, B., Cousin, T., Sulpice, B., Chamontin, J., Ferrières, J.-F., Tanti, G. R., Gibson, L., Casteilla, N. M., Delzenne, M. C., Alessi, and R., Burcelin, 2007, Metabolic Endotoxemia Initiates Obesity and Insulin Resistance, Diabetes, Volume 56, p. 1761-1772.
5. Cunningham, C., S., Campion, K., Lunnon, C. L., Murray, J. F., Woods, R. M., Deacon, J. N., Rawlins, and V. H., Perry, 2009, Systemic inflammation induces acute behavioral and cognitive changes and accelerates neurodegenerative disease, Biological Psychiatry, Volume 65, p. 304-312.
6. DeArmond, S. J., K., Kristensson, and R. P., Bowler, 1992, PrPSc causes nerve cell death and stimulates astrocyte proliferation: A paradox, Progress in Brain Research, Volume 94, p. 437-446.

7. Diedrich, J. F., P. E., Bendheim, Y. S., Kim, R. I., Carp, and A. T., Haase, 1991, Scrapie-associated prion protein accumulates in astrocytes during scrapie infection, *PNAS*, Volume 88, p. 375-379.
8. Giese, A., D. R., Brown, M. H., Groschup, C., Feldmann, I., Haist, and H. A., Kretzschmar, 1998, Role of microglia in neuronal cell death in prion disease, *Brain Pathology*, Volume 8, p. 449-457.
9. Iwata, N., Y., Sato, Y., Higuchi, K., Nohtomi, N., Nagata, H., Hasegawa, M., Tobiume, Y., Nakamura, K., Hagiwara, H., Furuoka, M., Horiuchi, Y., Yamakawa, and T., Sata, 2006, Distribution of PrP(Sc) in cattle with bovine spongiform encephalopathy slaughtered at abattoirs in Japan, *Japanese Journal of Infectious Diseases*, Volume 59, p. 100-107.
10. Kim, H. O., G. P., Snyder, T. M., Blazey, R. E., Race, B., Chesebro, and P. J., Skinner, 2008, Prion disease induced alterations in gene expression in spleen and brain prior to clinical symptoms, *Advances and Applications in Bioinformatics and Chemistry*, Volume 1, p. 29-50.
11. Lee, J. W., Y. K., Lee, D. Y., Yuk, D. Y., Choi, S. B., Ban, K. W., Oh, and J. T., Hong, 2008, Neuro-inflammation induced by lipopolysaccharide causes cognitive impairment through enhancement of beta-amyloid generation, *Journal of Neuroinflammation*, Volume 5, p. 37-50.
12. Murray, C., D. J., Sanderson, C., Barkus, R. M., Deacon, J. N., Rawlins, D. M., Bannerman, and C., Cunningham, 2012, Systemic inflammation induces acute working memory deficits in the primed brain: relevance for delirium, *Neurobiology of Aging*, Volume 33, p. 603-616.

13. Noh, H., J., Jeon, and H., Seo, 2014, Systemic injection of LPS induces region-specific neuroinflammation and mitochondrial dysfunction in normal mouse brain, *Neurochemistry International*, Volume 69, p. 35-40.
14. Orge, L., A., Galo, C., Machado, C., Lima, C., Ochoa, J., Silva, M., Ramos, J. P., Simas, 2004, Identification of putative atypical scrapie in sheep in Portugal, *The Journal of General Virology*, Volume 85, p. 3487-3491.
15. Prusiner, S. B., 1998, Prions, *PNAS*, Volume 95, p. 13363-13383.
16. Qin, L., X., Wu, M. L., Block, Y., Liu, G. R., Breese, J. S., Hong, D. J., Knapp, and F. T., Crews, 2007, Systemic LPS causes chronic neuroinflammation and progressive neurodegeneration, *Glia*, Volume 55, p. 453-62.
17. Raeber, A., Race, R. E., Brandner, S., Priola, S. A., Sailer, A., Bessen, R. A., Mucke, L., Manson, J., Aguzzi, A., Oldstone, M. B. A., Weissmann, C., and Chesebro, B., 1997, Astrocyte-specific expression of hamster prion protein (PrP) renders PrP knockout mice susceptible to hamster scrapie, *The EMBO Journal*, Volume 16, p. 6057-6065.
18. Safar, J., H., Wille, V., Itri, D., Groth, H., Serban, M., Torchia, F. E., Cohen, and S. B., Prusiner, 1998, Eight prion strains have PrP^{Sc} molecules with different conformations, *Nature Medicine*, Volume 4, p. 1157-1165.
19. Sheng, J. G., S. H., Bora, G., Xu, D. R., Borchelt, D. L., Price, and V. E., Koliatsos, 2003, Lipopolysaccharide-induced-neuroinflammation increases intracellular accumulation of amyloid precursor protein and amyloid beta peptide in APP^{swe} transgenic mice, *Neurobiology of Disease*, Volume 14, p. 133-145.

20. Watts, J. C., K., Giles, S. K., Grillo, A., Lemus, S. J., DeArmond, and S. B., Prusiner, 2011, Bioluminescence imaging of Aβ deposition in bigenic mouse models of Alzheimer's disease, PNAS, Volume 108, p. 2528-33.
21. Westaway, D., S., Genovesi, N., Daude, R., Brown, A., Lau, I., Lee, C. E., Mays, J., Coomaraswamy, B., Canine, R., Pitstick, A., Herbst, J., Yang, K. W., Ko, G., Schmitt-Ulms, S. J., Dearmond, D., McKenzie, L., Hood, and G. A., Carlson, 2011, Down-regulation of Shadoo in prion infections traces a pre-clinical event inversely related to PrP(Sc) accumulation, PLoS Pathogen, Volume 7, p.e1002391.
22. Zhu, B., Z. G., Wang, J., Ding, N., Liu, D. M., Wang, L. C., Ding, and C., Yang, 2014, Chronic lipopolysaccharide exposure induces cognitive dysfunction without affecting BDNF expression in the rat hippocampus, Experimental and Therapeutic Medicine, Volume 7, p. 750-754.